



Melatti, Carmen (2018) Mitochondrial division in *T. gondii*: analysis of the Dynamin-related protein C and of its putative interactors. PhD thesis.

<https://theses.gla.ac.uk/38972/>

Copyright and moral rights for this work are retained by the author

A copy can be downloaded for personal non-commercial research or study, without prior permission or charge

This work cannot be reproduced or quoted extensively from without first obtaining permission in writing from the author

The content must not be changed in any way or sold commercially in any format or medium without the formal permission of the author

When referring to this work, full bibliographic details including the author, title, awarding institution and date of the thesis must be given

Enlighten: Theses

<https://theses.gla.ac.uk/>
research-enlighten@glasgow.ac.uk

**Mitochondrial division in *T. gondii*:
analysis of the Dynamin-related
protein C and of its putative
interactors**

By

Carmen Melatti
B.Sc., M. Res. (Hons)

Submitted in fulfilment of the requirements for the
Degree of Doctor of Philosophy

School of Life Sciences
College of Medical, Veterinary & Life Science
Institute of Infection, Immunity & Inflammation
University of Glasgow

Abstract

Apicomplexa parasites such as *Plasmodium spp.* and *Toxoplasma gondii* are characterised by a single, lasso-shaped mitochondrion. This organelle is critical during all phases of the parasite life cycle, and is a validated drug target against parasites of the Apicomplexa phylum. In contrast to other eukaryotes, replication of the mitochondrion in these parasites is tightly linked to the cell cycle. A key step in mitochondrial segregation is the fission event, which in many eukaryotes requires the action of Dynamin-related proteins: these mechanochemical enzymes are recruited at the outer membrane of the mitochondria and mediate membrane constriction. To date, none of the components of the apicomplexan fission machinery have been identified and validated. In this work, I investigated the role of DrpC, a highly divergent, Apicomplexa-specific putative Dynamin-related protein, in *T. gondii*. Endogenous tagging showed that DrpC is adjacent to the mitochondrion, and is localised both at its periphery and at its basal part, where fission is expected to occur. Depletion and dominant negative expression of DrpC results in interconnected mitochondria and ultimately in drastic changes in mitochondrial morphology, leading to parasite death. These data indicate that DrpC is essential for mitochondrial biogenesis in *T. gondii*. To better understand the fission mechanism, DrpC potential interactors were investigated in this study; intriguingly, it is here shown that the conserved mitochondrial protein Fis1, which in other eukaryotes recruits the Dynamin-related protein during fission, is not required for mitochondrial fission in *T. gondii*. Conversely, immunoprecipitation data suggest an interaction between DrpC and the microtubule scaffold; as DrpC is also seen at the periphery of the parasite, these data could suggest a second role for this atypical Dynamin-related protein.

Table of Contents

Abstract.....	2
Table of Contents	3
List of Tables.....	7
List of Figures.....	7
Acknowledgements.....	9
Author’s Declaration	10
Publications arising from this work and collaborations	11
Definitions/abbreviations	12
1 Introduction.....	15
1.1 Taxonomy of <i>T. gondii</i>	15
1.2 Life cycle of <i>T. gondii</i>	16
1.2.1 Life cycle in the definitive host	17
1.2.2 Life cycle in the intermediate host	18
1.3 Pathogenesis and clinical features.....	23
1.4 Characterisation of essential genes in <i>T. gondii</i>	24
1.4.1 DiCre system and Conditional U1 Gene Silencing	25
1.4.2 The tetracycline-inducible system	26
1.4.3 The ddFKBP system.....	27
1.4.4 CRISPR/Cas9 in <i>T.gondii</i>	28
1.4.5 The auxin-inducible degron (AID) system	29
1.5 Ultrastructure of <i>T. gondii</i> tachyzoites	30
1.5.1 The apical complex and secretory organelles	31
1.5.2 The apicoplast	33
1.5.3 The IMC	34
1.5.4 The microtubule network	35
1.5.5 The mitochondrion	38
1.6 Endodyogeny	40
1.7 Mitochondrial dynamics in higher eukaryotes	45
1.7.1 Mitochondria motility	47
1.7.2 Mitochondrial fusion.....	48
1.7.3 Mitochondrial fission	50
1.8 Dynamin superfamily: universal membrane remodelling effectors	53
1.8.1 Dynamin-related proteins: mode of action	54
1.8.2 Dynamin-related proteins in <i>T. gondii</i>	56
1.9 Aim of study	60
2 Materials and Methods.....	61

2.1	Equipment	61
2.2	Computer Software.....	61
2.3	Consumables, biological and chemical reagent	62
2.4	Kits.....	63
2.5	Buffers, solutions and media.....	63
2.6	Antibodies	65
2.7	Oligonucleotides	66
2.8	Plasmids.....	66
2.9	Cell strains.....	67
2.9.1	Bacteria strains	67
2.9.2	<i>Toxoplasma gondii</i> strains.....	67
2.9.3	Mammalian cell lines.....	68
2.10	Molecular biology	68
2.10.1	Isolation of genomic DNA from <i>T. gondii</i>	68
2.10.2	mRNA extraction and cDNA synthesis	68
2.10.3	qRT-PCR	69
2.10.4	Polymerase chain reaction.....	69
2.10.5	Agarose gel electrophoresis	71
2.10.6	Restriction endonuclease digest	71
2.10.7	Dephosphorylation of digested DNA plasmids.....	72
2.10.8	Purification of DNA	72
2.10.9	Determination of nucleic acid concentrations.....	72
2.10.10	Ligation of DNA fragments.....	72
2.10.11	Plasmid transformation into bacteria	73
2.10.12	Isolation of plasmid DNA from bacteria.....	73
2.10.13	DNA sequencing	74
2.10.14	Cloning performed in this study.....	74
2.10.15	Ethanol precipitation	75
2.11	Cell biology	76
2.11.1	<i>Toxoplasma gondii</i> tachyzoites and mammalian cells <i>in vitro</i> culturing	76
2.11.2	Trypsin/EDTA treatment of mammalian cell lines	76
2.11.3	Cryopreservation of <i>T. gondii</i> and thawing of stabilates.....	76
2.11.4	Transfection of <i>T. gondii</i>	77
2.11.5	Isolation of clonal parasite lines by limited dilution.....	79
2.12	Tachyzoite phenotypic analysis	79
2.12.1	Immunofluorescence assay	79
2.12.2	Plaque assay	79
2.12.3	Replication assay	80

2.12.4	Time-lapse video microscopy.....	80
2.13	Biochemistry	80
2.13.1	Preparation of parasite cell lysates	80
2.13.2	Sodium dodecyl sulphate polyacrylamide gel electrophoresis	81
2.13.3	Western blotting	81
2.13.4	Ponceau-staining	81
2.13.5	Immunostaining.....	82
2.13.6	Visualisation and quantification of the protein bands	82
2.13.7	Stripping.....	82
2.13.8	Immunoprecipitation	82
2.13.9	Co-immunoprecipitation	83
2.14	Bioinformatics	84
2.14.1	Sequence alignments	84
2.14.2	Homology modelling	84
2.14.3	Data and statistical analysis	84
3	Characterisation of the Dynamin-related protein DrpC in <i>T. gondii</i>	85
3.1	Generation and confirmation of the knock-in strain <i>DrpC-YFP</i>	86
3.2	Analysis of DrpC localisation	88
3.3	Analysis of DrpC knockdown	94
3.4	Generation of a dominant negative form of DrpC	100
3.5	Overexpression of full-length and truncated forms of DrpC	105
3.6	Conclusions	108
4	Analysis of potential interactors of DrpC in <i>T. gondii</i>	111
4.1	Conservation of the fission complex in <i>T. gondii</i>	112
4.2	Overexpression of Fis1	115
4.3	Knockdown of Fis1.....	119
4.4	Immunoprecipitation experiments.....	122
4.4	Conclusions	124
5	Outlook: localisation and function of p50 in <i>T. gondii</i>	128
5.1	Generation of an inducible knockdown of p50	130
5.2	Analysis of p50 localisation and function	132
5.3	Conclusions	139
6	General discussion	142
6.1	DrpC mediates mitochondria fission during endodyogeny	142
6.2	Fis1 function in <i>T. gondii</i>	148
6.3	DrpC puncta at the parasite periphery	150
6.4	Conclusion.....	156
	Accompanying material.....	159
	Bibliography	160

List of Tables

Table 2.1-1. Equipment	61
Table 2.2-1. Software.....	61
Table 2.3-1. Biological and chemical reagents.....	62
Table 2.4-1. Nucleic acid extraction and amplification kits	63
Table 2.5-1. Buffers for DNA Analysis	63
Table 2.5-2. Buffers for Western blot analysis.....	63
Table 2.5-3. Buffers and media for bacterial culture	64
Table 2.5-4. Buffers and media for <i>T. gondii</i> tachyzoites and mammalian cell culture	64
Table 2.6-1. Primary antibodies.....	65
Table 2.6-2. Secondary antibodies, fluorescent ligands and stains	65
Table 2.7-1: Oligonucleotides used in this study	66
Table 2.8-1. Main plasmids used in this study for cloning and expression in <i>T. gondii</i>	66
Table 2.9-1. <i>Escherichia coli</i> competent cells for plasmid transformation	67
Table 2.9-2: <i>T. gondii</i> strains used in this study.....	67
Table 2.10-1. qPCR master mix	69
Table 2.10-2. qPCR thermic profile.....	69
Table 2.10-3. Q5®Taq reaction	70
Table 2.10-4. Q5® Taq amplification thermic profile.....	70
Table 2.10-5. Taq DNA polymerase PCR reaction.....	70
Table 2.10-6. Taq DNA polymerase thermic profile	70
Table 4.1-1: Conservation of the known mitochondrial fission complex in <i>T. gondii</i>	113
Table 3-1: DrpC pull-down results	123
Table 6-1: Summary of current knowledge about putative conserved effectors mitochondrial dynamics in Apicomplexa parasites.	157

List of Figures

Figure 1-1: The life cycle of <i>Toxoplasma gondii</i>	17
Figure 1-2: The lytic cycle of <i>T. gondii</i>	19
Figure 1-3: Ultrastructure of <i>T. gondii</i> tachyzoite.	30
Figure 1-4: Structure of the single mitochondrion of <i>T. gondii</i>	40
Figure 1-5: Endodyogeny of <i>T. gondii</i>	43
Figure 1-6: Dynamics of mitochondrial replication in <i>T. gondii</i>	45
Figure 1-7: Mitochondrial dynamics and the balance between fission and fusion	49
Figure 1-8: Structure and assembly of classical Dynamin and mitochondrial Dynamin-related proteins.	55
Figure 1-9: Dynamin-related proteins in <i>T. gondii</i>	59
Figure 3-1: Endogenous tagging of DrpC	87
Figure 3-2: Localisation of DrpC.....	89
Figure 3-3: DrpC associates with the mitochondrion in <i>T. gondii</i>	90
Figure 3-4: DrpC localisation in different stages of mitochondria replication and segregation.	92
Figure 3-5: Analysis of the dynamic localisation of DrpC during mitochondrial fission.	93

Figure 3-6: DrpC puncta colocalise with mitochondrial interconnections.....	94
Figure 3-7: Rapamycin induction efficiently promotes DrpC downregulation	96
Figure 3-8: Analysis of DrpC knock-down on different organelles of <i>T. gondii</i> ...	97
Figure 3-9: DrpC knock-down leads to abnormal mitochondria morphology.....	99
Figure 3-10: Shield-1 mediated expression of a dominant negative form of DrpC impairs parasite growth.	101
Figure 3-11: Over-expression of a dominant-negative form of TgDrpC leads to interconnected mitochondria.....	104
Figure 3-12: Modelling of the GTP binding domain of DrpC	105
Figure 3-13: Overexpression of wild-type and truncated forms of DrpC	107
Figure 4-1: Fis1 alignment	114
Figure 4-2: Fis1 localisation and overexpression.....	116
Figure 4-3: Analysis of Fis1 and DrpC putative interaction.....	118
Figure 4-4: Fis1 Knockdown.....	121
Figure 4-5: Immunoprecipitation on the strain <i>DD-GFP-DrpCwt</i>	122
Figure 5-1: Generation of the strain <i>p50-mAID-HA</i>	132
Figure 5-2: p50 localisation and downregulation in the strain <i>p50-mAID-HA</i>	133
Figure 5-3: Colocalisation analysis in the strain <i>p50-mAID-HA</i>	134
Figure 5-4: Quantification of growth in <i>p50-mAID-HA</i> parasites in presence and absence of IAA	135
Figure 5-5: Analysis of replication in <i>p50-mAID-HA</i> parasite strain	136
Figure 5-6: Analysis of p50 knockdown effect on different organelles of <i>T. gondii</i>	137
Figure 5-7: p50 knockdown leads to abnormal mitochondria morphology in 30% of counted vacuoles	138
Figure 5-8: p50 knockdown results in a defect in rhoptry biogenesis	139

Acknowledgements

I would like to thank Prof. Markus Meissner for giving me the opportunity to work in his group, for his enthusiasm for science and the generosity he showed me during my PhD. I am also grateful to my second supervisor, Dr. Lilach Sheiner, for her advice and helpful inputs in this project. Finally, to my assessors, Professors Richard McCulloch, Paul Garside and Sylke Müller, for their encouragement, advice and kindness.

I much enjoyed working in the Meissner lab, and profited from the help and advice of many members of the group; in particular, I would like to thank Doctors Mariana Serpeloni, Elena Jimenez Ruiz and Maria Fernanda LaTorre Barragan, who were always ready to help me and taught me much. I am also grateful to Dr Javier Periz, Dr. Gurman Pall and Matthew Gow, for their support in the lab and for stimulating discussions.

Finally, I feel lucky to have met so many good friends in Glasgow: Mari and Fer, who annoyingly called me “maaaama” for years, and made the lab so much fun; Johannes and Mario, the “last men standing” whose friendship in this last year was precious, and who lent me a hand whenever I needed; and finally, Nati and Andrea, my crazy salsa friends, for all the adventures we shared.

And a special thank you to two great people: Phe, my friend who manages to feel close even when I am freezing in Scotland and he is roasting in Naples; and to Tomás, who supports and encourages me every day, in that caring, funny, rock’n’roll way of his.

Author's Declaration

I, Carmen Melatti hereby declare that I am the sole author of this thesis and performed all of the work presented, with the following exceptions highlighted below. No part of this thesis has been previously submitted for a degree at this or another university.

Chapter 1:

3D reconstruction of DrpC puncta was performed in collaboration with Dr. Leandro Lemgruber, WTCMP imaging technologist, University of Glasgow, UK.

Homology modelling of DrpC GTPase domain was performed by Dr. Ehke Pohl, Durham University, UK.

Publications arising from this work and collaborations

Carmen Melatti, Manuela Pieperhoff, Leandro Lemgruber, Ehmke Pohl, Lilach Sheiner, and Markus Meissner. “A unique Dynamin-related protein is essential for mitochondrial fission in apicomplexan parasites”. *Submitted for publication*

Pieperhoff MS, Pall GS, Jimenez-Ruiz E, Das S, Melatti C, et al. (2015): “Conditional U1 Gene Silencing in *Toxoplasma gondii*”. PLoS One 10: e0130356.

Definitions/abbreviations

°C	Degree Celsius	<i>E. coli</i>	<i>Escherichia coli</i>
Aa	Amino acid	EDTA	Ethylene diamine tetraacetic acid
AID	Auxin-inducible degron	ER	Endoplasmic reticulum
AMA1	Apical membrane antigen 1	EtOH	Ethanol
Amp	Ampicillin	FBS	Fetal bovine serum
ADP	Adenosine diphosphate	fw	Forward
ATP	Adenosine triphosphate	g	Gram or Gravity (context dependent)
BLAST	Basic Local Alignment Search Tool	GAP	Glideosome associated protein
bp	Base pair	gDNA	Genomic deoxyribonucleic acid
BSA	Bovine serum albumin	GFP	Green fluorescent protein
Ca ²⁺	Calcium	GOI	Gene of interest
CAT	Chloramphenicol acetyltransferase	GED	GTPase Effector Domain
cDNA	Complementary deoxyribonucleic acid	GPI	Glycophosphatidylinositol
Cas9	Caspase9	GRASP	Golgi Reassembly and Stacking Protein
CDPK	Calcium-dependent protein kinase	GSH	Glutathione
CIP	Calf intestinal phosphatase	GTP	Guanosine triphosphate
C-terminal	Carboxyl terminal	h	Hour
CRISPR	Clustered Regularly Interspaced Short Palindromic Repeats	H ₂ O	Water
DD	Destabilisation domain	HEPES	4-(2-Hydroxyethyl)-piperazineethanesulphonic acid
DHFR	Dihydrofolate reductase	HFF	Human foreskin fibroblast
DiCre	Dimerisable Cre	HSP	Heat shock protein
DMEM	Dulbecco's Modified Eagle's Medium	Hx or hxgprt	Hypoxanthine-xanthine-guanine phosphoribosyl transferase
DMSO	Dimethyl sulfoxide	IAA	indole-3-acetic acid
DN	Dominant negative	IFA	Immunofluorescence analysis
DNA	Deoxyribonucleic acid	IMC	Inner membrane complex
dNTP	Deoxynucleotide 5'-triphosphate	IMM	Inner Mitochondrial membrane
Drp	Dynamain related protein	IPTG	Isopropyl-O-D-thiogalactopyranoside
		kbp	Kilo base pair
		KD	Knockdown
		kDa	Kilo Dalton
		KO	Knockout

LB	Luria-Bertani	rpm	revolutions per min
LoxP	Locus crossover in P1	RT	Room temperature
M	Molar	rev	Reverse
MCS	Multiple cloning site	s	Second
mg	Milligram	SAG1	Surface antigen 1
MIC	Micronemal protein	SD	Standard deviation
min	Minute	SDS-PAGE	Sodium dodecyl sulfate polyacrylamide gel electrophoresis
ml	Millilitre	SEM	Standard of the mean
mM	Milimolar	SOC	Super optimal broth with catabolite repression
MPA	Mycophenolic acid	<i>spp.</i>	Species
mRNA	Messenger ribonucleic acid	SSR	Site specific recombination
MT	Microtubule	t	Time
Myo	Myosin	<i>T. gondii</i> or <i>Tg</i>	<i>Toxoplasma gondii</i>
NCBI	National Center for Biotechnology Information	TAE	Tris-acetate-EDTA
ng	Nanogram	TOM	Transporter of the Outer Membrane
nm	Nanometer	TEMED	N,N,N',N'-tetramethylethyle nediamine
N-terminal	Amino terminal	TJ	Tight junction
o/n	Over night	TM	Transmembrane
OMM	Outer Mitochondrial Membrane	Tris	Tris [hydroxymethyl] aminomethane
ORF	Open reading frame	U	Unit
<i>P. berghei</i> or <i>Pb</i>	<i>Plasmodium berghei</i>	UTR	Untranslated region
<i>P. falciparum</i>	<i>Plasmodium falciparum</i>	UV	Ultraviolet
PBS	Phosphate buffered saline	V	Volts
PCR	Polymerase chain reaction	v/v	Volume/volume percentage

PFA	Paraformaldehyde	w/v	Weight/volume percentage
P _i	Inorganic phosphate	WB	Western blot
PH	Pleckstrin homology		
PM	Plasma membrane	WHO	World health organisation
POI	Protein of interest	WT	Wild-type
PV	Parasitophorous vacuole	Xan	Xanthosine monophosphate
PVM	Parasitophorous vacuole membrane	X-Gal	5-bromo-4-chloro-3-indoyl- β -D-Galactopyranoside
PRD	Proline-Rich domain		
r	Resistant	YFP	Yellow fluorescent protein
RFP	Red fluorescent protein	μ g	Microgram
RNA	Ribonucleic acid	μ l	Microliter
RON	Rhoptry neck protein	μ m	Micrometer
ROP	Rhoptry protein	μ M	Micromolar

1 Introduction

Since its discovery in 1908 (Nicolle and Manceaux, 1908), *Toxoplasma gondii* has become one of the most studied protozoa of the Apicomplexa phylum. The interest in this unicellular obligate parasite comes from different factors. Firstly, it has great medical and veterinary importance: one-third of the human population is estimated to be chronically infected, and huge economic losses are caused by abortion in sheep and cattle as a result of toxoplasmosis (Torrey and Yolken, 2013).

Moreover, thanks to its amenability to genetic manipulation and *in vitro* culturing, *T. gondii* is a good model organism for research on conserved aspects of Apicomplexa biology, as it is more experimentally accessible than other members of its phylum.

Finally, this parasite presents a number of unique features -like its mechanisms of motility, host cell entry, and division - which make it an interesting model for cell biology; comparing some of its distinctive features with the ones of other eukaryotic systems can give new insights into their origin and evolution.

In this introduction, the main aspects of *T. gondii* biology will be reviewed. Moreover, particular emphasis will be given to the unusual replication mechanism which *T. gondii* adopts during its lytic cycle, and to the behaviour of its single mitochondrion during that stage.

1.1 Taxonomy of *T. gondii*

Despite its worldwide distribution and wide host range, *T. gondii* is the only species of the *Toxoplasma* genus; its name derives from its shape (toxoplasma = arc-like form) and from the organism in which it was first isolated, the rodent *Ctenodactylus gundi* (Nicolle and Manceaux, 1908). *T. gondii* is a member of the class of cyst-forming Coccidia, which belongs to the phylum of Apicomplexa, a large group of unicellular protozoan parasites (Levine et al., 1980). More than 6000 species have been described in this phylum, and many more (almost a million, according to a recent estimate) remain unnamed (Adl et al., 2007). In addition to *T. gondii*, other members of this phylum are of great medical and

veterinary importance: the most dangerous for human health is *Plasmodium falciparum*, the agent of human malaria, which caused more than 400.000 deaths in 2016 (World Health Organization: World malaria report 2017). Another apicomplexan parasite, *Cryptosporidium spp.*, is able to infect humans and causes severe gastrointestinal illnesses, especially among children and people who are immunocompromised or malnourished (Checkley et al., 2015). Moreover, *Eimeria spp.* (the agent of coccidiosis in poultry), *Babesia spp.*, *Neospora spp.* and *Theileria spp.* all affect livestock and cause heavy economic losses (Sharman et al., 2010, Giles et al., 2014, Maharana et al., 2016).

Apicomplexa are obligate intracellular parasites; they all have an apical complex, a unique structure which gives the name to the phylum (see paragraph 1.5.1). Another feature common to Apicomplexa is a system of membranous sacs, called alveoli, which subtends the plasma membrane; alveoli are the unifying morphological characteristic of the infrakingdom Alveolata, which comprises also Dinoflagellates and Ciliates (Cavalier-Smith, 1993, Adl et al., 2005). While Apicomplexa are all defined by their obligate parasitic lifestyle, ciliates and dinoflagellates show a wider range of symbiotic behaviours, suggesting that Apicomplexa evolved from free-living, photosynthetic organisms (Blader et al., 2015, Moore et al., 2008).

1.2 Life cycle of *T. gondii*

T. gondii is a facultative heteroxenous parasite, as its life cycle is completed in two different kinds of hosts. While the lytic cycle can occur in virtually any warm-blooded animal, this parasite can replicate sexually only in the Felidae family, its definitive host.

The complete life cycle (Figure 1-1) was first described with the discovery of sexual stages in the small intestine of cats (Hutchison, 1965, Dubey et al., 1970b, Dubey et al., 1970a). Notably, *T. gondii* has no need to go through the sexual cycle before infecting a new host, as it can be transmitted orally in the form of a tissue cyst (Su et al., 2003).

During its life cycle, *T. gondii* can present three different infectious stages: tachyzoites, the fast growing forms; bradyzoites, contained in tissue cysts; and sporozoites, contained in sporulated oocysts. Hosts (definitive or intermediate) can be infected by any of these three stages, either through horizontal transmission (i.e., ingesting either oocysts disseminated in the environment, or tissue cysts usually present in undercooked meat) or vertically, by transplacental transmission of tachyzoites.

1.2.1 Life cycle in the definitive host

Members of the Felidae family can become infected with tachyzoites, sporozoites or bradyzoites; currently, most experiments to elucidate the sexual cycle have used bradyzoite-induced infections (Fig. 1-1) (Dubey and Frenkel, 1976, Dubey, 2006).

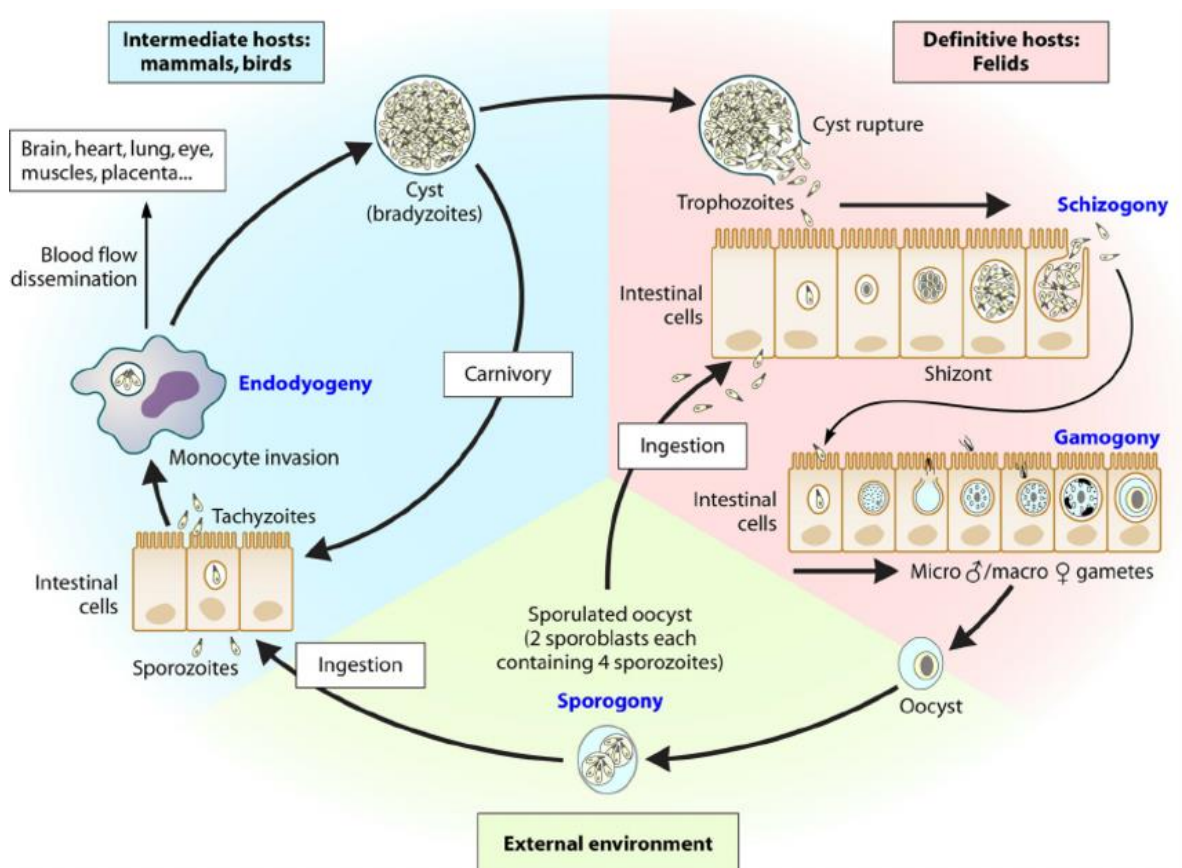


Figure 1-1: The life cycle of *Toxoplasma gondii*.

Sexual reproduction occurs in felids, the definitive hosts, while asexual replication can take place in any warm-blooded vertebrate. Schizogony and gamogony take place in the gut of the cat; the fusion of male and female gametes produces diploid oocysts, which are shed with the faeces. Sporulation occurs in the external environment, and sporulated oocyst can be taken up by intermediate hosts. Once sporozoites are released, asexual reproduction takes place, and tachyzoites disseminate in the body during the acute phase of infection. Host immune response triggers differentiation in slow growing, cyst forming bradyzoites. Figure reprinted from (Robert-Gangneux and Darde, 2012). Copyright © 2012, American Society for Microbiology

When ingested by a cat, the tissue cyst wall is digested in the lumen of the gut; the released bradyzoites invade the epithelial cells of the small intestine and replicate asexually, giving rise to five different stages (A- to E-schizonts). In the last three stages, merozoites are formed by endopolygony, a process where the nuclei divide several times before cytoplasmic segmentation takes place. At this point starts the sexual phase of the life cycle, which typically occurs four days after tissue cyst ingestion: merozoites develop into either male (microgametocyte) or female (macrogametocyte) gametocytes (Speer and Dubey, 2005). During microgamony, merozoites differentiate in microgamonts, large cells that undergo nuclear division to form up to 21 biflagellate male microgametes; after budding, microgamonts swim and fertilize the single macrogamete, which is the product of macrogamony. The resulting zygote then builds a rigid wall, forming an oocyst (Ferguson et al., 1975).

Upon rupture of the infected epithelium cells of the intestine, millions of unsporulated (non-infective) oocysts are released into the intestinal lumen and passed with the cat's faeces into the environment (Dubey, 2001). Aeration and change of temperature induce sporulation (meiotic division) of the oocyst, which results in the formation of two sporocysts, each containing four sporozoites (Cornelissen et al., 1984, Speer and Dubey, 1998). Thanks to its multi-layered wall, a sporulated oocyst can maintain its infectivity for several years under ordinary environmental conditions (Dubey, 1998).

1.2.2 Life cycle in the intermediate host

T. gondii reproduction in the intermediate host is exclusively asexual. When the sporulated oocyst is ingested by an intermediate host, sporozoites are released in the lumen of the small intestine and infect the cells of the lamina propria (Speer and Dubey, 1998). There, they undergo replication to form the fast-growing, banana-shaped tachyzoites, which disseminate throughout the body. In this phase of acute infection, tachyzoites undergo a lytic cycle consisting of invasion of host cells, replication inside a parasitophorous vacuole (PV), and egress (Fig. 1-2); these processes will be detailed in the following paragraphs.

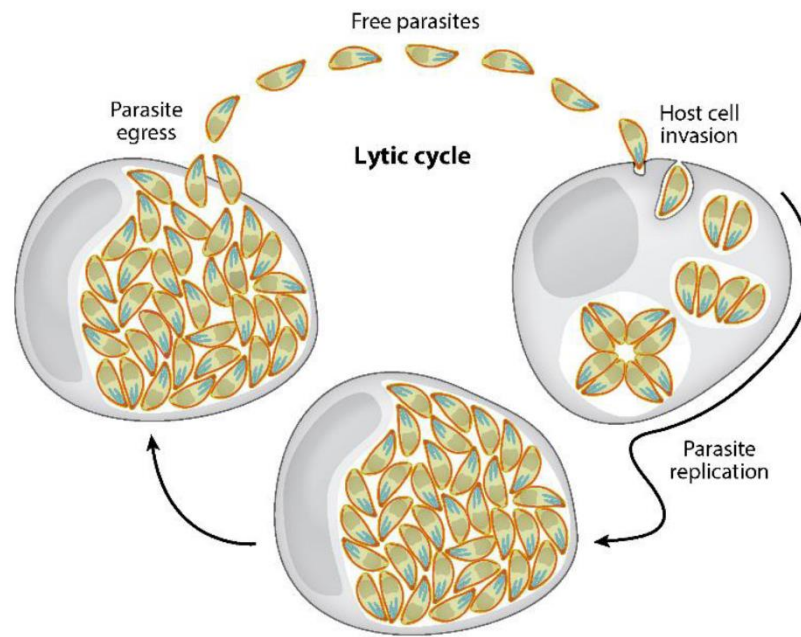


Figure 1-2: The lytic cycle of *T. gondii*.

Extracellular tachyzoites use their gliding machinery to locate a host cell; after attachment to the host surface, they actively penetrate the cell, and in the process a protective PVM is formed. Replication by endodyogeny takes place within the PV. After multiple rounds of division, tachyzoites egress the host, move to neighbouring cells by gliding motility and re-invade new cells. Reprinted from (Blader et al., 2015). Copyright © Annu. Rev. Microbiol. 2015.

1.2.2.1 Gliding, attachment and invasion

At the start of the lytic cycle, *T. gondii* tachyzoites move to reach the host cell, re-orientate and finally enter. To accomplish these steps, the parasite uses a complex form of movement called gliding motility, coupled with the coordinated discharge of micronemes and rhoptries, secretory organelles essential for virulence.

When analysed on 2D substrates, *T. gondii* gliding motility demonstrates three distinct motions; twirling, circular and helical (Hakansson et al., 1999). When a 3D matrix is used, parasites move exclusively in a left-handed corkscrew (Leung et al., 2014); these assays probably reflect different patterns of motility, and are both useful if put in the appropriate context. For example, 3D assays are probably more useful to study tissue migration, when parasites can travel long distances before reaching their target cells, and need to easily change direction of movement, as shown for *Plasmodium ssp.* (Amino et al., 2006).

According to the classical model of apicomplexa motility, gliding motility is powered by an acto-myosin motor, integrated in a complex called the glideosome, which anchors the Myosin A motor protein to the inner membrane complex (IMC) through the interaction of myosin light chain MLC1 and the Glideosome-associated proteins GAP45, GAP50 and GAP40 (as reviewed in (Tardieux and Baum, 2016, Frenal et al., 2017) . To propel the parasite forward, the glideosome also needs to interact with extracellular receptors; this is mediated by adhesins, micronemal proteins which after secretion are inserted into the parasite membrane to mediate interaction with extracellular molecules (Carruthers et al., 2000, Huynh et al., 2003). Thus, according to the linear model of gliding motility, Myosin A, housed in the narrow space (20-40 nm) between the plasma membrane and the IMC, moves short, unstable actin filaments (Herm-Gotz et al., 2002, Meissner et al., 2002, Wetzal et al., 2003); when Myosin A pulls the actin filaments rearwards, this movement is transmitted through a linker to the adhesins-substrate complex. The latter is translocated rearwards, resulting in the forward movement of the parasite over the substrate (Soldati and Meissner, 2004).

Some aspects of this elegant model for gliding motility are not yet explained, or have been challenged by new evidence. Aldolase, which was long thought to be the linker between the motor and the adhesins, has been shown to be dispensable for motility; instead, the glideosome-associated connector (GAC) protein has been proposed to serve as the connector (Shen and Sibley, 2014, Jacot et al., 2016). Moreover, the viable knockout of several key glideosome factors, which were thought to be essential for motor function, and the discovery that *T. gondii* actin forms an extensive F-actin network, showed that more work is needed to better understand how the acto-myosin motor powers *T. gondii* gliding and invasion (Andenmatten et al., 2013, Egarter et al., 2014, Whitelaw et al., 2017, Periz et al., 2017).

Thanks to the action of the acto-myosin motor, *T. gondii* is able to invade host cells in an active, very rapid process.

At first, the parasite loosely attaches itself to the host cell, through low-affinity lateral contacts with the host cell surface (Carruthers and Boothroyd, 2007); afterwards, the regulated discharge of micronemes mediates a firmer

attachment to host cell receptors, which results in a reorientation of the parasite at its apical end (Carruthers et al., 1999). Rhoptry neck proteins (RONs) are subsequently secreted in the host cytosol, and a “tight junction” (TJ) at the parasite/host cell interface is formed: TJ formation is mediated by the interaction between the micronemal protein AMA1 at the plasma membrane of the parasite, and RON2, a rhoptry neck protein inserted in the host plasma membrane (Alexander et al., 2005, Carruthers et al., 1999, Carruthers and Boothroyd, 2007, Frenal et al., 2017, Lamarque et al., 2011, Mital et al., 2005). RON2 interacts with micronemal proteins RON4, RON5 and RON8, which are secreted in the host cytoplasm, and are also required for subverting host cell functions (Besteiro et al., 2009, Lebrun et al., 2005, Guerin et al., 2017). Importantly, it has been shown that parasites lacking AMA1 can still form a TJ (Bargieri et al., 2013); it is proposed that homologs of AMA1 and RON2 can be upregulated to perform invasion (Lamarque et al., 2014).

After junction formation, as the parasite pushes further into the host cell the AMA1-RON2 junction at the tachyzoite apical tip is translocated to the posterior end; from the invaginated host membrane derives the parasitophorous vacuole, which is established thanks to the action of Rhoptry bulb proteins (ROP) and Dense Granules proteins, and finally pinched off by a fission pore (Suss-Toby et al., 1996, Dubremetz, 2007).

Thus, at the end of invasion the tachyzoite resides within the PV; this structure is important to isolate the parasite from the host lysosomal system, while also acting as a molecular sieve to permit diffusion of nutrients that *T. gondii* scavenges from the host (Jones and Hirsch, 1972, Clough and Frickel, 2017). Once formed, the PV is rapidly encaged by the host cytoskeleton (Coppens et al., 2006), and the PVM recruits host cell mitochondria and endoplasmic reticulum (Sinai et al., 1997, Sinai and Joiner, 2001).

1.2.2.2 Replication and egress

Once the PV is established, the invading tachyzoite undergoes replication through a process termed endodyogeny, in which two daughter cells are formed inside the mother until they are ready to bud; this process will be illustrated in detail in paragraph 1.6.

Duplication time through endodyogeny is usually of around six hours; the replication process is repeated several times, until egress is triggered.

Scanning electron microscopy revealed that egress is not a simple rupture of the host cell, but an active process, which can be triggered by calcium ionophores (Caldas et al., 2010) and, just as invasion, depends on gliding motility and microneme secretion. The increase in intracellular calcium levels is likely a response to environmental signals triggered by host cell damage or permeabilisation; the calcium-dependent kinase CDPK3 was shown to be essential for microneme secretion and subsequent egress (McCoy et al., 2012, Lourido et al., 2012), even if the mechanisms underlying these process are not yet completely understood. It is known that the micronemal perforin-like protein (PLP1) has an essential role in disrupting the parasitophorous vacuole membrane (PVM) (Kafsack et al., 2009); moreover, it was recently shown that the Lecithin-cholesterol acyltransferase (LCAT) is secreted from dense granules to contribute to PVM permeabilisation and to the disruption of the host plasma membrane (Schultz and Carruthers, 2018). This disruption of host cell-derived membranes, coupled with the activation of the gliding machinery (Egarter et al., 2014), leads to successful release of the parasites in the extracellular environment, where they are ready to start a new round of the lytic cycle.

1.2.2.3 The end of the lytic cycle: differentiation of the bradyzoite cyst

During their lytic cycle, tachyzoites can spread throughout the body; in particular, infection of monocytes and dendritic cells helps dissemination in the brain (Lambert et al., 2006, Courret et al., 2006), even if a recent report showed that tachyzoites are able to directly cross the blood-brain barrier (Konradt et al., 2016).

This acute phase of infection, which can lead to the clinical manifestation of toxoplasmosis, is restricted by a strong cell-mediated response, which usually acts in a timely fashion to prevent the appearance of symptoms (Yap and Sher, 1999). Even if this immune response is usually highly efficient at killing tachyzoites, some escape destruction and transform into bradyzoites (from the Greek brady = slow), protected by a tissue cyst which is a modified parasitophorous vacuole. EM analysis of bradyzoites shows that they are quite

similar in structure to tachyzoites, and that their cytoplasm contains numerous granules of amylopectin, required for energy storage and for the correct formation of the cyst wall (Frenkel, 1973, Dubey et al., 1998). Bradyzoites inside the tissue cyst are not dormant, but have replication potential (Watts et al., 2015); moreover, tissue cysts are not static, but probably rupture periodically to give rise to a new lytic cycle. Tissue cysts are impervious to drugs, can avoid immune-mediated destruction, and are responsible for transmission to new intermediate hosts, or to a definitive host; unfortunately, many technical challenges render difficult the study of bradyzoites and the discovery of treatments for latent infection (Alday and Doggett, 2017).

1.3 Pathogenesis and clinical features

While *T. gondii* was first isolated in rodent species in 1908 (Nicolle and Manceaux, 1908), its medical importance was discovered only in 1939, when it was isolated in tissues of a congenitally-infected infant (Wolf et al., 1939). Furthermore, its veterinary importance became known when it was found to cause mass abortion in sheep (Hartley and Marshall, 1957); years later, the use of a specific antibody test, the Sabin-Feldman dye test (Sabin and Feldman, 1948), paved the way to the recognition of *T. gondii* as one of the most successful parasites, distributed worldwide and able to infect a wide range of warm-blooded hosts.

It is assumed that in most cases *T. gondii* infections do not cause clinical disease in immunocompetent hosts; this notion has been challenged by outbreaks of toxoplasmosis epidemics, linked to oocyst contamination of water (Bowie et al., 1997, Baldursson and Karanis, 2011). In general, both competent and immunocompromised individuals can develop the disease, especially ocular toxoplasmosis (Flegr et al., 2014). However, the most dangerous outcomes of toxoplasmosis are found in two high-risk groups: pregnant women who become infected with *T. gondii* for the first time during the pregnancy, and immunosuppressed individuals.

Primary infection in pregnant women can be very dangerous for the unborn child, especially in the first trimester, if focal lesions develop in the placenta and tachyzoites reach the foetus. Usually, infection is cleared in the visceral

tissues of the foetus but not in the central nervous system, leading in the most severe cases to spontaneous abortion or stillbirth, or to new-borns developing congenital toxoplasmosis, with ocular and neurological pathologies (Dunn et al., 1999).

In immunosuppressed patients, the infection can lead to life-threatening cerebral toxoplasmosis: caused by re-activation of cysts in the brain, it can result in lethal cerebral lesions. Thanks to the advent of the highly active antiretroviral therapy (HAART), the number of AIDS patients suffering from toxoplasmic encephalitis has been drastically reduced compared to the levels reached in the nineties, when it was estimated that approximately 10% of AIDS patients in the USA, and up to 30% in Europe, had died from toxoplasmosis (Luft and Remington, 1992).

T. gondii strains show different virulence and pathogenicity in different hosts, probably as a result of co-evolution with their respective hosts. In Europe, Africa and North America, three dominant groups have traditionally be identified (Howe and Sibley, 1995), characterised by different levels of virulence, as they manipulate the host cell response in distinct ways. Notably, types II and III are less virulent, and show a lower growth rate, than Type I parasites (Yang et al., 2013). In addition, many atypical groups have been identified, especially in South America.

1.4 Characterisation of essential genes in *T. gondii*

Among Apicomplexa parasites, *T. gondii* is the most amenable to genetic manipulation, thanks to its ease of culturing, its high replication rate, and efficiency of transfection. Its haploid genome is sequenced, and it is regularly updated on the community database ToxoDB (<http://toxodb.org/toxo/>); it is constituted of 14 chromosomes, for a total genome size of around 65 Mb (Sibley and Boothroyd, 1992, Khan et al., 2005, Lau et al., 2016).

T. gondii can be transfected with DNA either transiently or stably (Kim et al., 1993, Soldati and Boothroyd, 1993a). While *Plasmodium spp.* can maintain episomes for long periods (O'Donnell et al., 2001), non-integrated episomal DNA is much less stable in *T. gondii*.

Conversely, stable transfection techniques rely on the targeted or random insertion of DNA into the parasite genome. In *T. gondii*, random integration is easily achieved, due to the action of the parasite non-homologous end joining (NHEJ) repair mechanism, which directly ligates broken ends of DNA Double Strand Breaks (DSB).

Stable transfections based on homologous recombination between the parasite genome and homology sequences in a plasmid are more difficult to achieve; this limitation has been addressed through the generation of the $\Delta ku80$ line, which lacks Ku80, the main effector protein of NHEJ repair mechanism (Huynh and Carruthers, 2009b, Fox et al., 2009). Several markers have been developed to select for stable transformants, as the efficiency of transfection is usually rather low (Wang et al., 2016).

Since *T. gondii* genome is haploid, the characterization of essential genes requires the employment of conditional systems of knock-down and over-expression. In recent years, many such systems have been adapted to *T. gondii*; in the following section, the ones which have been used in this thesis will be illustrated.

1.4.1 DiCre system and Conditional U1 Gene Silencing

The DiCre system has been successfully used in *T. gondii* (Andenmatten et al., 2013), and in *Plasmodium* spp (Collins et al., 2013). It is based on the Cre-lox system originally described by Sauer and Henderson, who showed that the Site-Specific Recombinase (SSR) Cre can be used to specifically remove DNA-sequences flanked by loxP recognition sites (Sauer and Henderson, 1988). In the conditional DiCre system, Cre is expressed in the form of two separate polypeptides, each fused to a different rapamycin-binding protein (FKBP12 and FRB) (Jullien et al., 2003, Jullien et al., 2007). When rapamycin is added to the media, it brings together the two parts of the protein, and the resulting dimerization restores recombinase activity. In *T. gondii*, this system is highly efficient; expression of the DiCre cassette in $\Delta Ku80$ parasites was shown to result in 90% excision of a LoxP-flanked *lacZ* (Andenmatten et al., 2013).

The DiCre system was subsequently modified by Pieperhoff et al., merging it with the U1 gene silencing system (Pieperhoff et al., 2015). The latter is based on the regulatory function of U1 snRNP, a splicing factor that can also block polyadenylation of a pre-mRNA when it binds it near its stop codon. This mechanism is used by mammalian cells and viruses to regulate gene expression of some transcripts, since block of polyadenylation causes destabilisation and degradation of pre-mRNA (Gunderson et al., 1998, Kaida, 2016); previous literature shows that it is possible to harness this system *in vitro*, to specifically downregulate transcripts through U1-binding at their 3' end (Beckley et al., 2001, Fortes et al., 2003, Abad et al., 2008).

In *T. gondii*, the U1-mediated silencing was merged with the DiCre system to make it inducible: U1-recognition sequences are integrated (in the $\Delta ku80::DiCre$ strain) at the 3'UTR of the gene of interest, but are separated from its stop codon by a loxP-flanked sequence. Upon Rapamycin addition, the DiCre recombinase is reconstituted and excises the loxP-flanked region, so that the U1-binding sequences are now close to the stop codon of the gene of interest, resulting in degradation of its mRNA. As discussed in Chapter 3, this strategy was successfully adopted to obtain a conditional Knock-down of DrpC; upon Rapamycin addition, a recombination rate of $\approx 98\%$ was observed, and U1 sequences efficiently promoted DrpC downregulation (Pieperhoff et al., 2015). While this technique was successfully implemented for DrpC Knock-down, it has some drawbacks: integration of loxP sequences in the 3'-UTR region can result in reduced transcription levels even before Rapamycin induction, as will be discussed. Moreover, the kinetics of down-regulation can be slow, depending on the stability of the protein (Jimenez-Ruiz et al., 2014).

1.4.2 The tetracycline-inducible system

One of the most used systems for transcriptional regulation in *T. gondii* is the tetracycline-inducible transactivator system. Based on the tetracycline resistance operon of *E. coli*, this system was harnessed for regulation of mammalian gene expression by Gossen and Bujard. In this strategy, the Tet protein TetR, a transcriptional repressor which binds the Tet-operator DNA repeats (TetO) in a tetracyclin-dependent manner, is fused to the VP16 activation domain (derived from Herpes simplex virus), generating an efficient

tetracycline-dependent trans-activator (tTA). Thus, if the TetO sequences are located upstream of a minimal promoter, tTA binding leads to the recruitment of the transcription initiation machinery; when tetracycline is added, it binds to TetR, leading to a conformational change that abolishes DNA-binding (Gossen and Bujard, 1992).

In *T. gondii*, the original trans-activator derived from Herpes Simplex Virus does not interact with the transcription machinery; to overcome this problem, a genetic screen was performed, where TetR was randomly inserted into the genome to identify functional activation domains. This led to the isolation of the trans-activator TATi-1 (trans-activator trap identified), which is regulated by the tetracycline analog ATc in a tight, inducible manner (Meissner et al., 2002). Moreover, the generation of a parasite parental strain which expresses this transactivator (*RHΔKu80 TATi-1*) has allowed efficient control of transcription simply through the replacement of the GOI endogenous promoter with a Tet-inducible promoter (Sheiner et al., 2011).

The tetracycline-inducible system has some disadvantages that need to be considered during phenotypic analysis of a gene knock-down: the expression under the non-endogenous promoter can be problematic for some GOIs (for example, the ones that are not highly expressed in wild-type parasites), and ATc-mediated downregulation can allow some residual activity (Jimenez-Ruiz et al., 2014). Nevertheless, this system is a very useful tool which has allowed the generation of many knock-down strains in *T. gondii*.

1.4.3 The ddFKBP system

A faster way of regulation is represented by the ddFKBP system, which allows rapid modulation of protein stability. Devised by Banaszynski et al., it is based on the Rapamycin-binding protein FKBP, which was modified so that it is unstable unless it is bound to a permeable Rapamycin analogue, named Shield-1. Thus, the fusion of a protein of interest to this FKBP destabilisation domain (ddFKBP) leads to its degradation, unless Shield-1 is added to stabilize the fusion protein (Banaszynski et al., 2006).

This system has been successfully adapted in Apicomplexa (Armstrong and Goldberg, 2007, Herm-Gotz et al., 2007), but it is important to note that Shield-mediated stabilisation in *T.gondii* is in some instances not tightly regulated. In *T. gondii*, the ddFKBP strategy has been mostly used for analysing over-expression phenotypes and for the regulated expression of dominant negative mutants (Kremer et al., 2013, Agop-Nersesian et al., 2009); in particular, it has been useful in the study of Dynamin-related proteins of *T. gondii*, as the analysis of dominant-negative versions of DrpA and DrpB has been instrumental in the characterisation of their function (van Dooren et al., 2009, Breinich et al., 2009).

1.4.4 CRISPR/Cas9 in *T.gondii*

To date, CRISPR/Cas9 is the system that holds more promise for easy genome manipulation in Apicomplexa parasites. This mechanism was discovered in archaea and bacteria (Mojica et al., 2005, Gasiunas et al., 2012, Jinek et al., 2012), which use it as a prokaryotic immune system, as reviewed in (Lander, 2016). Following studies that implemented this technique for genome engineering in mammals (Cong et al., 2013, Mali et al., 2013), this system has been successfully adapted in *T. gondii* (Shen et al., 2014a, Sidik et al., 2014): the nuclease Cas9 is expressed together with a single guide RNA (sgRNA), composed of the 20-nucleotide CRISPR RNA (crRNA) - which contains the homology region that will guide the nuclease to its DNA target - fused to a transactivating RNA (tracrRNA) scaffold, essential for correct processing of the crRNA and for Cas9 activity. When Cas9 binds the gRNA, it is guided to homology sequences in the genome, and there it will mediate a Double-Strand Break (DSB). Importantly, the Cas9 complex will target only genomic sequences which are complementary to the 20-bp gRNA and are followed by a PAM (protospacer-adjacent motif), which is composed by the nucleotides NGG; this allows the complex to distinguish between the target DNA and the crRNA-coding sequences.

In *T. gondii*, CRISPR/Cas9 has been implemented for two different strategies. It has been used as a tool for creating mutants, harnessing the high rates of non-homologous end-joining (NHEJ) repair to obtain gene disruption: in fact, the parasite uses this low-fidelity mechanism to repair the Cas9-mediated DSB, creating frame-shift mutations and insertions at the cleavage site (Sidik et al.,

2014). Notably, this method has been successfully used for a CRISPR/Cas9-based genome-wide genetic screen in *T. gondii*, which is a valuable resource for the community (Sidik et al., 2016).

Secondly, CRISPR/Cas9 can be used to achieve gene editing: when providing a repair template, the DSB can be repaired through homologous recombination, allowing the precise insertion of epitope tags, point mutations or long sequences (Di Cristina and Carruthers, 2018).

1.4.5 The auxin-inducible degron (AID) system

To allow rapid regulation at the protein level, the auxin-inducible degron (AID) system has recently been adapted for genomic manipulation in *T. gondii* (Brown et al., 2017). The system is based on the auxin-dependent degradation pathway that plants have evolved to control gene expression in many developmental and growth processes (Teale et al., 2006), in a mechanism that is now well understood.

Transcription of the phytohormone Auxin is repressed by the AUX/IAA transcription repressors. When a signal arrives for this repression to be lifted, Auxin itself is recruited to bind to the AUX/IAA repressors; this binding promotes the interaction of the E3 ubiquitin ligase SCF-TIR1 with the AUX/IAA proteins, which as a result are polyubiquitylated and finally rapidly degraded by the proteasome. Importantly, a “degron” domain in the AUX/IAA transcription repressors is crucial for their interaction with auxin and with SCF-TIR1 (Lavy and Estelle, 2016).

This mechanism was successfully adapted in yeast, and subsequently in Apicomplexa such as *Plasmodium* *ssp.* and *T. gondii* (Nishimura et al., 2009, Kreidenweiss et al., 2013, Philip and Waters, 2015, Brown et al., 2017). As orthologs of TIR1 and AUX/IAAs are only found in plant species, the adaptation of this system to other organism always requires the expression of TIR1 and the fusion of the target protein with the “degron” domain.

In *T. gondii*, a line was generated that stably expresses a codon-optimised Tir1 in the $\Delta ku80$ background; moreover, a small Degron domain was optimised and

fused to a target gene. When auxin was added, protein depletion was observed, as soon as four hours after induction (Brown et al., 2017).

1.5 Ultrastructure of *T. gondii* tachyzoites

The crescent-shaped tachyzoite is the most studied form of *T. gondii*; measuring approximately $2 \times 7 \mu\text{m}$, with a pointed anterior and a more rounded posterior end (Fig. 1-3), it exhibits most characteristics of a standard eukaryotic cell, such as the presence of a mitochondrion, an ER/Golgi system, and a nucleus surrounded by a nuclear envelope and in contact with the ER. Notably, some of these structures show atypical characteristics and functions: for example, the mitochondrion is present as a single organelle with a distinctive lasso shape, and the trafficking system has been modified on a molecular level to support the formation of secretory organelles.

In addition, *T. gondii* is characterised by novel structures and organelles, such as the apical complex, the inner membrane complex and the apicoplast, whose key characteristics are summarised here, before illustrating the two structures that are of most interest for this thesis: the mitochondrion and the cytoskeleton.

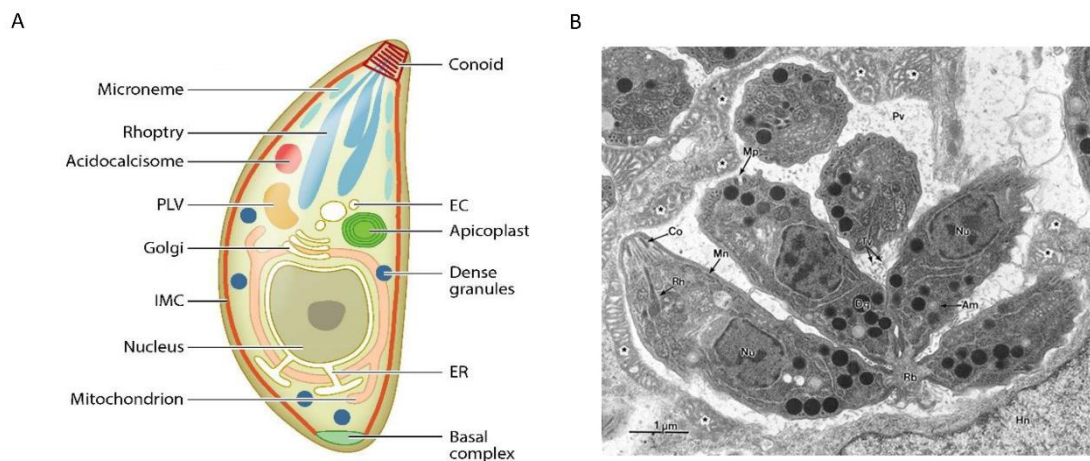


Figure 1-3: Ultrastructure of *T. gondii* tachyzoite.

(A) Schematic representation of the ultrastructure of *T. gondii* tachyzoite. The parasite is protected by a pellicle, formed by the plasma membrane (in brown) and the inner membrane complex (IMC) shown in red. Specialised secretory organelles, micronemes (turquoise) and rhoptries (blue) are located at the apical end of the parasites under the conoid (dark red); dense granules (dark blue) are distributed throughout the cytoplasm. At the centre of the parasite body is the nucleus, connected with the ER (yellow). The endosymbiotic organelles, apicoplast (green) and mitochondrion (pink) are in association during interphase. Other organelles shown are the Golgi (yellow), the endosome compartment (EC), the plant-like vacuole (PLV). At the base of the parasite, the basal complex is shown in green. Adapted from (Blader et al., 2015). Copyright Annu.

Rev. Microbiol. 2015. (B) Morphology of a typical rosette. Transmission electron micrograph showing four tachyzoites in the final stages of endodyogeny, still attached by their posterior ends to a common residual body (Rb); at the apical end, the apical complex is clearly visible (Co: conoid; Mn; microneme; Rh: rhoptry). The parasitophorous vacuole (Pv) surrounds the parasites. Reprinted from (Dubey et al., 1998). Copyright © 1998, American Society for Microbiology.

1.5.1 The apical complex and secretory organelles

The apical complex, which gives the phylum its name, exhibits variable morphologies in different Apicomplexa. In *T. gondii*, it is built around the conoid, a system of atypical tubulin fibers arranged in a spiral; inside it run two microtubules, housed between the preconoidal ring (from which the conoid fibers originate) and the polar ring, which acts as a microtubule organising centre.

It was observed that the conoid is extruded in the first stages of invasion in a calcium-dependent manner (Mondragon and Frixione, 1996), suggesting that this protrusion has a mechanical function during attachment or invasion (Hu et al., 2002, Del Carmen et al., 2009). In addition, the conoid has an essential role in providing a regulated gateway for the release of secretory organelles during attachment, invasion and formation of the parasitophorous vacuole (Katris et al., 2014).

Three types of secretory organelles are present in *T. gondii*: micronemes, rhoptries and dense granules.

Micronemes play a key role in invasion and egress (Carruthers et al., 1999), as already described in paragraph 1.2.2.1. To date, over 50 micronemal proteins have been described; together with the rhoptries, micronemes are synthesised *de novo* during endodyogeny, in a process which requires trafficking through the endosomal pathway and maturation of the precursor proteins through proteolytic processing (Ngo et al., 2003, Harper et al., 2006).

The Dynamin-related protein DrpB is essential for biogenesis of the apical secretory organelles, as it mediates the budding of vesicles containing micronemal and rhoptry proteins from the Golgi (Breinich et al., 2009); these vesicles are then trafficked from the Golgi to endosomal-related compartments

thanks to the cargo receptor TgSORTLR (Sloves et al., 2012). Moreover, Rab proteins Rab5A and Rab5C are essential for correct trafficking of all rhoptry proteins and of some micronemal proteins (Kremer et al., 2013). Interestingly, a recycling pathway mediated by Vps35-Vps26-Vps29 core complex was recently discovered in *T. gondii* tachyzoites, indicating that microneme and rhoptry biogenesis does not depend solely on *de novo* production (Sangare et al., 2016).

Rhoptries are club-shaped organelles, usually in a number of 8-10 per cell (Dubremetz, 2007), formed by two compartments: the upper “neck” contains RON (rhoptry-neck) proteins, while the ROP proteins are housed in the bulbous compartment below it.

While RON proteins have an important function during invasion (see paragraph 1.2.2.1), ROP proteins are involved in different processes. Some ROPs, like ROP4 and the ROP2 family, are required for the establishment and maintenance of the parasitophorous vacuole (Carey et al., 2004, El Hajj et al., 2007); in addition, some ROP kinases act as virulence factors, as they are secreted to control gene expression of key immune response regulators of the host (Boothroyd and Dubremetz, 2008, Taylor et al., 2006, Yamamoto et al., 2011). The best studied examples are ROP18 and ROP5, which are at the surface of the PV, where they phosphorylate host immune-related GTPase (IRGs) and prevent them from accumulating on the membrane and destroying the parasite vacuole (Fentress et al., 2010, Steinfeldt et al., 2010, Behnke et al., 2015).

As previously mentioned, rhoptry proteins are trafficked thorough the same pathways as micronemal proteins; at the end of this process, rhoptry organelles are attached to the apical end of the parasite through the action of an armadillo-repeat protein (ARO), in a process that has been proposed to be dependent on actin and Myosin F (Mueller et al., 2013, Mueller et al., 2016).

Dense granules are the third type of secretory organelle of *T. gondii*; these electron-dense compartments are observable throughout the cytoplasm, and measure around 200 nm in diameter. It was recently shown that dense granules movement is dependent on Myosin F-mediated transport along long filaments of actin (Heaslip et al., 2016, Periz et al., 2017). Dense granules proteins (GRA) are important for formation and maintenance of the PV (Mercier et al., 2005);

moreover, some GRA proteins, as for example GRA2, are essential for the formation of the membranous nanotubular network, which is formed post-invasion and expanded as the number of parasites inside the PV increases (Mercier et al., 2002). Finally, similarly to rhoptry kinases, some GRA proteins are also responsible for the modulation of the host cell response, acting as virulence factors (Bougdour et al., 2014, Braun et al., 2013, Curt-Varesano et al., 2016).

1.5.2 The apicoplast

The apicoplast is a chloroplast-like organelle found in all Apicomplexa (except in *Cryptosporidium* spp., where it was secondarily lost) (Zhu et al., 2000).

It is derived from an event of secondary endosymbiosis, as an ancestor protist took up a red alga, retained it and transformed it into a fully dependent endosymbiont organelle (Arisue and Hashimoto, 2015) ; its photosynthetic function was lost during evolution, as Apicomplexa moved towards a parasitic lifestyle (van Dooren and Striepen, 2013). Nevertheless, the organelle is essential for parasite survival at all stages, and it supports three essential metabolic pathways: the heme synthesis pathway (which is also partly mediated by the mitochondrion), the type II fatty acid biosynthesis and the isoprenoid precursors production (Sheiner et al., 2013, Mazumdar et al., 2006, van Dooren et al., 2012, Nair et al., 2011). As such, the apicoplast is the target of a number of anti-parasitic drugs (Fichera and Roos, 1997, Jomaa et al., 1999, Dahl and Rosenthal, 2008). Apicoplast loss still allows parasites to reinvade, but they succumb to delayed death when they begin to replicate; *P. falciparum* merozoites have been shown to survive without an apicoplast if the culture is supplemented with isopentenyl phosphate (IPP), but this effect is not observed in *T. gondii* (Yeh and DeRisi, 2011).

Similar to the mitochondrial genome, the genome of the apicoplast is greatly reduced, as most proteins are encoded in the nucleus. As a result, a complex trafficking system is required to ensure that apicoplast proteins are targeted to the right compartment in the four-membrane organelle; the apicoplast thioredoxin Atrx1 has recently been characterised as involved in the control of protein trafficking to this organelle (Biddau et al., 2018).

During endodyogeny, the apicoplast needs to be elongated and divided to allow correct segregation in daughter cells; it was shown that the Dynamin-related protein DrpA is required for the division step, while segregation is actin and Myosin F dependent (van Dooren et al., 2009, Jacot et al., 2013, Egarter et al., 2014).

1.5.3 The IMC

T. gondii pellicle is a unique triple bilayer structure, formed by the plasma membrane and the inner membrane complex (IMC), a system of flattened membranous sacs sutured together. These sacs are called alveoli; characteristic of all Alveolates, in *T. gondii* the alveoli are derived from vesicles trafficked through the Golgi in a process mediated by the small GTPases Rab11A and B (Sheffield and Melton, 1968, Agop-Nersesian et al., 2010, Agop-Nersesian et al., 2009).

The IMC extends through the whole length of the parasite's body, except at the apical and posterior ends, where the apical and basal bodies are located, respectively. Several IMC sub-compartments can be identified, which are formed by different classes of proteins, such as the IMC sub-compartment proteins (ISPs) and the gliding associated proteins (GAPs). While GAP45 and GAP50 can be detected along the whole length of the parasite with exception of the apical cap, proteins like ISP1 and GAP70 can only be visualised apically; GAP80 is only at the posterior region and ISP1 and ISP3 are in the middle and posterior regions (Beck et al., 2010, Fréna1 et al., 2010, Fréna1 et al., 2014). Recently, a novel class of proteins in the IMC has been discovered: named the IMC sutures components (ISCs), they localize to the transverse and longitudinal sutures that demark the junctions between the alveolar sacs (Chen et al., 2015, Chen et al., 2017).

As already discussed, according to the linear motor model the IMC mediates the anchorage and stabilisation of the acto-myosin motor. Myosin A interacts through the myosin light chain MLC1 with GAP45, a gliding associated protein which is anchored at its N-terminus to the plasma membrane; at its C-terminus, GAP45 interacts with the IMC components GAP40 and GAP50, thus anchoring the motor to the IMC (Gaskins et al., 2004, Fréna1 et al., 2010, Gilk et al., 2009).

Importantly, GAP40 and GAP50 have been shown to be also involved in IMC biogenesis; their ablation results in significant IMC morphology defects and ultimately in the collapse of the parasite ultrastructure. This suggests that the IMC has an essential role in parasite structural stability, especially during daughter cell formation (Harding et al., 2016).

On its cytoplasmic face, the IMC is supported by a meshwork (called sometimes “alveolin network”) of intermediate filament-like (IF-like) proteins, known as IMC proteins; so far, 14 IMC proteins have been characterised, which have specific and distinct roles and localisations. These proteins are sequentially assembled into the cytoskeleton of budding daughters during replication, and thus they can be used as markers of distinct budding steps. For example, IMC15 is the first to be recruited during replication; IMC7 is excluded from the budding daughters, and is only present in the mother; IMC1 and IMC3 are both present in mother and daughter cytoskeletons, and they are commonly used to visualise parasites that are in the first stages of endodyogeny (Mann and Beckers, 2001, Anderson-White et al., 2012, Dubey et al., 2017).

Below this network run the subpellicular microtubules, which will be described in the next paragraph; it has been proposed that a family of glideosome-associated proteins with multiple-membrane spans (GAPMs) connects the inner membrane complex to the alveolin network and possibly to the microtubules (Bullen et al., 2009, Frenal et al., 2017), but more research is needed to prove this hypothesis (Harding et al., 2016).

1.5.4 The microtubule network

Tubulin makes up five essential structures in *T. gondii* tachyzoites: the conoid and the intraconoid microtubules in the apical complex; the replicative structures of spindle microtubules and centrioles; and the subpellicular microtubules, part of the cortical cytoskeleton, whose structural role will be illustrated in detail here.

Three α and three β tubulin isotypes are present in the *Toxoplasma* genome (Nagel and Boothroyd, 1988, Xiao et al., 2010, Morrissette, 2015); while β isotypes are expressed similarly in different stages and show almost 98% of

sequence identity, α isotypes are characterised by different expression profiles, suggesting that they are required for the formation of different structures. Additionally, *T. gondii* genome contains also genes for γ , δ and ϵ tubulin, but only γ tubulin is expressed in tachyzoites (Morrisette, 2015).

The subpellicular microtubules are typically composed of α 1- β 1 heterodimers assembled head-to-tail to form protofilaments; the lateral association of 13 protofilaments results in a microtubule. The twenty-two subpellicular microtubules originate from the Apical Ring located below the conoid, which functions as a microtubule organising centre; thus, in *T. gondii* the plus-end of microtubules is the one growing away from the apical region of the parasite (Russell and Burns, 1984). Running below the pellicle, the microtubules form a left-handed spiral extending from the apical end to approximately two-thirds of the parasite body (Nichols and Chiappino, 1987, Morrisette et al., 1997). These microtubules are extremely stable compared to those of vertebrate cells, probably thanks to parasite-specific microtubule-binding proteins which heavily decorate them, such as SPM1, TrxL1 and TLAP2 (Tran et al., 2012, Liu et al., 2013, Liu et al., 2016).

These data suggest that the main role for subpellicular microtubules is structural; their close association with the IMC is essential, especially during parasite division, when the coordinated growth of cortical microtubules and the IMC regulates daughter cells packaging inside the mother. Inhibition of microtubule growth by the depolymerizing drug oryzalin induces abnormal IMC assembly and non-viable daughter cells (Morejohn et al., 1987, Stokkermans et al., 1996, Shaw et al., 2000, Morrisette and Sibley, 2002, Hu, 2008).

In eukaryotes, microtubule tracks are also usually required for vesicular transport along the cell and for the movement of organelles; both processes are powered by the microtubule motors kinesin and dynein, ATPases that use the energy derived from ATP hydrolysis to move along microtubule tracks (Vale, 2003).

In general, most kinesins direct the movement towards the plus end of the microtubules (that is, the growing end). Their small, well-conserved motor domains power movement through ATP hydrolysis and mediate the interaction

with microtubules; the tail domains are more variable, and are required for cargo binding and for interaction with regulatory proteins (Hirokawa and Tanaka, 2015). In *T. gondii* genome, 19 kinesins are present (Morrissette, 2015). Of these, only two have been characterised: Kinesin A localises to the apical ring and is thought to be required for its stability, while Kinesin B was localised to the cortical microtubules, but its function remains unknown (Leung et al., 2017).

Movement towards the minus end of microtubules is mainly powered by dynein complexes, which in mammals are divided between “cytoplasmic dyneins” and “flagellar dyneins”. In these proteins dimers, the force to move along microtubules is generated by their large heavy chain subunits, each containing six ATPase modules forming a ring (Hirokawa and Tanaka, 2015, Roberts et al., 2013). In most cases, efficient dynein movement along microtubules requires the interaction with the cofactor dynactin; this complex of proteins binds to the intermediate chains of dynein to facilitate motor processivity and the anchoring to microtubules (Schroer, 2004). Ten dynein heavy chains are found in *T. gondii* genome, together with several types of intermediate and light chains; while some of these are probably “flagellar dyneins”, important for flagellar movement in the sexual stages of the parasite, others are hypothesised to be “cytoplasmic dyneins”. Moreover, some components of dynactin, namely Arp1, p25, p27, p62 and p50, are conserved (Morrissette, 2015).

So far, only the dynein light chain 8-a (DLC8-a) has been characterised in *T. gondii*; when overexpressed, it localises to the conoid, spindle poles, centrosomes and basal end of the parasite. A later study showed only an apical localisation for DLC8-a, and also determined a cytosolic distribution for other three members of the dynein LC8 subfamily (TgDLC8-b, TgDLC8-c, and TgDLC8-d) (Hu et al., 2006, Qureshi et al., 2013).

As kinesin and dynein motor proteins remain amply uncharacterised in *T. gondii*, it is not possible to determine if they are required for organelle transport or vesicular traffic. Moreover, as previously discussed, dense granules have been shown to be dependent on a Myosin F motor to be moved along actin filaments, and rhoptry positioning at the apical end of the parasite is also mediated by a acto-myosin F mechanism (Mueller et al., 2013, Heaslip et al., 2016). In mammalian cells, organelles like mitochondria have been shown to be

transported along microtubules by kinesin and dynein, as will be discussed in paragraph 1.7.1; to date, no data are available about mitochondria transport in *T. gondii*.

1.5.5 The mitochondrion

Mitochondria are the result of an endosymbiotic event which occurred 1.5 billion years ago, when a bacterium was internalised into a larger host cell and adapted to intracellular life (Wang and Wu, 2015). In all eukaryotes, mitochondria are delimited by the outer and the inner mitochondrial membrane (OMM and IMM, respectively) (Pernas and Scorrano, 2016). Inside, two aqueous mitochondrial sub-compartments, the intermembrane space (IMS) and the matrix, are present; moreover, a third, crucial sub-compartment is formed by deep invaginations of the IMM protruding in the mitochondrial matrix. These structures, known as cristae membranes, house the respiratory chain complexes and the ATP synthase, and are of crucial importance for energy production (Mannella, 2006).

Traditionally, mitochondria have been described as the powerhouse of the eukaryotic cell, as they are the site of cellular respiration and many other fundamental metabolic and bioenergetics processes, such as β -oxidation of fatty acids and Krebs cycle, heme biosynthesis, iron/sulfur cluster assembly, and the metabolism of certain amino acids. In recent years, however, research has focused on different unique mitochondrial functions, such as their role in apoptosis and ageing, the mechanisms of mtDNA maintenance, and the complex regulation of mitochondrial dynamics (Jiang and Wang, 2004, Fang et al., 2016, Pernas and Scorrano, 2016). Here, an overview on mitochondrial functions and morphology in *T. gondii* will be given, before discussing in detail mitochondrial dynamics during endodyogeny.

In *T. gondii*, the mitochondrion has the same basic characteristics found in all eukaryotes: it is delimited by two membranes and has a high density matrix, with cristae showing a peculiar omega shape (Melo et al., 2000) (Fig. 1-4). The TCA cycle was shown to be fully active in *T. gondii* (MacRae et al., 2012), as well as the mitochondrial electron transport chain (ETC) for oxidative phosphorylation (Vercesi et al., 1998). Moreover, the parasite mitochondrion is important for the production of precursors of other pathways, like pyrimidine

and heme biosynthesis; as the latter process is shared between apicoplast and mitochondrion, during interphase these two organelles are seen in close physical association (Seeber et al., 2008, Vaidya and Mather, 2009, Sheiner et al., 2013). Thus, the mitochondrion is essential for *T. gondii* survival at all stages, and it is a validated drug target for both *Plasmodium* spp. and *T. gondii* (Mather and Vaidya, 2008, Goodman et al., 2017); currently, it is targeted by compounds such as atovaquone and myxothiazol, which inhibit the ETC by acting as ubiquinone analogues (Srivastava et al., 1997).

Only a handful of the proteins required for the above-mentioned pathways are encoded in the mitochondrial genome of the parasite. In fact, though sequencing of the mitochondrial genome in *T. gondii* has been hindered by the presence of mtDNA-like sequences in the nucleus (Ossorio et al., 1991, Garbuz and Arrizabalaga, 2017), it is known that all Apicomplexa have an extremely reduced mitochondrial genome, with the exception of *Cryptosporidium* spp., where the mtDNA was completely lost (Putignani et al., 2004). Based on studies on *P. falciparum* mitochondrion, *T. gondii* mitochondrial genome is thought to encode only three proteins (cytochrome b, cytochrome c oxidase I Cox1, and cytochrome c oxidase III Cox3) and a few highly fragmented rRNA genes, while all other mitochondrial proteins need to be imported from the cytoplasm (Feagin et al., 1991, Vaidya et al., 1989). As mitochondrial genome reduction is a shared feature of all eukaryotes (though in Apicomplexa it has occurred in a remarkably bigger scale), the import of mitochondrial proteins from the cytosol is a conserved mechanism, which is dependent on the translocons of the outer and inner mitochondrial membranes (TOM and TIM, respectively) (Dudek et al., 2013, Manganas et al., 2017). In *T. gondii*, it was shown that a TOM complex is conserved, containing Tom40 (which forms the central pore of the complex), Tom22 and Tom7, but not receptor proteins Tom70 and Tom20 (van Dooren et al., 2016). Bioinformatics analysis has also shown that some components of the TIM translocon are conserved in *T. gondii*, but the complex remains uncharacterised (van Dooren et al., 2016).

One of the most divergent aspects of *T. gondii* mitochondrion is probably its morphology; in fact, like most Apicomplexa but very differently from most other eukaryotes, this parasite has a single, ramified mitochondrion, which usually has

a lasso shape in intracellular tachyzoites, extending all around the periphery of the parasite (Melo et al., 2000). This morphology seems to change in extracellular parasites, where most mitochondria partially detach from the parasite periphery, and in some cases completely collapse. Parasites with a collapsed mitochondrion are viable, and during invasion they re-expand the organelle and establish the typical intracellular morphology (Ovciarikova et al., 2017).

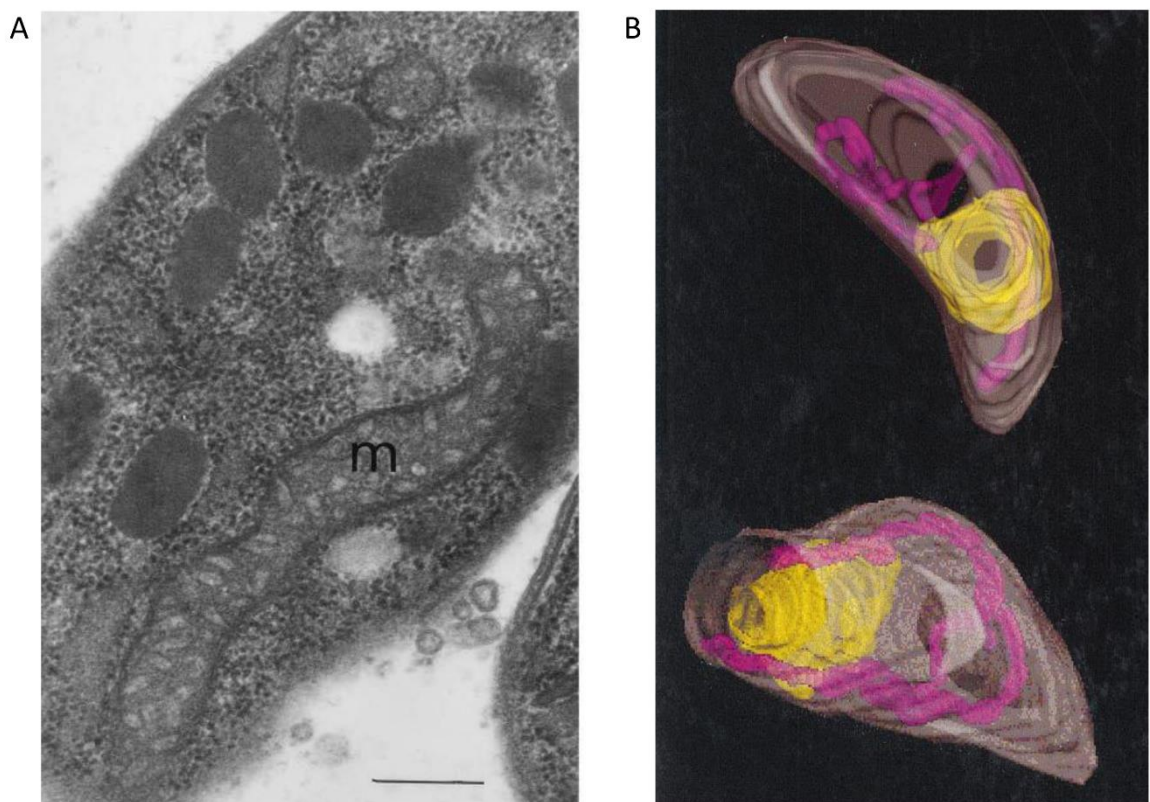


Figure 1-4: Structure of the single mitochondrion of *T. gondii*.

(A) Transmission electron micrographs of the single mitochondrion (m) in *T. gondii* tachyzoites. Scale bar: 0.5 μm . (B) Three-dimensional reconstruction of extracellular tachyzoites of *T. gondii*. The nucleus is in yellow, and the pellicle is in transparent white. The mitochondria is in purple, showing that its branches go around the periphery of the parasite. Modified from (Melo et al., 2000). Copyright © 2000 Academic Press.

1.6 Endodyogeny

The asexual replication of *T. gondii* tachyzoites, termed endodyogeny, is a division process where daughter cells are not formed by fission, but rather

assembled within the mother until they are ready to bud (Fig. 1-5) (Goldman et al., 1958, Sheffield and Melton, 1968, Nishi et al., 2008).

The G1 phase comprises half of the cell cycle; towards the end of this stage, the Golgi elongates and the centriole starts to divide, an event that marks the transition to the S phase (Pelletier et al., 2002, Hartmann et al., 2006, Suvorova et al., 2015). While the DNA is replicating, the apicoplast elongates (Striepen et al., 2000); in the late S phase, the first cytoskeleton elements of the daughter cells are assembled, marking the initiation of budding. Daughter buds are assembled in an apical to basal direction (which is established through the centrosome), starting from their conoid and apical ring, from where the subpellicular microtubules are nucleated (Hu et al., 2006).

After a very short (or absent) G2 phase (Francia and Striepen, 2014), the M phase starts, overlapping with cytokinesis. In this phase, the nucleus and the apicoplast are divided and then segregated in the growing daughter cells, together with newly-formed branches of the endoplasmic reticulum (ER). At this point, the other organelles need to be duplicated or elongated in order to be segregated; thus, in the last stages of endodyogeny the daughter cells acquire the mitochondrion and their own set of secretory organelles, as will be detailed later in this paragraph.

Budding of the daughter cells is completed through the constriction of their basal end. Although the mechanisms underlying this constriction are not well understood, it is proposed that the parasite's basal complex, which is formed by MORN-1, Centrin -2 and several basal IMC proteins, acts as a contractile ring in the last stages of division. MORN-1 signal is detected at the start of endodyogeny, when it is in close juxtaposition to the apical end of the nascent daughters; while the budding cells grow, the MORN-1 ring encircles the growing ends of the daughter's cytoskeleton, and is finally found at the basal part of the parasites when cytokinesis occurs (Hu et al., 2006, Hu, 2008, Gubbels et al., 2006). When MORN-1 is ablated, double-headed parasites are formed, where the daughters are conjoined at their basal ends, as no cytokinesis takes place in this mutant (Lorestani et al., 2010, Heaslip et al., 2010).

At the end of endodyogeny, the cytoskeleton of the mother is disassembled and the plasma membrane is incorporated by the daughter parasites in a Rab11A-dependent process (Agop-Nersesian et al., 2009). A residual body (RB) is formed, which is thought to help organise the rosette; this function is also effected by the membranous nanotubular network (MNN), a complex of membranes that connect the parasites together and to the PV membrane (Sibley et al., 1995, Mercier et al., 2002). The RB usually contains some secretory organelles, together with mitochondrial and nuclear fragments; the membrane connections between the RB and the tachyzoites in the PV can persist until they egress (Muñiz-Hernández et al., 2011). It was recently shown that an intravacuolar actin network runs through these interconnections, and is important for transport of material between parasites in the same rosette (Periz et al., 2017).

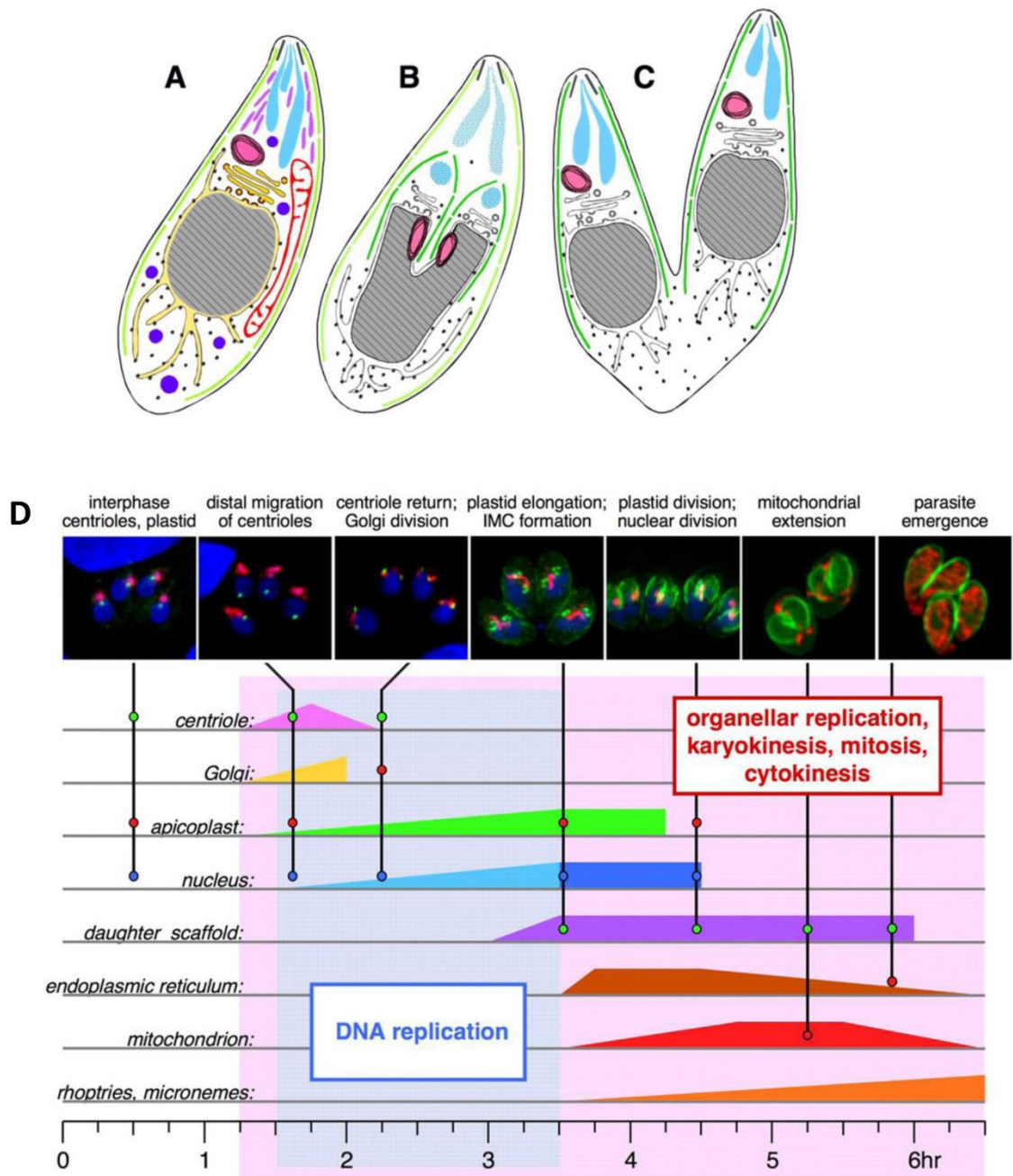


Figure 1-5: Endodyogeny of *T. gondii*.

(A) *T. gondii* tachyzoites during interphase. (B) During endodyogeny, the daughter cells develop in an apical to basal direction; Golgi and apicoplast replicate and divide in the early stages, and are incorporated in the growing buds; secretory organelles are degraded inside the mother, and newly synthesised in the daughter cells. (C) Towards the end of the process, when the buds are almost ready to emerge, cytokinesis occurs at the basal end, and the plasma membrane of the mother is acquired by the daughters. (D) Timeline of events taking place during endodyogeny. Mitochondria division occurs late in replication, together with organelle biosynthesis and ER replication. Reproduced from (Nishi et al., 2008). Copyright © 2008 Company of Biologists.

The use of time-lapse microscopy has greatly increased our knowledge on organellar dynamics during endodyogeny (Hu, 2008, Nishi et al., 2008); the

molecular mechanisms underlying these processes, however, are not yet fully understood.

As previously discussed, it is proposed that secretory organelles are synthesized *de novo* by budding and fusion of vesicles emerging from the ER and Golgi, in a process driven by the Dynamin-related protein B; evolutionary conserved regulators of endosomal trafficking, such as HOPS/CORVET complex subunits, Rab5a and the sortilin-like receptor TgSORTLR, have been shown to be involved in the process (Breinich et al., 2009, Morlon-Guyot et al., 2015, Kremer et al., 2013, Sloves et al., 2012). Moreover, it has been recently suggested that micronemes and rhoptries from the mother are degraded and their components recycled in the daughter cells (Jimenez-Ruiz et al., 2016, Sangare et al., 2016).

On the contrary, organelles of endosymbiotic origin cannot be formed *de novo*: during evolution, their successful acquisition always requires the establishment of a mechanism to divide and partition them between the progeny. In *T. gondii*, these processes follow the cell cycle, requiring a coordination between daughter formation and organelle division.

In the case of the apicoplast, it has been proposed that this coordination is achieved by anchoring the organelle to the newly duplicated centrosomes before daughter cell budding starts. In this way, when the daughter IMC begins to extend the apicoplast is extended as well, forming a U-shape that is constricted at the basal end of the growing parasites by the basal complex. At this point, a Dynamin-related protein called DrpA mediates fission (for more detail, see paragraph 1.8.2), so that each of the daughters has its own organelle (van Dooren et al., 2009, Lorestani et al., 2010).

The mechanism of mitochondrial fission in *T. gondii* has not been characterised, and is the focus of this thesis. Time-lapse microscopy (Nishi et al., 2008) has shown that the mitochondrion of the mother cell starts elongating at an early stage of daughter IMC formation, branching in multiple locations; these elongations remain in the plasma membrane of the mother until the last stages of cell division. Finally, the elongated organelle's branches are inserted inside the daughter buds, and seemingly pulled up, till the two interconnected, lasso-shaped organelles are surrounding the periphery of the daughter cells; the connection between them is

subsequently cleaved, so that independent organelles are now present in each daughter cell (Fig. 1-6).

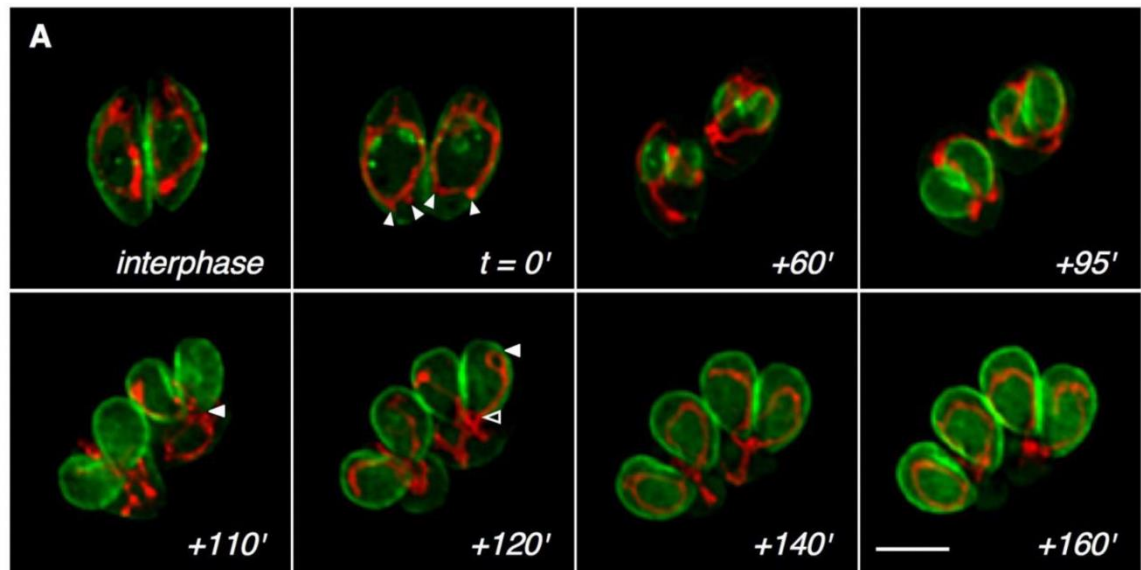


Figure 1-6: Dynamics of mitochondrial replication in *T. gondii*.

(A) Time-lapse microscopy of parasites during endodyogeny, showing IMC (labelled with IMC1-YFP, in green) and the mitochondrion (labelled with HSP60-RFP, in red). In interphase, the mitochondrion has the typical lasso shape; when daughter cells start to form ($t=0$), the mitochondrion forms branches (arrowheads), which later ($t=60'$) elongate and encircle the buds ($t=95'$) but do not enter them; when the daughters are emerging from the mother, the mitochondrial branches quickly enter them ($t=110'$) and are pulled towards the cell periphery ($t=120'$). The mitochondria remain connected for a variable time ($t=140$), and at the end of endodyogeny a mitochondrial portion is visible in the residual body ($t=160$). Scale bar: 5 μm . Reproduced from (Nishi et al., 2008). Copyright © 2008 Company of Biologists.

Thus, at least two mitochondrial dynamics seem at play during endodyogeny: fission, to cleave the connection and form two distinct mitochondria, and motility. In the following paragraph, I will illustrate how mitochondrial dynamics are at play in other eukaryotes, where the molecular effectors of these processes have been studied in detail.

1.7 Mitochondrial dynamics in higher eukaryotes

Mitochondrial dynamics have been extensively studied both in yeast - an excellent system for forward genetic screens - and in human cells, especially since altered mitochondrial dynamics have been linked to diseases such as cancer, Parkinson's and Alzheimer's dementia, and amyotrophic lateral sclerosis (Nunnari and Suomalainen, 2012, Chen and Chan, 2009).

Extensive research has shown that mitochondria in yeast and humans are not independent, discrete organelles; rather, during interphase they form a “mitochondrial network”. This network needs to be strictly integrated with other cellular compartments, and, above all, highly dynamic, capable to constantly change its organisation in correlation with the needs of the cell. To effect these dynamic changes, the mitochondrial network depends on the processes of division, fusion, and transport: these mechanisms are in a highly regulated balance which determines the shape, number, fitness and correct location of mitochondria in cells, as reviewed in (Ramachandran, 2017) (Fig. 1-7).

When this balance is misregulated, pathology ensues; in particular, there is a strong link between neurodegenerative disease and perturbed mitochondrial dynamics, as the latter influence not only ATP production, but also apoptosis regulation and reactive oxygen species production (Gao et al., 2017). Thus, excessive mitochondrial fragmentation is a common factor in neurodegeneration, and it has been shown to be induced by factors associated with these diseases; for example, the phosphorylated protein Tau and mutant Htt (associated with Alzheimer and Huntington diseases, respectively) induce mitochondrial fission and impair fusion, leading to impaired mitochondrial function and increased cell death (Kandimalla et al., 2016, Shirendeb et al., 2012).

Mitochondrial dynamics change drastically upon cell division. Just before mitosis, mitochondrial fusion rates are increased, probably to organise mitochondrial distribution (Horbay and Bilyy, 2016). However, during mitosis mitochondria are extensively fragmented by the Dynamin related protein Drp1, which is activated by the mitotic kinases Aurora A and cyclin B-cyclin-dependent kinase (CDK)1 (Taguchi et al., 2007). Moreover, mitochondrial motility is observed in polarised cells which require mitochondrial transport to the bud (Kanfer and Kornmann, 2016). After cytokinesis, Drp1 activity decreases and fusion rates are increased, leading to the establishment of the mitochondrial network.

1.7.1 Mitochondria motility

The mechanisms of mitochondria transport in yeast greatly differ from the ones used by specialised human cells such as neurons, reflecting their respective complexity and needs. In yeast, mitochondrial motility and tethering are mainly required upon cell budding, to ensure that both mother and daughter cells are equipped with their own mitochondrial network (Labbe et al., 2014). To this end, mitochondria are transported in an active process involving actin and the myosin motor Myo2, whose depletion results in defective mitochondrial distribution in the buds (Altmann et al., 2008, Fortsch et al., 2011). Myo2 interacts with at least two adaptors on the mitochondria surface, Mmr1 and Ypt11 (Itoh et al., 2002, Itoh et al., 2004); interestingly, Mmr1 functions also as a tether between mitochondria and ER in the daughter cell (Swayne et al., 2011).

In mammalian cells, mitochondria movement has been mostly studied in neurons, where transport to the axons is essential to provide these active regions with the necessary source of energy and metabolites (Lackner et al., 2013). In contrast to yeast, mammalian mitochondria move across microtubules. The small Rho-GTPase Miro, inserted in the mitochondrial outer membrane, mediates bidirectional movement; when Miro-1 is depleted, neurons show altered mitochondrial distribution and motility (Misko et al., 2010).

Immunoprecipitation experiments uncovered that this transmembrane protein interacts with the Kinesin Kif5 (through the TRAK/Milton family of molecular adaptors) for anterograde transport, and with Dynein/dynactin complex for retrograde movement (Glater et al., 2006, Morlino et al., 2014, Russo et al., 2009). Recently, Miro has also been shown to recruit the actin motor Myo19 on the mitochondria membrane, suggesting that it has an additional role in coupling the mitochondria to the actin cytoskeleton; this function could be important for mitochondrial segregation during mitosis (Lopez-Domenech et al., 2018, Tang, 2018).

Similarly to what observed in yeast, mitochondrial positioning in axons is also regulated by static anchor complexes. Immobilisation of axonal mitochondria requires the mitochondrial outer membrane protein syntaphilin, which is proposed to function as “brake”: it can anchor mitochondria to microtubules,

and at the same time inhibit KIF5, the microtubule motor which mediates anterograde motility. Thus, positioning of mitochondria is regulated through a molecular interplay between motor and docking proteins (Chen and Sheng, 2013, Kraft and Lackner, 2017).

1.7.2 Mitochondrial fusion

Similarly to what just described for mitochondria positioning, the number and shape of the mitochondria are determined by a balance of two opposing mechanisms: mitochondrial fusion and fission (Fig. 1-7). This balance is essential for the correct function and structure of the mitochondrial network, and the equilibrium can be shifted in response to cytosolic cues to accommodate the cell needs. For example, it was observed that, upon cell starvation, fission is attenuated: as a result, the mitochondrial network becomes more fused, which is associated with an increased production of ATP (probably thanks to enhanced exchanges in the network of metabolites and mtDNA) (Gomes et al., 2011, Rambold et al., 2011). Furthermore, it is well established that apoptotic signalling requires mitochondrial fragmentation to release cytochrome c in the cytoplasm; this fragmentation is induced through increased fission activity and through inhibition of fusion (Suen et al., 2008).

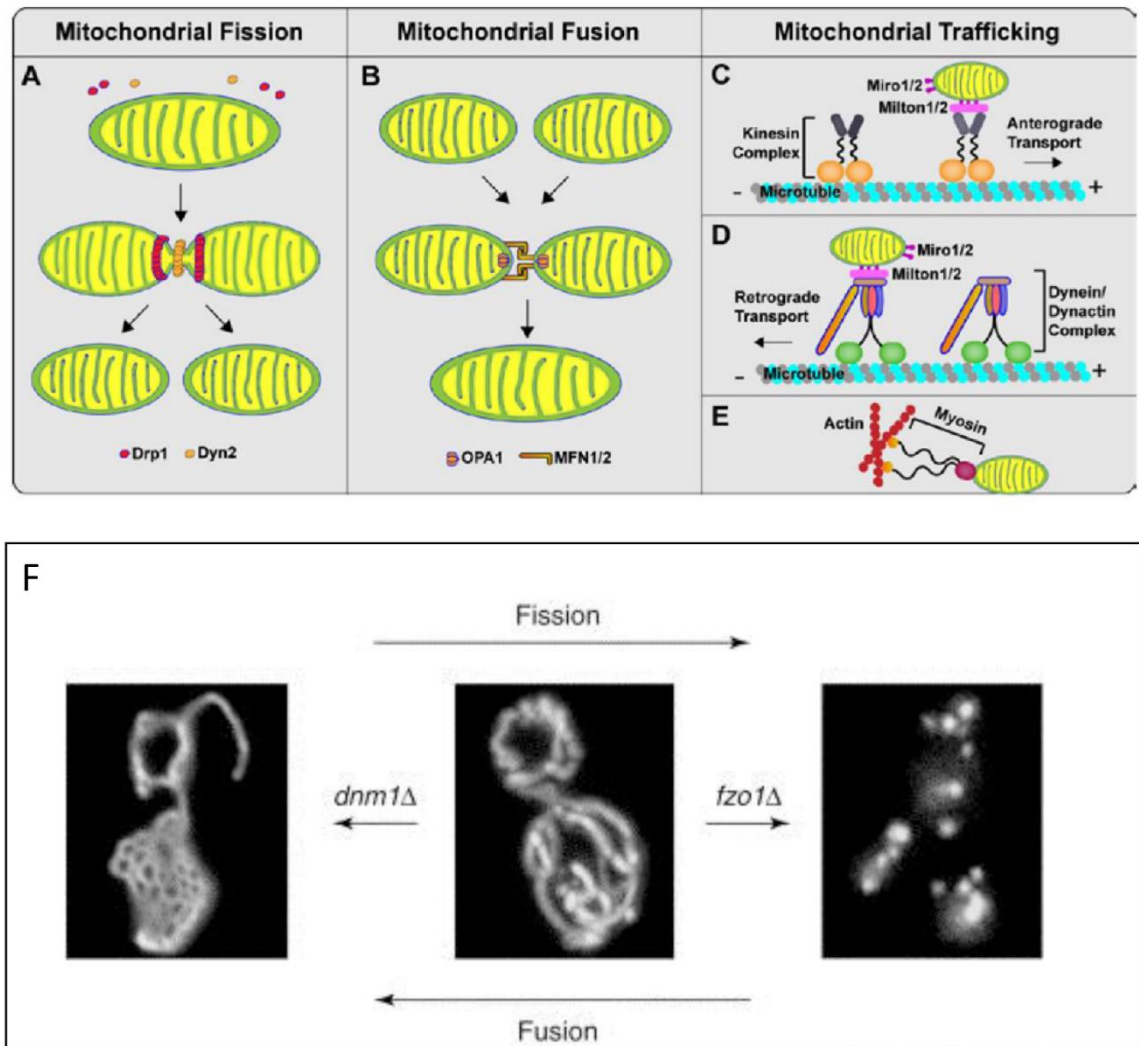


Figure 1-7: Mitochondrial dynamics and the balance between fission and fusion

(A) Mitochondrial dynamics in mammalian cells depend on the opposing forces of fission and fusion, and on the movement on microtubule or actin tracks. In mammals, the key agents of mitochondrial fission are Drp1 and Dyn2, both belonging to the Dynamin superfamily (B) Fusion is a two-step process; in mammalian cells, outer membrane fusion is mediated by Mfn1-2, while OPA-1 is the key effector of inner membrane fusion. (C, D and E) Mitochondrial movement in mammals is largely microtubule-mediated, though actin filaments have been associated with short-distance mitochondrial movement. Microtubule-based movement is mediated by the anterograde motor kinesin-1 and by the retrograde motor dynein/dynactin; interaction with the mitochondrial proteins Milton and Miro is essential for movement. Panel reprinted from (Gao et al., 2017). (F) The balance between mitochondrial fusion and fission is important for the maintenance of the mitochondrial network. In yeast, Dnm1 and Fzo1p are the key agent of fission and fusion, respectively; in wild-type yeast, their balanced action maintains a tubular mitochondrial network (middle). When Dnm1 is ablated, unopposed mitochondrial fusion results in a mitochondrial net (left); conversely, loss of Fzo1p leads to excessive fragmentation owing to unregulated mitochondrial fission (right). Figure reprinted from (Shaw and Nunnari, 2002). Copyright © 2002 Elsevier Science Ltd.

Mitochondrial fusion is an essential merging event that ensures homogeneity in the mitochondrial population of a cell through the exchange of proteins, mtDNA, lipids and metabolites. Fusion starts with two mitochondria coming in close

contact (probably through the regulation of the actin cytoskeleton); successively, both the Outer and the Inner Mitochondrial Membrane (OMM and IMM, respectively) need to undergo fusion, through distinct mechanisms which are mediated by Dynamin-related proteins (Drps), large GTPase proteins of the Dynamin superfamily (as reviewed in (Lee and Yoon, 2016)).

OMM fusion is mediated by the OMM integral protein Fzo1/Mitofusin1-2 (in yeast and humans, respectively) (Hermann et al., 1998, Chen et al., 2003). Mitofusin complexes need to be present in both adjacent mitochondria (Koshiba et al., 2004), and their trans-interaction tethers the two organelles together; subsequent GTPase activity brings them closer, forming a “docking ring”, and fusion occurs at the periphery of this ring (Brandt et al., 2016).

IMM fusion is performed through the action of the transmembrane IMM protein OPA1 (Mgm1 in yeast), a Dynamin-related protein which is also involved in mtDNA maintenance and cristae integrity (Cipolat et al., 2004, Meeusen et al., 2006, Pernas and Scorrano, 2016). In contrast to what observed for Fzo1/Mitofusin, the activation of OPA1 activity on just one of the fusing mitochondria is sufficient for IMM fusion (Song et al., 2009). IMM fusion mechanism is not completely understood; moreover, while it is clear that in yeast OMM and IMM fusion events are coordinated (Sesaki and Jensen, 2004), it is not known how this is accomplished in mammalian cells.

1.7.3 Mitochondrial fission

Mitochondrial fission is the division process where the constriction and cleavage of a pre-existing “mother mitochondrion” gives rise to new organelles. This process is important in dividing cells, as mitochondria cannot be created *de novo*. In budding yeast, mitochondria are first expanded in size, then divided and partitioned in daughter cells (Friedman and Nunnari, 2014, Ramachandran, 2017). When mitochondrial fission is impaired, yeast cells can still complete meiosis, but mitochondria are not correctly partitioned in the progeny. Similarly, inhibiting fission during meiosis leads to the production of inviable progeny in mammals (Gorsich and Shaw, 2004, Waterham et al., 2007, Ishihara et al., 2009).

Recently, it has been proposed that fission and replication of mitochondrial DNA (mtDNA) are strictly connected, as replication of mtDNA occurs near sites that are marked for fission, to ensure that the daughter mitochondria inherit their own genome (Lewis et al., 2016).

As recently reviewed (Kraus and Ryan, 2017), mitochondrial fission is also important in post-mitotic cells, where is essential to: 1) maintain a healthy population through the fragmentation of damaged mitochondria, which are then targeted for degradation (a process termed mitophagy) (Twig et al., 2008) ; 2) facilitate mitochondrial transport, since smaller organelles are more easily transported along cytoskeletal tracks, especially in narrow regions like the thin axonal processes of neurons (Verstreken et al., 2005), and 3) enhance the release of cytochrome-c after apoptotic induction (Montessuit et al., 2010).

Mitochondrial fission is mediated by the coordinated action of cytoskeletal elements and proteins residing both in the cytoplasm and on the mitochondrion, and both the OMM and IMM are severed as a result. The first molecule found to have a key role in this process was the yeast Dynamin related protein Dnm1. A forward genetic screen showed that knockout of this protein caused the mitochondrial network to become highly elongated and interconnected. It was shown that Dnm1 has a cytoplasmic pool, but also forms puncta along the mitochondria, and that the GTPase activity was essential for its function (Otsuga et al., 1998). At the same time, a mitochondrial function and localisation were observed for its human homolog, Drp1 (Smirnova et al., 1998). Importantly, Drp1 function is also essential for peroxisome fission (Koch et al., 2003, Li and Gould, 2003).

Subsequent research has shown that Dnm1/Drp1 are key effectors of mitochondria membrane constriction (Bleazard et al., 1999, Smirnova et al., 2001). These mechanochemical enzymes wrap around the mitochondrial membrane and form spirals; upon GTPase hydrolysis, conformational changes in Drp1 helices cause a two-fold decrease in ring diameter to facilitate membrane constriction (Mears et al., 2011, Koirala et al., 2013) (see paragraph 1.8). Moreover, additional players of mitochondrial fission have been uncovered, which will be discussed here.

Not all the puncta of Dnm1/Drp1 on the mitochondria lead to fission; future sites of mitochondrial fission are usually marked by a “pre-constriction step”, which is needed to reduce the diameter of the mitochondrial tubule (which normally measures ~300-500 nm) to ~150 nm, the width of the Dnm1/Drp1 helix (Ingerman et al., 2005). This pre-constriction step is mediated by the concerted action of Endoplasmic Reticulum (ER) and actin: the ER wraps around mitochondria at sites of future fission (Friedman et al., 2011) and in those sites actin polymerization occurs, mediated by the ER-localised Formin 2 (INF2) and by the mitochondrial protein Spire1C (Korobova et al., 2013, Manor et al., 2015). It is proposed that myosin II is subsequently recruited to these sites to help pre-constrict the mitochondrial tubules (Korobova et al., 2014). However, it was recently noted that mitochondrial fission can also be elicited by mechano-stimulation in mammalian cells (Helle et al., 2017).

To further constrict the membrane, the oligomerisation of Dnm1/Drp1 is required; as already mentioned, this protein has a cytoplasmic pool, and needs to be recruited to the mitochondrial outer membrane, a function carried out by a number of different adaptors/receptors (Pagliuso et al., 2018). In yeast, the transmembrane OMM protein Fis1 is the main adaptor, binding the yeast-specific receptors Mdv1 and Caf4 to recruit Dnm1 and promote its assembly (Mozdy et al., 2000, Lackner et al., 2009, Griffin et al., 2005). Human cells also express Fis1, but it is dispensable for fission (Otera et al., 2010, Osellame et al., 2016). Nevertheless, its knockdown induces a mild elongation phenotype; this could suggest that Fis1 could play a role in Drp1 recruitment under some physiological conditions (Loson et al., 2013). Drp1 recruitment and assembly at constriction sites in mammalian cells is mediated by the primary adaptor Mff, conserved in all metazoans (Gandre-Babbe and van der Bliek, 2008), and by the chordate-specific OMM proteins MiD49 and MiD51 (Palmer et al., 2011). Strikingly, these adaptors can work independently to recruit Drp1 (Koirala et al., 2013), and the activity of Drp1 can be modulated differently by these interchangeable adaptors. For example, it has been shown that when mitochondrial fission is induced by apoptotic signals, Drp1 recruitment is mediated by MiD49 and MiD51, not Mff (Otera et al., 2016). Furthermore, Drp1/Dnm1-mediated fission can also be modulated by phosphorylation, sumoylation and ubiquitination; thus, Drp1 activity to the OMM relies not only on its receptor complex, but also on

numerous posttranslational modifications (Pagliuso et al., 2018, Kanfer and Kornmann, 2016, Taguchi et al., 2007).

Dnm1/Drp1 recruitment leads to the formation of helices on the membrane, which contribute to the tubule constriction (see paragraph 1.8). It was recently found that the final severing step requires an additional mechanochemical enzyme, the classical Dynamin Dyn2 (Lee et al., 2016). Dyn2 is transiently recruited to constricted mitochondrial sites to facilitate severing of the membrane; moreover, its ablation led to elongated mitochondria, which in some regions were constricted by Drp1, but not severed. It is thus proposed that Drp1-mediated constriction facilitates the assembly of Dyn2, which then completes division.

As already noted, mitochondrial fission interests both IMM and OMM, but it is not clear if the two membranes are cleaved in distinct steps. To date, no inner membrane fission machinery has been identified. Whether the constriction of the OMM pushes the IMM together until it fuses, or additional proteins are involved in coordinating inner membrane fission, it is not known; intriguingly, recent work has suggested a coordination between the fission machinery and OPA-1, the regulator of IMM fusion (Anand et al., 2014).

1.8 Dynamin superfamily: universal membrane remodelling effectors

As discussed above, mitochondrial division and fusion are mediated by the action of Dynamin-related proteins (Drps), which belong to the superfamily of Dynamins, large mechanochemical enzymes that mediate different membrane remodelling processes. Members of this family share two key characteristics: a large GTPase domain at their N-terminus, which is the most conserved region throughout the family, and shows low GTP-binding affinity; and a GTPase activation mechanism that is oligomerization-dependent (Praefcke and McMahon, 2004, Faelber et al., 2013).

Dynamin was first characterised as a GTPase that associates with microtubules in vitro (Shpetner and Vallee, 1989, Obar et al., 1990); subsequent studies in *D. melanogaster* showed that temperature-sensitive mutants lacking Dynamin do

not perform endocytosis, as scission of clathrin-coated vesicles from the plasma membrane is blocked (Kosaka and Ikeda, 1983, van der Bliek and Meyerowitz, 1991).

Today, members of the Dynamin superfamily have been described in most eukaryotes and even in bacteria, and are divided in classical Dynamins and Dynamin-related proteins. While the former are best known for their role in endocytosis, Dynamin-related proteins have evolved to perform different membrane remodelling processes, from organelle division and fusion, to plant cytokinesis (Heymann and Hinshaw, 2009).

In addition to the GTPase domain, members of this superfamily are usually characterised also by a Middle domain and a GTPase Effector domain (GED). Classical Dynamins, but not Dynamin-related proteins, also present a Pleckstrin-Homolgy (PH) domain and a Proline-Rich domain (PRD), which are important for membrane binding, as they mediate lipid and protein interaction, respectively (van der Bliek, 1999). Dynamin-related proteins are thought to rely mostly on protein interactions to bind target membranes; however, in place of the PH domain they present a unique sequence called insert B (InsB), which in some cases has been shown to mediate interaction with the lipid cardiolipin (Bustillo-Zabalbeitia et al., 2014, Ugarte-Urbe et al., 2014, Stepanyants et al., 2015).

1.8.1 Dynamin-related proteins: mode of action

Most of our knowledge on Drps mechanism of action is based on classical Dynamins; when the crystal structure of Drp1 was uncovered, its polymerisation and constriction mechanisms were shown to be similar to classical Dynamins, though some modifications were also evident (see Fig. 1-8) (Frohlich et al., 2013, Ford et al., 2011).

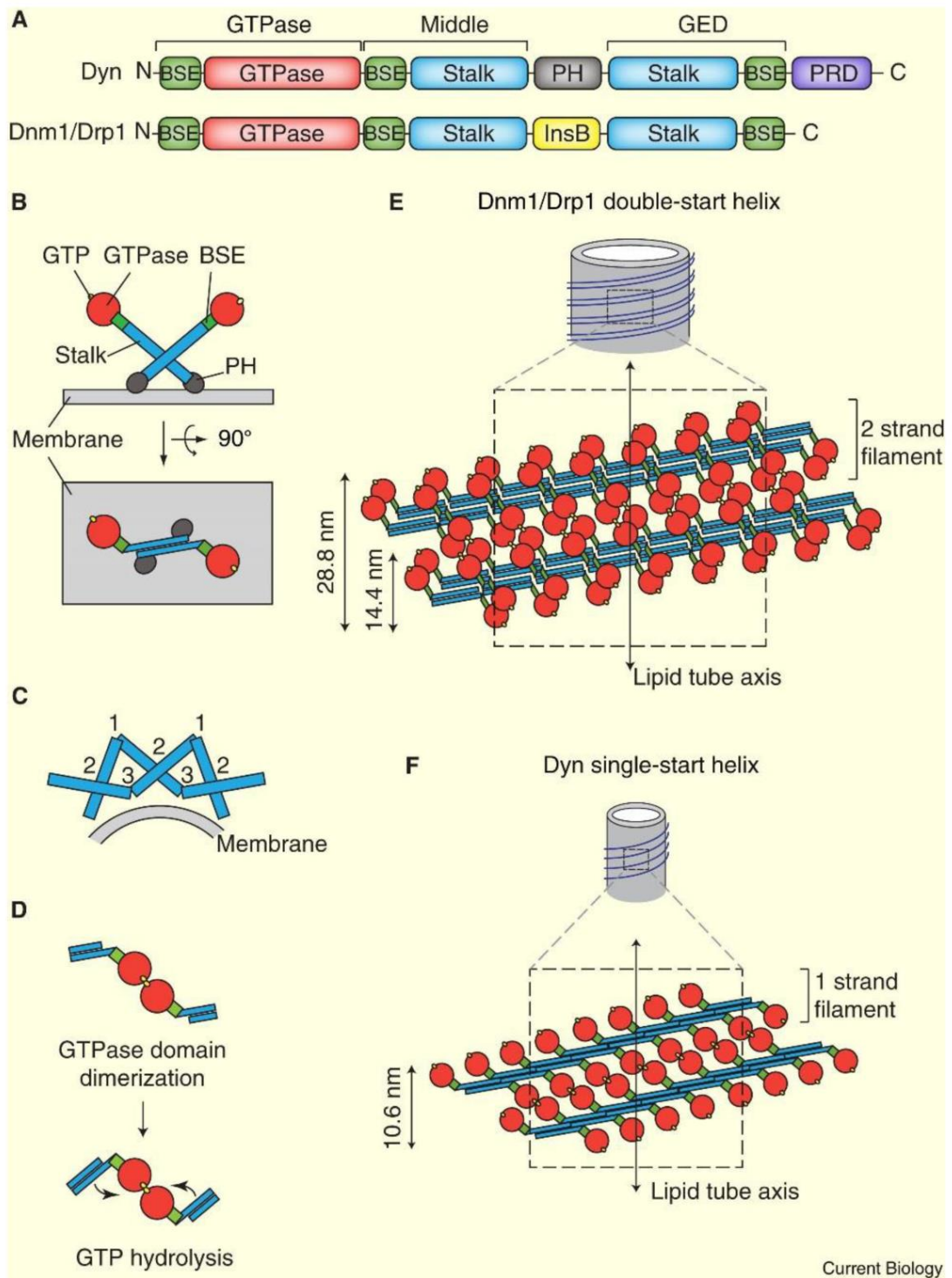


Figure 1-8: Structure and assembly of classical Dynamin and mitochondrial Dynamin-related proteins.

(A) Comparison of the domain architectures of classical Dynamin (Dyn) and mitochondrial Dynamin-related proteins Dnm1/Drp1. (B) Once recruited to the membrane, all member of the Dynamin superfamily polymerise thanks to interactions mediated by their stalk domains; the GTPase domain (bound to GTP, in yellow) projects from the spiral backbone. (C) The regions of the stalk that mediate dimerization (interface 2) are distinct from the ones that mediate polymerisation (interface 1 and 3). (D) Interaction of the GTPase domains between adjacent strands of the Dynamin spiral stimulates GTPase hydrolysis, which in turn changes the conformation of the stalks, leading to constriction of the spiral. (E, F) While classical Dynamins form a single-start helix around membranes, Drp1/Dnm1 form double-start spirals. (GED: GTPase

effector domain; PRD: proline-rich domain; BSE: bundle signalling element; PH: pleckstrin homology; InsB: insert B. Domains are color-coded in the same manner throughout the figure. Reproduced from (Bui and Shaw, 2013). Copyright © 2013 Elsevier Ltd.

Fission Drps contain the characteristic N-terminal GTPase domain, which binds a single molecule of GTP through four GTP-binding motifs (G1-G4): the P-loop in the G1 motif coordinates the phosphates, while a Threonine in the G2 motif is required for catalysis; a conserved Glycine in the G3 motif forms a hydrogen bond with the γ -phosphate of GTP, and the G4 motif is important for the coordination of the base and ribose part of the molecule (Reubold et al., 2005, Praefcke and McMahon, 2004).

Drp1/Dnm1 is recruited to the mitochondrial membrane in its GTP-bound state *in vivo* (Ingerman et al., 2005). Once recruited, the Middle and GED domains fold to form a “stalk”, while the GTPase domain faces away from the membrane (van der Bliek et al., 2013, Bui and Shaw, 2013). Microscopy and crystallography analyses show that the interaction between stalks of different subunits is required to mediate the formation of multimeric spirals typical of all Dynamins (Chappie et al., 2011, Gao et al., 2010). In Dynamin-related proteins, this polymerisation results in the formation of a double-start helix, where the GTPase domains project from the back-bone in opposite directions; this causes the GTPase domain of molecules in two adjacent rungs of to interact, and as a result the GTPase activity is highly stimulated (Wenger et al., 2013).

GTP hydrolysis induces a conformational change in the BSE (bundle signalling element), a segment positioned between the GTPase domain and the stalk; it is proposed that, similar to what observed in classical Dynamins, this acts as a “power-stroke” which is then transmitted to the stalk region, changing the geometry of the helix around the membrane and finally causing membrane constriction (Chappie et al., 2011, Mears et al., 2011, Zhang and Hinshaw, 2001).

1.8.2 Dynamin-related proteins in *T. gondii*

Three Dynamin-related protein are present in *T. gondii* genome (Breinich et al., 2009, van Dooren et al., 2009, Pieperhoff et al., 2015): DrpA, DrpB and DrpC.

Localisation of DrpA shows that it forms small patches in the cytosol, but is also strongly associated with the apicoplast; during endodyogeny, DrpA is both at the tips of the organelle and at the region where division occurs, strongly suggesting a role in apicoplast fission (van Dooren et al., 2009). To confirm this hypothesis, a mutated form of DrpA, bearing a point mutation in a key residue of the GTPase domain, was expressed: this strategy has been used with success in various studies on Dynamins, as it is proven that mutations in the GTPase domain specifically disrupt Dynamin function in a dominant-negative fashion, through abolition of its GTPase activity (van der Blik et al., 1993, Otsuga et al., 1998, Herskovits et al., 1993). Expression of a dominant-negative form of DrpA led to severe apicoplast defects, as the organelle failed to divide (van Dooren et al., 2009).

Thus, DrpA is a key effector of apicoplast fission; its mode of action, though, is not well understood. The authors hypothesised that formation of DrpA helices during apicoplast division requires a pre-constriction step, as the diameter of the unconstricted organelle is too wide to allow DrpA polymerisation around it. This pre-constriction was proposed to be mediated by the MORN1 ring in the basal complex, which is essential for cytokinesis (see paragraph 1.6). In the proposed model, the apicoplast is anchored to the centrosome at the start of endodyogeny; when daughter buds start to extend inside the mother, the apicoplast is pulled down and stretched, assuming a U shape. It is hypothesised that the base of the U is constricted by the MORN-1 ring, allowing DrpA polymerisation on the apicoplast membrane (van Dooren et al., 2009); this model is supported by the observation that apicoplast fission is abolished in mutants lacking MORN-1, suggesting that, in absence of this pre-constriction step, DrpA helices cannot assemble (Lorestani et al., 2010, Gubbels et al., 2006, Heaslip et al., 2010).

As already discussed, DrpB is a key factor in secretory organelle biogenesis and maintenance (Breinich et al., 2009). This protein is concentrated at the Golgi, and a dominant-negative DrpB mutant was shown to result in aberrant trafficking of secretory proteins. When expression of the dominant-negative DrpB is induced, *de novo* biogenesis of secretory organelles is blocked, and micronemal and rhoptry proteins are re-routed to the constitutive secretion pathway; thus,

they are not found at the apical complex, but either in the lumen of the parasitophorous vacuole or at the plasma membrane. Thus, DrpB is essential for the biogenesis of secretory organelles; however, new data suggest that it could also be involved in other processes, such as recycling of proteins from the mother to daughter cells during replication.

Phylogenetic analysis shows that DrpA and DrpB are alveolate-specific, and show the three characteristic domains of Drps: GTPase, Middle and GED domains (Fig. 1-9). In contrast, in the sequence of DrpC only the GTPase domain can be identified, and the protein is Apicomplexa-specific; moreover, it was previously shown that it has an essential role in *T. gondii*, as its ablation results in drastically impaired parasite growth (Pieperhoff et al., 2015). Further characterisation of this protein and of its interactors is the aim of this thesis.

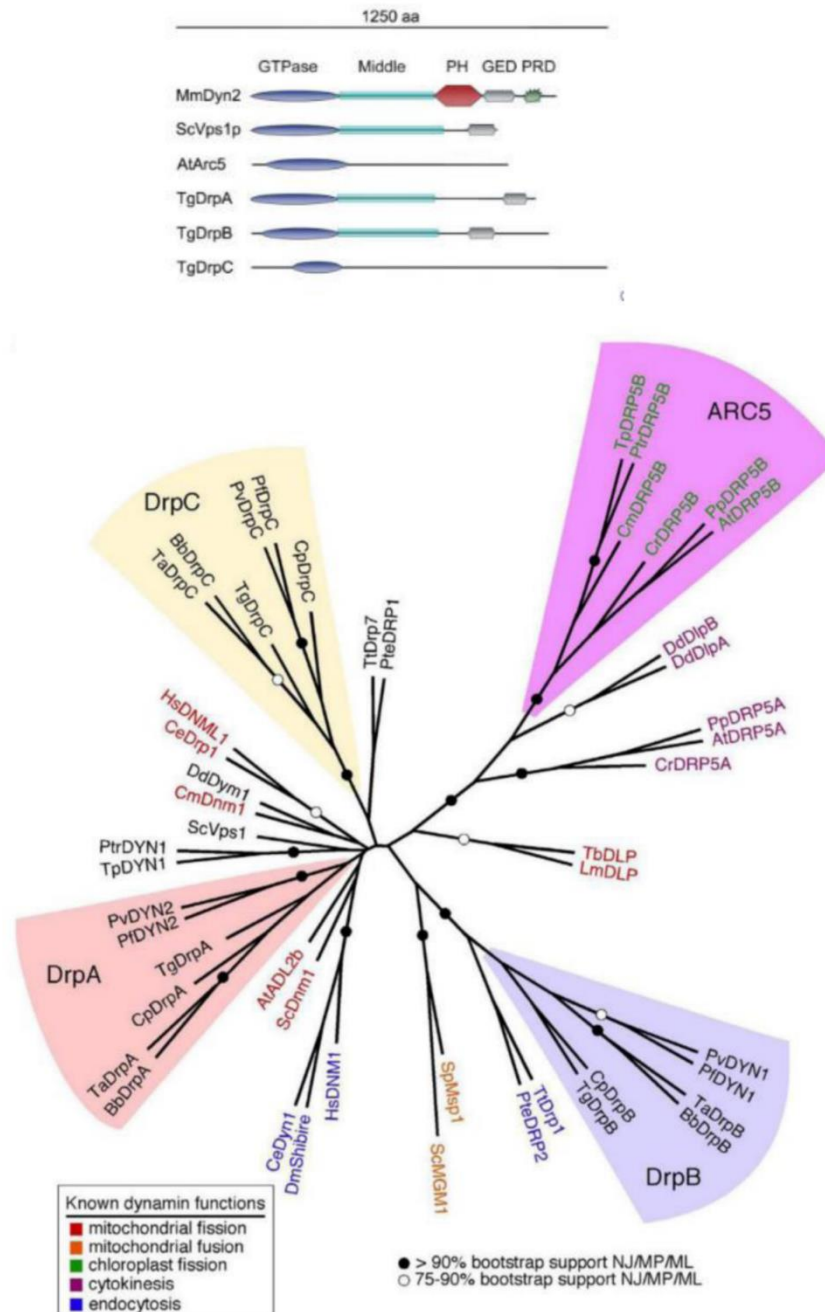


Figure 1-9: Dynamin-related proteins in *T. gondii*

(A) Scheme of the domains architecture of different representative of the Dynamin superfamily. While the Dynamin Dyn2 shows the five domains typical of classical Dynamins, Dynamin-related proteins usually are formed by a GTPase, Middle and GED domains. *T. gondii* DrpA and DrpB show this typical architecture, while DrpC presents only the large GTPase domain (Sc: *Saccharomyces cerevisiae*; Mm: *Mus musculus*; At: *Arabidopsis thaliana*; Tg: *Toxoplasma gondii*). (B) Multiple sequence alignment of the GTPase domain of 49 Dynamin-related proteins, showing that three Dynamin-related proteins are conserved in *T.gondii*. Panel (A) reprinted from (Breinich et al., 2009); panel B reprinted from (van Dooren et al., 2009). Copyright © 2009, CellPress.

1.9 Aim of study

Of the three Dynamin-related proteins present in *T. gondii*, DrpC is the only one that is Apicomplexa-specific (Breinich et al., 2009, van Dooren et al., 2009); moreover, it shows a highly divergent domain architecture, as its GTPase is the only recognisable domain in its structure. Finally, it was shown that ablation of DrpC results in parasite death (Pieperhoff et al., 2015). Thus, DrpC could prove an interesting drug target, as it is essential, highly divergent from mammal dynamin-related proteins, and conserved in parasites that are showing resistance to traditional therapies, such as *Plasmodium spp.* (World Health Organization: World malaria report 2017). However, the function of this protein is still unknown in *T. gondii*.

Thus, this work aims to:

- Characterise DrpC localisation and function in *T. gondii*;
- Assess whether its GTPase domain is required for parasite fitness;
- Investigate the mechanism of mitochondrial fission in *T. gondii*;
- Characterise potential interactors of DrpC.

2 Materials and Methods

2.1 Equipment

Table 2.1-1. Equipment

Applied Biosystems	Real-time PCR light cycler (Prism 7500), MicroAmp® optical 96-well reaction plate, MicroAmp® optical adhesive film
Applied Precision	DeltaVision® Core microscope
BD Biosciences	Syringes, Needles (23-25 gauge), FACS tubes with cell strainer cap
BioRad	Agarose gel electrophoreses equipment, UV transilluminator, SDS-PAGE system, Blotting apparatus (Transblot SD and Mini transblot electrophoretic transfer cell), gel documentation system, gene Pulser Xcell, Micropulser, S3e™ Cell sorter
BTX	Electroporation cuvettes and system (ElectroSquare Pore 830)
Eppendorf	Thermocycler (Mastercycler Eppgradient), Thermomixer compact
Fished Scientific	Ultrasound water bath FB15047
GE healthcare	Nitrocellulose membrane (Hybond ECL),
Grant	Water bath
Heraeus Instruments	Incubator
Ibidi	15 µ-Slide 10.8 Luer collagen IV chambers
KD scientific	Syringe pump
Kuehner	Shaking incubator (ISF-1-W)
Li-COR	Odyssey CLx
Lonza	4D-Nucleofactor™X electroporation unit, Single 100 µl Nucleovette™
Milipore	MilliQ water deionising facility, 3 µm Millipore filters
Photometrics	CoolSNAP HQ2CCD camera
Sanyo	CO2- incubator tissue culture
Satorius	Analytical balances
Sciquip	Sigma 6K 15 centrifuge (1150 rotor and 12500 rotor)
StarLab	ErgoOne Single & Multi-Channel pipettes, StarPet Pro pipette controller
Stuart	Heat block, Roller mixer, Orbital Shaker
ThermoFisher scientific	CO2- incubator tissue culture, Nanodrop spectrophotometer, Centrifuge (sorvall legend XFR), Table top centrifuge Heraeus Pico 21, Tabletop cooling centrifuge Heraeus Fresco 21, Invitrogen™ DynaMag™ magnets.
Zeiss	Axioskop 2 (mot plus) fluorescence microscope with AxioCam MRm CCD camera, Primo Vert (light microscope), Axiovert 40 CFL fluorescence microscope with AxioCam ICc1, Axiovert A1 fluorescence microscope with AxioCam IMc1, ELYRA PS.1 Super-resolution microscope, sCMOS pco SIM camera, Plan Aplanachromat 63x lens

2.2 Computer Software

Table 2.2-1. Software

Adobe Systems Inc.	Adobe design premium CS4
AcaClone software	pDraw32
Applied Precision	SoftWoRx explorer and SoftWoRx suite
BioRad	ProSort™
Carl Zeiss Microscopy	Zen Black and Zen blue
CellProfiler	Cell Profiler 2.1.1 Analyst software
CLC Bio	CLC Genomics Workbench 6
GraphPad software Inc.	GraphPad Prism version 7.3
Li-COR	Image Studio 5.0
Microsoft Corporation	Windows 7, Microsoft Office 2010
<i>National Institute for Biotechnology Information (NCBI)</i>	Basic Local Alignment search tool (BLAST) (Altschul et al., 1990)
<i>National Institute of Allergy and Infectious Diseases (NIAID)</i>	ToxoDB (Gajria et al., 2007)
National Institutes of Health	ImageJ (Schindelin et al., 2015), Fiji (Schindelin et al., 2012)
New England Biolabs (NEB)	NEB tools™: Double Digest Finder, Enzyme Finder, NEBCutter®, NEBBioCalculator®, Tm Calculator
OligoCalc	Oligo Analysis tool (Kibbe, 2007)
PerkinElmer	Volocity 3D Image Analysis Software
Thermo Scientific	Thermo Scientific web tools: Tm Calculator
Thomson Scientific	Endnote X8
University of Utah	ApE Plasmid Editor v2.0.53c Copyright© by M. Wayne Davies
BioEdit	BioEdit Sequence alignment editor

2.3 Consumables, biological and chemical reagent

Table 2.3-1. Biological and chemical reagents

Clontech	Shield-1
Formedium	Tryptone, yeast extract
Li-COR	Chameleon Duo Pre-stained protein ladder
Life technologies	Phosphate buffered saline 1X (PBS), Trypsin/EDTA (0.05%), PureLink® RNA mini kit, DNaseI, Platinum Taq DNA Polymerase High Fidelity, NuPage SDS loading buffer and reducing agent, Sodium bicarbonate, Ultrapure agarose
Marvel	Milk powder (skimmed)
Melford	Agar, ditriothreitol, IPTG, X-Gal
NEB	DNA ladder (1 kb), All Restriction enzymes and associated buffers, T4 DNA ligase, Taq polymerase, Phusion® and Q5® high-fidelity DNA polymerase, Calf intestinal phosphatase (CIP)
Phoenix Research Products	GelRed nucleic acid stain
Promega	pGEM®-T Easy vectors system
Roche	MgSO ₄ × 7H ₂ O, potassium hydroxide, paraformaldehyde
Sigma	Ammonium persulfate, Bromophenol blue sodium salt, Casein hydrosylate, Dulbecco's Modified Eagle Medium (DMEM), Ficoll, Ethylene glycol tetraacetic acid, Ponceau S, Isopropanol, Sodium dodecyl sulfate (SDS), dimethyl sulfoxide (DMSO), N,N,N',N'-tetramethylethylenediamine, Triton X-100, Rapamycin, beta mercaptoethanol, Tween20, Giemsa stain, RNase-ZAP, L-glutathione reduced, Adenosine 5'-triphosphate disodium salt hydrate, Glutamine, 30% acryl-

Southern Biotech	bisacrylamide mix, Sodium deoxycholate, K ₂ HPO ₄ , Magnesium chloride, Bleomycin (BLEO), Ampicillin sodium salt, Gentamicin, Xanthine, Chloramphenicol (CAT), Indole-3-acetic acid sodium salt (IAA, Auxin)
Thermo Scientific	Fluoromount G (with and without DAPI) Bovine serum albumin (BSA), Ethylene diamine tetraacetic acid, Glycerol, Glycine, Methanol, Tris, Sodium chloride, 40 nM FluoSpheres® Carboxylate-Modified Microspheres, Platinum Taq DNA Polymerase High Fidelity, Restore Western blot stripping buffer, Invitrogen™ Dynabeads™ magnetic beads.
VWR	CaCl ₂ × 2 H ₂ O, Glacial acetic acid, Ethanol, HEPES, Potassium chloride, Na ₂ HPO ₄ , KH ₂ PO ₄
Zeiss	Immersion oil

2.4 Kits

Table 2.4-1. Nucleic acid extraction and amplification kits

Qiagen	Spin Mini-prep, Plasmid Midi-prep, MinElute PCR Purification MinElute, QIAquick gel extraction kit, DNeasy blood and tissue
Roche	PureLink® RNA isolation mini kit, high Pure PCR product purification
Thermo scientific	Maxima SYBR green/ROX qPCR Mater Mix

2.5 Buffers, solutions and media

Table 2.5-1. Buffers for DNA Analysis

50X TAE buffer	2M Tris, 0.5M Na ₂ EDTA, 5.71% glacial acetic acid (v/v)
5X loading dye	15% Ficoll (v/v), 20 mM EDTA, 0.25% Bromophenol Blue in H ₂ O
NEB 1 kb + DNA ladder	150 µl 1kb ladder (1 µg/µl), 300 µl 5X DNA loading buffer, 1050 µl H ₂ O

Table 2.5-2. Buffers for Western blot analysis

RIPA buffer	50 mM Tris-HCl (pH 8.0), 150 mM NaCl, 1 mM EDTA, 0.5% sodium deoxycholate, 0.1% SDS (w/v), 1 % triton X-100 (v/v)
4X separating gel buffer	1.5 M Tris-HCl (pH 8.8), 0.4% SDS (w/v)
Separating gel	8-15% of 30% acryl-bisacrylamide, 25% 4X separating gel buffer, 0.1% APS 10% (w/v), 0.2% TEMED (v/v)
4X stacking gel buffer	0.5 M Tris/HCl (pH 6.8), 0.4% SDS (w/v)
Stacking gel	4% of 30% acryl-bisacrylamide, 25% 4X stacking gel buffer (v/v), 0.1% APS 10% (w/v), 0.2% TEMED (v/v)
SDS PAGE running buffer	25 mM Tris, 192 mM glycine, 0.1% SDS (w/v)
Transfer buffer for wet blot	48 mM Tris, 39 mM glycine, 20% methanol (v/v)
Blocking solution	0.2% Tween (v/v), 3% skimmed milk powder (W/v), 0.037 SDS (W/v)

Washing solution (PBS-Tween)	0.2% tween (v/v) in 1X PBS
1 M DTT	3.085 g 1,4-dithio-DL-threitol (DTT) in 20 ml 10 mM NaAc (pH 5.2)
10 % APS	1 g ammonium persulfate in 10 ml H ₂ O

Table 2.5-3. Buffers and media for bacterial culture

LB medium	10 g/l tryptone, 5 g/l yeast extract, 5 g/l NaCl
LB agar	1.5% (w/v) agar in LB medium
SOB medium	2% tryptone (w/v), 0.5% yeast extract (w/v), 0.05% NaCl (w/v), 2.5 mM KCl, 10mM MgCl ₂
SOC medium	20 mM glucose in SOB medium
NYZ broth	5 g/l NaCl, 2 g/l MgSO ₄ *7H ₂ O, 5 g/l yeast extract, 10 g/l casein hydrolysate, pH adjusted to 7.5 with NaOH
Ampicillin (1000X)	100 mg/ml in H ₂ O
IPTG (100 µl/petri dish)	100 mM IPTG in H ₂ O
X-Gal (20 µl/petri dish)	50 mg/ml in N,N-dimethylformamide

Table 2.5-4. Buffers and media for *T. gondii* tachyzoites and mammalian cell culture

DMEM _{COMPLETE}	500 ml DMEM, 10 % FCS (v/v), 2 mM glutamine, 20 µg/ml gentamicin
2 x Freezing solution	25 % FCS (v/v), 10 % DMSO (v/v) in DMEM _{COMPLETE}
Electroporation buffer (Cytomix)	10 mM K ₂ HPO ₄ /KH ₂ PO ₄ , 25 mM HEPES, 2 mM EGTA pH 7.6, 120 mM KCl, 0.15 mM CaCl ₂ , 5 mM MgCl ₂ with 5 mM KOH adjusted to pH 7.6, 3 mM ATP, 3 mM GSH
Giemsa staining solution	10 % Giemsa stain (v/v) in H ₂ O
MPA (500X)	12.5 mg/ml in methanol
XAN (500X)	20 mg/ml, 1M KOH
Pyrimethamine (1000X)	1 mM in EtOH
Shield-1 (1000X)	1 mM in 70 % EtOH
Rapamycin (1000X)	50 µM in DMSO
IAA (Auxin) (1000X)	500 mM in EtOH
ATc (1000X)	0.5 µg/ml
FACS buffer	1 % FCS, 1 mM EDTA in PBS
PFA fixing solution	4 % PFA (w/v) in PBS
Permeabilisation solution	0.2 % triton X-100 (v/v) in PBS
Blocking solution	2 % BSA (w/v) in permeabilisation solution

2.6 Antibodies

Table 2.6-1. Primary antibodies

Name	Species	Dilution		Source
		IFA	WB	
Aldolase	Rabbit	(-)	1:3000	Sibley, L. D.
Catalase	Rabbit	(-)	1:3000	Soldati, D.
GAP45	Rabbit	1:1000	(-)	Soldati, D.
GFP	Mouse	1:500	1:2000	Roche
HA	Rat	1:500	1:1000	Roche
HA	Mouse	1:100	(-)	Cell signaling
HSP60	Rabbit	1:2000	(-)	Sheiner, L.
IMC1	Mouse	1:1000	(-)	Ward, G.
TOM40	Rabbit	1:2000	(-)	Van dooren, G.
Mic4	Rabbit	1:3000	(-)	Soldati, D.
Rop2,4	Mouse	1:500	(-)	Dubremetz, JF.
Gra5	Mouse	1:500	(-)	Delauw, M. F
CPN60	Rabbit	1:1000	(-)	Sheiner, L.
c-MYC	Mouse	1:250	1:500	Sigma
DrpB	Rat	1:1000	(-)	Keith Gull
Tubulin (acetylated)	Mouse	1:500	(-)	Sigma

Table 2.6-2. Secondary antibodies, fluorescent ligands and stains

Name	Species	Dilution			Source
		IFA	WB	Live-IM	
Alexa Fluor350 anti-mouse	Goat	1:3000	(-)	(-)	Life Technologies
Alexa Fluor488 anti-mouse	Goat	1:3000	(-)	(-)	Life Technologies
Alexa Fluor594 anti-mouse	Goat	1:3000	(-)	(-)	Life Technologies
Alexa Fluor633 anti-mouse	Goat	1:3000	(-)	(-)	Life Technologies
Alexa Fluor350 anti-rabbit	Goat	1:3000	(-)	(-)	Life Technologies
Alexa Fluor488 anti-rabbit	Goat	1:3000	(-)	(-)	Life Technologies
Alexa Fluor594 anti-rabbit	Goat	1:3000	(-)	(-)	Life Technologies
Alexa Fluor633 anti-rabbit	Goat	1:3000	(-)	(-)	Life Technologies
Alexa Fluor350 anti-rat	Goat	1:3000	(-)	(-)	Life Technologies
Alexa Fluor488 anti-rat	Goat	1:3000	(-)	(-)	Life Technologies
Alexa Fluor594 anti-rat	Goat	1:3000	(-)	(-)	Life Technologies
IRDye680RD anti-Mouse	Goat	(-)	1:5000	(-)	Li-Cor
IRDye800CW anti-Mouse	Goat	(-)	1:5000	(-)	Li-Cor
IRDye680RDanti-Rabbit	Goat	(-)	1:5000	(-)	Li-Cor
IRDye800CW anti-Rabbit	Goat	(-)	1:5000	(-)	Li-Cor

2.7 Oligonucleotides

Table 2.7-1: Oligonucleotides used in this study

Name	Sequence 5' → 3'	Purpose
DrpC-LIC fw	TACTTCCAATCCAATTTAATGCCCGAG	DrpC-YFP
DrpC-LIC rev	TCCTCCACTTCCAATTTTAGCAGCC	DrpC-YFP
DrpCYFP int fw	GCGCCACTCAGACGAAG	DrpCYFP integration PCR
DrpCYFP int rev	ATGGGCACCACCCCGG	DrpCYFP integration PCR
DrpC-HA-U1 fw	CAGGACCTCGAGGAGAGC	qRT-PCR DrpC-HA-U1
DrpC-HA-U1 rev	CCAACGCTCTGAACGAGGC	qRT-PCR DrpC-HA-U1
Q5wt fw	TTTAGATCTAAAAGGGAATCAAGAAAAAATG	p5RT70-GFP-DrpC
Q5wt rev	GCCATGGCCATGCATAGT	p5RT70-GFP-DrpC
Q5DN fw	GAGCATGGCGCGACGACCCCTTCTC	p5RT70-DD-GFP-DrpCDN
Q5DN rev	TGCTGCCGAAGACGACA	p5RT70-DD-GFP-DrpCDN
Q5GTPase only fw	TAATCACCCTGTGCTCAC	p5RT70-DD-GFP-DrpC GTPase only
Q5GTPase only rev	CTCACTCAAGAGGCTCTG	p5RT70-DD-GFP-DrpC GTPase only
DD-DrpCtrunc fw	CCTTAATTAATTACGCCCATCAACGGTGACGGAAGC	p5RT70-DD-GFP-DrpCTRUNC
DD-DrpCtrunc rev	CCATGCATGGAGCCTTCGAGAGTTTCATTCTCTGCACCTCC	p5RT70-DD-GFP-DrpCTRUNC
DD-Fis1 fw	ggcCCTAGGTACCATACGATGTTCCAGATTACGCTATGGAAGACTCCAACCTCAG	p5RT70-DD-HA-mCherry-Fis1
DD-Fis1 rev	gggTTAATTAATTAATTTTATGATAGCGTCCAC	p5RT70-DD-HA-mCherry-Fis1
Fis1 5' fw	GGGTCATGAGTCTCTTTGAAGACGTGCACCG	Tet07-Sag1-Fis1 5'
Fis1 5' rev	ggGGATCCTCTCGTACAGTGCTCACAACAAAAACG	Tet07-Sag1-Fis1 5'
Fis1 N-t fw	cccAGATCTATGGAAGACTCCAACCTCAGTC	Tet07-Sag1-Fis1 N-t
Fis1 N-t rev	gggACTAGTGGCGAAACACGCAAGTAAC	Tet07-Sag1-Fis1 N-t
Tet07-Sag1-Fis1 int fw	GCTGCACCATTCTATTCTTCTCTG	Tet07-Sag1-Fis1 integration PCR
Tet07-Sag1-Fis1 int rev	GCTATAAACACAGCCGAGGCGAC	Tet07-Sag1-Fis1 integration PCR
p50-mAID-HA fw	GAGGAGAAGAGCAACGATGTAATAATCAGAACTGATACCCAG GCTAGCAAGGGCTCGG	p50-mAID-HA
p50-mAID-HA rev	catgcgttctggacactgcagcagccctatgtgcagcgacc GTAATACGACTCACTATAGGGC	p50-mAID-HA
p50 gRNA fw	AAGTTgtctttggctgctgacatagG	p50 gRNA
p50 gRNA rev	AAAAcctatgtgcagcgaccaagacA	p50 gRNA

2.8 Plasmids

Table 2.8-1. Main plasmids used in this study for cloning and expression in *T. gondii*

Expression vector	Resistance	Reference
DrpC-YFP	DHFR	This study
DrpC-HA-U1	HX	(Pieperhoff et al., 2015)
TdTomato- TGME49_2154	CAT	(Ovciarikova et al., 2017)
p5RT70-GFP-DrpC	HX	This study
p5RT70-DD-GFP-DrpCDN	HX	This study
p5RT70-DD-GFP-DrpCwt	HX	(Pieperhoff, unpublished)
p5RT70-DD-GFP-DrpGTPaseonly	HX	This study
p5RT70-DD-GFP-DrpCTRUNC	HX	This study
p5RT70-DD-HA-mCherry-Fis1	HX	This study
Tet07-Sag1-Fis1	HX	This study
p50 gRNA	No selection	This study

2.9 Cell strains

2.9.1 Bacteria strains

Bacteria strains used in this study are listed in Table 2-13.

Table 2.9-1. *Escherichia coli* competent cells for plasmid transformation

XL10-Gold	Stratagene	Chemically competent
DH5 α	NEB	Chemically competent

2.9.2 *Toxoplasma gondii* strains

T. gondii strains used in this study are listed in Table 2-14.

Table 2.9-2: *T. gondii* strains used in this study

Strain (full name)	Selectable Marker	Reference
<i>RHΔhxcprt</i>	-	(Donald and Roos, 1993)
<i>RHΔku80</i>	-	(Huyn and Carruthers, 2009)
<i>RHΔku80 DrpC-YFP</i>	DHFR	This study
<i>RHΔku80DrpC-YFP::TdTomato-TGME49_215430</i>	DHFR,CAT	This study
<i>RHΔku80DiCre DrpC-HA-U1</i>	HX	(Pieperhoff et al., 2015)
<i>RH p5RT70-DD-GFP-DrpCDN</i>	HX	This study
<i>RH p5RT70-DD-GFPDrpC_{GTPaseonly}</i>	HX	This study
<i>RH p5RT70-DD-GFP-DrpCTRUNC</i>	HX	This study
<i>RHΔku80 TATi</i>	-	(Sheiner et al., 2011)
<i>RHΔku80 TATi Tet07-Sag1-Fis1</i>	HX	This study
<i>RH p5RT70-DD-HA-mCherry-Fis1</i>	HX	This study
<i>Tir1Δku80</i>	CAT	(Brown et al., 2017)
<i>Tir1Δku80 p50-mAID-HA</i>	HX, CAT	This study

2.9.3 Mammalian cell lines

Tachyzoites were grown in human foreskin fibroblasts (HFFs, purchased from ATCC), cultured up to passage 23. These primary cells grow in a monolayer due to contact inhibition, and were used for maintenance, transfection, subcloning and phenotypic characterisation of *T. gondii*.

2.10 Molecular biology

2.10.1 Isolation of genomic DNA from *T. gondii*

The extraction of genomic DNA (gDNA) was performed using the DNeasy® blood & tissue Kit. Parasites were collected either when freshly egressed, or when forming big vacuoles inside the host cells (in the latter case, scratching and syringing through a 25-gauge needle was performed to release parasites and disrupt the host cells). Parasites were subsequently pelleted by centrifugation (1200 g for 10 min), and resuspended in 200 µl of PBS 1X. gDNA extraction was accomplished by following the protocol described by the manufacturer, with a final elution in 200 µl H₂O.

2.10.2 mRNA extraction and cDNA synthesis

Parasites were pelleted by 600 g centrifugation for 5 min at 4°C and kept on ice all the time. Total RNA was isolated using the PureLink® RNA mini kit following the manufacturer's specifications. All equipment was cleaned using RNase-ZAP before use. The integrity of the RNA material was evaluated by running an agarose gel (app. 6ng per lane). In the gel, separation of the 28S and 18S bands could be observed after 10-15 min at 100V (Aranda et al., 2012). 1 µg of total RNA was used as template to synthesize cDNA using the reverse transcriptase SuperScript™ III kit (Invitrogen®) and random primer sets, according to manufacturer's protocol. For the reverse transcription reaction, an initial incubation step of 25 °C for 10 minutes was followed by 15-minute incubation at 50 °C and final step of 85 °C to terminate the reaction.

2.10.3 qRT-PCR

For qRT-PCR, mRNA was extracted from approximately 2×10^7 parasites of the strains *RHΔku80DiCre DrpC-HA-U1* (\pm 72 h 50 nM rapamycin induction) and *RH*. mRNA was extracted and cDNA synthesised as described in 1.10.2. qPCR reactions were performed with Power SYBR Green PCR Master Mix (Life Technologies) with 50 ng cDNA using a 7500 Real-Time PCR machine (Applied Biosystems); the master mix (Table 2-15) was prepared in duplicate per each sample, containing a negative control to discard contamination of the mix components or DNA material. Reactions were set up in MicroAmp® optical 96-well reaction plates and sealed with MicroAmp® optical adhesive films, then run using the thermic profile described in Table 2-16. Primer efficiencies were confirmed to be within the 90-110% recommended efficiency range using qPCR reactions with 2-fold serial dilutions of cDNA. For each gene of interest, mRNA levels were calculated relative to housekeeping act1 (TGGT1_209030).

Table 2.10-1. qPCR master mix

Component	Volume (μ l)
Maxima SYBR® green (2X)	6.25
Fw primer	0.5
Rv primer	0.5
Nuclease free H2O	4.25
Template [50ng]	1

Table 2.10-2. qPCR thermic profile

Temperature	Time	Cycles
50°C	2 min	
95°C	10 min	
95°C	15 sec	} x40
60°C	1 min	

2.10.4 Polymerase chain reaction

PCR was used in this study for different purposes: to amplify DNA fragments for molecular cloning, for colony screening in transformed bacteria, and to test genetically modified *T. gondii* strains for correct integration of transfected DNA in the parasite genome.

To reduce the occurrence of mutations, high fidelity polymerases with proof-reading activity were used for molecular cloning. Q5® High-Fidelity DNA Polymerase (NEB) was mainly used in this study. Mix preparation and thermic profiles are listed in Tables 2-17 and 2-18.

Table 2.10-3. Q5®Taq reaction

Component	Volume (μl)
5X Q5 Reaction Buffer	5
10mM dNTP Mix	0.5
10 μM Fw primer	1.25
10 μM Rv primer	1.25
Q5® Taq DNA pol	0.25
Template (10-50 ng)	1
H ₂ O	To 25

Table 2.10-4. Q5® Taq amplification thermic profile

Temperature	Time	Cycles
98°C	30 sec	} X30
98°C	10 sec	
50°C-72°C*	30 sec	
72°C	30 sec/kb [^]	
72°C	5 min	
4°C	indefinitely	

(*) Calculated based on primers T_m

([^]) Calculated based on amplicon size

Taq DNA polymerase (NEB) was used to amplify products for colony screening and analytical purposes. PCR reaction and thermal cycler conditions are listed in Tables 2-19 and 2-20.

Table 2.10-5. Taq DNA polymerase PCR reaction

Component	Volume (μl)
10X ThermoPol buffer	2.5
10mM dNTP Mix	0.5
10 μM Fw primer	0.5
10 μM Rv primer	0.5
Platinum® Taq DNA pol	0.125
Template (>1000 ng)	1
H ₂ O	To 25

Table 2.10-6. Taq DNA polymerase thermic profile

Temperature	Time	Cycles
95°C	30 sec	

95°C	30 sec	} X30
45°C-68°C*	60 sec	
68°C	1 min/kb [^]	
68°C	5 min	
4°C	indefinitely	

(*) Calculated based on primers T_m

([^]) Calculated based on amplicon size

2.10.5 Agarose gel electrophoresis

Agarose gel electrophoresis was used to separate DNA fragments and amplicons according to their size (Lee et al., 2012). Gels were prepared diluting agarose (0.8 - 2%) in 1X TAE (W/V) by boiling in a microwave; to visualise the bands, 0.01% GelRed was added. Sample DNA was mixed with 6x DNA loading dye and loaded into the wells; 5 µl of 1 kb plus DNA ladder (Thermo Scientific™) was used as a reference. Agarose gels were run in an electrophoresis chamber filled with 1X TAE for 1 hour at 100 V. The DNA was visualised using a UV trans illuminator.

2.10.6 Restriction endonuclease digest

DNA digestion with restriction endonucleases was used throughout this study for molecular cloning, plasmid verification and linearization of constructs for transfection. All restriction enzymes and buffers were supplied by NEB®; reactions were usually carried out for 3 hours.

For molecular cloning, 3 µg of PCR product or 0.5 µg of plasmid were digested with the appropriated restriction enzymes according to specifications of the manufacturer.

Plasmid DNA isolated from the bacteria was verified using diagnostic digests, using 100 ng of DNA.

For stable transfections, plasmids were linearized with a single cutting enzyme; moreover, certain plasmids were double cut to dispose of the backbone. For transfections in BioRad® electroporator, 60 µg of the plasmid of interest was

digested. For Amaxa[®] transfections, 20 µg the plasmid of interest was digested following manufacturer's directions.

2.10.7 Dephosphorylation of digested DNA plasmids

For molecular cloning, the digested plasmids were treated with alkaline calf intestinal phosphatase (CIP), which mediates the dephosphorylation of the 5' end of DNA, to prevent the re-ligation of the backbone. Incubation of 10 U/µl (0.5 µl) of CIP with the sample at 37°C for 1 hour is enough to treat the plasmids before purification.

2.10.8 Purification of DNA

After running the digested plasmid in agarose gels, purification of DNA bands was performed using the QiAquick gel Extraction kit. The desired band was cut from the agarose gel using a sterile scalpel blade over a UV transilluminator. The piece of agarose containing the band was weighed, extracted following the specifications of the manufacturer, and eluted in 10 µl H₂O. 0.5 µl elution was run on an agarose gel to assess contamination with other DNA fragments.

2.10.9 Determination of nucleic acid concentrations

Nucleic acid concentrations were determined using a nanodrop spectrophotometer to measure absorbance at 260 nm, and to check for the presence of proteins or other chemical contaminants (Desjardins and Conklin, 2010).

2.10.10 Ligation of DNA fragments

To obtain covalent binding of insert and plasmid backbone for molecular cloning, T4 DNA ligase (NEB[®]) was used. This enzyme catalyses the formation of phosphodiester bonds between the 5' phosphate and 3' hydroxyl ends in dsDNA. Reactions were performed by mixing the backbone and the insert at a molar ratio of 1:3; 50 ng of backbone were used. 1 µl of T4 DNA ligase Buffer, 1 µl of T4 DNA Ligase and H₂O were added in a final volume of 10 µl. Ligations were incubated overnight at room temperature.

2.10.11 Plasmid transformation into bacteria

The ligation reaction was transformed in chemically competent *E. coli* to amplify the desired plasmid. Bacterial recipients were thawed on ice; 50 µl of bacteria were used per reaction. Bacteria were mixed with 5 µl of the ligation reaction and incubated together for 30 min; after this time, they were heat shocked at 42°C for 30 sec, and returned to ice for 2 min. 450 µl of NZY rich broth was added, and bacteria were left to recover for one hour at 37°C shaking. They were subsequently plated on LB-ampicillin agar plates, and incubated at 37°C overnight. Colonies were screened by analytical digest or by colony PCR; positive colonies were cultured by shaking in LB broth at 37°C overnight.

2.10.12 Isolation of plasmid DNA from bacteria

To extract plasmid DNA from bacteria, overnight grown cultures were pelleted by centrifugation, and the pellet was resuspended in a buffer containing EDTA and RNase A. Bacteria were subsequently lysed using a lysis buffer containing SDS and NaOH, which breaks the cells open and denatures proteins. Moreover, NaOH disrupts the hydrogen bonding between DNA bases, separating the double-stranded DNA into single-stranded DNA. Next, the lysis step is stopped using a solution containing potassium acetate, which neutralizes the alkaline conditions of the lysis buffer; in this environment, hydrogen bonds can reform, allowing the small, single strands of the plasmid DNA, but not the longer strands of the bacterial genomic DNA, to reanneal. The high concentration of salts precipitates the cellular debris; by high-speed centrifugation, all unwanted contaminants from the lysis will be pelleted, thus yielding a solution containing the plasmid DNA. From this point, plasmid DNA was purified by using silica columns provided in QiAprep spin Miniprep and Midiprep kits (Qiagen®). Alternatively, ethanol precipitation was used to obtain large amounts of plasmid. In this case, ethanol 100% was added after centrifugation. The precipitation was facilitated by keeping the mix at -80°C for 30 min or -20°C overnight. DNA and ethanol 100% were separated by ultracentrifugation, followed by a washing step with ethanol 70%. Finally, plasmid DNA was eluted in 100 µl ddH₂O, yielding around 500 µg to 1 mg of DNA material.

2.10.12.1 Small scale DNA plasmid extraction

When relatively small amounts of DNA plasmid yields were required, plasmid DNA was purified by QiAprep spin Miniprep (Qiagen®). For this, colonies containing the plasmid of interest were grown overnight in 4 ml of LB broth shaking. After this time, cells were lysed as described above, and DNA extracted using QiAprep spin Miniprep kit (Qiagen®) following the manufacturer's protocol. The DNA material was eluted in a final volume of 50 µl in ddH₂O, yielding around 5-20 µg of plasmid.

2.10.12.2 Medium and large scale DNA plasmid extraction

Large amounts of plasmid DNA are required for parasite transfection; for this reason, cells containing the final plasmids were grown overnight in 50 ml LB broth shaking. Bacteria were pelleted by centrifugation and plasmid DNA was extracted by following QiAprep spin Midiprep kit (Qiagen®) specifications. This protocol yields between 50 and 300 µg of plasmid DNA diluted in a final volume of 200 µl in ddH₂O.

2.10.13 DNA sequencing

DNA sequencing was used to verify inserts and final vectors prior transfection. DNA samples were prepared under specifications of GATC® Biotech in a final volume of 10 µl containing 5 µl of purified DNA [80-100 ng/µl], and 5 µl of primer [5 pmol/µl].

2.10.14 Cloning performed in this study

All primers used in this study are listed in Table 2-11.

To generate the plasmid TgDrpC-YFP LIC, the C-terminal part of the gene was amplified using the primers DrpC-LIC fw and DrpC-LIC rev; the resulting PCR product was inserted into the plasmid pLIC-YFP by ligation independent cloning (Huynh and Carruthers, 2009a, Fox et al., 2009).

The parental strain p5RT70-DD-GFP-DrpC_wt (previously generated by Manuela Pieperhoff) was modified with Q5 modification kit (New England BioLabs,

Catalog number E0554S) to delete the DD cassette, and obtain the plasmid p5RT70-GFP-DrpCwt, using primers Q5wt-fw and Q5wt-rev. Similarly, the vectors p5RT70-DD-GFP-DrpCDN and p5RT70-DD-GFP-DrpCGTPase only were obtained through modification of the p5RT70-DD-GFP-DrpCwt plasmid, using the primers Q5DN-fw and Q5DN-rev, and Q5GTPase only-fw and Q5GTPase only-rev, respectively.

To generate the plasmid p50RT70-DD-GFP-DrpCtruncated, DrpC cDNA was amplified using oligonucleotides DD-DrpCtruncated-fw and DD-DrpCtruncated-rev, respectively. Subsequently, ligation through NsiI-NotI restriction into the parental vector p5RT70-DD-myc-GFP-HX was performed.

The plasmid p5RT70-DD-mCherry-HA-Fis1 was generated by amplifying Fis1 coding sequence with primers DD-Fis1-fw and DD-Fis1-rev; the PCR product was inserted in the parental vector p5RT70-DD-mCherry-HA-HX via AvrII/PacI cloning.

To generate the plasmid Tet07-Sag1-Fis1, Fis1 5'UTR was amplified with primers Fis5'-fw and fis5'-rev, and the N-terminus of Fis1 was amplified with primers Fis N-terminus-fw and FisN-terminus-rev. All fragments were cloned into the parental vector Tet07-Sag1-HX, and the linearised plasmid was transfected in the strain *TAT1ΔKu80ΔHX*.

For p50 ablation, a plasmid containing the coding sequence of mAID in frame with a HA epitope tag, and followed by the 3'UTR of the DHFR gene (Brown et al., 2017), was amplified with the primers p50-mAID-HA-fw and p50-mAID-HA-rev. To facilitate tagging, this PCR product was co-transfected with the vector pTOXO_Cas9-CRISPR (Curt-Varesano et al., 2016), which expresses Cas9 under a constitutive promoter, and harbours the TgU6 promoter upstream of the single guideRNA (sgRNA) cloning site (BsaI). Oligonucleotides p50 gRNA-fw and p50 gRNArev were cloned using the Golden Gate strategy.

2.10.15 Ethanol precipitation

Verified and purified final vectors were precipitated using ethanol prior transfection. For this, plasmid DNA was mixed with 1/10 of 3M sodium acetate (pH 5.2), and 3 volumes of ice-cold 100% ethanol. Plasmids were precipitated by

centrifugation at 13,000 rpm at 4°C for 30 min, followed by two washes with 70% ethanol to remove salts. Ethanol was discarded and the pellet was air-dried before resuspending it in either cytomix or P3 buffer, depending on the electroporator used (BioRad® or Amaxa®, respectively).

2.11 Cell biology

2.11.1 *Toxoplasma gondii* tachyzoites and mammalian cells *in vitro* culturing

Toxoplasma gondii tachyzoites were grown in human foreskin fibroblast monolayer (HFF), cultured in Dulbecco's modified Eagle's medium (DMEM), which was supplemented with 10 % fetal bovine serum (FBS), 4 mM L-Glutamine and 10 µg/ml gentamycin. Cells were grown at 37°C and 5% CO₂ in a humidified incubator. Parasites were maintained by passing extracellular tachyzoites to fresh confluent HFF monolayers; alternatively, intracellular parasites were artificially released from their vacuoles. In the latter case, the HFF monolayer was scratched with a cell scraper, and host cells were lysed by passing them through a 23 G needle three times. The volume of parasites passaged varied according to the experiment to perform.

2.11.2 Trypsin/EDTA treatment of mammalian cell lines

HFFs were split 1:4 weekly by Matthew Gow. Cell splitting was performed using trypsin protease to detach cells from the bottom of the culturing flasks. Host cells were washed three times with 1XPBS to remove all residual media, trypsin/EDTA was added to cover the monolayer, and culturing flasks were left at 37°C for 5 min. At this point, flasks were tapped to facilitate detachment. The reaction was stopped by adding DMEM_{COMPLETE} to a volume 1:4 to pass the cells to new containers.

2.11.3 Cryopreservation of *T. gondii* and thawing of stabilates

To generate parasite stabilates, large intracellular vacuoles were frozen in cryotubes. To this end, host monolayers heavily infected with *T. gondii* were gently scratched using a cell scraper, and pelleted by centrifugation. Pellets were resuspended in 750 µl DMEM and an equal volume of 2x freezing media

(Table 2-8); the suspension was transferred to 2 ml cryotubes, which were immediately put at -20°C. Subsequently, cryotubes were transferred to a -80°C freezer where they can be stored for several weeks; however, storage in liquid nitrogen is necessary for long term preservation.

Frozen *T. gondii* stabilates were thawed at 37°C, and parasites added to confluent host cells. The next day, fresh media was added to help their recovery.

2.11.4 Transfection of *T. gondii*

In *T. gondii*, electroporation is used to achieve transient or stable transfection of exogenous DNA (Soldati and Boothroyd, 1993b); throughout this study, transfections were performed using either BioRad or Amaxa electroporators. These machines differ in efficiency and buffers required. BioRad electroporator yields up to 30% transfection efficiency, and uses a homemade buffer called cytomix (Table 2-8) which mimics intracellular ion composition. In contrast, Amaxa nucleofactor works with commercially available buffer P3, and yields up to 90% transfection efficiency.

2.11.4.1 Transient transfections

Transient transfections are used in *T. gondii* to express circular exogenous DNA; the circular plasmid is not integrated in the genome, but stays extra-chromosomal and is lost after a series of cell divisions (Suarez et al., 2017). Transient transfections were performed using Amaxa equipment to achieve high transfection efficiency. Briefly, 10⁶ parasites were pelleted and resuspended in Lonza P3 buffer. At the same time, 10-20 µg of plasmid DNA were precipitated, and the pellet was resuspended with 50 µl of Lonza® P3 buffer. The two components were mixed in an electroporation cuvette. Following transfection, parasites were inoculated onto HFFs grown on coverslips and incubated between 24 and 72 hours prior to fixation and analysis.

2.11.4.2 Stable transfection

Stable transfection techniques rely on the targeted or random insertion of DNA into the parasite genome. As discussed in paragraph 1.4, random integration of

exogenous DNA in *T. gondii* is facilitated by the action of the parasite non-homologous end joining (NHEJ) repair mechanism, which is mediated by the Ku80 enzyme (Donald and Roos, 1993).

In this study, overexpression vectors were randomly integrated in *T. gondii* genome using BioRad electroporator. 60 µg of plasmid DNA were linearized; after checking complete linearization by gel electrophoresis, the DNA was precipitated and dissolved in 100 µl of Cytomix. 10^7 parasites were resuspended in 640 µl of cytomix, to which 30 µl ATP (100 mM) and 30 µl GSH (100 mM) were added. DNA and parasites were subsequent mixed, and 10 units of the restriction enzyme used for linearization were added to the transfection mix before electroporation. This technique, called restriction enzyme mediated insertion (REMI) is used to increase transfection efficiency: REMI was shown to activate the DNA repair machinery, and results in elevated recombination event (Black et al., 1995).

Stable transfections based on homologous recombination between the parasite genome and homology sequences in a plasmid are carried out in $\Delta ku80$ parasites: as this parental strain is not able to use the NHEJ repair mechanism, transfection efficiency of endogenous tagging and gene replacements constructs is highly increased (Huynh and Carruthers, 2009, Fox et al., 2009).

In this study, the line *DrpC-YFP* was obtained through linearization and transfection of 30 µg of the plasmid *DrpC-YFP* in the strain $\Delta ku80$, using BioRad electroporator. To generate the line *Tet07-Sag1-Fis1*, 20 µg of the plasmid *Tet07-Sag1-Fis1* were linearised and transfected with the Amaxa electroporator in the parental strain *TATI $\Delta ku80\Delta HX$* . The strain *p50-mAID-HA* was obtained through co-transfection of 20 µg of p50 gRNA plasmid and the PCR product (see paragraph 2.10.14) with Amaxa electroporator.

2.11.4.3 Drug-mediated positive selection

After transfection, drug selection is necessary to enrich transfected parasites in the pool. Several markers have been developed in *T. gondii*; in this study, parasites were either selected in presence of 25 mg/ml mycophenolic acid and 40 mg/ml xanthine (which select for HXGPRT resistance cassette) (Donald and

Roos, 1993), or by using 1 μ M pyrimethamine for the dihydrofolate reductase-thymidylate synthase allele DHFR-TD (Donald et al., 1996).

2.11.5 Isolation of clonal parasite lines by limited dilution

The isolation of stable, clonal parasite lines was obtained through limited dilution of a stable pool on a 96 well plate. After 5-7 days, plaques were formed in the host cell monolayer; wells with one plaque indicate a single parasite clone, because only one parasite was initially present in this well. Clonal populations were transferred to 24 well plates, and checked by immunofluorescence analysis, Western Blot and integration PCR.

2.12 Tachyzoite phenotypic analysis

2.12.1 Immunofluorescence assay

Immunofluorescence analysis (IFA) was used to determine localisation of proteins and to assess expression of mutants. For immunofluorescence analysis, HFF cells grown on cover slips were inoculated with *T. gondii*; infected HFF monolayers were fixed in 4% paraformaldehyde for 20 min at room temperature, and washed once with PBS. Next, coverslips containing parasites were blocked for 40 min in permeabilising conditions (0.2% triton X-100, 2% BSA in 1X PBS). Probing with primary antibodies was performed for 60 min in a wet chamber: coverslips were placed upside down into a petri dish that contained wet paper towel, parafilm and 30 μ l drops of primary antibody diluted in blocking solution. Afterwards, coverslips were washed 4 times and incubated with secondary antibodies in blocking buffer for 1 hour. Finally, coverslips were washed 4 times with PBS, and fixed using Fluoromount™ containing DAPI. All procedures were performed at room temperature.

2.12.2 Plaque assay

1×10^3 parasites were inoculated on confluent HFF monolayers grown in 6-well plates. The plates were incubated at 37°C, 5% CO₂ for 7 days. After this time, monolayers were gently washed once in PBS and fixed with cold methanol for 20 min. Fixative was removed and cultures were stained with Giemsa (1:10 in H₂O)

for 45 min, then washed three times with PBS. Images were acquired using Axiovert 40 fluorescence microscope with AxioCam. When required, plaque size was measured using ImageJ software and normalized to the appropriate control.

2.12.3 Replication assay

1×10^5 tachyzoites were inoculated onto HFF monolayers grown on glass coverslips. Infection was allowed under normal growth conditions for 1 hour; after this time, coverslips were washed in PBS to remove extracellular parasites and therefore synchronise replication. Parasites were allowed to replicate under standard culturing conditions for 24 hours prior fixation. Samples were labelled using α IMC1; 100 vacuoles were counted, and categorised by number of parasites contained in each vacuole (2, 4, 8, 16, >32). Numbers were expressed as percentage. Assays were done in triplicate in three independent experiments.

2.12.4 Time-lapse video microscopy

Video microscopy was conducted with the DeltaVision Core microscope, equipped with a temperature and gas control chamber which was used to maintain culture conditions (37°C and supplying 5% CO₂). Parasites were grown in glass bottom live cell dishes (Ibidi μ -dish^{35mm-high}). Obtained videos were analysed using SoftWoRx® or Fiji software.

2.13 Biochemistry

2.13.1 Preparation of parasite cell lysates

10^7 parasites were used for Western Blot analysis. Parasites were scratched and syringed, filtered and pelleted by centrifugation at 1500 g for 5 min at 4°C, then washed twice in cold PBS. Subsequently, parasites were resuspended and counted; then, the volume containing around 1×10^7 parasites was pelleted and the supernatant was removed. Parasite pellet was lysed on ice (to prevent protein degradation) with 8 μ l RIPA buffer (see Table 2-6) for 5 minutes; the insoluble material was subsequently removed by centrifugation at 4 °C for 10 minutes at maximum speed. The supernatant was transferred to a fresh

Eppendorf with 1.2 µl reducing agent (Invitrogen©) and 3 µl NuPage® 4x loading dye. Samples were boiled for 10 minutes at 95 °C.

2.13.2 Sodium dodecyl sulphate polyacrylamide gel electrophoresis

Protein separation was achieved by sodium dodecyl sulphate polyacrylamide gel electrophoresis (SDS-PAGE) (Laemmli, 1970). SDS-polyacrylamide gels were made in a 1.5 mm thick glass cassette at 8% .APS and TEMED were used to catalyse polymerisation; therefore, they were added right before the gels were poured. The resolving gel (see Table 2-6) was first poured, and isopropanol was added on top, to avoid uneven polymerization in the gel upper surface; after its polymerisation, the stacking gel mix was added on top, together with a 10-well comb. Gel cassettes were assembled in the Bio-Rad© mini-PROTEAN® Tetra Cell with 1 x SDS running buffer; parasite lysates were loaded, and 2µl Chameleon™ Duo protein ladder (Li-COR) was included to assess gel migration and protein size. Samples were run at 90 V for 10 minutes through the stacking gel, then the voltage was increased to 120 V (for 50 minutes) for separating the proteins in the resolving gel.

2.13.3 Western blotting

For Western blotting, proteins were transferred from the polyacrylamide gel to Hybond® ECL™ nitrocellulose membranes (Sigma-Aldrich®), by using a wet transfer method. To this end, membrane and gel were “sandwiched”, on each side, by 3xWhatman filter paper and a foam pad; everything was pre-soaked in transfer buffer. This assembly was placed in Bio-Rad© mini-PROTEAN® Tetra Cell and submerged with transfer buffer (See Table 2-6). Protein transfer was performed at 100 V for 60 minutes on ice in a cold room to prevent overheating.

2.13.4 Ponceau-staining

Protein transfer to the membrane was verified by Ponceau staining. Membranes were stained with Ponceau S solution for 5 min at RT, shaking. After visualization, the dye was removed by washing twice with PBS for 5 min.

2.13.5 Immunostaining

Membranes were blocked for 1 hour in 3% skimmed milk in PBST (see Table 2-6) at room temperature while shaking. Afterwards, membranes were incubated overnight at 4°C in a wet chamber with the primary antibody diluted in 1 mL blocking buffer. Afterwards, membranes were washed three times with PBST, and finally incubated with the secondary antibody (IRDye® LiCor®) diluted in 6 mL blocking buffer for 1 hour while shaking. Finally, the membranes were washed three times in PBST and twice in PBS.

2.13.6 Visualisation and quantification of the protein bands

Proteins were detected using the Li-Cor® Odyssey® equipment. This system allows highly accurate quantitative infrared detection of the protein of interest.

2.13.7 Stripping

Membranes can be re-probed by removing previous antibodies. This was achieved by incubating membranes in Li-COR® stripping buffer for 20 min shaking. Afterwards, membranes were washed three times in PBS to remove all the stripping buffer and detached antibodies, and at this point immunostaining could be performed again.

2.13.8 Immunoprecipitation

To find potential interactors of DrpC, immunoprecipitation experiments were performed on the strain *p5RT70-DD-GFP-DrpC^{wt}. RH-GFP* parasites were used as a control; experiments were performed in triplicate. Dynabeads™ Goat Anti-Mouse IgG (Invitrogen) beads were used in combination with Invitrogen™ DynaMag™ magnets.

Intracellular tachyzoites (1×10^9 parasites were used per condition) were incubated with 0.2 μM of Shld-1 for 4h, and then scratched and syringed. After filtering to avoid host cell contamination, parasites were counted, washed with PBS, and finally lysed in a salt buffer containing 50 mM TrisHCl pH 7.5, 50 mM Sodium Citrate, 0,1% CHAPS, 0,7% Nonidet P-40 (NP-40), and a phosphate inhibitor cocktail (P-5726). Lysis was carried out on ice for 20 minutes;

microscopy was used to make sure that parasites had been properly lysed. The samples were centrifuged at 15,000 g for 30 min (at 4°C). In the meantime, the magnetic beads Dynabeads™ Goat Anti-Mouse IgG (Invitrogen) were prepared. 50 µl of beads were used per reaction; after washing them with PBS, they were incubated in blocking solution (1 mL PBS-BSA 4%) for 15 minutes. Afterwards, they were treated with PBS-Tween 0.02% for 15 minutes, and finally incubated for 30 minutes in 1 mL solution containing 10 µl of α-GFP antibody (Mouse, Roche) (4 µg of antibody were used for 50 µl of beads) diluted in PBS Tween-20. GFP-conjugated beads were then crosslinked as per manufacturer instructions to avoid co-elution of the antibody, and finally incubated in the lysis buffer. At this point, the supernatant obtained after centrifugation of the parasite lysate was incubated with the GFP-conjugated beads for 1 h at 4°C while shaking. Afterwards, the beads were washed three times in the same buffer solution and antigens were eluted from the beads with 60 µl of elution buffer (20 mM TrisHCl, 2% SDS). Samples were boiled for 20 min at 72° before elution; NuPage and DTT were finally added to the eluate. Western Blot analysis was performed on the immunoprecipitation fractions, and the eluate for each pull-down was analysed by mass spectrometry.

2.13.9 Co-immunoprecipitation

To assess the putative interaction between Fis1 and DrpC, co-immunoprecipitation experiments were performed in the strain *DD-mCherry-HA-Fis1:: DrpC-YFP*.

DD-mCherry-HA-Fis1:: DrpC-YFP parasites was induced with 0.2 µM of Shield-1 for 4 hours, to obtain a weak overexpression of Fis1. The lysate was subjected to IP with beads conjugated with α-GFP antibody (as described in the previous paragraph). The eluate was used for Western Blot analysis, probing with α-GFP and α-HA antibodies to assess the presence of DrpC and Fis1, respectively.

2.14 Bioinformatics

2.14.1 Sequence alignments

DNA and protein sequences were aligned using BioEdit Sequence alignment editor, which was also used to check the chromatogram of sequenced samples.

DNA or amino acid sequences were searched and/or aligned using BLAST® local alignment tool (Altschul et al., 1990) available in either ToxoDB (<http://toxodb.org/toxo/>), UniProt (<https://www.uniprot.org/>) or NCBI (<https://blast.ncbi.nlm.nih.gov/Blast.cgi>) web pages.

2.14.2 Homology modelling

In order to construct a reliable homology for DrpC, BLAST+ was used to identify related sequences in the UniProt data base (The UniProt Consortium, 2016). The conserved N-terminal GTPase domain comprising of approximately 300 residues was then used to construct the homology model using SWISSMODEL (Bertoni et al., 2017, Biasini et al., 2014). All potential models were evaluated manually with the model based on PDB:3L43 determined at a resolution of 2.3 Å, which shares a sequence identity of approximately 22%, being the most reliable (30% over the GTPase domain.) Visual inspections, structural comparisons, least-squares superpositions and figures were prepared using Pymol (DeLano, 2002). This analysis was conducted by Dr. Ehmke Pohl, Durham University.

2.14.3 Data and statistical analysis

Primary data entry was done using Microsoft Excel and GraphPad Prism® 7.03. Statistical analysis was performed using GraphPad Prism® 7.03. When comparing two groups, the P value was calculated using an unpaired Student's t-test. When comparing multiple groups, the P value was determined using One-way ANOVA accompanied by Dunnet's multiple comparison test.

3 Characterisation of the Dynamin-related protein DrpC in *T. gondii*

Dynamins constitute a conserved superfamily of proteins performing a variety of essential roles, from membrane budding to organelle division and cytokinesis (Praefcke and McMahon, 2004). This superfamily includes classical Dynamins and Dynamin-related proteins; their mechanism of action is very similar, as all members are mechanochemical enzymes which polymerise around membranes and use GTP hydrolysis to catalyse membrane constriction. As discussed in paragraph 1.8, Dynamins are the major effectors of endocytosis, and are characterised by five domains; Dynamin-related proteins display a wider range of functions, and show only three of these domains: the GTPase, Middle and GED domains (Ramachandran, 2017).

Previous bioinformatics analyses have revealed that *T. gondii* encodes for two well conserved Dynamin-related proteins, DrpA and DrpB; DrpA plays an essential role in apicoplast division (van Dooren et al., 2009) while DrpB is required for secretory organelle biogenesis (Breinich et al., 2009) (see paragraph 1.8.2). DrpC, a protein which is only conserved in Apicomplexa, was identified as a third potential member of the Dynamin superfamily. While DrpA and DrpB display conservation of the three domains typical of Dynamin-related proteins (GTPase, Middle and GED regions), DrpC domain architecture is highly divergent. This protein is characterised by a large GTPase domain (Breinich et al., 2009, van Dooren et al., 2009, Purkanti and Thattai, 2015), but Middle and GED domains are not recognisable in its long, disorganised C-terminus.

DrpC was shown to be essential, as its depletion leads to parasite death (Pieperhoff et al., 2015), but no detailed functional analysis has been performed; here, I will illustrate how DrpC localisation and function was further characterised during my thesis project.

3.1 Generation and confirmation of the knock-in strain *DrpC-YFP*

DrpC localisation was assessed using an endogenous tagging approach developed in *T. gondii* by Huynh and Carruthers (Huynh and Carruthers, 2009b). The 3' genomic region of *DrpC* (not including its stop codon) was amplified and the resulting PCR product inserted into the plasmid LIC-YFP by ligation independent cloning (see paragraph 2.10.14); thus, a portion of *DrpC* C-terminal region is fused to YFP in the plasmid *DrpC-YFP*. This vector was transfected in the $\Delta ku80$ strain, where homologous integration is favoured (Fox et al., 2009, Huynh and Carruthers, 2009b), so that the region of homology in the construct recombined with the homologous sequences in the endogenous gene (Fig. 3-1a). Correct integration at the 3' end of *DrpC* was verified by analytical PCR on genomic DNA: two separate PCR reactions amplified specific amplicons in the strain *RH $\Delta ku80$ DrpC-YFP* (hereafter called *DrpC-YFP*), which were not amplified in the recipient strain (Fig. 3-1b). Western Blot analysis confirmed fusion of GFP at *DrpC* C-terminus, showing the expected band size of ≈ 160 kDa (Fig. 3-1c).

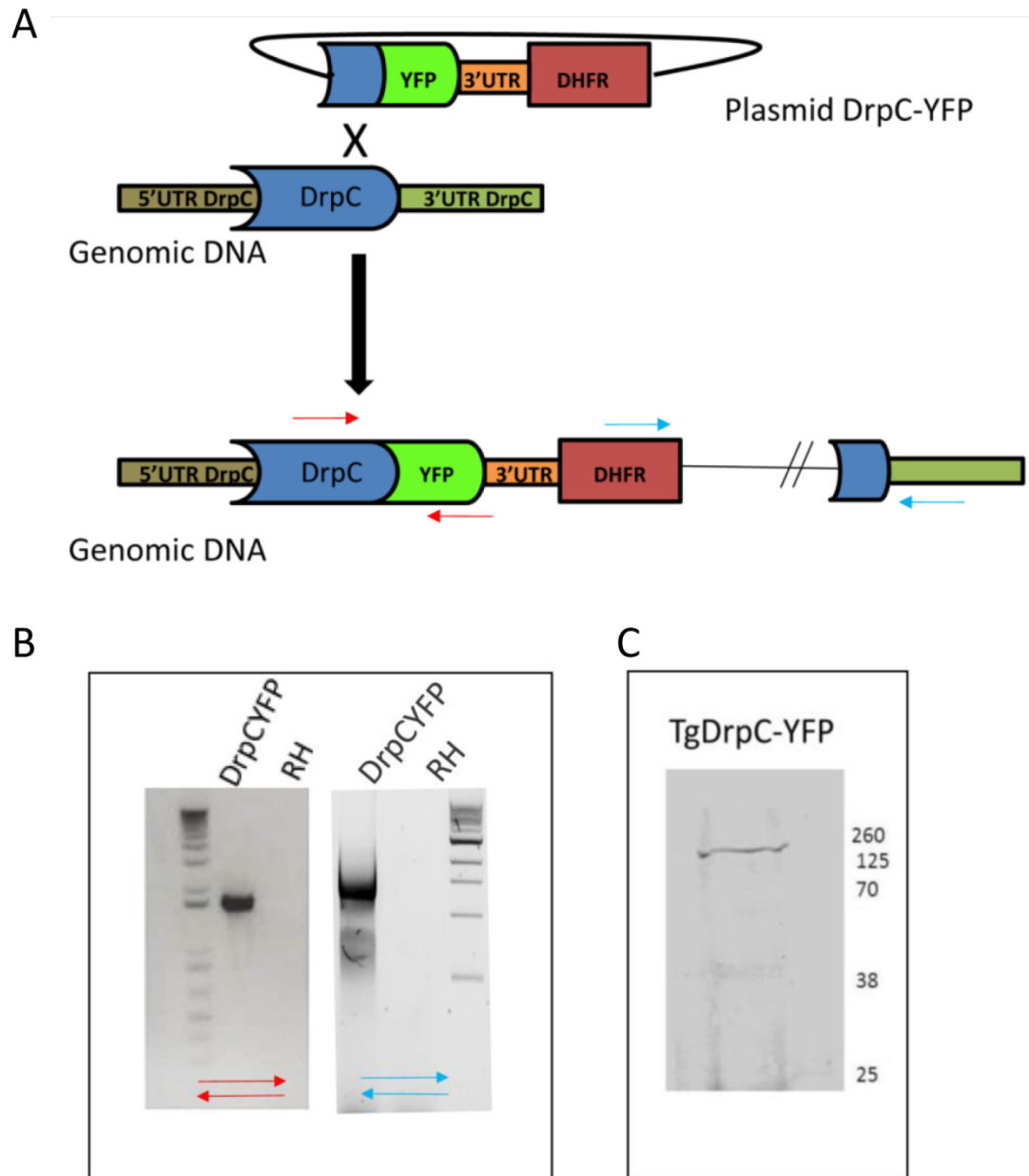


Figure 3-1: Endogenous tagging of DrpC

(A) Scheme of endogenous tagging strategy; a single crossover event allows genomic integration of *DrpC* fused to YFP; the plasmid contains a DHFR resistance cassette that allows selection of integrants. (B) Analytical PCR confirms correct integration in the *DrpC*-YFP strain; the two pairs of primers used (to confirm 5' and 3' integration) are indicated as red and blue arrows in (A) and (B). (C) Western blotting on the *DrpC*-YFP strain using α -GFP antibody shows the expected band for the fusion protein (≈ 160 KDa).

3.2 Analysis of DrpC localisation

To determine DrpC localisation in *T. gondii* intracellular tachyzoites, immunofluorescence analysis was performed on IFA plates inoculated with *DrpC-YFP* parasites; *RH* parasites were used as a control. As DrpC is not strongly expressed, α -GFP antibody was used. While in *RH* parasites no signal for YFP was detected, in the *DrpC-YFP* line a specific signal was found. DrpC-YFP has a distinct pattern of punctate structures distributed both along the periphery and at the basal part of the parasite; moreover, a faint but specific cytoplasmic signal is also detected (Fig. 3-2a). Further analysis revealed that DrpC puncta do not have a significant colocalisation with apicoplast, Golgi, rhoptries, micronemes, or the dynamin-related protein DrpB (Fig. 3-2b). Conversely, a distinct colocalisation with the mitochondrion was observed: quantification confirmed that most puncta of DrpC appear associated with the mitochondrial tubule (Fig. 3-2b and c), though some puncta seem associated with the parasite periphery, and not with the mitochondrion, as will be discussed later.

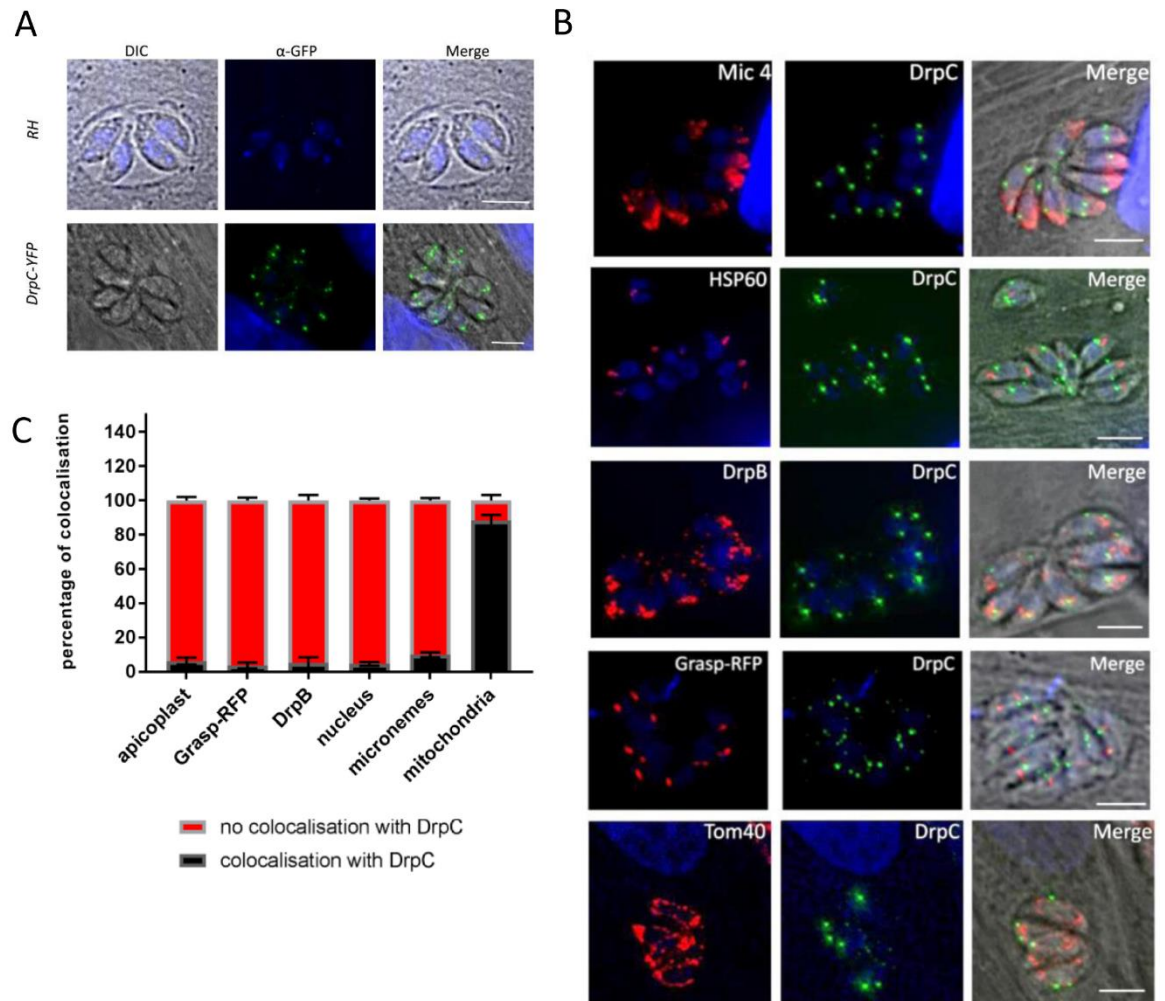


Figure 3-2: Localisation of DrpC

(A) IFA on *RH* and *DrpC-YFP* parasite lines reveals a specific YFP signal (green) in the latter strain. (B) Colocalisation analysis shows that DrpC does not colocalise to micronemes (Mic4, red), apicoplast (HSP60, red), Golgi (DrpB, red) and ER (Grasp-RFP). Conversely, co-staining with Tom40, a marker for the mitochondrial outer membrane, reveals an association between DrpC and the mitochondrion. Scale bars: 5 μ m. (C) Quantification of the colocalisation between DrpC and the indicated organelles: the analysis was carried by counting DrpC puncta that seemed to be coinciding with the signal of different organelles ($n=3$, 100 vacuoles counted per each condition).

Structured Illumination Microscopy (SIM) shows that the number and size of these structures are highly variable: at times, spiral-like structures of DrpC are visible around the mitochondrial tubule (Fig. 3-3a, upper inset), while in other cases the puncta are small and resemble dots (Fig. 3-3a, lower inset). 3D reconstructions confirm that the majority of puncta are in close proximity with the mitochondrion (Fig. 3-3b), concentrated both at the periphery and at the basal end of its outer membrane. As already described in Fig. 3-2c, a small but significant percentage of DrpC foci are found to not colocalise with the

mitochondrion (Fig. 3-3a); these puncta are usually at the periphery of the parasite, while at the basal end DrpC foci more consistently coincide with Tom40 signal.

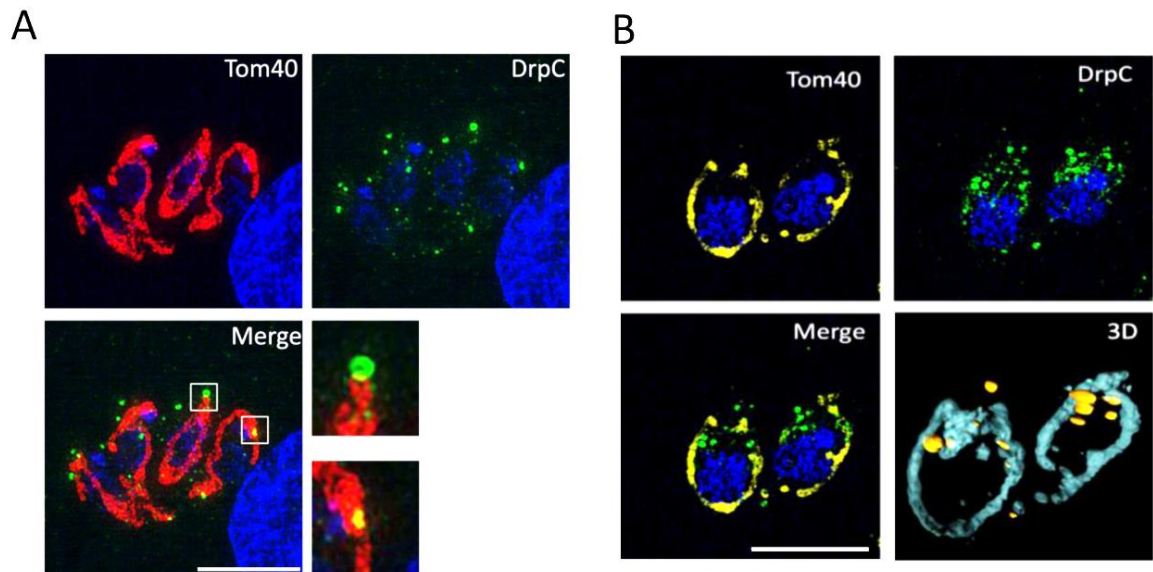


Figure 3-3: DrpC associates with the mitochondrion in *T. gondii*.

(A) SIM analysis on *DrpC-YFP* parasites, using α -GFP (green) and α -Tom40 (red) antibodies, shows that puncta on the mitochondrion can have different shapes: in some cases, a ring is seen on the membrane (upper inset), while other puncta form smaller dots. (B) 3D rendering confirms that the majority of DrpC puncta (in yellow) are at the mitochondrial membrane; this image was made by Leandro Lemgruber (cyan). Scale bars: 5 μ m.

To gain insight into the meaning of this interaction, DrpC localisation was analysed during endodyogeny and put in relation to mitochondria dynamics during parasite replication. Parasites were inoculated on IFA coverslips, the cultures were synchronised and then stopped after 4 hours, when most of the parasites were undergoing endodyogeny; IFA was performed using antibodies α -YFP (to assess DrpC localisation), α -Tom40 and α -tubulin (to assess mitochondria position and endodyogeny progression, respectively).

As previously discussed, mitochondria dynamics in *T. gondii* closely follow the cell cycle: the mitochondrion of the mother is replicated during endodyogeny and subsequently partitioned in the daughter cells (Nishi et al., 2008). As shown in Fig. 3-4a, when the daughter buds start to assemble (in white), the mitochondrion (in red) starts forming new branches; the signal of DrpC (in green) is associated with the new ramifications, and in some occasion it is possible to see that it encircles them (Fig. 3-4a, inset).

While the budding daughters' cytoskeleton continues to grow, the new mitochondrial branches remain associated with the mother; only towards the end of endodyogeny the mitochondrial branches associate with the basal end of the buds, and are subsequently inserted inside, as shown in figure 3-4b. From this stage, it is possible to observe two different population of DrpC puncta. In one group are the puncta which are recruited to the basal end of the budding parasites, colocalising to the mitochondrial bundle that is still outside of the daughter cells (Fig. 3-4b, asterisk); this population persists at the basal end of the organelle when the mitochondrial branches are completing their migration inside the daughter cells, as seen in Fig. 3-4c. As already discussed, mitochondria remain attached to each other at their base for a variable period of time, until the interconnections are cleaved to allow each daughter to acquire an autonomous, single organelle. In this stage, the concentration of DrpC puncta at the basal end colocalises with these mitochondrial interconnections (Fig. 3-4c, asterisk).

The second population of DrpC signal shows a very different localisation; when mitochondria are still largely outside the daughter cells, puncta of DrpC are not in contact with the mitochondrial membrane, but rather are at the periphery of daughter cells (Fig. 3-4b, arrowheads). This population is seen again in contact to mitochondrial branches once these have entered the buds and start encircling their periphery (Fig. 3-4c, arrowheads).

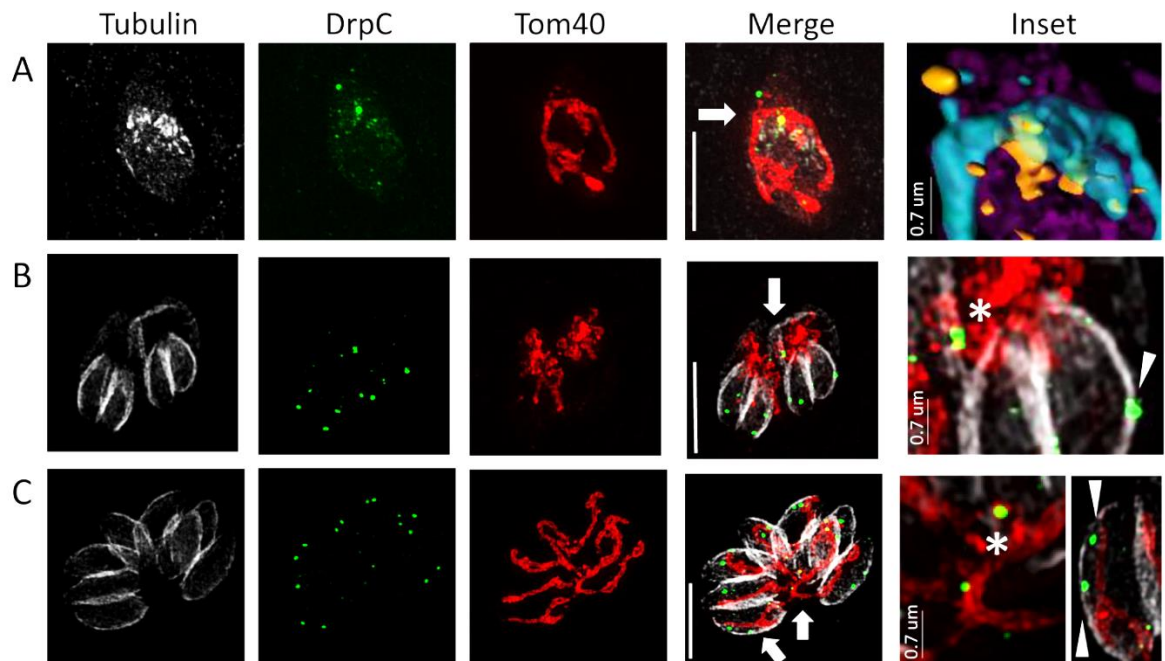


Figure 3-4: DrpC localisation in different stages of mitochondria replication and segregation.

(A) At the start of daughter cell formation (grey), the mitochondrion (in red) starts forming new branches; the signal of DrpC (in green) is associated with these ramifications. In the inset, the same picture is showed with 3D rendering, to show DrpC (in yellow) half-encircling the mitochondrial membrane (cyan). (B) When buds are almost completely formed, the mitochondria enter them from their basal end. At this stage, DrpC signal is visible both at the basal end of the parasite, colocalising with the mitochondrion (asterisk in the inset), but also at the periphery of the parasite, seemingly in close proximity to the cytoskeleton (arrowhead in inset). (C) Once the mitochondria have entered the buds, they migrate till they fully encircle the parasites periphery. The DrpC puncta that in the previous stage seemed in contact to the cytoskeleton are now in close proximity to the extending mitochondrial branches (arrowheads). At this stage, the mitochondria in the vacuole are still interconnected between each other; the second population of DrpC puncta colocalises with the interconnections (asterisk). Vacuoles were stained with α -tubulin, α -GFP and α -Tom40 antibodies. Arrows highlight the regions that are shown at a higher magnification in the insets. Scale bars are = 5 μ m, unless otherwise stated in the figure.

The localisation of DrpC puncta at the interconnections is very intriguing, as it is highly reminiscent of the mitochondrial recruitment observed in other eukaryotes for Drp1 and Dnm1, Dynamin-related proteins which are important for mitochondrial fission (Pagliuso et al., 2018). Thus, the behaviour of DrpC in the last phases of endodyogeny, in particular in the stages when the interconnected mitochondria are finally cleaved, needed to be more investigated.

To this end, the *DrpC-YFP* strain was transfected with the plasmid TdTomato-TGME49_215430, as verified by Western Blot analysis (Fig. 3-5a). In this construct, a strong promoter drives the expression of the Outer Mitochondrial

marker TGME49_215430 fused to the fluorescent protein tdTomato (Ovcariikova et al., 2017); thus, in the strain *DrpC-YFP::TdTomato- TGME49_215430*, the localisation of DrpC and of the mitochondrion can be followed by live microscopy.

As shown in Fig. 3-5b, we focused on parasites at the last stages of replication, which present mitochondria that are still interconnected at the basal end. In the example movie shown, two DrpC puncta are visible at the periphery of the mitochondrion, and their localisation is quite static; conversely, the two puncta at the basal connection between the two mitochondria (time point 00:20) are highly dynamic. At time point 00:40, one of the DrpC foci coincides with a constriction of the mitochondrial membrane, which goes on to be cleaved in this region (time point 1:24); at 1:27, DrpC is now at the terminal end of the mitochondria tubule, as a result of the cleavage of the interconnection. The puncta remain at the basal end of the newly formed parasites even after the interconnections have been cleaved.

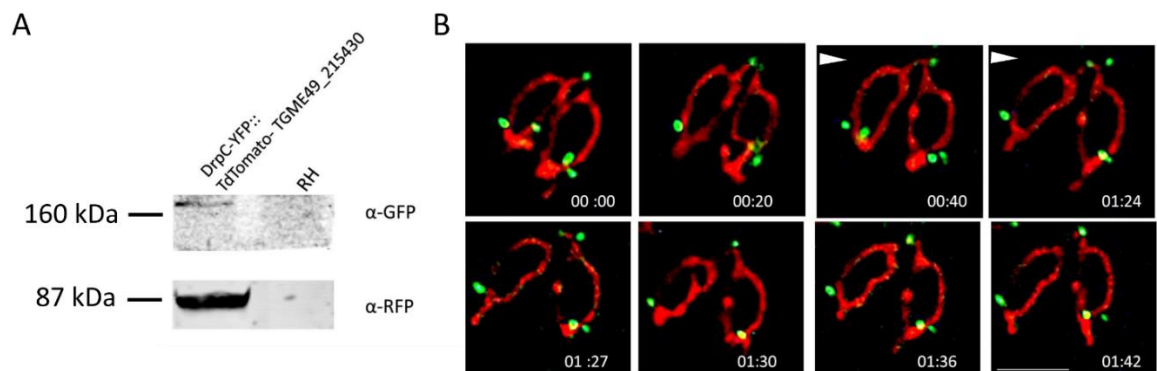


Figure 3-5: Analysis of the dynamic localisation of DrpC during mitochondrial fission.

(A) Western blot analysis using the antibodies reported in the figure confirms the generation of the *DrpC-YFP::TdTomato- TGME49_215430* strain, where the plasmid TdTomato-TGME49_215430 (probed with α -RFP antibody) is randomly integrated in the genome of the *DrpC-YFP* strain. (B) Time-lapse analysis on the same strain illustrates dynamic localisation of DrpC during the last stages of mitochondria fission (in red, TGME49_215430-tdTomato; in green, DrpC-YFP). TgDrpC is at the mitochondria periphery and at the basal interconnection; the signal at the basal end is highly dynamic and localises to region of constriction and fission of the mitochondrial membrane. Time is indicated in minutes. Scale bar: 5 μ m.

These observations were confirmed by SIM analysis performed on the *DrpC-YFP::tdTomato-TGME49_215430* strain, choosing replicating vacuoles of different size (two-, four- or eight- parasite stages) where the mitochondria are interconnected (as TGME49_215430 is fused to the fluorescent protein TdTomato, no antibody is necessary to visualise the signal of this outer mitochondrial membrane marker in this strain). As shown in Fig. 3-6, multiple puncta of DrpC are visible at the interconnections of the mitochondria; in some cases it is possible to notice the invagination and what seems like a constriction of membranes colocalising with DrpC signal.

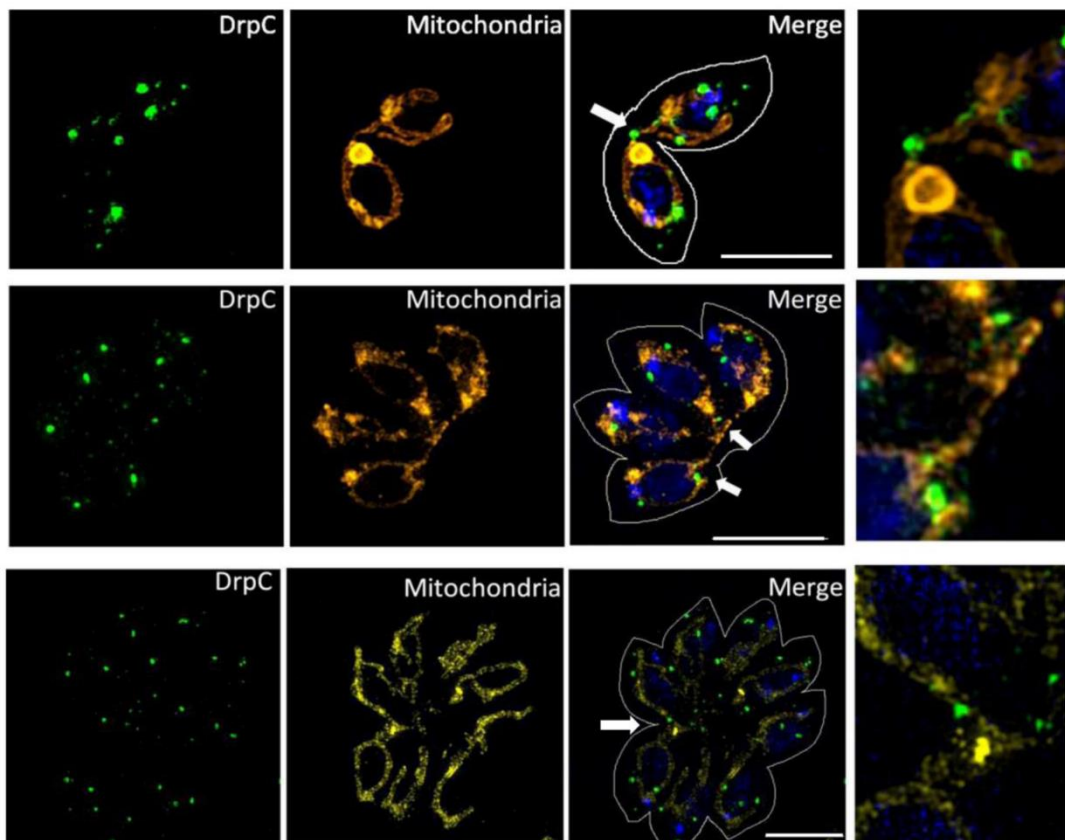


Figure 3-6: DrpC puncta colocalise with mitochondrial interconnections

DrpC signal (in green, α -GFP) was imaged with SIM microscopy in parasites presenting interconnected mitochondria (in yellow, TdTomato- TGME49_215430). Arrows indicate regions that are enlarged in the insets. The signal of DrpC at the basal ends coincides with the interconnections, and at times a constriction is observable at these foci. Scale bars: 5 μ m.

3.3 Analysis of DrpC knockdown

In a previous study, a DiCre-U1 knockdown strategy was successfully used to obtain the downregulation of DrpC in the *DiCre Δ ku80* parental strain (Pieperhoff et al., 2015). As shown in Fig. 3-7a, *DrpC* genomic locus in the *RH Δ ku80DiCre*

DrpC-HA-U1 line (which will be called hereafter *DrpC-HA-U1*) is modified so that *DrpC* is fused at its 3' to an HA epitope tag, which is followed by a floxed region containing *Sag1* 3'UTR and a resistance cassette; four U1 sequences are placed downstream of this region. When Rapamycin is added, DiCre recombinase is reconstituted; its activity leads to excision of the loxP-flanked region downstream of the modified *DrpC* locus. As a result, the U1 sequences are translocated close to the stop codon of *DrpC*, thus mediating degradation of its mRNA (for more detail, see introduction paragraph 1.4.1).

Pieperhoff et al. showed that the excision event was highly efficient, and that it results in downregulation of *DrpC* in the strain *DrpC-HA-U1*. Further characterisation was needed to understand the role of this protein.

In my analysis, *DrpC* knock-down in the *DrpC-HA-U1* strain was analysed both at mRNA and protein levels. qRT-PCR showed that mRNA levels of *DrpC* are significantly downregulated 72 hours after Rapamycin treatment, as shown in Fig. 3-7b: comparing Rapamycin-induced *DrpC-HA-U1* with *RH* (Wild-type) parasites, a reduction of more than 80% in *DrpC* transcript levels is seen. It was also found that tagging of *DrpC* results in significantly reduced mRNA levels prior to Rapamycin induction, an effect that was seen in other cases where this strategy was applied; it is proposed that this is due to integration of loxP sequences within the 3'UTR (Pieperhoff et al., 2015). This however does not affect viability of this strain in absence of Rapamycin, as shown by plaque assay (Fig. 3-7d).

Western Blot analysis probing with α -HA antibody confirmed efficient Rapamycin- induced *DrpC* downregulation: after 72 hours of induction, α -HA signal is no longer detected (Fig. 3-7c).

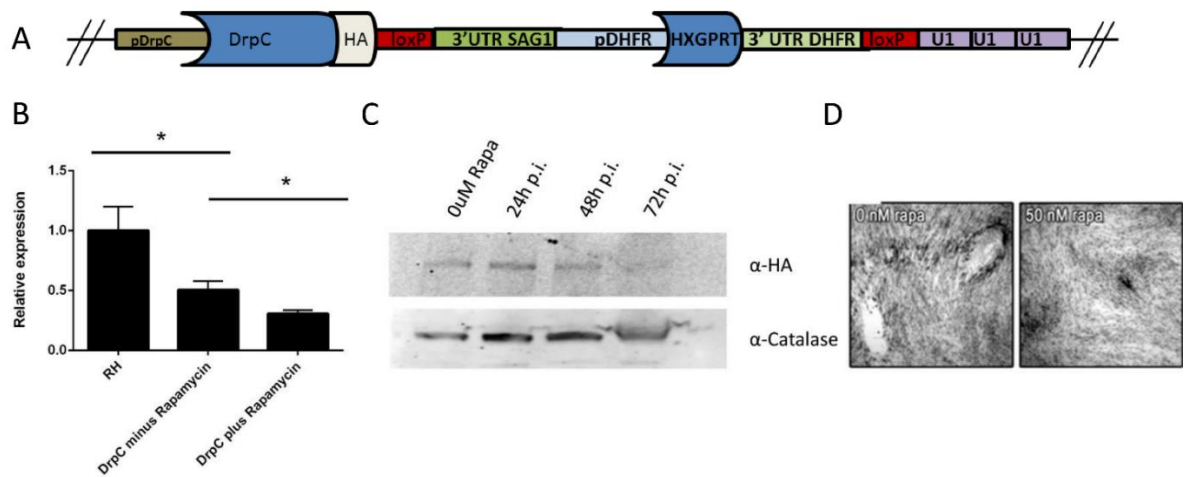


Figure 3-7: Rapamycin induction efficiently promotes DrpC downregulation

(A) Scheme of the modified locus of *DrpC* in the *DrpC-HA-U1* strain. (B) qRT-PCR measuring transcription levels of *DrpC* shows that in the strain *DrpC-HA-U1*, a 50% reduction of *DrpC* mRNA levels is seen compared to the level measured in RH parasites. 72 hours after Rapamycin induction, a further downregulation of *DrpC* is evident, so that the residual expression is only 20% of the transcript levels in wild-type parasites. Quantitative RT-PCR was conducted in duplicate of three biological replicas; data shows mean \pm SEM (* $p < 0.005$, unpaired two-tailed Student's T-test). (C) Western Blot analysis with α -HA antibodies shows that *DrpC* signal is virtually undetectable 72 hours post Rapamycin induction. (D) Plaque assay shows that *DrpC* depletion is lethal for *T. gondii*. Plaque assay reproduced from (Pieperhoff et al., 2015).

These results were confirmed by IFA analysis, which showed that *DrpC* puncta are no longer visible 72 hours after Rapamycin induction. At this time point, I found that *DrpC* down-regulation has no significant effect on the biogenesis of micronemes and rhoptries. Apicoplast biogenesis and rosette organisation are likewise not significantly affected by *DrpC* knock-down. Golgi morphology was assessed by transient transfection of the GRASP-RFP marker (Pelletier et al., 2002) in the *DrpC-HA-U1* line, and no significant differences in Golgi morphology between induced and non-induced parasites 72 hours after induction were found (Fig. 3-8a and b).

In contrast, while in non-induced *DrpC-HA-U1* parasites 96% of the mitochondria have normal morphology, in Rapamycin-treated parasites around 90% of the mitochondria look misshapen (Fig. 3-8b). Importantly, when wild-type parasites are treated with Rapamycin, $\approx 95\%$ of the vacuoles show normal, lasso-shaped mitochondria (data from two independent experiments).

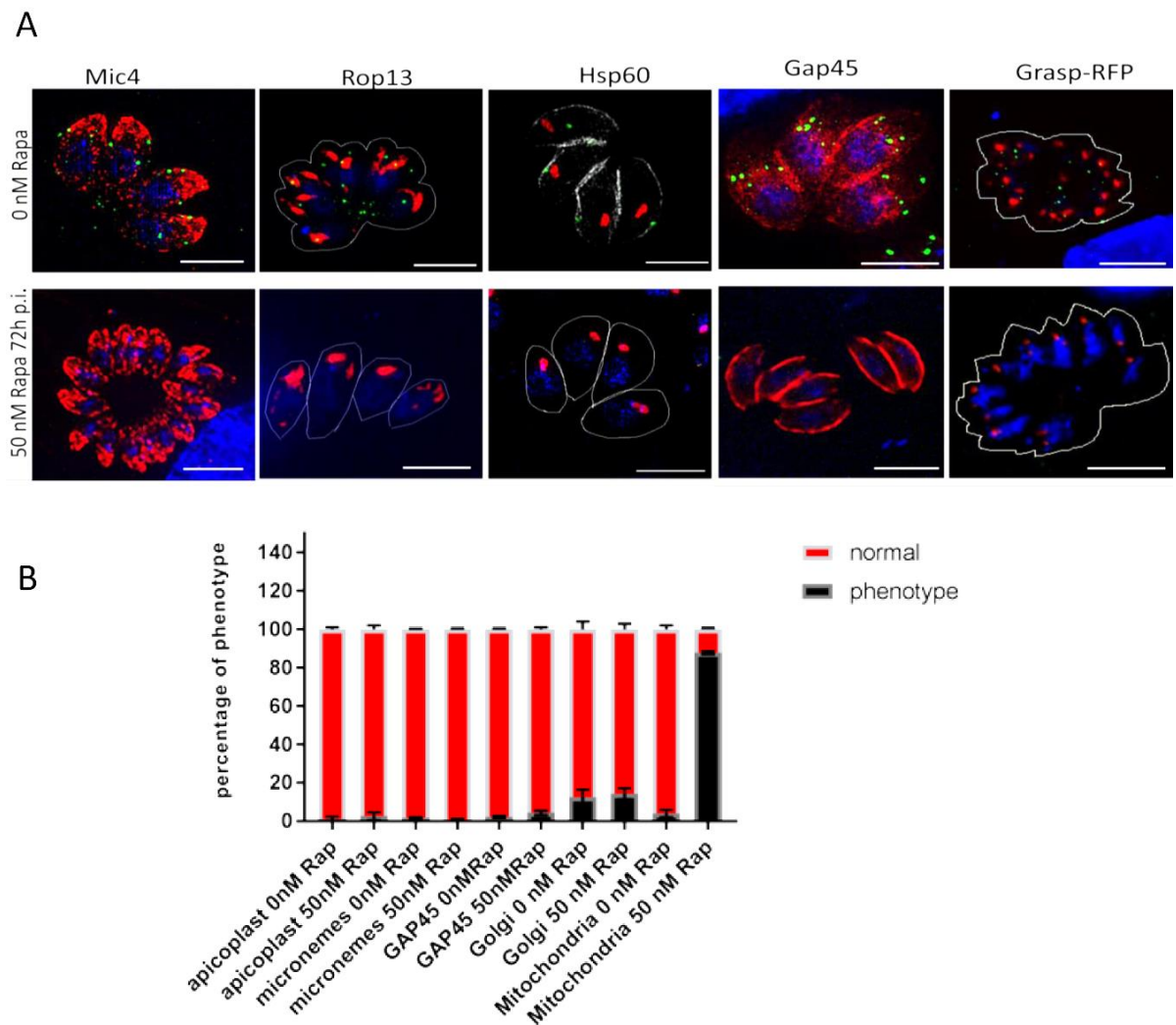


Figure 3-8: Analysis of DrpC knock-down on different organelles of *T. gondii*

(A) IFA analysis shows that 72 hours post induction, DrpC down-regulation does not affect secretory organelles such as micronemes (probed with α -Mic4) and rhoptries (probed with α -Rop13). Similarly, apicoplast, IMC and Golgi (markers α -HSP60, α -Gap45 and Grasp-RFP, respectively) show normal morphologies at these time point. Scale bars: 5 μ m. (B) Quantification (n=3, 100 vacuoles counted per experiment) shows that DrpC down-regulation has a specific effect on mitochondrial morphology: at 72 hours post-induction, around 90% of the vacuoles show aberrant mitochondrial morphologies, while the other indicated organelles do not show significant differences.

Three different mitochondria phenotypes were identified. In the induced parasites, 41% of the vacuoles contain mitochondria that remain interconnected with each other. 39.2% of the vacuoles show mitochondria membranes that are severely misshapen, a phenotype we refer to as “thick membranes”, while around 7% of the vacuoles show mitochondria that are reduced to small, closed circles (“collapsed”) (Fig. 3-9a and 3-9c).

To confirm that the mitochondria phenotype is specific, a complementation experiment was carried out. To this end, the plasmid p5RT70 -GFP-DrpC was generated, encoding a copy of *DrpC* tagged with GFP and under the control of p5RT70 ,a constitutive promoter composed of the fusion between the five-repeat element of *sag1* 5'UTR and the minimal promoter of *α-tubulin* (Soldati and Boothroyd, 1995) . When the plasmid was transiently transfected in induced *DrpC-HA-U1* parasites, IFA analysis revealed that GFP-DrpC fully rescues the mitochondria defect observed upon DrpC down-regulation (Fig. 3-9b and c).

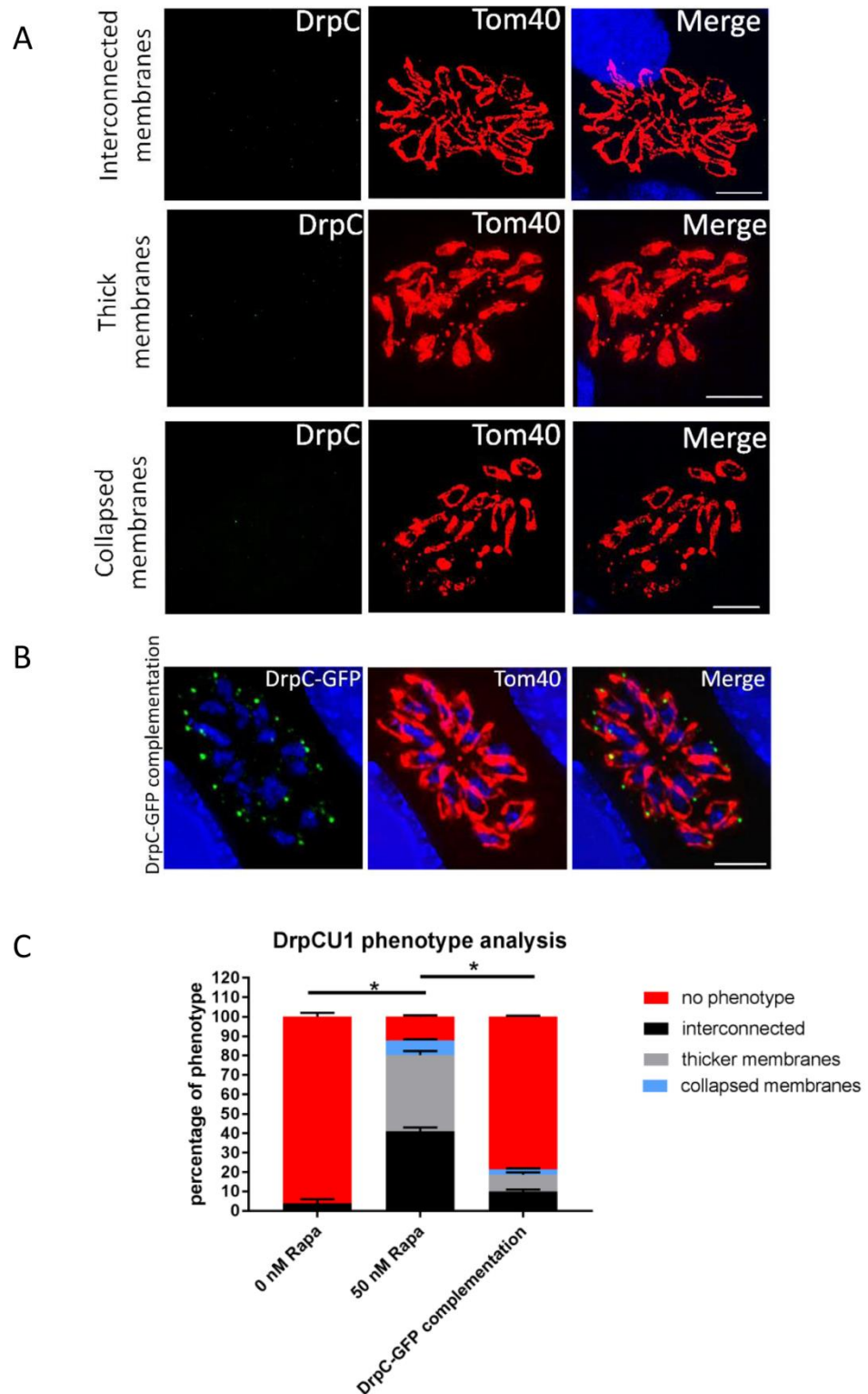


Figure 3-9: DrpC knock-down leads to abnormal mitochondria morphology

(A) Immunofluorescence analysis at 72 hours post induction of DrpC down-regulation shows three types of abnormal mitochondrial morphology: interconnected mitochondria, thick membranes and small, circular mitochondria (“collapsed”). (B) Complementation experiments show that expression of DrpC-GFP rescues DrpC knockdown phenotypes, as quantified in (C). Scale bars: 5 μ m. (C) Quantification was obtained through comparison of three independent experiments, each with at least 300 vacuoles, and statistical analysis performed to compare the observed distributions. Error bars show SD, and asterisks indicate significant difference ($P < 0.001$ multiple t-test).

3.4 Generation of a dominant negative form of DrpC

DrpC down-regulation showed that this protein is implicated in mitochondria biogenesis; this is in agreement with the mitochondrial localisation observed in the *DrpC-YFP* strain. The analysis of its specific role, though, was complicated by the observation that two main mitochondria phenotypes are seen upon *DrpC* knock-down. Two explanations are possible: the first is that DrpC contributes to different aspects of mitochondria biology; alternatively, it can be hypothesised that only one of the observed phenotypes is the primary effect of DrpC depletion, and the other is a knock-on effect due to general mitochondrial dysfunction.

To be able to differentiate between these possibilities and to identify the primary role of the protein, a more rapid system for DrpC functional ablation was required. It is well documented that dynamin activity can be blocked in a dominant-negative fashion when a second copy carrying a non-functional GTPase domain is introduced in the genome; several amino acid substitutions in the GTPase domain have been reported to block GTP hydrolysis (van der Bliek et al., 1993, Otsuga et al., 1998). This strategy has been successfully used in *T. gondii* for the study of DrpA and DrpB functions (van Dooren et al., 2009, Breinich et al., 2009); since the overexpression of dominant negative DrpA and DrpB is lethal for the parasite, the authors generated stable cell lines where the overexpression could be inducibly expressed using the ddFFKBP system (see introduction paragraph 1.4.3).

The same strategy was adopted for DrpC: its cDNA was cloned in the plasmid p5RT70 -DD-GFP to generate the construct p5RT70 -DD-GFP-DrpC_{wt}, where the constitutive promoter p5RT70 controls the expression of DrpC fused to GFP and to the destabilisation domain (DD), which in absence of Shield-1 causes degradation of the fused protein (this plasmid was generated by Manuela Pieperhoff). Further manipulation of this construct allowed me to introduce a specific mutation in the GTPase domain of DrpC; sequencing of the plasmid confirmed the generation of the new construct p5RT70 -DD-GFP- DrpC_{DN}, where the Lysine at the residue 129 of DrpC is mutated in Alanine (Fig. 3-10a). After transfection and selection in *RH* parasites, a stable line was obtained where the construct is randomly integrated in the genome. Western Blot analysis on

RHp5RT70-DD-GFP-DrpCDN parasites (which I will call *DD-GFP-DrpCDN*) shows that no signal is detected when they are grown in absence of Shield-1; upon Shield-1 addition, the signal of the expected band size is visible as soon as 4 hours post induction, and remains at stable levels at 24 hours p.i. (Fig. 3-10b). As expected, this line is not viable when grown in presence of Shield-1 for 7 days, as measured by plaque assay (Fig. 3-10c).

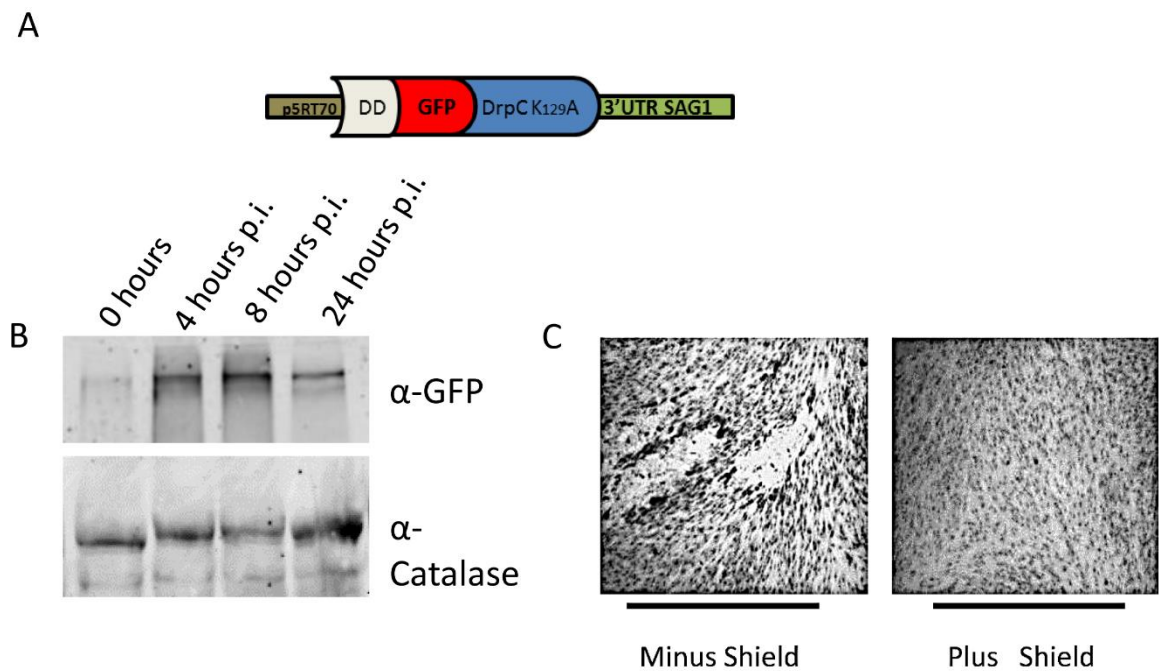


Figure 3-10: Shield-1 mediated expression of a dominant negative form of DrpC impairs parasite growth.

(A) Scheme of the plasmid randomly transfected in *RH* parasites to obtain the strain *DD-GFP-DrpCDN*, (B) Western blotting shows that Shield-1 rapidly stabilises the protein *DD-GFP-DrpCDN*; probing with α -GFP antibody reveals expression of the protein as soon as 4 hours post induction, and the expression levels remain stable at 24 hours post induction. (C) Plaque assay shows that *T.gondii* tachyzoite growth is severely impaired upon *DD-GFP-DrpCDN* induction.

Immunofluorescence analysis on this line at 24 hours post induction reveals no effects on secretory organelles, apicoplast or IMC (Fig. 3-11a). Conversely, the localisation of *DD-GFP-DrpCDN* changes at different times of Shield-1 induction; this correlates to a drastic effect in mitochondrial morphology, as the mitochondria in the vacuoles become increasingly interconnected (Fig. 3-11b and c). At 4 hours post-induction, *DD-GFP-DrpCDN* puncta are at the periphery and at the basal part of the mitochondrion; quantification shows that at this time point only 9% of the vacuoles have interconnected mitochondria. At 8 hours post-induction, almost all the signal is accumulated at the basal part of the mitochondrion, and the percentage of interconnected mitochondria rises to 23%;

at 24 hours post-induction, 53.6% of the vacuoles have this phenotype, and DD-GFP-DrpCDN signal completely covers the interconnection.

This analysis provides support for the hypothesis that DrpC has a specific mitochondrial function; moreover, in the strain *DD-GFP-DrpCDN* only one mitochondrial phenotype is observed, while the other abnormal morphologies seen upon *DrpC-HA-U1* knockdown (thicker membranes and “collapsed” mitochondria) were not revealed. This suggests that the primary effect of DrpC functional ablation is a failure in mitochondrial fission.

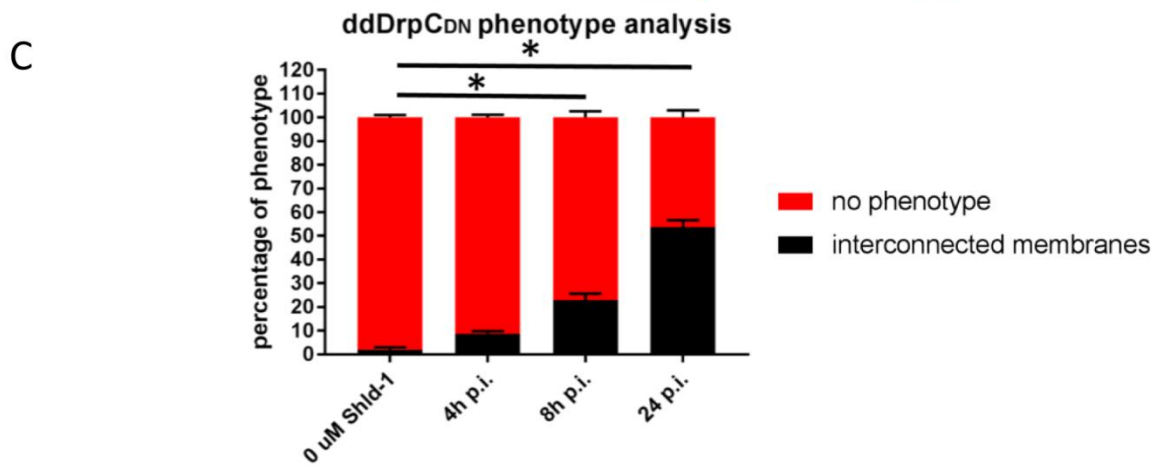
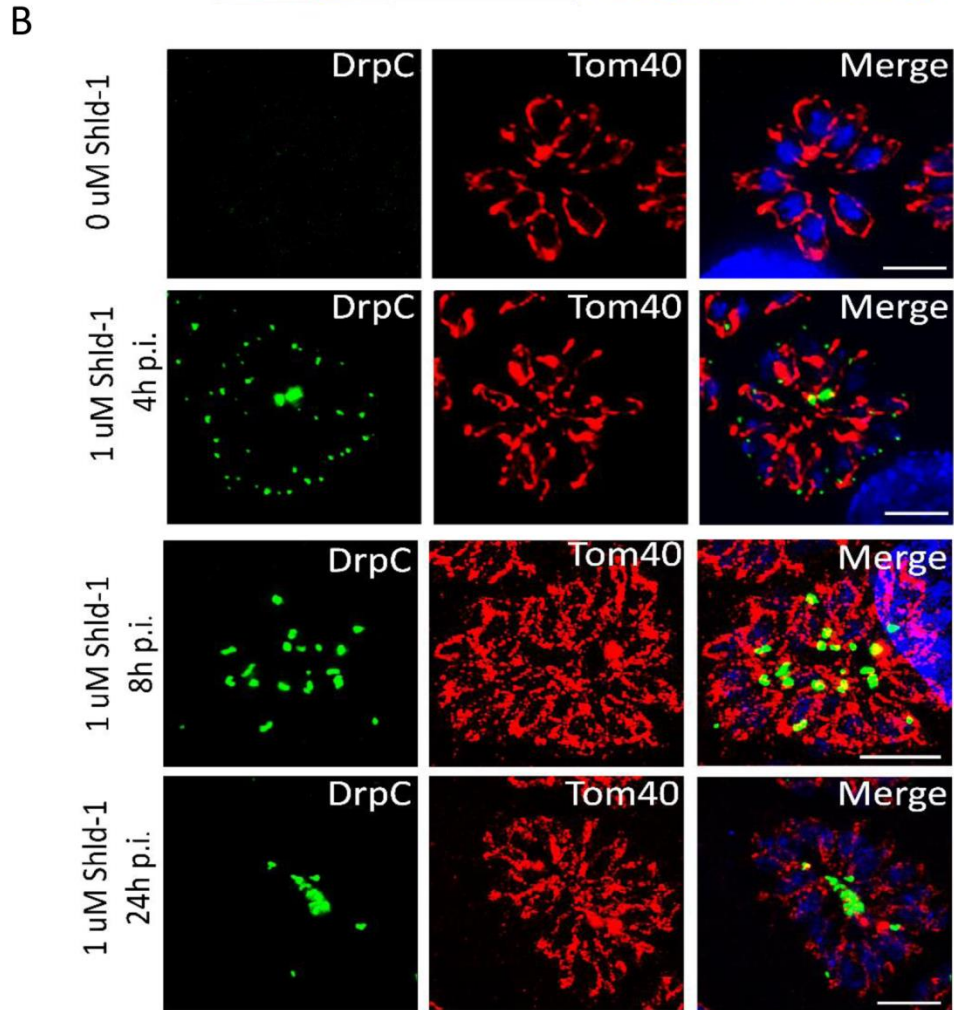
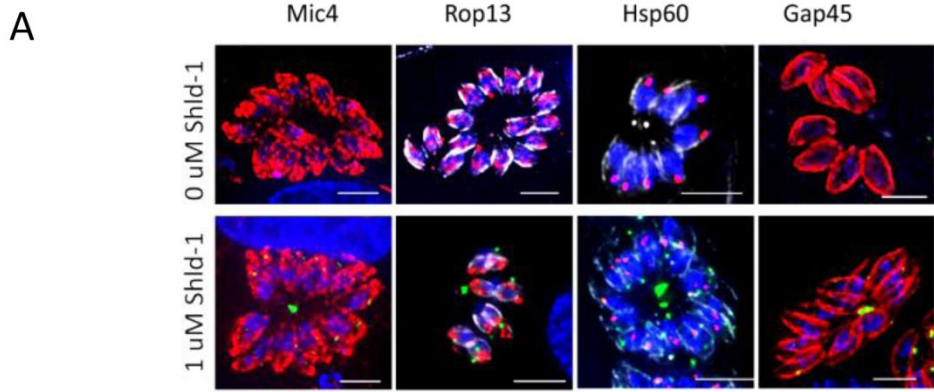


Figure 3-11: Over-expression of a dominant-negative form of TgDrpC leads to interconnected mitochondria.

(A) IFA analysis on the *DD-GFP-DrpCDN* line at 24 hours in presence and absence of Shield-1 shows that the dominant negative DrpC has no effect on micronemes (probed with α -mic4), rhoptries (α -Rop13), apicoplast (α -HSP60) or IMC (α -Gap45). (B) Immunofluorescence analysis showing mitochondrial phenotype in induced *DD-GFP-DrpCDN* parasites. Four hours after Shield-1 stabilisation, puncta of the overexpressed protein are visible at the periphery and basal part of the mitochondrion; at 8 and 24 hours, an accumulation of the signal on the basal part of mitochondria, which become increasingly interconnected, is seen. The quantification of this set of experiments is shown in (C); at least 100 parasitophorous vacuoles were counted in triplicate, and statistical analysis performed to compare the observed distributions. Error bars represent SD from the three independent experiments. Asterisks indicate significant difference ($P < 0.001$ multiple t-test). Scale bar: 5 μ m.

These experiments show that GTPase activity is essential for DrpC function; a detailed *in silico* analysis performed by Dr. Ehmke Pohler supports the notion of GTPase activity for DrpC. In order to provide molecular insight into the putative GTPase activity of this protein, he constructed a homology model using SWISSmodel (Biasini et al., 2014): the closest model in the protein data base as identified by BLAST (Camacho et al., 2009) is the crystal structure of the human Dynamin 3 GTPase domain (PDB: 3L43), determined by the Toronto Structural Genomics Consortium at a resolution of 2.3 Å.

DrpC and human Dynamin 3 share a sequence identity of 31% over the GTPase domain (amino-acids 118-401); thus, a reliable homology model for the overall structure of this domain could be calculated for DrpC, even if a number of insertions and deletions, in particular on the C-terminal side of DrpC GTPase domain, were found. While these differences will lead to significant local structural changes, the overall fold is predicted to be conserved, as shown in Fig. 3-12a. The GTP binding site is mainly conserved, with the diphosphate-contacting P-loop (shown in yellow in Fig.3-12a) displaying only small changes. Moreover, based on the homodimeric human Dynamin 3 structure (Bertoni et al., 2017), DrpC GTPase is predicted to adopt a similar homodimer (Fig. 3-12b); the oligomeric structure of the full-length DrpC, however, remains to be elucidated.

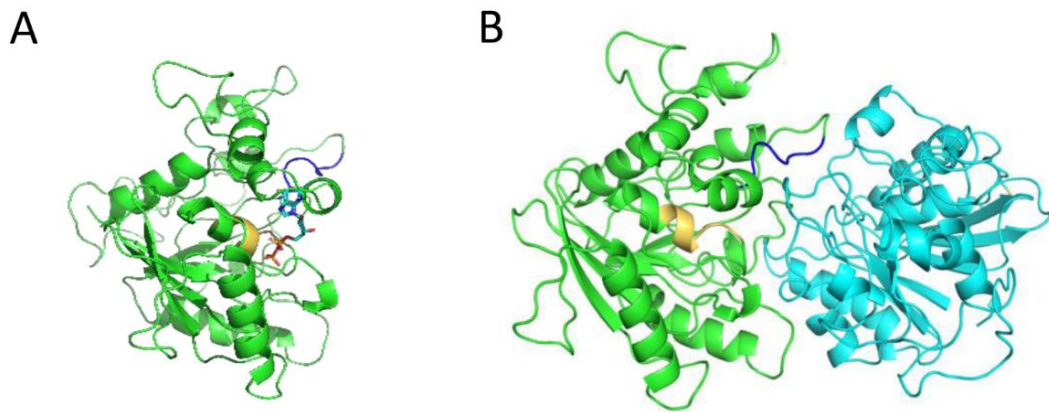


Figure 3-12: Modelling of the GTP binding domain of DrpC

(A) Monomer model for DrpC GTPase domain. The P-loop is indicated in yellow, while the less conserved region is in blue. (B) Model of the dimerization of DrpC GTPase domains. Data obtained by Dr. Ehmke Pohl.

3.5 Overexpression of full-length and truncated forms of DrpC

Next, the phenotype caused by the overexpression of DrpC was analysed. Drp1 overexpression causes fragmentation of the mitochondrial network in *C. elegans* (Labrousse et al., 1999); in mammalian cells, however, there are contrasting reports: some authors showed that Drp1 overexpression leads to mitochondria fragmentation (Szabadkai et al., 2004), while others find that mitochondria are fragmented only when Drp1 receptors- such as Mff and Fis1- are overexpressed (Smirnova et al., 2001, Otera et al., 2010, Loson et al., 2013).

Analysis of the stable line *RHp5RT70-DD-GFP-DrpCwt* (which was previously generated by Manuela Pieperhoff, and will be called here *DD-GFP-DrpCwt*) was carried out (Fig. 3-13 a). In this strain, DrpC overexpression is efficiently induced by Shield-1: Western Blotting analysis on parasites grown for 24 hours in presence and absence of Shield-1 reveals a protein of the expected band size only in induced parasites (Fig. 3-13 b). DrpC overexpression does not affect parasite growth: plaque assay (Fig. 3-13 c) on *DD-GFP-DrpCwt* parasites shows no difference between induced and non-induced parasites. IFA analysis reveals that overexpressed *DD-GFP-DrpCwt* localises correctly on the mitochondrion, and no fragmentation is visible (Fig. 3-13 d).

Next, the ddFKBP system was harnessed to express truncated version of the protein, in the attempt to gain information about the domains required for DrpC recruitment to the mitochondrion. To this end, the plasmid p5RT70-DD-GFP-DrpCwt was modified by Q5 mutagenesis, and the plasmid p5RT70-DD-GFP-DrpCGTPase only (expressing only the N-terminus of DrpC, which encodes for the GTPase domain) was obtained (Fig. 3-13 e). Moreover, a p5RT70-DD-GFP-DrpCTRUNCATED plasmid was generated by amplifying the C-terminus of DrpC (without the GTPase domain) and cloning it into the plasmid p5RT70 -DD-GFP (Fig. 3-13 i). After transfection and selection, the two stable lines *DD-GFP-DrpCGTPase only* and *DD-GFP-DrpCTRUNCATED* were obtained. Western Blot confirmed efficient stabilisation of *DD-GFP-DrpCGTPase only* and *DD-GFP-DrpCTRUNCATED* when the respective strains were grown in presence of 1 μ M Shield-1 for 24 hours (Fig. 3-13 f and 3-13 j, respectively).

Surprisingly, IFA analysis showed that mitochondria recruitment of DrpC is abolished when *DD-GFP-DrpCGTPase only* (Fig. 3-13 h) and *DD-GFP-DrpCTRUNCATED* (Fig. 3-13 l) are stabilised for 24 hours with Shield-1. Both the overexpressed versions of DrpC are instead found exclusively in the cytoplasm; since they don't localise on the mitochondrion, no dominant effect is expected. Plaque assay confirmed this prediction: *DD-GFP-DrpCGTPase only* and *DD-GFP-DrpCTRUNCATED* parasites grown in presence of Shield-1 do not present any growth defect, as shown in Fig. 3-13 g and 3-13 k, respectively.

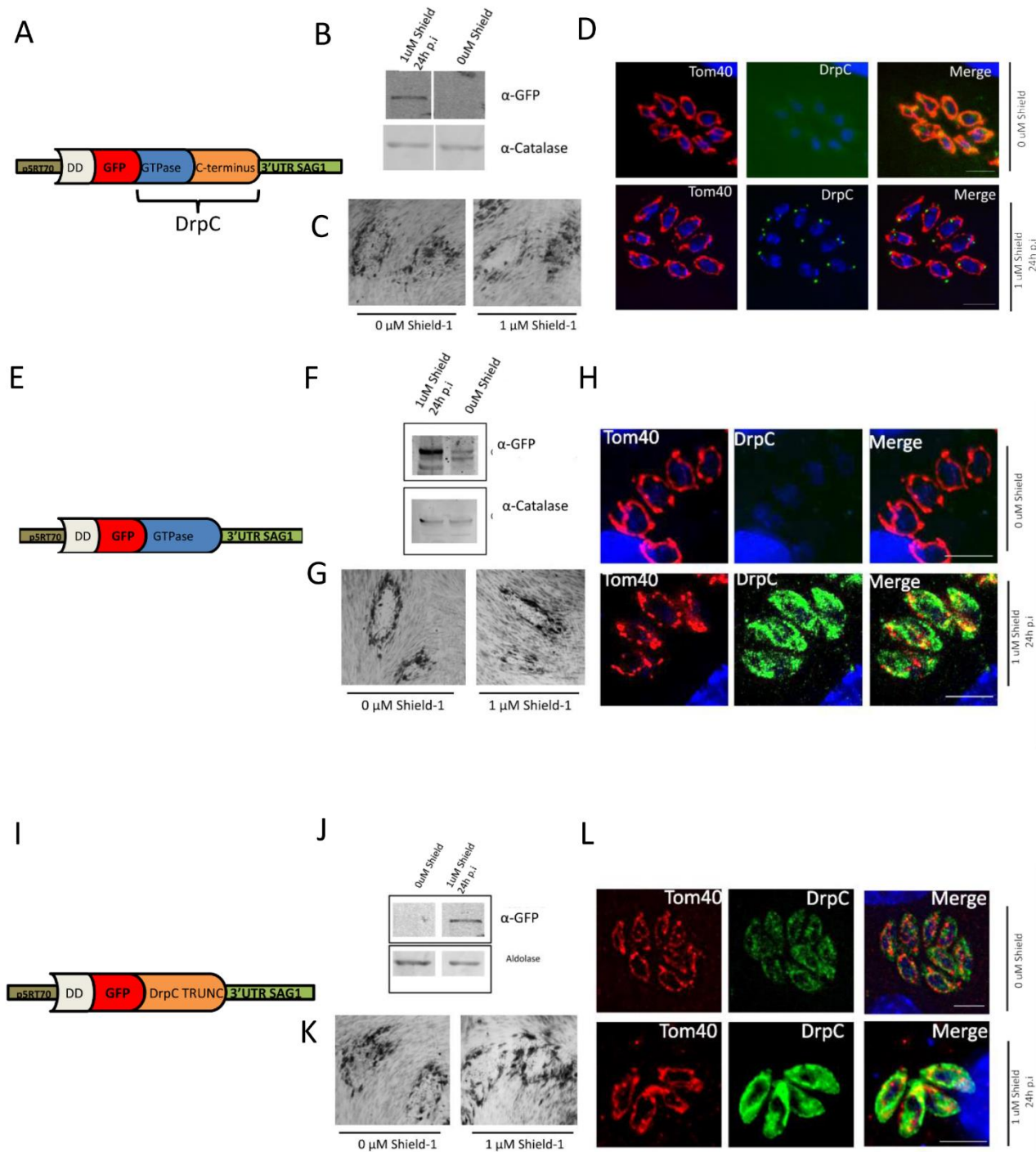


Figure 3-13: Overexpression of wild-type and truncated forms of DrpC

Plasmids DD-GFP-DrpC_{wt} (A), DD-GFP-DrpC_{GTPase} only (E) and DD-GFP-DrpC_{Truncated} (I) were stably transfected in RH parasites; Western Blot analysis using antibodies α -GFP and α -Catalase confirms that 24-hour exposure to 1 μ M Shield-1 efficiently stabilises the randomly integrated proteins DD-GFP-DrpC_{wt} (B), DD-GFP-DrpC_{GTPase} only (F) and DD-GFP-DrpC_{Truncated} (J) in the respective strains. Plaque assays shows that the in the strains DD-GFP-DrpC_{wt} (C), DD-GFP-DrpC_{GTPase} only (G) and DD-GFP-DrpC_{Truncated} (K), parasite growth is not impaired when Shield-1 is added to the media. Localisation analysis demonstrates that DD-GFP-DrpC_{wt} forms puncta that localise on the mitochondrion (D); conversely, DrpC_{GTPase} only (H) and DD-GFP-DrpC_{Truncated} (I) localise on the cytoplasm, and do not form puncta. IFA analysis was conducted with α -GFP (in green) and α -Tom40 (in red) antibodies. Scale bars: 5 μ m.

3.6 Conclusions

Though the main events taking place during *T. gondii* endodyogeny have been described (Nishi et al., 2008), the mechanisms underlying mitochondria replication and segregation have not been characterised. In this chapter, functional analysis of Apicomplexa-specific protein DrpC is presented, and leads to the conclusion that this *bona fide* Dynamin-related protein is essential for mitochondria biogenesis.

Endogenous tagging reveals that DrpC forms a cytoplasmic pool but is also found in foci at the periphery and basal part of the parasites; a significant portion of these puncta colocalise with the resting mitochondrion, as shown through colocalisation with the two outer membrane markers Tom40 and TGME49_215430. Recruitment at the basal part of the organelle seems to be important during the last steps of endodyogeny, when the replicated mitochondrion is present as an interconnected structure between the daughter cells: time-lapse and fixed microscopy show that DrpC is at these mitochondrial interconnections, and in some cases an invagination of the mitochondrial tubule is visible where DrpC has been recruited.

These observations led me to hypothesise that *T. gondii* DrpC acts as a functional homolog of Drp1/Dnm1, key effectors of mitochondrial fission in human and yeast. When Drp1 and Dnm1 are down-regulated, fission is blocked; as a result, fusion is unopposed, and the mitochondria forming the typical network observed in higher eukaryotes become all connected with each other (Smirnova et al., 2001, Otsuga et al., 1998) .

In *T. gondii*, there is no mitochondrial network, but rather a single, usually lasso-shaped mitochondrion; the only fission step that has been observed takes place when - following mother mitochondrion elongation and the insertion of the new branches in the budding cells - the mitochondrial connections between the two daughter cells need to be cleaved. If DrpC is involved in fission, then it is logical to expect that its absence would result in an abnormal persistence of mitochondrial interconnections between daughter cells in a vacuole.

To verify this model, two different strategies for DrpC functional ablation were utilised; phenotypic analysis in the strain *DrpC-HA-U1* showed a specific mitochondrial effect upon DrpC down-regulation, as more than 90% of vacuoles present defects in mitochondria biogenesis, which result in parasite death. Of these vacuoles, more than 40% show an “interconnected mitochondria” phenotype.

These observations were confirmed by the analysis of the *DD-DrpCDN* strain: Shield-mediated stabilisation of a dominant-negative form of DrpC leads to the rapid formation of vacuoles with interconnected mitochondria. Conversely, inducible overexpression of a wild-type copy of DrpC is shown to not have any effect on mitochondrial biogenesis. Truncated version of DrpC (*DD-GFP-DrpCGTPase* only and *DD-GFP-DrpCTRUNCATED*) do not polymerise on the mitochondria: as a result, only a cytoplasmic signal is detected. No dominant negative effect is detected upon overexpression of these exogenous, truncated proteins; this is probably due to the fact that these truncated forms cannot bind the mitochondrion, and thus the endogenous, wild-type DrpC can still carry out its function. Conversely, in the *DD-DrpCDN* strain, the mutated protein (which carries only a single mutation in its GTPase domain, making it inactive) is still able to bind the mitochondrion, thus impairing the function of the endogenous DrpC.

Thus, this chapter proposes that DrpC primary function in *T. gondii* is in mitochondrial fission; the GTPase domain is essential for the protein function, and homology modelling supports the notion of GTPase activity.

However, some observations could point to a second role of DrpC. As already mentioned, a second population of DrpC puncta is observed at the periphery of the resting mitochondrion, but no membrane constriction is seen in correspondence with these foci. Moreover, at the endodyogeny stage when the replicated mitochondrion is present as a “bundle” still outside of the daughter cells, these puncta are already visible at the periphery of the daughter cells, and seem to contact the mitochondrial branches only when they start entering the buds. This observation could mean that DrpC has also a role as a bridge between the parasite structural elements and the mitochondrion. This could be in accord with the data on DrpC down-regulation: in fact, upon Rapamycin

addition, a second phenotype is visible, where mitochondria are club-shaped, as if the two sides of the lasso are collapsed on each other. Could this suggest that DrpC additional role is in tethering the lasso to the cytoskeleton of the parasite? If so, why is this phenotype not observed upon induction of the dominant-negative form of DrpC? Both points will be discussed in more detail in the general discussion chapter (see pages 150-154).

4 Analysis of potential interactors of DrpC in *T. gondii*

Data shown in the previous chapter suggest that DrpC is recruited to the mitochondria to promote fission; next, the potential mechanisms that ensure DrpC binding on the mitochondrial tubule were investigated.

As described in paragraph 1.7.3, Dynamins bind to their target membranes in different ways. Classical Dynamins are recruited to sites of membrane budding through the concerted action of two domains: the Proline-Rich domain (PRD), which mediates protein-protein interactions, and the Pleckstrin Homology domain (PH), which has a high affinity for phosphatidylinositol 4,5-bisphosphate (Shpetner et al., 1996, Okamoto et al., 1997, Bethoney et al., 2009).

Conversely, Dynamin-related proteins, which do not display PRD and PH domains, are usually recruited by adaptor proteins; in recent years, the mechanisms underlying mitochondria recruitment of the Dynamin-related proteins Drp1 and Dnm1 have been well studied. Though Drp1 can directly interact with some lipids such as cardiolipin (Bustillo-Zabalbeitia et al., 2014, Stepanyants et al., 2015), Drp1/Dnm1 specific binding to the mitochondrion is mainly achieved through interaction with a “fission complex”, a system of adaptor proteins on the mitochondrial membrane (Pagliuso et al., 2018). Mitochondrial recruitment of yeast Dnm1 is mediated by the complex Fis1-Caf4-Mdv1; Fis1, a transmembrane mitochondrial protein, is essential for fission and directly interacts with Dnm1 (see paragraph 1.7.3) (Mozdy et al., 2000, Tieu et al., 2002, Griffin et al., 2005). While Fis1 is highly conserved, its role in mammals has long been controversial: today, it is believed that mammalian Drp1 is primarily recruited through the adaptors Mff, MiD49 and MiD50 (Gandre-Babbe and van der Bliek, 2008, Palmer et al., 2011), and that human Fis1 is not essential for fission. In fact, only a moderate elongation phenotype is visible upon Fis1 depletion in mammalian cells (Loson et al., 2013); recently, it was proposed that in mammalian cells Fis1 plays a specific role in stress-induced mitochondrial fission (Shen et al., 2014b).

Intriguingly, both Fis1 and Mff are also present on peroxisomal membranes, and both have been involved in Drp1 recruitment during peroxisome fission, though Fis1 downregulation does not affect peroxisome morphology (Schrader et al., 2016).

Here, I aimed to identify the adaptor proteins required to recruit DrpC to the mitochondrial membrane, an attempt which led me to characterise the Fis1 homolog conserved in the parasite genome.

4.1 Conservation of the fission complex in *T. gondii*

In order to identify *T. gondii* “fission complex”, I performed a literature search and collected the amino acid sequence of proteins which are identified as mitochondrial adaptors in human, yeast and plants. Next, I performed a BLAST-P search to find *T. gondii* homologs of these molecules. As seen in Table 4-1, only the protein Fis1 was found to have a significant degree of conservation, as a BLAST-P search using the human homolog Fis1 retrieves *T. gondii* protein TGME49_263323 with a e-value of 1e-12 (the Clustal-Omega alignment between the two proteins is shown in Fig. 4-1). Reciprocal BLAST with *T. gondii* TGME49_263323 in the NCBI database identifies it as a member of the Fis1 family, and it can be hypothesised that it is a functional homolog of human Fis1. To test this hypothesis, the localisation and function of TGME49_263323 (which will be referred to as Fis1 in this chapter) were assessed.

Protein	Function	<i>Toxoplasma gondii</i>
Fis1 (human, yeast, plants)	Mitochondrial outer membrane adaptor	TgFis1 (TGME49_263323) Phenotype score: +0.94 (Sidik et al., 2016) Location: mitochondrion (Padgett et al., 2017)
Mdv1/Caf4/Num1/Mdm36 (yeast)	Mitochondrial receptor for Dnm1	-
Mff (human)	Recruits Drp1 on the mitochondrial membrane	-
MiD49/50 (human)	Drp1 receptors	-
ELM1 (plants)	Recruits Drp3 to the mitochondrial membrane	-

Table 4.1-1: Conservation of the known mitochondrial fission complex in *T. gondii*

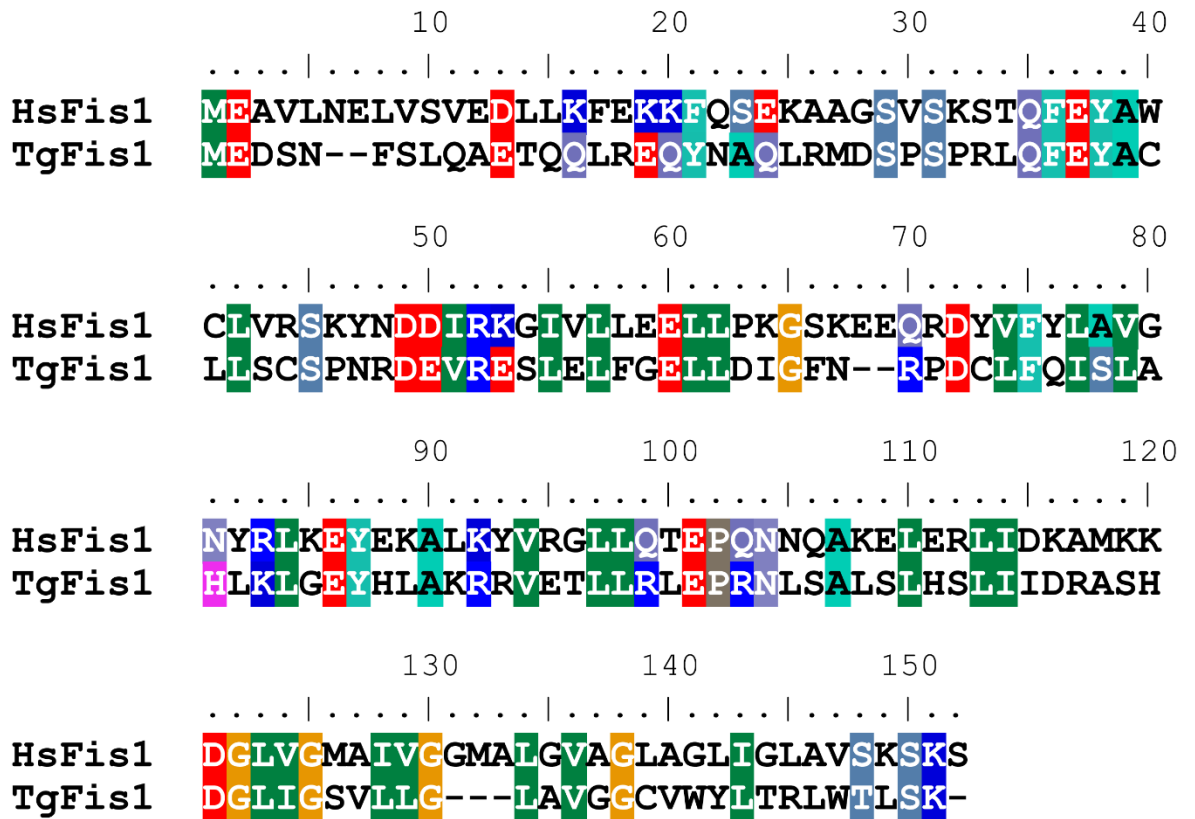


Figure 4-1: Fis1 alignment

Clustal - Omega alignment of human Fis1 and *T. gondii* Fis1. Identity/similarity threshold for shading is 70%.

4.2 Overexpression of Fis1

In the database ToxoDB, Fis1 is identified as a tetratricopeptide repeat-containing protein; transcriptome data shows that the protein maintains stable expression levels during the cell cycle in tachyzoites, and it is predicted to have a transmembrane domain at its C-terminus. This suggests that tagging at its C-terminus could perturb Fis1 function; thus, to assess its localisation, Fis1 cDNA was cloned in the plasmid p5RT70-DD-mCherry-HA, to generate the construct p5RT70-DD-mCherry-HA-Fis1 (Fig. 4-2a). The plasmid was randomly integrated in the strain *DrpC-YFP*, and parasites $\Delta ku80p5RT70DD-mCherry-HA-Fis1:: DrpC-YFP$ (hereafter called *DD-mCherry-HA-Fis1:: DrpC-YFP*) were analysed. In this line, Fis1 is N-terminally tagged, and its expression can be modulated using Shield-1 at different concentrations and induction times; moreover, since in the parental strain DrpC is endogenously tagged (as described in the previous chapter of results), it is possible to assess the effects of Fis1 overexpression on DrpC localisation and function.

In absence of Shield-1, a weak signal for DD-mCherry-HA-Fis1 of the expected size of ≈ 57 kDa was detected by Western Blot probing with α -HA antibody; IFA analysis using α -HA antibody does not show any signal under these conditions (Fig. 4-2b and 4-2c). To assess Fis1 localisation, a weak overexpression was induced, by treating the strain with $0.2 \mu\text{M}$ of Shield-1 for 4 hours; Western Blot analysis shows a faint band of the expected size. In these conditions, the overexpressed protein is also detectable by IFA analysis: the signal of α -HA antibody is evenly distributed on the mitochondrion and overlaps with the marker of the outer membrane Tom40.

Subsequently, the effects of Fis1 overexpression were assessed by inducing *DD-mCherry-HA-Fis1:: DrpC-YFP* with $1 \mu\text{M}$ of Shield-1 for 24 hours; at this time point, Western Blotting shows a strong signal for DD-mCherry-HA-Fis1 (Fig. 4-2c). IFA analysis confirms that Fis1 signal overlaps with Tom40; strikingly, the overexpression leads to a severe defect in mitochondrial morphology, while the structure of the parasite is not compromised. Quantification revealed that more

than 80% of vacuoles present an abnormal mitochondria phenotype: the mitochondria are completely collapsed at their base, with only few branches visible inside the connected parasites (Fig. 4-2b and 4-2d). Plaque assay confirmed a strong phenotypic effect: while *DD-mCherry-HA-Fis1:: DrpC-YFP* parasites grown in absence of Shield-1 can form normal plaques, their growth is completely abolished when they are induced with 1 μ M of Shield-1 (Fig. 4-2e).

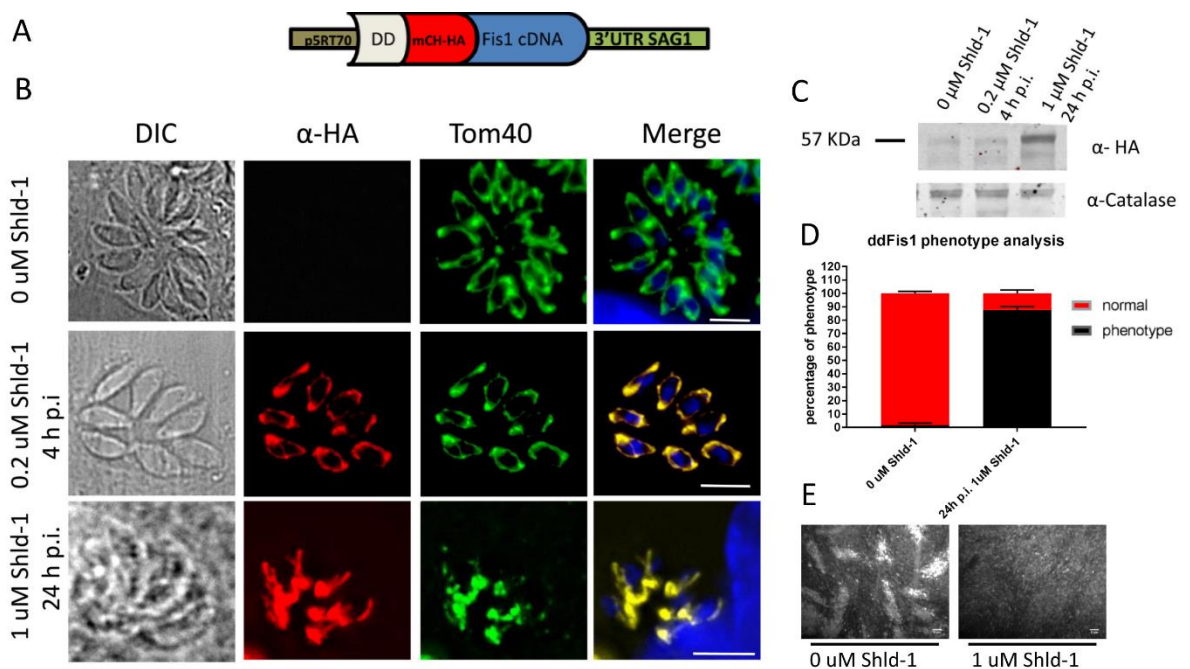


Figure 4-2: Fis1 localisation and overexpression

(A) Scheme of the plasmid randomly transfected in *DrpC-YFP* parasites to obtain the strain *DD-mCherry-HA-Fis1:: DrpC-YFP*. (B) Immunofluorescence analysis shows that in absence of Shield-1, no signal is detected when probing with α -HA antibody; after 4 hours induction with 0.2 μ M Shield-1, α -HA signal overlaps with the mitochondrial marker Tom40. Induction of *DD-mCherry-HA-Fis1:: DrpC-YFP* strain for 24 hours with 1 μ M of Shield results in a severe mitochondrial phenotype, where the mitochondria look thick at their base, and the mitochondrial branches are greatly reduced. Scale bars: 5 μ m. (C) Western blot probing with α -HA antibody shows that upon induction with 0.2 μ M of Shield-1, a weak expression of Fis1 is achieved; treatment with 1 μ M of Shield-1 for 24 hours results in high expression levels of the protein. (D) Quantifications carried out at 24 hours post induction (with 1 μ M of Shield-1) show that at this time point, 84% of the vacuoles present a severe mitochondrial phenotype. The experiment was carried out in triplicate, counting 100 vacuoles per each replicate. (E) Plaque assay shows that *T.gondii* tachyzoite growth is severely impaired upon *DD-mCherry-HA-Fis1* induction.

Next, the effect of Fis1 overexpression on DrpC localisation was analysed. Since at 24 hours post induction the mitochondrial phenotype is severe, I decided to include an intermediate time point, analysing mitochondria phenotype and DrpC localisation at 0, 12 and 24 hours post induction with 1 μ M of Shield (Fig. 4-3a and 4-3b). Western Blotting at these time points confirms that Fis1 is not detected by α -HA probing at 0 hours, while at 12 and 24 hours post induction a

strong expression is observed (Fig. 4-3a). In absence of Shield-1 no defect in mitochondria morphology are detected by IFA analysis using the mitochondrial marker Tom40. Moreover, as described in Chapter 3, two populations of DrpC puncta are visible: one population is at the periphery of the mitochondrion, while the other is recruited at the basal part of the organelle (Fig. 4-3b). At twelve hours post induction, it is possible to notice a thickening of the mitochondria; at this time point, DrpC foci still decorate both their periphery and basal part. At twenty-four hours post-induction, when around 80% of vacuoles show mitochondria which are almost completely collapsed at their centre, DrpC puncta which are normally found at the periphery appear to retain their localisation, even though they are no longer in contact with the mitochondrion; the population which is usually at the basal part of the organelle seems to be reduced, though this was not quantified (Fig. 4-3b).

Next, the interaction between Fis1 and DrpC in *T. gondii* was investigated by co-immunoprecipitation in the strain *DD-mCherry-HA-Fis1:: DrpC-YFP*. To this end, the *DD-mCherry-HA-Fis1:: DrpC-YFP* strain was induced with 0.2 μ M of Shield-1 for 4 hours, to obtain a weak overexpression of Fis1. The lysate was subjected to IP with beads conjugated with α -GFP antibody, and Western Blot analysis was performed using α -GFP and α -HA antibodies to assess the presence of DrpC and Fis1, respectively. As shown in Fig. 4-3c, both the signal for DrpC and Fis1 are found in the input and output fractions, but in the eluted fraction only the signal of DrpC is found; thus, the experiment did not demonstrate an interaction between Fis1 and DrpC.

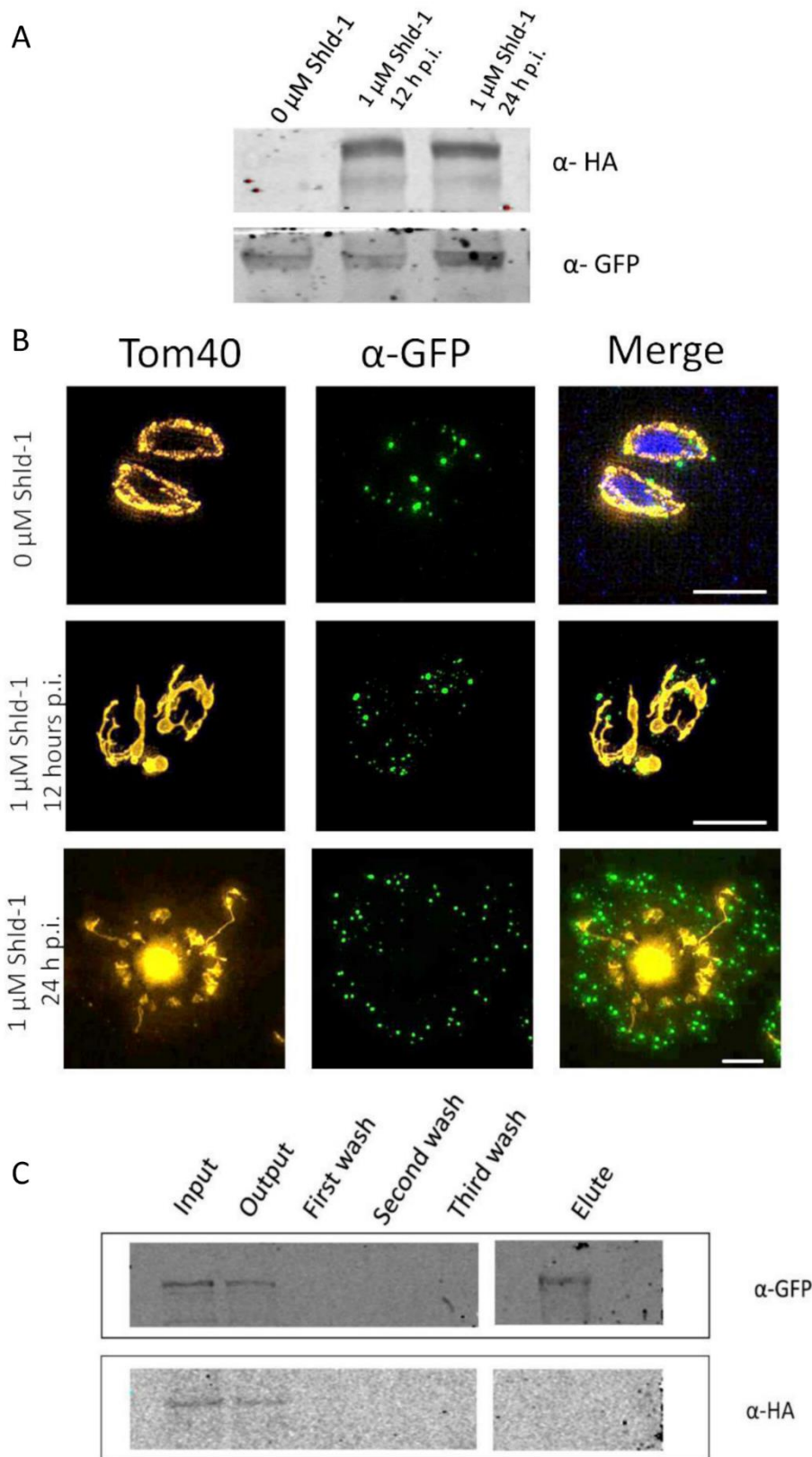


Figure 4-3: Analysis of Fis1 and DrpC putative interaction

(A) Western blot analysis assessing the expression levels of Fis1 at the indicated time points; Fis1 overexpression is not detected in absence of Shield--1, but is efficiently induced at 12 and 24 hours post induction. (B) IFA analysis assessing the effect of Fis1 overexpression on DrpC localisation. In absence of Shield-1, the mitochondrion shows a normal morphology, and DrpC puncta are found both at the periphery and at the basal part. At 12 hours post induction (1 μM of Shield-1), the mitochondrion shows a thicker membrane, but still maintains its usual lasso-shape, and DrpC localisation is kept at the periphery and basal part of the organelle. At 24 h post-induction, the mitochondrion is present as a thick dot at the basal end of the parasite and shows only few

branches; DrpC is found at the periphery of the parasite, but is not in contact with the mitochondrion. DrpC signal at the base of the organelle seemed reduced, but this effect could not be quantified. Scale bars: 5 μm . (C) Western blot analysis of the co-immunoprecipitation of HA-tagged Fis1 and GFP-tagged DrpC captured with GFP-conjugated beads.

4.3 Knockdown of Fis1

While the data derived from overexpression could suggest an essential role of Fis1 in mitochondrial integrity, a recent genome wide screen for essential genes suggests that Fis1 is not important for parasite growth in vitro (phenotypic score: +0.94) (as a comparison, DrpC has a phenotypic score of -4.54) (Sidik et al., 2016).

Therefore, it was decided to investigate Fis1 function by employing the tetracycline inducible transactivator system to induce Fis1 knockdown. This system was chosen because, as detailed in paragraph 1.4.2, it is widely used for generation of knockdown strains in *T. gondii*; it allows also endogenous tagging at the N-terminus of the GOI (as Fis1 has a transmembrane domain at its C-terminus, it is predicted that a tag in that region could affect its function; thus, the DiCreU1 system could not be used). It requires the replacement of the GOI endogenous promoter with the tetO7-Sag1 inducible cassette (consisting of seven tetracycline-operator sequences fused to the *Surface antigen 1 (SAG1)* minimal promoter) in the parental line *TATI Δ Ku80 Δ HX*, where the transactivator TATi-1 is under the control of a constitutive promoter. When the GOI is under the control of the TetO7-SAG1 cassette in this strain, its expression is induced by the TATi-1 transactivator; upon ATc induction, downregulation of the GOI is achieved (see paragraph 1.4.2) (Meissner et al., 2002).

A 978-bp portion of the N-terminus of Fis1 (starting from the annotated start codon) and a 994 bp-region upstream of the ATG were amplified and cloned in the plasmid TetO7-Sag1-HX. The linearized plasmid was transfected in the strain *TATI Δ Ku80 Δ HX* (Sheiner et al., 2011, Salamun et al., 2014); upon double homologous recombination, the line *TATI Δ Ku80TetO7-Sag1-Fis1* (hereby called *TetO7-Sag1-Fis1*) was generated, where Fis1 is N-terminally tagged with c-myc epitope tag and is under the control of the conditional promoter TetO7Sag1 (Fig.

4-4 a). Integration was confirmed by analytical PCR using the primers highlighted in fig. 4-4 a. A specific band of 1.1 kb is amplified in the *Tet07-Sag1-Fis1* strain and not in the parental line with the primers highlighted in red, and the primers highlighted in blue confirmed that the endogenous locus has been successfully replaced in the mutated strain (Fig. 4-4 b). In absence of ATc, Western Blot analysis shows a band of the expected size (≈ 16 kDa) when probing with α -myc antibody (Fig. 4-4 c); IFA analysis confirms that Fis1 is evenly distributed on the mitochondrial surface, overlapping with the signal of Tom40 (Fig. 4-4 e). Efficient downregulation was demonstrated by immunoblot and immunofluorescence analyses, which reveal that the signal of Fis1 is undetectable at 72 hours post induction with ATc (Fig. 4-4 c and 4-4 e, respectively).

The effect of Fis1 depletion was first measured by plaque analysis; surprisingly, *T. gondii* growth was not significantly affected upon ATc induction (Fig. 4-4 d). This observation was further confirmed by IFA analysis on parasites grown in presence of ATc for 72 hours: no phenotype was observed in the induced parasites, and mitochondria morphology was not affected by Fis1 knockdown (Fig. 4-4 e). These results suggest that Fis1 is not essential for *T. gondii* growth *in vitro*; moreover, Fis1 localises on the mitochondrion but its down-regulation does not affect the organelle morphology.

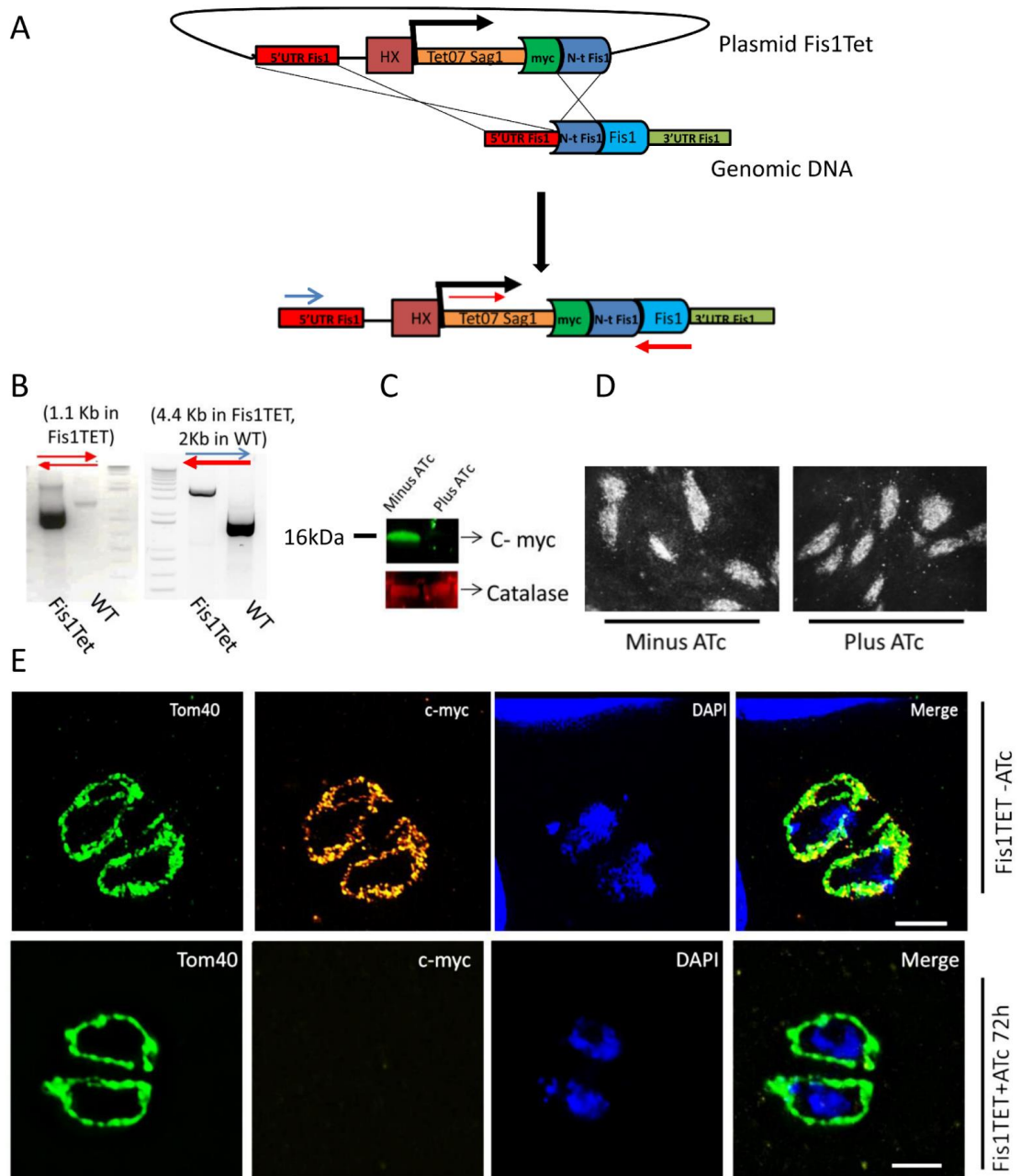


Figure 4-4: Fis1 Knockdown

(A) Scheme of knockdown strategy: a double cross-over event allows the replacement of Fis1 endogenous promoter with TetO7-Sag1 inducible cassette, and the endogenous tagging at Fis1 N-terminus with c-myc epitope. (B) Integration PCR with primers indicated as red and blue arrows in (A) confirms successful integration. (C) Confirmation of ATc-mediated protein knockdown. In absence of ATc, Western Blot analysis shows the expected protein size of 16 kDa, tagged with c-Myc; the induction of TgFis1 Knock-down with ATc shows that at 48 hours the protein is no longer detectable by Western Blot. (D) Plaque assay shows that Fis1 deletion does not impair parasite growth. (E) Immunofluorescence analysis confirms that TgFis1 is evenly distributed in the mitochondrial outer membrane. In presence of ATc, the signal of Fis1 is no longer detectable, but mitochondria morphology is not affected. Scale bar: 2 μ m

4.4 Immunoprecipitation experiments

Next, immunoprecipitation on DrpC was performed to find potential interactors. As DrpC is not highly expressed and rather unstable, it was decided to use the strain *DD-GFP-DrpCwt*, which was induced with 0.2 μ M of Shield-1 for 4 hours to obtain a weak overexpression of DrpC. Pull-down experiments were performed in triplicate with parasites expressing inducible *DD-GFP-DrpCwt*, and with a control line *RH-GFP*. Fig. 4-5 shows a representative Western blot of one of these pull-down experiments; since Shield-1 induction was performed for only 4 hours, it is possible to notice some degradation of the protein *DD-GFP-DrpCwt*.

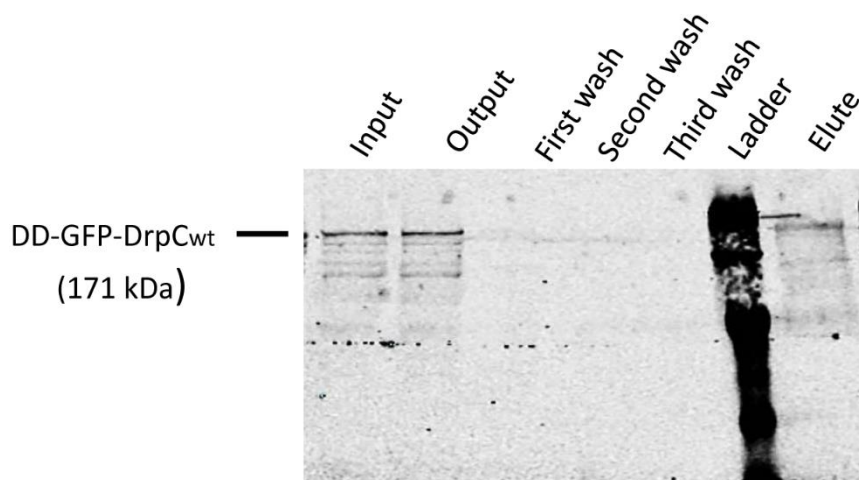


Figure 4-5: Immunoprecipitation on the strain *DD-GFP-DrpCwt*

Western Blot analysis on the indicated fractions of immunoprecipitation performed on the strain *DD-GFP-DrpCwt* probing with α -GFP antibody

The whole eluate for each pull-down was analysed by mass spectrometry. Table 1 lists the identified proteins that appeared in the triplicates of *DD-GFP-DrpCwt* immunoprecipitates. The proteins listed are the ones which were identified by more than two peptides, with Mascot probability score of 20 or above; moreover, they were always absent from the triplicates of parental line control.

ToxoDB ID	Replicate			Information from sequence analysis
	1	2	3	
TGME49_270690	+	+	+	DrpC
TGME49_221620	+	-	+	β -tubulin
TGME49_286660	+	-	+	Kinesin, putative
TGME49_309980	+	-	-	Dynein heavy chain
TGME49_246740	-	-	+	p50 (hypothetical protein)
TGME49_263520	-	-	+	microtubule associated protein SPM1 (SPM1)
TGME49_231630	-	+	-	alveolin domain containing intermediate filament IMC4 (ALV4)

Table 3-1: DrpC pull-down results

As shown in Table 1, DrpC was the protein found with the highest score in all three immunoprecipitation experiment. Unfortunately, no putative receptor on the mitochondrial membrane could be identified. Previous literature in other organisms shows that the interaction of Drp1/Dnm1 with the adaptor complex is highly transient (Otera et al., 2010, Liu and Chan, 2015); thus, it seems that the conditions here used for the immunoprecipitation experiments do not capture the binding of DrpC to mitochondrial proteins. Conversely, a potential interaction of DrpC to the microtubule cytoskeleton was highlighted, as a β -tubulin (TGME49_221620) and microtubule-associated proteins are pulled down in these experiments. In particular, three of these proteins are identified as part of microtubule-based motors: TGME49_286660 (which was present with high score in two of the three replicates) is identified in ToxoDB as a putative kinesin, while TGME49_309980 is described as a dynein heavy chain, and TGME49_46740 as p50 (also known as dynamitin), a component of the dynactin protein complex, which is an essential regulator of dynein movement along microtubule tracks.

While kinesin and the dynein-dynactin complexes were found in two of the three experiments, two other hits were present with high score in just one of the

replicates: TGME49_263520, which has been characterised as the microtubule-associated protein SPM1 (Tran et al., 2012), and TGME49_231630, a cytoskeletal protein.

Overall, five of the more robust hits in these experiments can be defined as microtubule-associated proteins (MAPs) (Morrissette, 2015); moreover, three of these are subunits of motor complexes which are responsible for movement along microtubules, and which have not been characterised in *T. gondii*. In the next chapter, I will illustrate the characterisation of one of these proteins, the dynactin subunit p50. However, during my work I also tried to investigate the role of the kinesin protein (TGME49_286660) which was also consistently present in the eluate of DrpC immunoprecipitation experiments; unfortunately, my endeavours to tag the kinesin at its 3' end and to downregulate it with the DiCre U1 system were not successful. Further work (possibly trying a different knock-down strategy) will be required to investigate the interaction between DrpC and TGME49_286660.

4.4 Conclusions

Dynamamin-related proteins do not directly bind lipids, but rely on protein-protein interactions to be recruited on their target membranes (Bethoney et al., 2009). In the previous chapter, DrpC has been shown to be a key factor in mitochondria biogenesis, but further study was necessary to understand the mechanisms underlying its recruitment on the mitochondrion during fission.

My analysis started with the hypothesis that *T. gondii* could show conservation of the “fission complex”, a system of adaptor proteins which recruit Dynamamin-related proteins onto the mitochondria membrane in other eukaryotes (Pagliuso et al., 2018). Starting with this hypothesis, I performed BLAST-P searches in the *T. gondii* genome to identify potential homologs of known proteins of the fission complex in human, yeast and plants.

The composition of this complex greatly varies among model organisms; a BLAST-P search in *T. gondii* found that only one of these members, the transmembrane protein Fis1, is conserved in the parasite genome. The interpretation of this result, however, needs to take in account another possibility: as DrpC is a highly

divergent Dynamin-related protein, its adaptor on the membrane could likewise be dissimilar from the proteins described in common model organisms, and as such it would not be identified by standard BLAST-P searches.

As Fis1 shows high sequence similarity to its human homolog, it was decided to investigate its function. The ddFKBP system was successfully adopted to modulate the overexpression levels of Fis1, and thus to investigate its localisation (in conditions of weak overexpression) and the effects of its strong overexpression on parasite viability. It was found that in conditions of low expression, Fis1 is evenly distributed on the mitochondria surface; this was recently confirmed by Padgett et al., who identified Fis1 as a Tail-anchored protein, and showed that when ectopically expressed it localises at the mitochondrion (Padgett et al., 2017). Surprisingly, we saw that high overexpression levels of Fis1 cause a lethal phenotype, causing the mitochondrion, as soon as 12 hours post induction, to develop abnormally thick membranes; at 24 hours post induction, the mitochondrion looks collapsed on itself in the basal part of the parasite, and only few mitochondrial branches are visible. DrpC puncta are still visible at the periphery of the parasite, but are no longer in contact with the mitochondrion. Conversely, the concentration DrpC puncta at the basal region seems to be reduced.

Interpretation of this data is rather difficult. It was hypothesised at the end of the previous chapter that DrpC puncta form two populations, which have different roles: while the puncta at the basal end are essential during endodyogeny to ensure cleavage of mitochondria interconnections, the ones at the periphery are not bound to the mitochondrion at all times, as they maintain this localisation even when mitochondria branches are excluded from daughter cells during endodyogeny. Thus, it can be proposed that, when Fis1 overexpression leads to mitochondrial collapse, DrpC recruitment at the base is no longer possible; conversely, DrpC puncta at the periphery are kept in their position, as their localisation is not dependent on the mitochondrion.

Why does Fis1 overexpression cause such a striking mitochondrial phenotype? If Fis1 is the receptor of DrpC during mitochondrial fission, then Fis1 overexpression would be expected to result in a higher recruitment of DrpC at the mitochondrial basal region, with the mitochondrion becoming more

fragmented in that area; however, the experiments shown in this chapter show no such effect. Moreover, co-immunoprecipitation data shows no direct interaction between DrpC and Fis1 in the strain *DD-mCherry-HA-Fis1:: DrpC-YFP*. Thus, the phenotype observed upon induction could be due to a general collapse of the mitochondrion, whose biogenesis could be affected by the abnormally high levels of one of its membrane proteins: if so, the phenotype observed in the induced *DD-mCherry-HA-Fis1:: DrpC-YFP* strain is only a knock-on effect of Fis1 overexpression, not its direct consequence.

To reach a better understanding on Fis1 role in *T. gondii*, a different approach was needed; to this end, a knockdown strategy was implemented to assess the effect of Fis1 downregulation on *T. gondii* fitness and on mitochondrial morphology. The use of the TET system allowed me to obtain a strain where Fis1 depletion can be achieved by ATc induction (Meissner et al., 2002).

Thanks to this approach, it was shown that Fis1 knockdown is not deleterious for parasite fitness; moreover, no mitochondrial phenotype is visible in parasites where Fis1 expression is downregulated. These results suggest that Fis1 is not essential for parasite growth, and that it plays no role, at least in tachyzoites, in mitochondrial biogenesis. It is important to bear in mind, however, that the Tet-transactivator system has been shown to allow for some residual expression of target genes (Jimenez-Ruiz et al., 2014); as a result, it cannot be ruled out that ATc-mediated Fis1 downregulation is not complete, and that residual levels of Fis1 are sufficient to ensure parasite survival. A clean knockout would therefore be necessary to ensure that Fis1 is indeed not essential in *T. gondii*; however, Fis1 downregulation data are confirmed by a CRISPR/Cas9 genome-wide screen, where Fis1 is classified as “dispensable”, with a phenotypic score of +0.94 (Sidik et al., 2016).

Thus, the receptor responsible of DrpC recruitment during fission is still not known in *T. gondii*. In the attempt to find such receptor, GFP-tagged DrpC was used as bait in immunoprecipitation experiments; the analysis of these data showed that no putative mitochondrial protein was being pulled down with DrpC. Previous literature suggests that interactions between dynamin-related proteins and the mitochondrial fission complex are of low affinity or transient (Otera et al., 2010, Strack and Cribbs, 2012, Liu and Chan, 2015); thus, it is possible that a

more sensitive method should be adopted to capture such interaction in *T. gondii*.

Conversely, pull-down data suggests an interaction between DrpC and tubulin. Moreover, the immunoprecipitation data find that kinesin and dynein, motor complexes which mediate movement of different organelles along microtubule tracks, are pulled down with DrpC.

Interestingly, a link between dynamin-related proteins such as Drp1 and microtubules has been proposed in other eukaryotic systems, though its significance remains unclear. It was found that a Drp1 splice variant can bind to microtubules in mammalian cells; the authors proposed that this Drp1 sub-population was a cytoskeletal “reserve pool”, but suggested that, as microtubules mediate mitochondria movement in mammalian cells, their interaction with Drp1 could have a deeper relevance in mitochondria localisation (Strack et al., 2013).

Moreover, previous work on mammalian cells suggests that Drp1 can interact with the dynein-dynactin motor complex, which mediates organelle migration towards the minus end of microtubules: in mammalian cells, disruption of dynein function through the overexpression of dynactin subunit p50 (also known as dynamitin), leads to a reduced recruitment of Drp1, which in turn leads to the formation of elongated mitochondria (Varadi et al., 2004). Moreover, it was seen in *Drosophila melanogaster* larvae that at least one subunit of dynactin can interact directly with Drp1 (Drerup et al., 2017).

A conserved homolog of dynamitin is found in *T. gondii* genome; thus, it was decided to investigate its location and function in the parasite, to try to shed light on the link between mitochondria and microtubule cytoskeleton in the parasite. The preliminary results will be detailed in the next chapter.

5 Outlook: localisation and function of p50 in *T. gondii*

Microtubule-based transport of intracellular particles and organelles is a crucial process in eukaryotic cells; it relies on the interplay between two main motor complexes, kinesin and dynein. Kinesin usually drives movement towards the plus-end of the microtubules (i.e., their growing end), while migration towards the minus-end is mediated by cytoplasmic dynein, which forms a complex with its essential regulator dynactin (Vale, 2003, Reck-Peterson et al., 2018, Hirokawa, 1998, Hirokawa et al., 2009). Both motors interact with a huge array of different cargoes to regulate migration and spatial organization of intracellular vesicles, organelles and protein/RNA complexes.

One example of such cargo in mammalian cells is the mitochondrion. In fact, while in yeast these organelles travel along actin filaments, in mammals their long-range migration is dependent on microtubule-based motility (Schwarz, 2013). The mitochondrial proteins Miro and Milton are crucial in this process, as they mediate bidirectional movement through interaction with the kinesin KIF5 (which powers anterograde movement) and with the Dynein/dynactin complex for retrograde movement (Glater et al., 2006, Morlino et al., 2014, Russo et al., 2009) (for more detail, see paragraph 1.7.1).

In *T. gondii*, mitochondrial migration can be predicted to have an important function in the last stages of endodyogeny, when the replicated mitochondria rapidly enter the daughter cells. The mechanisms controlling their movement and localisation, however, are not yet understood. Disruption of actin filaments does not affect mitochondria morphology (Periz et al., 2017); conversely, the role of the microtubule cytoskeleton in mitochondrion biogenesis is not fully understood, and Miro and Milton do not seem to be conserved in the parasite genome.

The parasite microtubule scaffold can be selectively disrupted using dinitroaniline herbicides such as oryzalin, a compound that can completely disassemble cytoskeletal microtubules at low doses (Stokkermans et al., 1996, Morrisette and Sibley, 2002); in a previous study, this approach has been used to understand mitochondrial behaviour in replicating parasites whose microtubules are disassembled (Nishi et al., 2008). It was shown that, upon oryzalin treatment, mitochondria still associate with the parasite periphery, but they seem to remain interconnected with each other. However, analysis of mitochondria phenotype under these conditions is particularly complicated: as a result of oryzalin treatment, daughter cells are unable to complete endodyogeny, and division of the nucleus, ER and apicoplast are likewise impaired, leading to abnormal, enlarged cells (Nishi et al., 2008). Thus, it is very difficult to tease out the primary effect of oryzalin treatment under these conditions.

In this chapter, a different approach was taken to investigate whether microtubule-based motility is important for mitochondria biogenesis in *T. gondii*. As reported in the previous chapter, mass spectrometry data suggest an interaction between DrpC and β -tubulin; moreover, a kinesin motor protein (TGME49_286660), and two putative members of the dynein/dynactin complex (TGME49_309980 and TGME49_246740) co-precipitate with DrpC. These data could point to a role of DrpC in mediating mitochondrial movement, similarly to what seen for the mammalian dynamin-related protein Drp1, which can bind microtubules and has been shown to interact with dynactin (Strack et al., 2013, Varadi et al., 2004, Drerup et al., 2017).

In order to investigate this hypothesis, it was decided to characterise the function and localisation of one of the motor subunits that co-precipitate with DrpC. The protein p50, a subunit of the regulatory dynactin complex, was deemed a good target, since it was present in the IP pull-down, and was found to be essential in a CRISPR-Cas9 screen (phenotypic score: - 3.36) (Sidik et al., 2016). Moreover, numerous reports from other eukaryotic systems have proved that this subunit is essential for correct assembly of dynactin, which is an essential regulator of dynein processivity and cargo binding; as a result, knockdown or overexpression of p50 leads to the disruption of dynein/dynactin-

based motility (Schroer and Sheetz, 1991, Gill et al., 1991). Previous literature showed that this disruption causes multiple effects, from Golgi fragmentation and inhibition of mitotic spindle assembly, to block of mitochondrial motility and of transport of vesicles in the endomembrane system (Burkhardt et al., 1997, Valetti et al., 1999, Echeverri et al., 1996, Quintyne et al., 1999, Melkonian et al., 2007, Jacquot et al., 2010, Drerup et al., 2017, Reck-Peterson et al., 2018).

In this chapter, the localisation and role of p50 in *T. gondii* will be analysed; this preliminary characterisation shows that the protein has an important function in intracellular tachyzoites, but further work will be needed to fully understand its function.

5.1 Generation of an inducible knockdown of p50

To investigate p50 localisation and function, the auxin-inducible degron (AID) system was adopted, to achieve a rapid regulation of p50 protein levels (attempts to obtain p50 knockdown through the DiCre-U1 system had previously failed). As discussed in paragraph 1.4.5, the mechanism of auxin-mediated degradation was discovered in plants, where auxin (IAA) can modulate the action of AUX-IAA proteins by binding them through their so-called “degron” domain. The binding promotes the interaction of the E3 ubiquitin ligase SCF-TIR1 with the AUX/IAA proteins, which as a result are rapidly degraded by the proteasome (Teale et al., 2006).

This system was recently adapted for the generation of inducible mutants in *T. gondii* by Brown et al., (Brown et al., 2017), who engineered a strain which constitutively expresses the E3 ubiquitin ligase TIR1 (*Tir1Δku80*). C-terminus fusion of a gene of interest with the “mini auxin inducible degron” domain (mAID) in the strain *Tir1Δku80* allows IAA-mediated downregulation of protein levels (Brown et al., 2017).

To achieve p50 ablation, a plasmid containing the coding sequence of mAID in frame with a HA epitope tag, and followed by the 3'UTR of the *DHFR* gene, was amplified with specific primers that contain homologous tails to the 3' region of

p50. A CRISPR/Cas9 vector (Curt-Varesano et al., 2016) containing a gRNA that specifically cuts in the 3' region of *p50* was transiently transfected together with the PCR product in the strain *Tir1Δku80*. In this way, the double strand break induced in the 3' region of *p50* increases the probability of homologous recombination between the PCR product and *p50* locus, allowing the precise, in frame insertion of mAID and HA just before *p50* STOP codon (Fig. 5-1a) (Di Cristina and Carruthers, 2018).

Correct integration at the 3' end of *p50* was verified by analytical PCR on genomic DNA: a specific product of 3.3 kb was shown in the strain *Tir1Δku80p50-mAID-HA* (hereafter called *p50-mAID-HA*), and is not amplified in the parental strain (Fig. 5-1b). Western Blot analysis confirmed in frame fusion at *p50* C-terminus, showing the expected band size of ≈75 kDa. Though Brown et al. showed that this system allows downregulation of target proteins as soon as 4 hours post auxin induction (Brown et al., 2017), in the case of *p50* at least 24 hours of treatment with 500 μM of IAA were necessary to observe a reduction of protein levels (Fig. 5-1c).

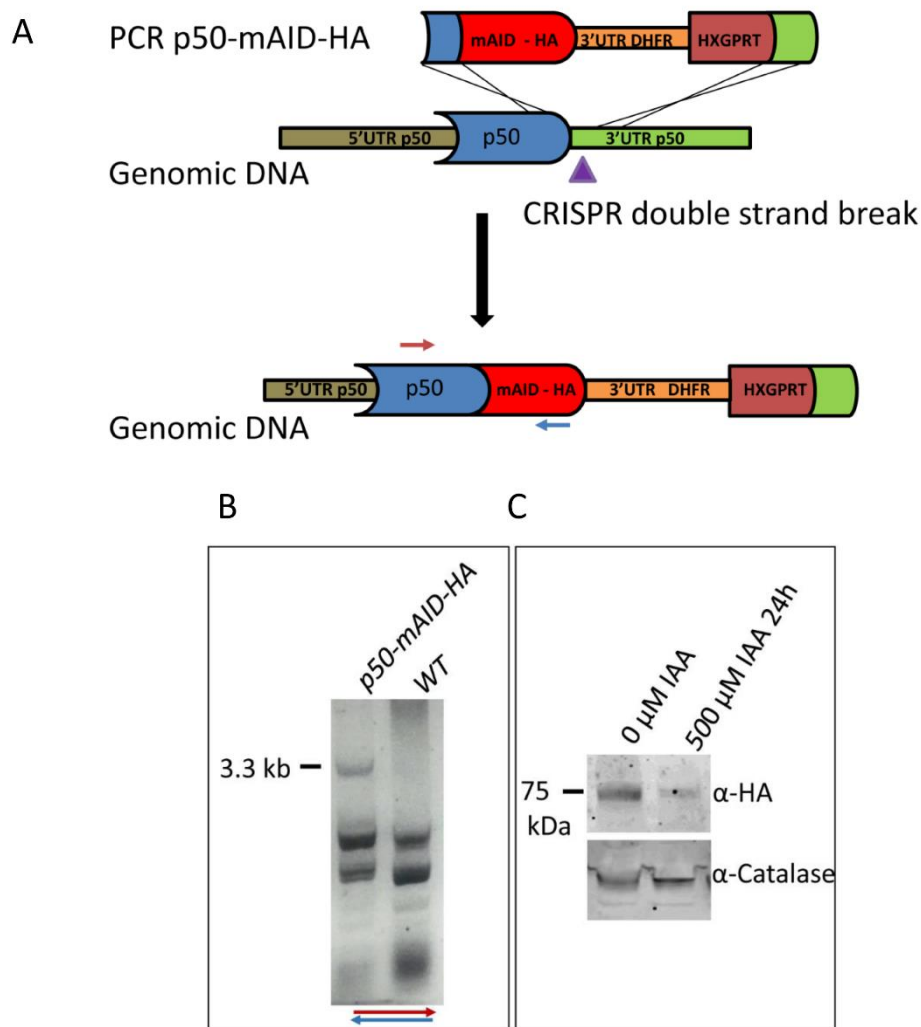


Figure 5-1: Generation of the strain *p50-mAID-HA*

(A) Scheme of knock-in strategy: a double crossover event allows fusion of mAID-HA to the 3' of p50; integration was facilitated by a double strand break caused by a CRISPR/Cas9 vector containing a p50-specific gRNA, which was transiently transfected in the strain *Tir1Δku80*. (B) Analytical PCR confirms correct integration in the *p50-mAID-HA* strain; a 3.3 kb product is amplified in the newly obtained strain, and not in the parental strain *Tir1Δku80* (WT); the primers used are indicated as red and blue arrows in (A). (C) Western blotting on the *p50-mAID-HA* strain using α -HA antibody shows the expected band for the fusion protein (≈ 75 KDa); after 24 hours of IAA treatment, the signal of p50-mAID-HA is highly reduced.

5.2 Analysis of p50 localisation and function

To assess the localisation and function of p50 in *T. gondii* intracellular tachyzoites, IFA analysis was carried out on the strain *p50-mAID-HA* grown for 24 hours in presence and absence of IAA. Staining with α -HA antibody shows a specific signal of p50 in non-induced parasites: a punctuated pattern distributed along the periphery of the parasite, but also found, at weaker levels, in the cytoplasm (Fig. 5-2, upper row). No signal is found in *p50-mAID-HA* parasites

probed with α -HA antibody after 24 hour induction with 500 μ M of IAA (Fig. 5-2, lower row).

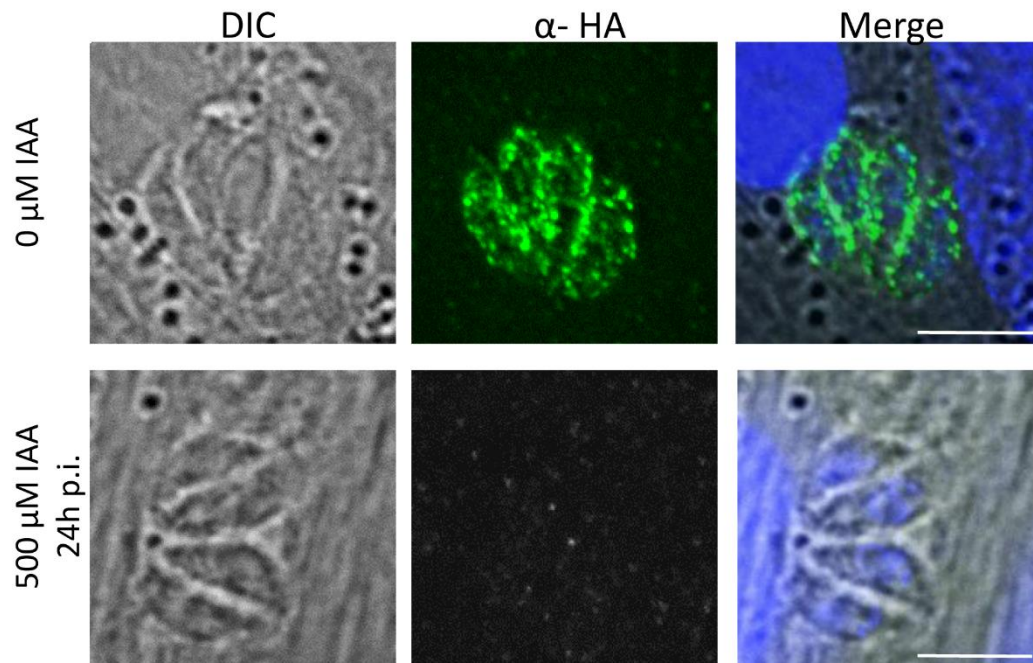


Figure 5-2: p50 localisation and downregulation in the strain *p50-mAID-HA*

IFA on the strain *p50-mAID-HA* parasite line reveals a specific HA signal (green) in non-induced parasites, which is not found after treatment with 500 μ M of IAA for 24 hours. Scale bars: 5 μ m.

As p50 signal is localised prevalently at the periphery of the parasite, colocalisation with other organelles shows a partial overlap with markers of the IMC, the mitochondrion and the apical organelles; however, no perfect colocalisation with these organelles was observed (Fig. 5-3).

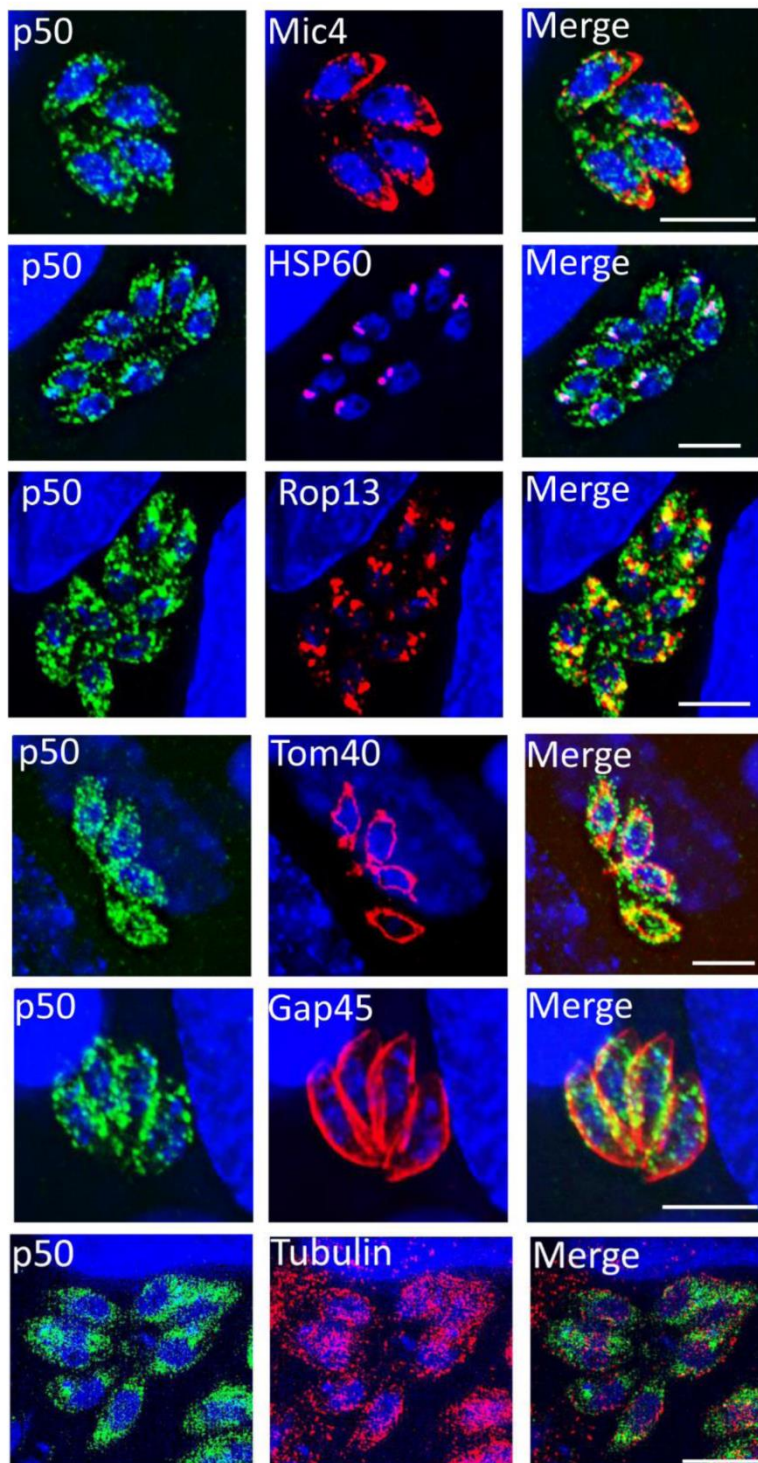


Figure 5-3: Colocalisation analysis in the strain *p50-mAID-HA*

Immunofluorescence analysis shows that p50 (α -HA, green) partially colocalises at the apical end with micronemes and rhoptries (Mic4 and Rop13, respectively). Along the parasite periphery, but not at its central and basal regions, p50 signal overlaps with the IMC (GAP45), microtubules (Tubulin) and the mitochondrion (Tom40). Scale bars: 5 μ m.

To assess the effect of p50 downregulation on parasite fitness, plaque assay was carried out on *p50-mAID-HA* parasites grown in presence and absence of 500 μ M IAA for seven days; the *RH* strain was used as a control. It was observed that

induced parasites can still form plaques, but the plaque area is highly reduced compared to non-induced parasites, as measured in Fig. 5-4; this result shows that p50 is important for parasite fitness. Moreover, the number of plaques observed was also highly reduced, which could suggest a defect in invasion.

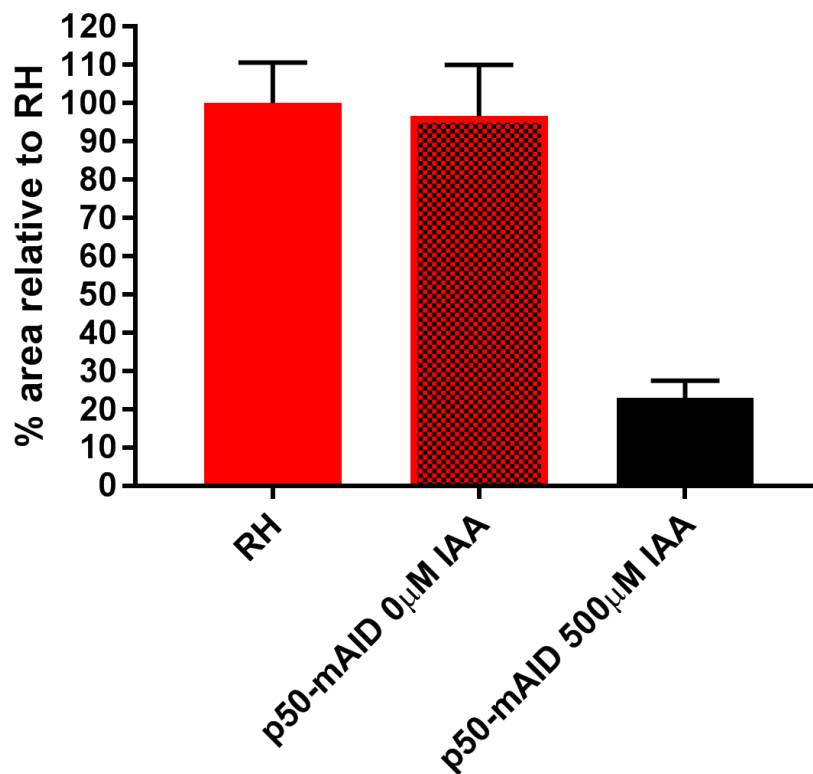


Figure 5-4: Quantification of growth in *p50-mAID-HA* parasites in presence and absence of IAA

Plaque assay was used to assess growth of *p50-mAID-HA* line compared to wild-type parasites. IAA-treated *p50-mAID-HA* parasites showed a marked reduction in plaque size. Plaque areas were measured using ImageJ drawing tool. Graphic shows average \pm SD. 10 plaques were analysed per each condition.

Replication assay confirmed this observation, as it was observed that induced *p50-mAID-HA* parasites display a severe delay in replication when compared to the wild type strain: the percentage of vacuoles containing 2 or 4 parasites is much higher than in the control, while vacuoles of 8 and 16 parasites are present in much smaller numbers (Fig. 5-5). It was also seen that *p50-mAID-HA* non-induced parasites show a slight delay in replication; this could point to a leakiness of the IAA system.

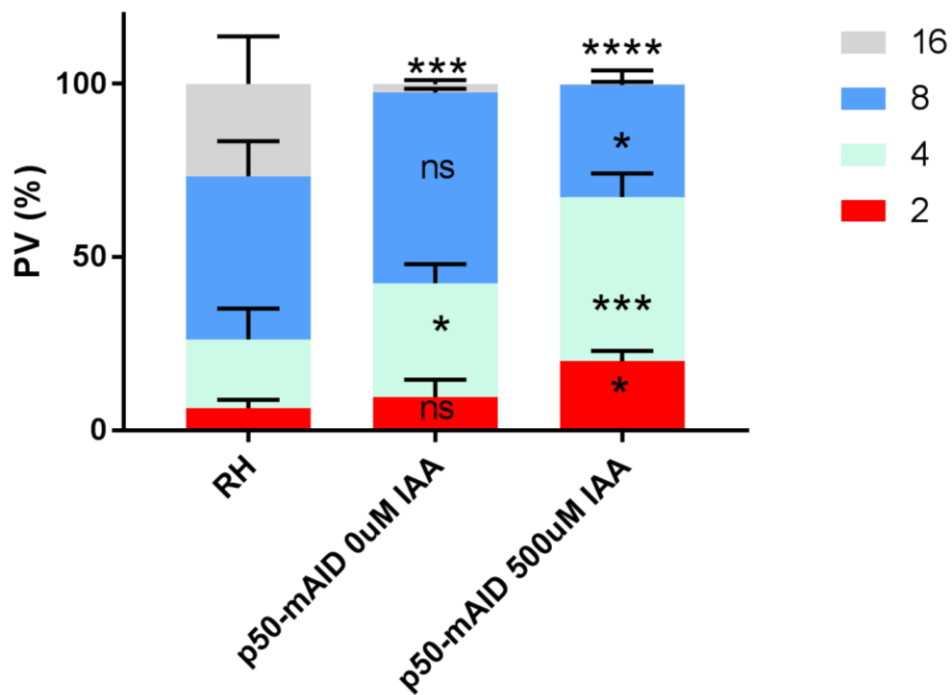


Figure 5-5: Analysis of replication in *p50-mAID-HA* parasite strain

Replication assay of RH and *p50-mAID-HA* parasites in presence or absence of IAA. Shows that p50 downregulation results in replication delay. The number of parasites per vacuole was counted 24 hours post infection. Graphic depicts mean \pm SD. One-way ANOVA followed by Dunnett test for multiple comparisons were used to analyse the data. **** $P \leq 0.0001$, *** $P \leq 0.0002$, * $P \leq 0.05$, not significant (ns) $P > 0.05$.

To understand the cause of the impaired growth observed upon p50 downregulation, IFA analysis on *p50-mAID-HA* parasites induced with 500 μ M IAA was carried out. As shown before, Western Blot and IFA analysis show that the signal of p50 is significantly decreased at 24 hours post induction. It was found that at this time point, nucleus morphology and rosette organisation are not significantly affected by p50 knockdown. Likewise, biogenesis of the apicoplast and of secretory organelles such as micronemes and dense granules was not altered (Fig.5-6a and b).

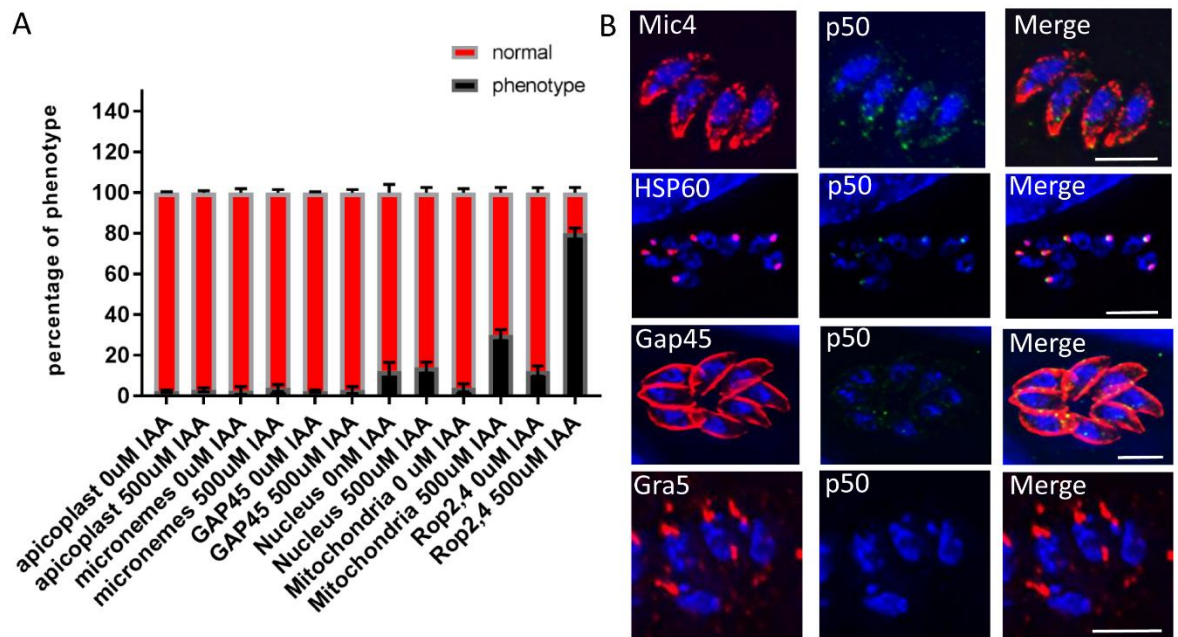


Figure 5-6: Analysis of p50 knockdown effect on different organelles of *T. gondii*

(A) Quantification (n=3, 100 vacuoles counted per experiment) shows that at 24 hours post induction, p50 down-regulation does not affect nucleus morphology (assessed with DAPI staining), parasite structure (measured with α -GAP45 antibody) or apicoplast and microneme biogenesis (probed with α -HSP60 and α -Mic4 respectively). In contrast, a significant ($p < 0.05$) increase in aberrant mitochondria and rhoptry biogenesis was observed. (B) Representative images of IFA analysis for Micronemes (α -Mic4), apicoplast (α -HSP60), IMC (α -GAP45), dense granules (α -Gra5) and nucleus (DAPI staining) in induced *p50-mAID-HA* parasites. Scale bars: 5 μ m.

Conversely, two organelles seemed to be affected by p50 ablation. IFA analysis and quantification in *p50-mAID-HA* parasites induced for 24 hours showed that p50 downregulation has an effect on mitochondria biogenesis, as 30% of the mitochondria displayed an aberrant morphology. In these vacuoles, the mitochondrial lost their characteristic lasso-shape, and were found clustered at one side of the parasite; thus, as a result of p50 downregulation, the mitochondrial membrane seemed to have lost contact with the parasite periphery (Fig.5-7, arrows). However, 70% of the vacuoles showed healthy, lasso-shaped mitochondria. Further analysis at later time points will be required to confirm a role of p50 in mitochondria morphology.

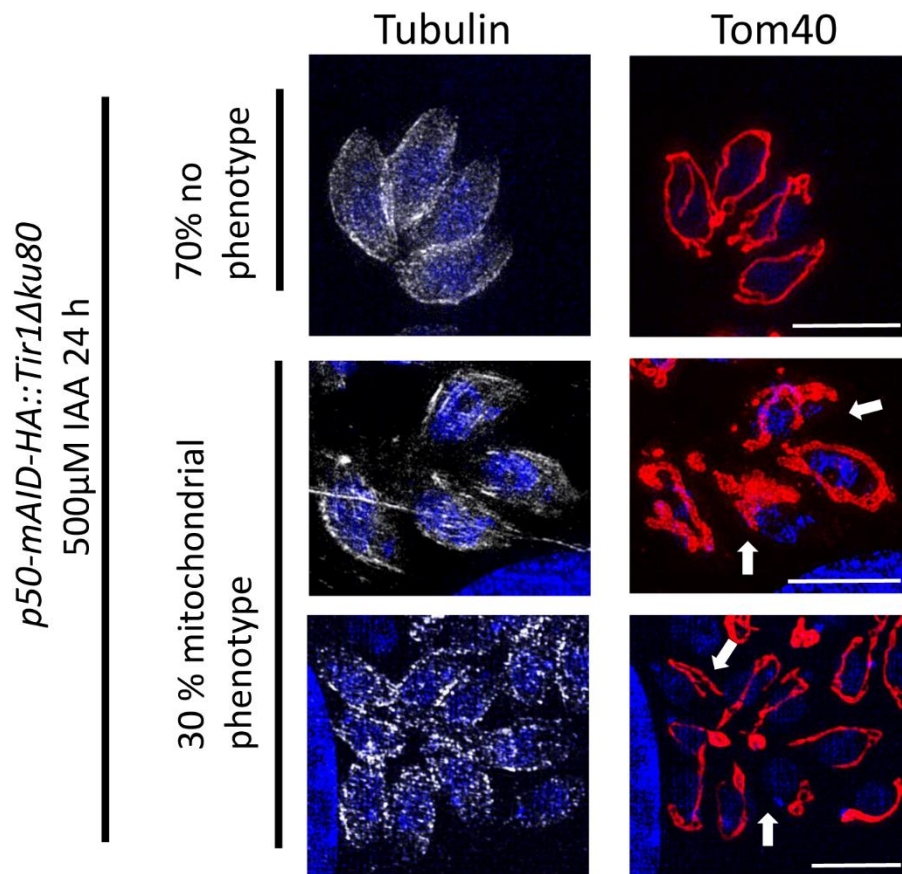


Figure 5-7: p50 knockdown leads to abnormal mitochondria morphology in 30% of counted vacuoles

IFA analysis shows that at 24 hours post induction 70% of parasites *p50-mAID-HA* show healthy mitochondria; however, the remaining 30% presents mitochondria which have lost their lasso shape, and are clustered at one side of the parasite periphery (arrows). Red, mitochondrial marker Tom40; in grey, α -tubulin. Scale bars: 5 μ m.

Surprisingly, upon p50 knockdown 80% of the vacuoles showed a defect in rhoptry distribution: staining with the marker Rop 2,4 shows that in induced parasites, rhoptries are not concentrated at the apical complex, but rather form filamentous structures along the whole length of the parasite (Fig.5-8). This is a different distribution from the one that is observed in dividing parasites, where newly-formed rhoptries are found in the body of developing daughter cells and in the residual body (Nishi et al., 2008); parasites undergoing division were not counted in the experiment (an example of rhoptry distribution in dividing parasites is shown in Fig. 5-8, asterisk).

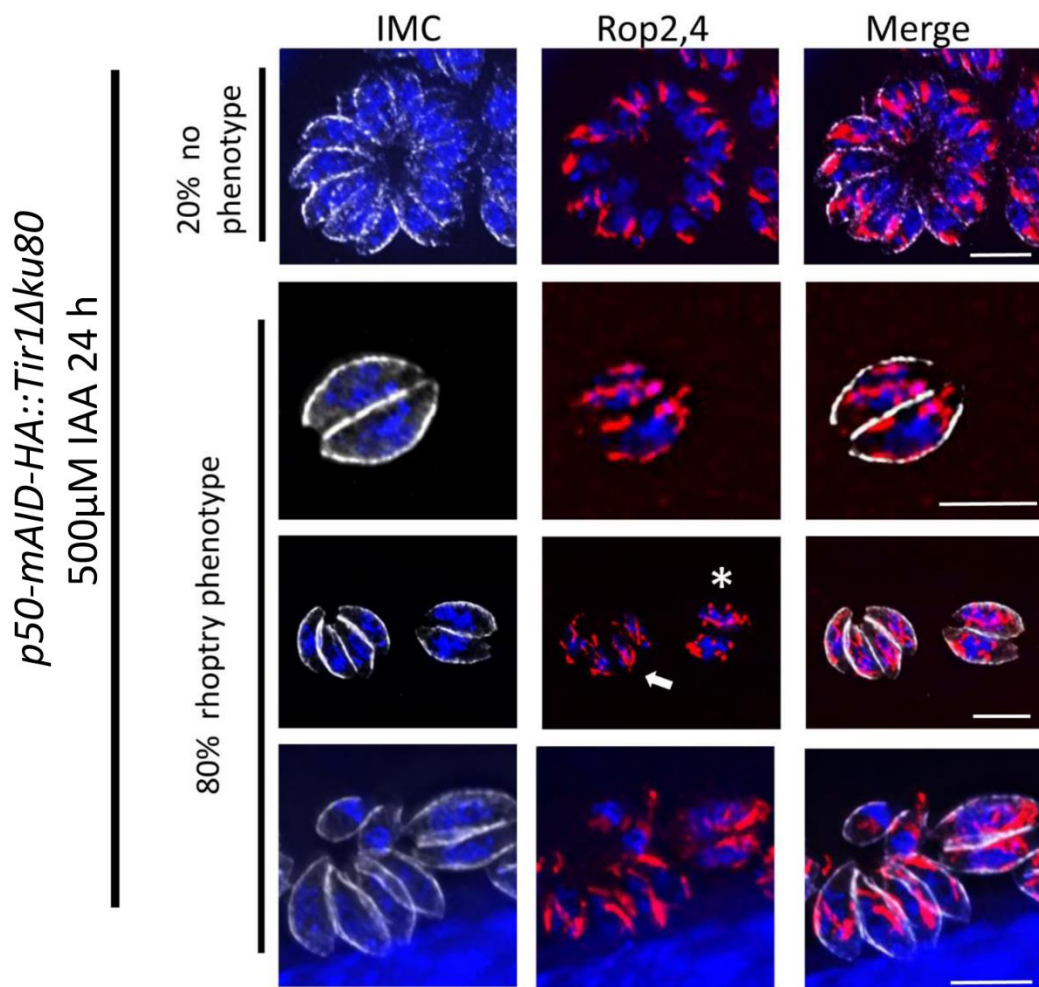


Figure 5-8: p50 knockdown results in a defect in rhoptry biogenesis

IFA analysis shows that at 24 hours post induction, p50 down-regulation leads to a defect in rhoptry distribution in 80% of the vacuoles, which show rhoptries that are no longer concentrated at the apical end, but are distributed along the parasite body. Parasites undergoing division were not counted, as rhoptry distribution changes during endodyogeny (asterisk). Red, Rhoptry marker Rop2,4; in grey GAP45. Scale bars: 5 μ m

5.3 Conclusions

In this chapter, p50 localisation and function were analysed, since data shown in the previous sections suggested that the dynamin-related protein DrpC could be linked to microtubule-based dynamics. IP experiments had found a potential interaction between DrpC and the microtubule motor complex dynein/dynactin.

In *T. gondii*, the function of this motor has not been characterised.

Bioinformatics analysis showed that a conserved dynein complex is present in a majority of Apicomplexans; moreover, as discussed in paragraph 1.5.4, dynactin subunits such as Arp1, p25, p27 p62 and p50 are conserved in *T. gondii* and *P. falciparum* (Gordon and Sibley, 2005, Morrissette, 2015). This suggests that a

functional dynein/dynamitin complex is active in these parasites, though its function has not been investigated.

Here, the function of p50 in *T. gondii* was analysed. This subunit has been shown to be essential for the correct formation of the dynein/dynactin complex in higher eukaryotes, and its ablation or overexpression have been often used to study the function of this complex (Burkhardt et al., 1997, Echeverri et al., 1996, Valetti et al., 1999, Melkonian et al., 2007).

It was found that in *T. gondii* tachyzoites p50 is distributed along the parasite periphery, but is also distributed in the cytoplasm. Moreover, using the Auxin-Degron system a downregulation of the protein was obtained. p50 knockdown is found to be deleterious for the parasite, as plaque assay shows a great reduction in plaque area in induced *p50-mAID-HA* parasites. This is confirmed by replication assays, which found a severe delay in division rates when p50 knockdown is induced.

Western Blot and IFA analyses indicated that 24 hours of IAA treatment were necessary to induce a significant down-regulation of p50; thus, a preliminary characterisation of p50 knockdown effects was done at this time point. It was seen that, while nucleus, micronemes and IMC are not affected by p50 ablation, a significant percentage of mitochondria show a phenotype: they do not encircle the parasite with their characteristic lasso shape, but rather they cluster at one side of the parasite periphery.

Thus, these observations could indicate a role of the dynein/dynactin complex in mitochondria movement; in other systems, it is well known that the dynein/dynactin complex mediates mitochondria migration towards the minus end of the microtubules (Morlino et al., 2014, Russo et al., 2009). As already discussed, *T. gondii* subpellicular microtubules emanate from the polar ring, a microtubule-organizing centre located at the apical end of the parasite; thus, the minus-end of the microtubules is at the apical end of the parasite. In an hypothetical model where the dynein/dynactin complex is important for mitochondrial migration, we could expect that inhibition of complex formation would result in a block of mitochondria migration towards the apical end of the parasite. This could be lead to a defect in mitochondria biogenesis during

endodyogeny, when the replicated mitochondrial branches need to enter the newly formed daughter cells; the clustered mitochondria observed in induced *p50-mAID-HA* parasites could be a result of a block of mitochondrial movement. However, it must be mentioned that upon p50 knockdown, the mitochondrial phenotype is observed only in 30% of the parasites; moreover, not all the mitochondria in a vacuole show this abnormal morphology.

The analysis of the mitochondrial phenotype is complicated by the observation of another, more recurrent phenotype: a mislocalisation of rhoptries, which are secretory organelles of the parasite apical complex. Upon p50 down-regulation, the signal of the rhoptry marker Rop2,4 (and also of the marker Rop1) is found all along the parasite body, in 80% of the vacuoles.

This data correlates with observations in other systems, where it was shown that inactivation of the dynein/dynactin complex through p50 overexpression impairs correct vesicular trafficking (Burkhardt et al., 1997). Interestingly, rhoptry transport to the apical complex in *T. gondii* was also shown to depend on actin filaments, and to be mediated by the motor protein Myosin F and by the armadillo repeat protein ARO (Mueller et al., 2013, Mueller et al., 2016). This could suggest that rhoptries are transported in a 2-step process, involving actin- and microtubule-based mechanisms.

Thus, more work is needed to understand p50 function in *T. gondii*. Invasion assays should be carried out to confirm a depletion of rhoptries from the apical complex upon induction of p50 knockdown; moreover, a more detailed phenotypic analysis, which should also encompass Golgi and ER morphology, along with other markers of rhoptry organelles, is needed, as well as co-immunoprecipitation experiments to confirm the interaction between p50 and DrpC.

Finally, mitochondrial behaviour in induced *p50-mAID-HA* parasites should be investigated after longer induction periods, to assess whether the percentage of abnormal mitochondria increases with time; mitochondria migration upon p50 downregulation is likewise being investigated in ongoing work in my research group.

6 General discussion

6.1 DrpC mediates mitochondria fission during endodyogeny

In most eukaryotes, mitochondria are essential for cell viability. They are the main source of energy for the cell, coupling the electron transport chain (ETC) with ATP production; they carry out crucial biochemical pathways, such as β -oxidation of fatty acids and Krebs cycle, heme biosynthesis, iron/sulfur cluster assembly, and the metabolism of certain amino acids; moreover, they are key regulators of apoptosis and senescence (Friedman and Nunnari, 2014, Nicholls and Ferguson, 2013).

As a consequence, these organelles need to quickly respond to changes in the environment; in many organisms, mitochondrial plasticity is ensured through the formation of a highly dynamic mitochondrial network during interphase. The number, functionality and shape of the mitochondria in the network depend on a highly regulated balance of fission, fusion, motility and tethering. During interphase, the interplay of these mechanisms is used to quickly remodel the network in response to extracellular stimuli or altered metabolic demands (Pagliuso et al., 2018, Ramachandran, 2017, van der Bliek et al., 2013, Lackner, 2014).

During mitosis, however, mitochondrial dynamics have a different function. Cells entering the M phase need to ensure partitioning of the mitochondria; thus, they fragment their mitochondrial network by increasing fission rates. After cytokinesis, the formation of the interphase mitochondrial network is restored by inhibition of the fission machinery, which leads to an increase in fusion rates; moreover, mitochondria are actively transported towards the periphery of the divided cells (Kanfer and Kornmann, 2016).

In Apicomplexa parasites such as *T. gondii*, conservation of such dynamics has not been investigated. Mitochondria adaptability is very important for organisms of this phylum, since their parasitic lifestyle exposes them to a great variation in energy supply. However, they do not present a mitochondrial network; most Apicomplexa, including *T. gondii* and *P. Falciparum*, are characterised by a single, elongated mitochondrion which surrounds the parasite periphery, and whose morphology does not change significantly in the asexual stages, at least in intracellular parasites (de Souza et al., 2009, Ovciarikova et al., 2017). Thus, it would seem that mitochondrial activity in these parasites is not modulated through remodelling of the mitochondrial shape (Zikova et al., 2016, MacRae et al., 2012, Sheiner et al., 2013).

Conversely, great changes in organelle morphology are observed in two different stages of the parasite lytic cycle: when, upon egress from the host cell, the mitochondrion drastically reduces its proximity to the periphery (Ovciarikova et al., 2017); and, most prominently, during parasite division (Nishi et al., 2008). As already described, new mitochondrial branches form during the early stage of *T. gondii* endodyogeny (Nishi et al., 2008); this event is likely coordinated with mtDNA replication, similarly to what is observed in *P. falciparum* (Preiser et al., 1996). The newly formed branches remain in the mother cell body till the last steps of endodyogeny, when they rapidly enter the budding daughter cells from their basal end, and remain interconnected at their base for variable periods, until a severing of the membrane leads to the formation of separate, independent organelles (Nishi et al., 2008). Thus, while no fusion event is apparent during endodyogeny, fission and motility could be required at least during the last steps of parasite division.

In this work, the conservation of the machinery for mitochondria fission was assessed. In most eukaryotes, Dynamin-related proteins are key effectors of this process, as these mechanoenzymes use energy from GTP hydrolysis to constrict membrane tubules. This membrane remodelling activity requires a pre-constriction step (usually mediated by the concerted action of ER and actin); moreover, receptors on the mitochondrial surface are necessary for Drps recruitment and activation (Pernas and Scorrano, 2016, Lackner et al., 2009, Lackner et al., 2013, Kraus and Ryan, 2017). Drp1 and Dnm1, involved in

mitochondrial fission in humans and yeast, show a conserved mechanism of action, though they bind to different receptors on the membrane.

T. gondii shows conservation of three Dynamin-related proteins. DrpA and DrpB are Alveolate-specific and show a typical domain architecture, with well-conserved GTPase, GED and Middle domains. These proteins were shown to play essential roles in apicoplast division (van Dooren et al., 2009) and in the biogenesis of the unique secretory organelles (Breinich et al., 2009) respectively. While a minor role for DrpA and DrpB in mitochondrial biogenesis could not be ruled out, no clear implication in mitochondrial division was found (van Dooren et al., 2009).

DrpC, a protein that shares no significant sequence identity with any protein outside the apicomplexan phylum, was identified as a third potential member of the Dynamin superfamily in these parasites (Breinich et al., 2009, Purkanti and Thattai, 2015, van Dooren et al., 2009); its downregulation was shown to be deleterious for parasite growth, but its role remained unknown (Pieperhoff et al., 2015).

My analysis started with the characterisation of DrpC function in *T. gondii* tachyzoites. While most of DrpC amino acid structure is highly divergent, the GTPase domain at its N-terminus shows low, yet significant sequence identity with other members of the Dynamin superfamily. As previously described, DrpC is Apicomplexa-specific, and shows high sequence similarity with its homolog in *Plasmodium spp.* (van Dooren et al., 2009, Breinich et al., 2009). It is also conserved in *Cryptosporidium parvum*, though this parasite presents only a relict mitochondria (Riordan et al., 2003, Keithly et al., 2005, Putignani et al., 2004).

Endogenous tagging showed that DrpC localises in puncta along the mitochondrial periphery and basal end. Binding at the basal end of the mitochondrion is evident in the last steps of endodyogeny; time-lapse and fixed microscopy showed that DrpC is at the interconnections between newly-formed mitochondrial branches until they are no longer visible. The significance of such recruitment is evident upon DrpC knock-down: in induced *DrpC-HA-U1* parasites, 90% of the vacuoles show severe mitochondrial phenotypes. The specificity of

such effect was confirmed by complementation experiments, where the introduction of a wild-type copy of DrpC in induced parasite restored normal mitochondrial morphology.

In particular, DrpC ablation caused two major phenotypes: 41% of vacuoles showed mitochondria remaining permanently interconnected, while 39% of the mitochondria assume a different phenotype, where the membranes seem thick, and the organelles become club-shaped. While the latter phenotype is of difficult interpretation, the interconnections seen in the majority of mitochondria is highly suggestive of a defect in fission after endodyogeny. To confirm this hypothesis, a dominant negative version of DrpC, with an inactive GTPase domain and tagged with YFP, was expressed, to achieve functional inhibition of the protein: as shown in Fig. 1-11, the mitochondria in a vacuole remained interconnected, and the inactive DrpC was concentrated at their basal part, decorating the interconnections.

These results strongly suggested that DrpC has a role in mitochondria biogenesis. More specifically, it can be assumed that DrpC is the functional homolog of Drp1 and Dnm1, mechanochemical enzymes which use the energy produced by a GTPase domain to catalyse mitochondria fission in humans and yeast, respectively. Homology modelling confirmed that its GTPase domain conserves the overall fold typical of the Dynamin superfamily, supporting the notion of GTPase activity. Interestingly, the expression of the protein DD-GFP-DrpCGTPase only and DD-GFP-DrpCTRUNCATED showed that binding and polymerisation around the mitochondrion is dependent on both the GTPase domain and the C-terminus tail, since these proteins were not able to form puncta, and were only found in the cytoplasm. Conversely, depletion of the GTPase domain of DrpB was shown to lead to a dominant negative effect, suggesting that the protein is able to bind membranes even in absence of this domain (Breinich et al., 2009); however, structural studies on other Dynamin-related proteins involved in mitochondrial fission revealed that, while oligomerisation is principally mediated by the “stalk” region, the GTPase domain is also required for the formation of spirals around the membranes (Frohlich et al., 2013, Marks et al., 2001).

Importantly, the foci at the basal part of the organelle seem to be actively involved in constriction only in a specific stage of the cell cycle. This suggests

that DrpC foci on the mitochondrion are usually kept inactive, until a specific signal triggers GTPase activity when mitochondrial fission is required. Two different mechanisms can be proposed to be in charge of such regulation.

DrpC activity could be regulated by the cell cycle: in dividing mammalian cells, Drp1 activity is stimulated during the M phase, leading to fragmentation of the mitochondrial network. Such fragmentation is directly stimulated by the mitotic kinases Aurora A and cyclin B-cyclin-dependent kinase (CDK)1, key regulators of cell cycle progression, which increase Drp1 GTPase activity through post-translational modifications (Kanfer and Kornmann, 2016, Taguchi et al., 2007). In a similar way, DrpC activity could be stimulated during endodyogeny by a regulator of cell division, to ensure that mitochondria and parasite division are coordinated; it was recently shown that *T. gondii* utilizes multiple Cdk-related kinases (Crks) to regulate different checkpoints during cell division, and some of them, such as Cdk1, control cytoplasmic mechanisms such as daughter assembly (Alvarez and Suvorova, 2017).

However, activation of DrpC GTPase domain could also require a mechanical stimulus. In the mitochondrial network, Drp1/Dnm1 puncta are found in different locations on the mitochondrial surface, but fission occurs only in sites marked by a “pre-constriction” step, which is mediated by two main actors: ER and actin. The ER wraps around mitochondria in sites of future fission (Friedman et al., 2011) and in those sites actin polymerization is induced, through the action of the ER-localised formin 2 (INF2) and the mitochondrial protein Spire1C (Korobova et al., 2013, Manor et al., 2015). Myosin II is subsequently recruited to these sites to help pre-constrict the mitochondrial tubules (Korobova et al., 2014).

Is a similar pre-constriction important for DrpC activity? Though ER and mitochondria seem to be strictly associated in *T. gondii*, a direct interaction between their membranes during endodyogeny was difficult to assess; better tools for the analysis of ER localisation and behaviour are required to further explore ER role in *T. gondii* mitochondrial fission. Moreover, no direct role of actin and myosin in mitochondrial fission has been observed in *T. gondii*. Actin depletion does not affect mitochondria morphology (Periz et al., 2017). Similarly, reagents that perturb the actin cytoskeleton have no effect on

parasite replication; though treated parasites show increased mitochondria profiles in their residual bodies, mitochondrial segregation is not affected (Shaw et al., 2000). Thus, actin would not seem to promote DrpC-mediated mitochondrial fission. Strikingly, mitochondria morphology is severely disrupted in *P. falciparum* gametocytes treated with the same reagents, suggesting a different role of the actin cytoskeleton in parasites at that stage, but not, however, in mitochondrial division (Hliscs et al., 2015).

It was recently shown that ER/actin-mediated pre-constriction is not the only mechanism that induces mitochondrial fission in mammalian cells, as other types of mechanical force can promote the same response (Helle et al., 2017); thus, in *T. gondii* the pre-constriction of the mitochondrion could be due to different mechanisms. For example, the extension of the daughter bud's IMC and the action of the basal body during cytokinesis (see paragraph 1.6) have been proposed to facilitate DrpA-mediated fission of the apicoplast in *T. gondii*, as their action could effect a pre-constriction which reduces the diameter of the organelle (van Dooren et al., 2009, Heaslip et al., 2010, Lorestani et al., 2010). Lorestani et al. proposed that knock out of MORN1 contractile ring at the basal body has an effect not only on apicoplast segregation, but also, at least partially, on the mitochondrion (Lorestani et al., 2010). Thus, it would be interesting to better analyse and quantify mitochondria fission defects in MORN1 knock-out lines, and to compare it to the effect seen upon DrpC ablation.

In conclusion, DrpC is a Dynamin-related protein which mediates mitochondrial fission in *T. gondii*, and whose ablation leads to parasite death. Interestingly, inhibition of mitochondrial fission is not always lethal in other eukaryotes: upon Dnm1 depletion, yeast mitochondrial network becomes a long, tubular structure which can still be transferred to buds during mitosis, but not meiosis (Otsuga et al., 1998). Conversely, defects in mitochondrial fission are lethal during embryo development in mice and humans, causing a wide range of effects: a newborn girl with a mutation in Drp1 GTPase domain showed developmental defects encompassing microcephaly and optic neuropathy (Ishihara et al., 2009, Waterham et al., 2007).

Thus, the results obtained in *T. gondii* confirm the essentiality of mitochondria dynamics in dividing cells, while their significance during interphase in yeast and mammalian cells is still debated (Kowald and Kirkwood, 2011).

6.2 Fis1 function in *T. gondii*

The role of Dynamin-related proteins in mitochondrial fission is widely conserved in eukaryotes: the last eukaryotic common ancestor (LECA) had a multifunctional ancestral Dynamin which likely mediated both mitochondrial and vesicle scission (Purkanti and Thattai, 2015). The mechanisms that lead to Drps recruitment onto the mitochondrial membrane, however, do not show a similar degree of conservation in higher eukaryotes: the composition of the so-called “fission complex”, the system of proteins which mediate Drps binding and activity on the mitochondrial membrane, greatly varies in different organisms (Pagliuso et al., 2018).

Yeast Dnm1 recruitment is mediated by the fungal-specific adaptor Mdv1 and by Fis1, a tail-anchored protein evenly distributed in the mitochondrial surface (Mozdy et al., 2000, Tieu et al., 2002, Naylor et al., 2006). Fis1 is also conserved in humans; its identification initially suggested that the whole machinery of mitochondrial fission is highly conserved in ophisthokonts. However, it is now clear that human Fis1 is not necessary for Drp1 recruitment, which is mediated by another tail-anchored protein, Mff, and by orthologs MiD49 and MiD51 (Gandre-Babbe and van der Bliek, 2008, Otera et al., 2010, Palmer et al., 2011). Thus, Fis1, although expressed in mammalian cells, does not conserve the function observed in yeast cells. This was elegantly proved by Koirala et al., who showed that, in yeast, fission defects caused by Fis1 depletion cannot be complemented by expression of human Fis1 (Koirala et al., 2013).

Similarly, the observation that in *T. gondii* a homolog of Fis1 is highly conserved initially led me to hypothesise that it could have a role in mitochondrial fission. This protein was recently identified as a tail-anchored protein in *T. gondii*; the authors showed that when ectopically expressed, Fis1 localises to the mitochondrion. This localisation is determined by a single transmembrane domain (TMD) at its C-terminus; moreover, a short C-terminus sequence was proposed to be important for mitochondrial localisation (Padgett et al., 2017).

Fis1 was recently reported to be also conserved and expressed in *P. falciparum*, though its role in that parasite was not investigated (Scarpelli et al., 2018).

In this study, weak overexpression of Fis1 and endogenous tagging after promoter replacement confirmed that Fis1 is evenly distributed on the mitochondrial surface.

Surprisingly, Fis1 overexpression led to a severe defect in mitochondria biogenesis, and resulted in parasite death; however, this result does not necessarily indicate a specific Fis1 effect. Similarly, interpretation of overexpression of human Fis1 has been controversial: while it was shown to result in an increase in autophagy rates, this was linked to mitochondrial dysfunction, rather than fragmentation *per se* (Gomes and Scorrano, 2008). Moreover, it is well known that overexpression of proteins which are targeted to specific cellular sub-compartments can lead to growth defects, due to an overloading of localisation resources in the cell (Moriya, 2015). In particular, a recent study showed that overexpression of GFP fused to mitochondrial targeting sequences caused a severe delay in yeast growth, which was linked to an overload of localisation processes, but also, surprisingly, to changes in transcriptional levels of mitochondrial genes (Kintaka et al., 2016).

Finally, Fis1 downregulation experiments lead me to propose that Fis1 is not responsible for DrpC mitochondrial recruitment. Because DrpC is essential, its receptor would be expected to be likewise required for parasite fitness; as shown in chapter 4, however, Fis1 knockdown did not lead to parasite death, or to any defect in mitochondrial biogenesis. While it cannot be excluded that ATC-mediated Fis1 downregulation is not complete (Jimenez-Ruiz et al., 2014), and that residual levels of Fis1 are sufficient to ensure parasite survival, it is interesting to note that a CRISPR/Cas9 genome-wide screen classified Fis1 as “dispensable”, with a phenotypic score of +0.94 (Sidik et al., 2016).

Finally, no evidence of Fis1 interaction with DrpC could be found by Co-IP experiments, though it cannot be excluded that a more sensitive technique would be needed to detect DrpC-Fis1 binding, as Drp1 and Dnm1 bind their respective receptors in a weak, transient fashion (Loson et al., 2013, Otera et al., 2010, Liu and Chan, 2015, Strack and Cribbs, 2012).

In conclusion, similarly to what observed in human cells, Fis1 conservation in *T. gondii* does not seem linked to any essential role in mitochondria fission; what, then, is the conserved function of Fis1? In mammalian cells, Fis1 role in mitochondrial fission was proposed to play a specific role in stress-induced mitochondrial fission, and to be important during apoptosis and mitophagy; these hypothesis, however, are still under debate, as its role in peroxisome fission. Similarly, *T.gondii* Fis1 could have a role in stress responses, though the role of apoptosis in the parasite is not well understood (Li et al., 2015, Ni Nyoman and Luder, 2013); thus, no clear answer as to Fis1 role can be given at the moment.

It is important to note that, while Fis1 was the only putative mitochondrial receptor found to be conserved in *T. gondii* genome, it cannot be excluded that other proteins are functionally conserved, but have been modified so that a simple BLAST-P search cannot recognise them. In fact, it has been often observed that evolution in eukaryotes can result in highly divergent molecules subtending to conserved functions. An example of this phenomenon was recently shown in the parasite *T. brucei*: the proteins of its Nuclear Pole Complex show considerable sequence diversity compared to their counterparts in ophisthokonts, but their secondary structure is overall remarkably similar (Rout et al., 2017). Similarly, the mitochondrial import machinery of this parasite shows a surprising degree of divergence from other organisms, but maintains its overall architecture (van Dooren et al., 2016). Thus, a bioinformatics approach could not be adequate to identify *T. gondii* fission complex; unfortunately, immunoprecipitation experiments did not help me identify any protein which could interact with DrpC on the mitochondrial membrane. However, these experiments suggest that DrpC can interact with elements of the cytoskeleton; these results, together with other observations on DrpC localisation, could suggest a second role for this Dynamin-related protein, as will be discussed in the following paragraph.

6.3 DrpC puncta at the parasite periphery

DrpC puncta are not only localised at mitochondria interconnections. As detailed in Chapter 3, two populations of DrpC foci can be distinguished: the ones recruited at the basal part of the mitochondrion, which catalyse the fission of

the membrane during endodyogeny; and those which are at the mitochondrial periphery throughout interphase.

Strikingly, this second population of DrpC puncta is not in contact with the mitochondrion at all times. As shown in figure 3-4, in the last steps of endodyogeny the replicated mitochondrion is excluded from budding cells, and stays in a bundle at their basal part until it migrates inside. At this point, DrpC puncta are already visible at the periphery of the nascent cells, but are not in contact with the mitochondrial membrane. However, they are seen again in close proximity to mitochondrial branches once these have entered the buds and start encircling their periphery. Thus, it would seem that DrpC localisation at the periphery is not dependent on the mitochondrion, since it is maintained when mitochondria branches are excluded from daughter cells during endodyogeny. Another example was seen upon Fis1 overexpression, which, as already discussed, leads to a severe mitochondrial defect. Upon 24 hours of Fis1 overexpression, the collapsed mitochondrion is at the basal end of the parasite and at the residual body, while only few branches extend at the parasite periphery. Also in this instance, DrpC puncta are kept at the periphery even if the mitochondrion is not interacting with them.

These data suggest that DrpC foci form two populations, which differ not only in their location but also in their mode of recruitment; do they also have different functions? Two different hypotheses could be formulated:

- 1) DrpC foci at the periphery could be in proximity, but not in contact with the mitochondrion; their localisation at the cell periphery could be required to mediate a different process, not linked to mitochondrial morphology. As already observed, it is hypothesised that in the last eukaryotic common ancestor only one Dynamin-related protein was expressed, which mediated both mitochondrial fission and vesicle scission. Similarly, DrpC could have been conserved to mediate not only mitochondrial fission during endodyogeny, but also other membrane remodelling mechanisms; the use of more sensitive pull-down techniques, such as proximity-dependent biotin identification (BioID), could reveal proteins that are in close proximity to DrpC, and help us understand its functions. Interestingly, unpublished work from the Meissner and Waller

groups proposes that proteins of the Adaptin family and the Kelch protein K13 could interact to mediate endocytosis in *T. gondii*; preliminary results show some colocalisation between these complexes and the foci of DrpC at the periphery, though no effect of DrpC on endocytosis has been uncovered till now (Ludek Korey and Chris Klinger, unpublished data).

- 2) DrpC foci at the periphery could contact the mitochondrial membrane at a specific stage, to mediate a different aspect of mitochondrial biogenesis.

This second hypothesis is in good accordance with data from yeast and mammals, where it is well known that only a fraction of Dynamin-related protein puncta seen on the mitochondrial outer membrane participates in mitochondrial division (Schauss et al., 2006, Naylor et al., 2006). In yeast, Dnm1 puncta that are not involved in mitochondrial fission form clusters that exhibit a polarized orientation facing the cell cortex, and are indeed thought to be anchored to it; the formation of these clusters seems to not be dependent on Mdv1 and Fis1 (which in yeast regulate Dnm1 recruitment as sites of fission), but on the receptor Caf4 (Schauss et al., 2006). Strikingly, it was shown that, when mitochondria retract from the periphery, some Dnm1 clusters stay at the cell cortex, losing contact with the mitochondrion (Schauss et al., 2006); this closely resembles the behaviour of DrpC puncta when the mitochondrion is not in contact with the parasite periphery.

However, the role of the puncta contacting the cell periphery in yeast and humans is not clear. They could simply constitute storage pools of inactive Drps, or mark future fission sites. However, a growing body of work suggests that these foci have a different, important role in mitochondria biogenesis. In particular, they have been proposed to be involved in two main processes: mitochondrial tethering to the cell periphery (Otsuga et al., 1998, Schauss et al., 2006, Cervený et al., 2007, Lackner et al., 2013) or mitochondrial motility (Drerup et al., 2017, Strack et al., 2013, Varadi et al., 2004).

Similarly, data shown in this work could suggest that DrpC foci at the periphery could serve either for mitochondrial tethering or to mediate movement. Importantly, immunoprecipitation experiments consistently show an interaction

between DrpC and tubulin. In *T. gondii*, microtubules form a left-handed spiral extending from the apical end to approximately two-thirds of the parasite body. It follows that DrpC puncta at the basal part of the mitochondrion would not be in contact with microtubules; conversely, the foci at the periphery could act as a bridge between the mitochondrion and the microtubule scaffold. This could find a confirmation in the observations made upon DrpC knock-down, which, as discussed before, leads to two different phenotypes: while the majority of mitochondria become interconnected at their base, another 39% of vacuoles show club-shaped, thick mitochondria. Since this second phenotype is not seen when a dominant-negative form of DrpC is expressed, it could be dismissed as a knock-on effect due to general mitochondrial dysfunction induced by absence of fission. However, an alternative explanation could be proposed: the population of DrpC foci at the periphery has a different role, and its ablation results in a distinct phenotype when the strain *DrpC-HA-U1*. In the strain *DD-GFP-DrpCDN*, the overexpressed mutated form is initially seen both at the periphery and at the basal end of the mitochondrion; at 8 hours post induction, however, the dominant negative form of DrpC is highly concentrated at the basal end. Thus, the endogenous, wild-type copy could be recruited to the periphery, and carry out its function.

The club-shaped mitochondria seen upon DrpC knockdown could suggest a role in tethering the lasso-shaped mitochondrion to the microtubule scaffold. In a similar way, Dnm1 has been proposed to interact with the protein Num1 to mediate tethering of the mitochondrion in yeast (Lackner et al., 2013). This seems in contrast with previous work, which showed that the mitochondrion of Apicomplexa parasites is in close juxtaposition with the IMC, and proposed that the mitochondrion is tethered to the IMC, not to microtubules (Ovcariikova et al., 2017, Kudryashev et al., 2010). However, since the microtubule scaffold is located under the IMC, it cannot be excluded that microtubules are likewise engaged in the formation of the mitochondrion-IMC tether. Further work would be required to properly assess the roles of IMC and microtubules in mitochondrial biogenesis. Interestingly, it was shown that knockdown of Gap40, which leads to incomplete assembly of the IMC scaffold, resulted also in abnormal mitochondria, which seem to collapse at one side of the parasite periphery

(Harding et al., 2016); localisation of DrpC puncta in this mutant strain could lead to a better understanding of mitochondrial tethers in *T. gondii*.

Alternatively, DrpC interaction with microtubules could suggest a role in mediating mitochondrial motility. Such function has been proposed in other systems: Strack et al. showed that a Drp1 isoform binds specifically microtubules, and proposed that Drp1 could modulate microtubule dynamics (Strack et al., 2013). Moreover, it was shown that Drp1 localisation can be influenced by the dynein/dynactin motor complex, and that such interaction can regulate mitochondria localisation (Varadi et al., 2004, Drerup et al., 2017).

Strikingly, kinesin and dynein, the motor complexes that mediate cargo movement along microtubule tracks, were also found to co-precipitate with DrpC in *T. gondii*. Upon finding such interaction, I decided to investigate the role of microtubule-based motility in mediating mitochondria movement, which, as already discussed, is important during endodyogeny, when the mitochondria migrate inside budding cells and encircle the periphery to assume their characteristic lasso shape. The use of microtubules depolymerizing drugs such as oryzalin has already been shown to greatly affect daughter cell formation, and to lead to pleiotropic effects (Nishi et al., 2008). It is thought, however, that mitochondrial entry in budding daughters is not affected by oryzalin treatment; in contrast, the characteristic lasso-shape of the mitochondrion is lost (Ovcariikova et al., 2017, Nishi et al., 2008). During my work, I repeated these experiments, and confirmed that oryzalin severely affects mitochondria morphology.

A similar result is shown here when p50, a component of the dynein/dynactin motor complex, is disrupted. This subunit has been shown to be essential for the functionality of the complex in ophistokonts, as it mediates the correct assembly of dynactin, an essential regulator of dynein function; as a result, knockdown or overexpression of p50 results in the disruption of dynein/dynactin- based motility (Schroer and Sheetz, 1991, Gill et al., 1991). It is shown here that, 24 hours post-induction of p50 knockdown, 30% of the vacuoles show mitochondria which fail to encircle the parasite, but rather are clustered at one side of the cell periphery. As the dynein/dynactin complex mediates motility towards the minus end of the microtubules, which in *T. gondii* is near the apical pole, the

phenotype observed could suggest that the dynein complex has a role in mitochondria migration at the periphery to establish their lasso shape. Interestingly, it was recently observed that axonal mitochondria transport in *D. melanogaster* neurons is dependent on the dynactin subunit Act10, which was seen to directly bind Drp1 (Drerup et al., 2017).

However, it must be considered that the mitochondrial defect is not the only result of p50 ablation; a more prominent defect in rhoptry distribution was observed. 24 hours after auxin-mediated p50 downregulation, 80% of the vacuoles show rhoptry mislocalisation. Rhoptries are usually concentrated at the apical part of the parasite body in a structure called Apical complex, where these organelles together with micronemes, another type of secretory organelles) are docked and released upon invasion. Upon p50 downregulation, staining with the rhoptry marker Rop2,4 showed that rhoptries were not at the apical complex, but formed filamentous structures along the whole length of the parasite; conversely, localisation of the micronemal protein Mic4 was not affected. The observed phenotype does not seem to indicate a defect in trafficking of rhoptry proteins. Rhoptries are mainly formed *de novo* during endodyogeny: fusion of vesicles deriving from the trans-Golgi network gives rise to pre-rhoptries, which eventually develop into mature organelles (Shaw et al., 1998). When correct trafficking is disrupted, rhoptries and micronemes are constitutively secreted, and found in the parasitophorous vacuole, as shown by inhibition of DrpB, TgSORTLR and Vps35, which are essential to guide proteins from the Golgi apparatus to pre-rhoptries or immature micronemes (for more detail, see paragraph 1.5.1) (Breinich et al., 2009, Sloves et al., 2012, Sangaré et al., 2016). p50 knockdown did not lead to constitutive secretion; the observed mislocalisation of rhoptries could be linked to a faulty transport of these organelles to the apical complex. A similar result was shown upon disruption of dynein/dynactin activity in mammalian cells: vesicular trafficking and correct membrane organelle distribution were severely impaired, and endocytic organelles were redistributed to the cell periphery (Burkhardt et al., 1997). The authors proposed that upon dynein/dynactin inhibition, the dynamic equilibrium between dynein and kinesin activity, which normally controls positioning of these organelles, was disrupted; unopposed action of the kinesin motor would

then lead to mislocalisation. A similar equilibrium could be present in *T. gondii*, where several kinesin subunits are conserved (as discussed in paragraph 1.5.4).

However, it is important to note that rhoptry positioning at the apical complex was previously shown to depend also on the armadillo repeat protein ARO, which can interact with the myosin motor MyoF, which has been also involved in dense granules motility, apicoplast segregation and centrosome positioning (Jacot et al., 2013, Heaslip et al., 2016). Moreover, actin depolymerisation was shown to affect rhoptry distribution, and the authors concluded that movement of these organelles to the apical complex is regulated by an acto/myosin mechanism (!!! INVALID CITATION !!!). Data shown here suggest that microtubule-based movement could also be important for rhoptry distribution; further analysis is being carried out in my research group to better understand this process and p50 function in *T. gondii*.

6.4 Conclusions

The findings of this thesis are summarised in Table 6-1. The main effectors of mitochondrial dynamics that were found to be conserved in *T. gondii* and that were studied in my work are reported, together with their homologs in *Plasmodium falciparum* (strain 3D7) and *Plasmodium berghei* (strain ANKA). Importantly, these three organisms have recently benefited from large-scale genetic analyses which aimed to systematically categorise genes based on their essentiality (Sidik et al., 2016, Gomes et al., 2015, Zhang et al., 2018); thus, the table reports - when this information was found to be available in the ToxoDB and PlasmoDB databases - if the mentioned genes were also found to be essential or dispensable in the respective organisms in these high-throughput screens. Finally, in the last column the putative function of these conserved genes in *T. gondii* (based on previous research and on the analysis provided in this thesis) is summarised.

Principal effectors of mitochondrial dynamics in humans and yeast	Homologs present in <i>T. gondii</i> , <i>P. falciparum</i> and <i>P. bergheii</i>	Essentiality in <i>-T. gondii</i> (Crispr screen), <i>- P. falciparum</i> (Piggyback insertion mutagenesis screen) <i>- P. bergheii</i> (PlasmoGEM KO screen)	Evidence for function in <i>T. gondii</i>	
Dynamin-related proteins: <ul style="list-style-type: none"> - Dnm1, Drp1 (main effectors of mitochondrial division in yeast and humans) - Fzo1/Mitofusin1-2; OPA1 (main effector of mitochondrial fusion in yeast and humans) 	DrpA <i>T.g.</i> : TGME49_267800 <i>P.f.</i> : PF3D7_1037500 <i>P.b.</i> : PBANKA_0520400	<i>T.g.</i> : Essential (phenotypic score -4.14) <i>P.f.</i> : Essential (mutagenesis index score 0.12) <i>P.b.</i> : Essential (relative growth rate 0.23)	Expression of DrpA dominant negative form leads to defect in apicoplast division (Van Dooren et al., 2009)	
	DrpB <i>T.g.</i> : TGME49_321620 <i>P.f.</i> : PF3D7_1145400 <i>P.b.</i> : PBANKA_0903600	<i>T.g.</i> : Essential (phenotypic score -4.91) <i>P.f.</i> : Essential (mutagenesis index score 0.12) <i>P.b.</i> : No data available		Expression of DrpA dominant negative form leads to defect in biogenesis of secretory organelles (Breinich et. al., 2009)
	DrpC <i>T.g.</i> : TGME49_270690 <i>P.f.</i> : PF3D7_1218500 <i>P.b.</i> : PBANKA_1434100	<i>T.g.</i> : Essential (phenotypic score -4.54) <i>P.f.</i> : Essential (mutagenesis index score 0.13) <i>P.b.</i> : No data available	Knock down and dominant negative forms cause defect in mitochondrial division (this study)	
	Fis1 <i>T.g.</i> : TGME49_263323 <i>P.f.</i> : PF3D7_1325600 <i>P.b.</i> : PBANKA_1340700	<i>T.g.</i> : Dispensable (phenotypic score 0.94) <i>P.f.</i> : Dispensable (mutagenesis index score 0.63) <i>P.b.</i> : No data available		Localised on the mitochondrion; its knockdown does not lead to reduced growth or mitochondrial defects (this study)
	Other receptors of yeast Dnm1 (Mdv1/Caf4/Num1/Mdm36) and human Drp1 (MiD49/50)	No homologs found in <i>T.g.</i> , <i>P.f.</i> and <i>P.b.</i>	-	
	Miro/ Milton (mediate microtubule-based motility)	No homologs found in <i>T.g.</i> , <i>P.f.</i> and <i>P.b.</i>	-	-
Kif5b (kinesin motor protein involved in anterograde transport of mitochondria in humans)	Several homologs found in Apicomplexa; of them, one is here mentioned: <i>T.g.</i> : TGME49_286660	<i>T.g.</i> : Dispensable (phenotypic score 1.08)	Suggested interaction with DrpC; attempts to tag it were unsuccessful (this study)	
Dynein/dynactin complex (mediates retrograde transport of mitochondria in humans)	Several subunits conserved in Apicomplexa; of them, one is here mentioned, (p50) <i>T.g.</i> : TGME49_246740	<i>T.g.</i> : Fitness conferring (phenotypic score -3.36)	Suggested interaction with DrpC; when down-regulated, a limited effect on mitochondria morphology was observed, along with a more pronounced defect in roptry distribution (this study).	
	<i>P.f.</i> : PF3D7_1346000	<i>P.f.</i> : Dispensable (mutagenesis index score 1)		
	<i>P.b.</i> : PBANKA_1358900	<i>P.b.</i> : Dispensable (relative growth rate 1)		

Table 6-1: Summary of current knowledge about putative conserved effectors mitochondrial dynamics in Apicomplexa parasites.

In conclusion, this work shows that the Apicomplexa-specific DrpC is a highly divergent Dynamin-related protein which mediates mitochondrial fission during *T. gondii* endodyogeny. Activity of its GTPase domain is essential for this function, and holds potential as a drug target against apicomplexan parasites. Moreover, two putative interactors of DrpC have been here characterised. The mitochondrial protein Fis1 is not essential for parasite growth, and does not seem to be required for mitochondria biogenesis or for DrpC-mediated fission; in my analysis, no interaction was found between the two proteins. Conversely, the dynactin subunit p50 was shown to be pulled-down in immunoprecipitation experiments that used DrpC as a bait; its ablation leads to a reduced mitochondrial defect, and to a striking rhoptry mislocalisation.

Accompanying material

Movie1

Live imaging performed on the strain *DrpC-YFP::TdTomato- TGME49_215430*, to follow DrpC localisation on the mitochondrion .

Bibliography

- ABAD, X., VERA, M., JUNG, S. P., OSWALD, E., ROMERO, I., AMIN, V., FORTES, P. & GUNDERSON, S. I. 2008. Requirements for gene silencing mediated by U1 snRNA binding to a target sequence. *Nucleic Acids Res*, 36, 2338-52.
- ADL, S. M., LEANDER, B. S., SIMPSON, A. G., ARCHIBALD, J. M., ANDERSON, O. R., BASS, D., BOWSER, S. S., BRUGEROLLE, G., FARMER, M. A., KARPOV, S., KOLISKO, M., LANE, C. E., LODGE, D. J., MANN, D. G., MEISTERFELD, R., MENDOZA, L., MOESTRUP, O., MOZLEY-STANDRIDGE, S. E., SMIRNOV, A. V. & SPIEGEL, F. 2007. Diversity, nomenclature, and taxonomy of protists. *Syst Biol*, 56, 684-9.
- ADL, S. M., SIMPSON, A. G., FARMER, M. A., ANDERSEN, R. A., ANDERSON, O. R., BARTA, J. R., BOWSER, S. S., BRUGEROLLE, G., FENSOME, R. A., FREDERICQ, S., JAMES, T. Y., KARPOV, S., KUGRENS, P., KRUG, J., LANE, C. E., LEWIS, L. A., LODGE, J., LYNN, D. H., MANN, D. G., MCCOURT, R. M., MENDOZA, L., MOESTRUP, O., MOZLEY-STANDRIDGE, S. E., NERAD, T. A., SHEARER, C. A., SMIRNOV, A. V., SPIEGEL, F. W. & TAYLOR, M. F. 2005. The new higher level classification of eukaryotes with emphasis on the taxonomy of protists. *J Eukaryot Microbiol*, 52, 399-451.
- AGOP-NERSESIAN, C., EGARTER, S., LANGSLEY, G., FOTH, B. J., FERGUSON, D. J. & MEISSNER, M. 2010. Biogenesis of the inner membrane complex is dependent on vesicular transport by the alveolate specific GTPase Rab11B. *PLoS Pathog*, 6, e1001029.
- AGOP-NERSESIAN, C., NAISSANT, B., BEN RACHED, F., RAUCH, M., KRETZSCHMAR, A., THIBERGE, S., MENARD, R., FERGUSON, D. J., MEISSNER, M. & LANGSLEY, G. 2009. Rab11A-controlled assembly of the inner membrane complex is required for completion of apicomplexan cytokinesis. *PLoS Pathog*, 5, e1000270.
- ALDAY, P. H. & DOGGETT, J. S. 2017. Drugs in development for toxoplasmosis: advances, challenges, and current status. *Drug design, development and therapy*, 11, 273.
- ALEXANDER, D. L., MITAL, J., WARD, G. E., BRADLEY, P. & BOOTHROYD, J. C. 2005. Identification of the moving junction complex of *Toxoplasma gondii*: a collaboration between distinct secretory organelles. *PLoS Pathog*, 1, e17.
- ALTMANN, K., FRANK, M., NEUMANN, D., JAKOBS, S. & WESTERMANN, B. 2008. The class V myosin motor protein, Myo2, plays a major role in mitochondrial motility in *Saccharomyces cerevisiae*. *J Cell Biol*, 181, 119-30.
- ALTSCHUL, S. F., GISH, W., MILLER, W., MYERS, E. W. & LIPMAN, D. J. 1990. Basic local alignment search tool. *Journal of molecular biology*, 215, 403-410.

- ALVAREZ, C. A. & SUVOROVA, E. S. 2017. Checkpoints of apicomplexan cell division identified in *Toxoplasma gondii*. *PLoS Pathog*, 13, e1006483.
- AMINO, R., THIBERGE, S., SHORTE, S., FRISCHKNECHT, F. & MENARD, R. 2006. Quantitative imaging of *Plasmodium* sporozoites in the mammalian host. *C R Biol*, 329, 858-62.
- ANAND, R., WAI, T., BAKER, M. J., KLADT, N., SCHAUSS, A. C., RUGARLI, E. & LANGER, T. 2014. The i-AAA protease YME1L and OMA1 cleave OPA1 to balance mitochondrial fusion and fission. *J Cell Biol*, 204, 919-29.
- ANDENMATTEN, N., EGARTER, S., JACKSON, A. J., JULLIEN, N., HERMAN, J. P. & MEISSNER, M. 2013. Conditional genome engineering in *Toxoplasma gondii* uncovers alternative invasion mechanisms. *Nat Methods*, 10, 125-7.
- ANDERSON-WHITE, B., BECK, J. R., CHEN, C. T., MEISSNER, M., BRADLEY, P. J. & GUBBELS, M. J. 2012. Cytoskeleton assembly in *Toxoplasma gondii* cell division. *Int Rev Cell Mol Biol*, 298, 1-31.
- ARANDA, P. S., LAJOIE, D. M. & JORCYK, C. L. 2012. Bleach gel: a simple agarose gel for analyzing RNA quality. *Electrophoresis*, 33, 366-9.
- ARISUE, N. & HASHIMOTO, T. 2015. Phylogeny and evolution of apicoplasts and apicomplexan parasites. *Parasitol Int*, 64, 254-9.
- ARMSTRONG, C. M. & GOLDBERG, D. E. 2007. An FKBP destabilization domain modulates protein levels in *Plasmodium falciparum*. *Nat Methods*, 4, 1007-9.
- BALDURSSON, S. & KARANIS, P. 2011. Waterborne transmission of protozoan parasites: review of worldwide outbreaks - an update 2004-2010. *Water Res*, 45, 6603-14.
- BANASZYNSKI, L. A., CHEN, L. C., MAYNARD-SMITH, L. A., OOI, A. G. & WANDLESS, T. J. 2006. A rapid, reversible, and tunable method to regulate protein function in living cells using synthetic small molecules. *Cell*, 126, 995-1004.
- BARGIERI, D. Y., ANDENMATTEN, N., LAGAL, V., THIBERGE, S., WHITELAW, J. A., TARDIEUX, I., MEISSNER, M. & MENARD, R. 2013. Apical membrane antigen 1 mediates apicomplexan parasite attachment but is dispensable for host cell invasion. *Nat Commun*, 4, 2552.
- BECK, J. R., RODRIGUEZ-FERNANDEZ, I. A., DE LEON, J. C., HUYNH, M.-H., CARRUTHERS, V. B., MORRISSETTE, N. S. & BRADLEY, P. J. 2010. A novel family of *Toxoplasma* IMC proteins displays a hierarchical organization and functions in coordinating parasite division. *PLoS pathogens*, 6, e1001094.
- BECKLEY, S. A., LIU, P., STOVER, M. L., GUNDERSON, S. I., LICHTLER, A. C. & ROWE, D. W. 2001. Reduction of target gene expression by a modified U1 snRNA. *Mol Cell Biol*, 21, 2815-25.
- BEHNKE, M. S., KHAN, A., LAURON, E. J., JIMAH, J. R., WANG, Q., TOLIA, N. H. & SIBLEY, L. D. 2015. Rhoptry Proteins ROP5 and ROP18 Are Major Murine Virulence Factors in Genetically Divergent South American Strains of *Toxoplasma gondii*. *PLOS Genetics*, 11, e1005434.

- BERTONI, M., KIEFER, F., BIASINI, M., BORDOLI, L. & SCHWEDE, T. 2017. Modeling protein quaternary structure of homo- and hetero-oligomers beyond binary interactions by homology. *Sci Rep*, 7, 10480.
- BESTEIRO, S., MICHELIN, A., PONCET, J., DUBREMETZ, J. F. & LEBRUN, M. 2009. Export of a *Toxoplasma gondii* rhoptry neck protein complex at the host cell membrane to form the moving junction during invasion. *PLoS Pathog*, 5, e1000309.
- BETHONEY, K. A., KING, M. C., HINSHAW, J. E., OSTAP, E. M. & LEMMON, M. A. 2009. A possible effector role for the pleckstrin homology (PH) domain of dynamin. *Proceedings of the National Academy of Sciences*, 106, 13359.
- BIASINI, M., BIENERT, S., WATERHOUSE, A., ARNOLD, K., STUDER, G., SCHMIDT, T., KIEFER, F., GALLO CASSARINO, T., BERTONI, M., BORDOLI, L. & SCHWEDE, T. 2014. SWISS-MODEL: modelling protein tertiary and quaternary structure using evolutionary information. *Nucleic Acids Res*, 42, W252-8.
- BIDDAU, M., BOUCHUT, A., MAJOR, J., SAVERIA, T., TOTTEY, J., OKA, O., VAN-LITH, M., JENNINGS, K. E., OVCIARIKOVA, J., DEROCHE, A., STRIEPEN, B., WALLER, R. F., PARSONS, M. & SHEINER, L. 2018. Two essential Thioredoxins mediate apicoplast biogenesis, protein import, and gene expression in *Toxoplasma gondii*. *PLoS Pathog*, 14, e1006836.
- BLACK, M., SEEBER, F., SOLDATI, D., KIM, K. & BOOTHROYD, J. C. 1995. Restriction enzyme-mediated integration elevates transformation frequency and enables co-transfection of *Toxoplasma gondii*. *Molecular and biochemical parasitology*, 74, 55-63.
- BLADER, I. J., COLEMAN, B. I., CHEN, C. T. & GUBBELS, M. J. 2015. Lytic Cycle of *Toxoplasma gondii*: 15 Years Later. *Annu Rev Microbiol*, 69, 463-85.
- BLEAZARD, W., MCCAFFERY, J. M., KING, E. J., BALE, S., MOZDY, A., TIEU, Q., NUNNARI, J. & SHAW, J. M. 1999. The dynamin-related GTPase Dnm1 regulates mitochondrial fission in yeast. *Nat Cell Biol*, 1, 298-304.
- BOOTHROYD, J. C. & DUBREMETZ, J. F. 2008. Kiss and spit: the dual roles of *Toxoplasma* rhoptries. *Nat Rev Microbiol*, 6, 79-88.
- BOUGDOUR, A., TARDIEUX, I. & HAKIMI, M. A. 2014. *Toxoplasma* exports dense granule proteins beyond the vacuole to the host cell nucleus and rewires the host genome expression. *Cell Microbiol*, 16, 334-43.
- BOWIE, W. R., KING, A. S., WERKER, D. H., ISAAC-RENTON, J. L., BELL, A., ENG, S. B. & MARION, S. A. 1997. Outbreak of toxoplasmosis associated with municipal drinking water. The BC *Toxoplasma* Investigation Team. *Lancet*, 350, 173-7.
- BRANDT, T., CAVELLINI, L., KÜHLBRANDT, W. & COHEN, M. M. 2016. A mitofusin-dependent docking ring complex triggers mitochondrial fusion in vitro. *Elife*, 5.
- BRAUN, L., BRENIER-PINCHART, M. P., YOGAVEL, M., CURT-VARESANO, A., CURT-BERTINI, R. L., HUSSAIN, T., KIEFFER-JAQUINOD, S., COUTE, Y., PELLOUX, H., TARDIEUX, I., SHARMA, A., BELRHALI, H., BOUGDOUR, A. & HAKIMI, M. A. 2013. A *Toxoplasma* dense granule protein, GRA24, modulates the early immune response

- to infection by promoting a direct and sustained host p38 MAPK activation. *J Exp Med*, 210, 2071-86.
- BREINICH, M. S., FERGUSON, D. J., FOTH, B. J., VAN DOOREN, G. G., LEBRUN, M., QUON, D. V., STRIEPEN, B., BRADLEY, P. J., FRISCHKNECHT, F., CARRUTHERS, V. B. & MEISSNER, M. 2009. A dynamin is required for the biogenesis of secretory organelles in *Toxoplasma gondii*. *Curr Biol*, 19, 277-86.
- BROWN, K. M., LONG, S. & SIBLEY, L. D. 2017. Plasma Membrane Association by N-Acylation Governs PKG Function in *Toxoplasma gondii*. *MBio*, 8.
- BUI, H. T. & SHAW, J. M. 2013. Dynamin assembly strategies and adaptor proteins in mitochondrial fission. *Curr Biol*, 23, R891-9.
- BULLEN, H. E., TONKIN, C. J., O'DONNELL, R. A., THAM, W. H., PAPENFUSS, A. T., GOULD, S., COWMAN, A. F., CRABB, B. S. & GILSON, P. R. 2009. A novel family of Apicomplexan glideosome-associated proteins with an inner membrane-anchoring role. *J Biol Chem*, 284, 25353-63.
- BURKHARDT, J. K., ECHEVERRI, C. J., NILSSON, T. & VALLEE, R. B. 1997. Overexpression of the dynaminin (p50) subunit of the dynactin complex disrupts dynein-dependent maintenance of membrane organelle distribution. *J Cell Biol*, 139, 469-84.
- BUSTILLO-ZABALBEITIA, I., MONTESSUIT, S., RAEMY, E., BASAÑEZ, G., TERRONES, O. & MARTINOU, J.-C. 2014. Specific Interaction with Cardiolipin Triggers Functional Activation of Dynamin-Related Protein 1. *PLOS ONE*, 9, e102738.
- CALDAS, L. A., DE SOUZA, W. & ATTIAS, M. 2010. Microscopic analysis of calcium ionophore activated egress of *Toxoplasma gondii* from the host cell. *Veterinary Parasitology*, 167, 8-18.
- CAMACHO, C., COULOURIS, G., AVAGYAN, V., MA, N., PAPADOPOULOS, J., BEALER, K. & MADDEN, T. L. 2009. BLAST+: architecture and applications. *BMC Bioinformatics*, 10, 421.
- CAREY, K. L., JONGCO, A. M., KIM, K. & WARD, G. E. 2004. The *Toxoplasma gondii* rhoptry protein ROP4 is secreted into the parasitophorous vacuole and becomes phosphorylated in infected cells. *Eukaryotic cell*, 3, 1320-1330.
- CARRUTHERS, V. & BOOTHROYD, J. C. 2007. Pulling together: an integrated model of *Toxoplasma* cell invasion. *Curr Opin Microbiol*, 10, 83-9.
- CARRUTHERS, V. B., GIDDINGS, O. K. & SIBLEY, L. D. 1999. Secretion of micronemal proteins is associated with *Toxoplasma* invasion of host cells. *Cellular microbiology*, 1, 225-235.
- CARRUTHERS, V. B., HAKANSSON, S., GIDDINGS, O. K. & SIBLEY, L. D. 2000. *Toxoplasma gondii* uses sulfated proteoglycans for substrate and host cell attachment. *Infect Immun*, 68, 4005-11.
- CAVALIER-SMITH, T. 1993. Kingdom protozoa and its 18 phyla. *Microbiol Rev*, 57, 953-94.

- CERVENY, K. L., STUDER, S. L., JENSEN, R. E. & SESAKI, H. 2007. Yeast mitochondrial division and distribution require the cortical num1 protein. *Dev Cell*, 12, 363-75.
- CHAPPIE, JOSHUA S., MEARS, JASON A., FANG, S., LEONARD, M., SCHMID, SANDRA L., MILLIGAN, RONALD A., HINSHAW, JENNY E. & DYDA, F. 2011. A Pseudoatomic Model of the Dynamin Polymer Identifies a Hydrolysis-Dependent Powerstroke. *Cell*, 147, 209-222.
- CHECKLEY, W., WHITE, A. C., JR., JAGANATH, D., ARROWOOD, M. J., CHALMERS, R. M., CHEN, X. M., FAYER, R., GRIFFITHS, J. K., GUERRANT, R. L., HEDSTROM, L., HUSTON, C. D., KOTLOFF, K. L., KANG, G., MEAD, J. R., MILLER, M., PETRI, W. A., JR., PRIEST, J. W., ROOS, D. S., STRIEPEN, B., THOMPSON, R. C., WARD, H. D., VAN VOORHIS, W. A., XIAO, L., ZHU, G. & HOUP, E. R. 2015. A review of the global burden, novel diagnostics, therapeutics, and vaccine targets for cryptosporidium. *Lancet Infect Dis*, 15, 85-94.
- CHEN, A. L., KIM, E. W., TOH, J. Y., VASHISHT, A. A., RASHOFF, A. Q., VAN, C., HUANG, A. S., MOON, A. S., BELL, H. N., BENTOLILA, L. A., WOHLSCHLEGEL, J. A. & BRADLEY, P. J. 2015. Novel components of the Toxoplasma inner membrane complex revealed by BioID. *MBio*, 6, e02357-14.
- CHEN, A. L., MOON, A. S., BELL, H. N., HUANG, A. S., VASHISHT, A. A., TOH, J. Y., LIN, A. H., NADIPURAM, S. M., KIM, E. W., CHOI, C. P., WOHLSCHLEGEL, J. A. & BRADLEY, P. J. 2017. Novel insights into the composition and function of the Toxoplasma IMC sutures. *Cell Microbiol*, 19.
- CHEN, H. & CHAN, D. C. 2009. Mitochondrial dynamics--fusion, fission, movement, and mitophagy--in neurodegenerative diseases. *Hum Mol Genet*, 18, R169-76.
- CHEN, H., DETMER, S. A., EWALD, A. J., GRIFFIN, E. E., FRASER, S. E. & CHAN, D. C. 2003. Mitofusins Mfn1 and Mfn2 coordinately regulate mitochondrial fusion and are essential for embryonic development. *J Cell Biol*, 160, 189-200.
- CHEN, Y. & SHENG, Z. H. 2013. Kinesin-1-syntrophin coupling mediates activity-dependent regulation of axonal mitochondrial transport. *J Cell Biol*, 202, 351-64.
- CIPOLAT, S., MARTINS DE BRITO, O., DAL ZILIO, B. & SCORRANO, L. 2004. OPA1 requires mitofusin 1 to promote mitochondrial fusion. *Proc Natl Acad Sci U S A*, 101, 15927-32.
- CLOUGH, B. & FRICKEL, E. M. 2017. The Toxoplasma Parasitophorous Vacuole: An Evolving Host-Parasite Frontier. *Trends Parasitol*, 33, 473-488.
- COLLINS, C. R., DAS, S., WONG, E. H., ANDENMATTEN, N., STALLMACH, R., HACKETT, F., HERMAN, J. P., MULLER, S., MEISSNER, M. & BLACKMAN, M. J. 2013. Robust inducible Cre recombinase activity in the human malaria parasite Plasmodium falciparum enables efficient gene deletion within a single asexual erythrocytic growth cycle. *Mol Microbiol*, 88, 687-701.

- CONG, L., RAN, F. A., COX, D., LIN, S., BARRETTO, R., HABIB, N., HSU, P. D., WU, X., JIANG, W. & MARRAFFINI, L. 2013. Multiplex genome engineering using CRISPR/Cas systems. *Science*, 1231143.
- COPPENS, I., DUNN, J. D., ROMANO, J. D., PYPAERT, M., ZHANG, H., BOOTHROYD, J. C. & JOINER, K. A. 2006. *Toxoplasma gondii* sequesters lysosomes from mammalian hosts in the vacuolar space. *Cell*, 125, 261-74.
- CORNELISSEN, A., OVERDULVE, J. & VAN DER PLOEG, M. 1984. Determination of nuclear DNA of five eucoccidian parasites, *Isospora* (*Toxoplasma*) *gondii*, *Sarcocystis cruzi*, *Eimeria tenella*, *E. acervulina* and *Plasmodium berghei*, with special reference to gamontogenesis and meiosis in *I.(T.) gondii*. *Parasitology*, 88, 531-553.
- COURRET, N., DARCHE, S., SONIGO, P., MILON, G., BUZONI-GATEL, D. & TARDIEUX, I. 2006. CD11c- and CD11b-expressing mouse leukocytes transport single *Toxoplasma gondii* tachyzoites to the brain. *Blood*, 107, 309-16.
- CURT-VARESANO, A., BRAUN, L., RANQUET, C., HAKIMI, M. A. & BOUGDOUR, A. 2016. The aspartyl protease TgASP5 mediates the export of the *Toxoplasma* GRA16 and GRA24 effectors into host cells. *Cell Microbiol*, 18, 151-67.
- CURT.VARESANO, A., BRAUN, L., RANQUET, C., HAKIMI, M. A. & BOUGDOUR, A. 2016. The aspartyl protease TgASP5 mediates the export of the *Toxoplasma* GRA16 and GRA24 effectors into host cells. *Cellular microbiology*, 18, 151-167.
- DAHL, E. L. & ROSENTHAL, P. J. 2008. Apicoplast translation, transcription and genome replication: targets for antimalarial antibiotics. *Trends in parasitology*, 24, 279-284.
- DE SOUZA, W., ATTIAS, M. & RODRIGUES, J. C. 2009. Particularities of mitochondrial structure in parasitic protists (Apicomplexa and Kinetoplastida). *Int J Biochem Cell Biol*, 41, 2069-80.
- DEL CARMEN, M. G., MONDRAGON, M., GONZALEZ, S. & MONDRAGON, R. 2009. Induction and regulation of conoid extrusion in *Toxoplasma gondii*. *Cell Microbiol*, 11, 967-82.
- DELANO, W. L. 2002. Pymol: An open-source molecular graphics tool. *CCP4 Newsletter On Protein Crystallography*, 40, 82-92.
- DESJARDINS, P. & CONKLIN, D. 2010. NanoDrop microvolume quantitation of nucleic acids. *Journal of visualized experiments: JoVE*.
- DI CRISTINA, M. & CARRUTHERS, V. B. 2018. New and emerging uses of CRISPR/Cas9 to genetically manipulate apicomplexan parasites. *Parasitology*, 1-8.
- DONALD, R. G., CARTER, D., ULLMAN, B. & ROOS, D. S. 1996. Insertional tagging, cloning, and expression of the *Toxoplasma gondii* hypoxanthine-xanthine-guanine phosphoribosyltransferase gene Use as a selectable marker for stable transformation. *Journal of Biological Chemistry*, 271, 14010-14019.
- DONALD, R. G. & ROOS, D. S. 1993. Stable molecular transformation of *Toxoplasma gondii*: a selectable dihydrofolate reductase-thymidylate synthase marker based on drug-resistance mutations in malaria. *Proc Natl Acad Sci U S A*, 90, 11703-7.

- DRERUP, C. M., HERBERT, A. L., MONK, K. R. & NECHIPORUK, A. V. 2017. Regulation of mitochondria-dynactin interaction and mitochondrial retrograde transport in axons. *Elife*, 6.
- DUBEY, J. 2006. Comparative infectivity of oocysts and bradyzoites of *Toxoplasma gondii* for intermediate (mice) and definitive (cats) hosts. *Veterinary parasitology*, 140, 69-75.
- DUBEY, J. & FRENKEL, J. 1976. Feline toxoplasmosis from acutely infected mice and the development of *Toxoplasma* cysts. *Journal of Eukaryotic Microbiology*, 23, 537-546.
- DUBEY, J., LINDSAY, D. & SPEER, C. 1998. Structures of *Toxoplasma gondii* tachyzoites, bradyzoites, and sporozoites and biology and development of tissue cysts. *Clinical microbiology reviews*, 11, 267-299.
- DUBEY, J., MILLER, N. L. & FRENKEL, J. 1970a. The *Toxoplasma gondii* oocyst from cat feces. *Journal of Experimental Medicine*, 132, 636-662.
- DUBEY, J. P. 1998. *Toxoplasma gondii* oocyst survival under defined temperatures. *J Parasitol*, 84, 862-5.
- DUBEY, J. P. 2001. Oocyst shedding by cats fed isolated bradyzoites and comparison of infectivity of bradyzoites of the VEG strain *Toxoplasma gondii* to cats and mice. *J Parasitol*, 87, 215-9.
- DUBEY, J. P., MILLER, N. L. & FRENKEL, J. K. 1970b. Characterization of the new fecal form of *Toxoplasma gondii*. *J Parasitol*, 56, 447-56.
- DUBEY, R., HARRISON, B., DANGOUDOUBIYAM, S., BANDINI, G., CHENG, K., KOSBER, A., AGOP-NERSESIAN, C., HOWE, D. K., SAMUELSON, J., FERGUSON, D. J. P. & GUBBELS, M. J. 2017. Differential Roles for Inner Membrane Complex Proteins across *Toxoplasma gondii* and *Sarcocystis neurona* Development. *mSphere*, 2.
- DUBREMETZ, J. F. 2007. Rhoptries are major players in *Toxoplasma gondii* invasion and host cell interaction. *Cellular microbiology*, 9, 841-848.
- DUDEK, J., REHLING, P. & VAN DER LAAN, M. 2013. Mitochondrial protein import: common principles and physiological networks. *Biochim Biophys Acta*, 1833, 274-85.
- DUNN, D., WALLON, M., PEYRON, F., PETERSEN, E., PECKHAM, C. & GILBERT, R. 1999. Mother-to-child transmission of toxoplasmosis: risk estimates for clinical counselling. *Lancet*, 353, 1829-33.
- ECHEVERRI, C. J., PASCHAL, B. M., VAUGHAN, K. T. & VALLEE, R. B. 1996. Molecular characterization of the 50-kD subunit of dynactin reveals function for the complex in chromosome alignment and spindle organization during mitosis. *J Cell Biol*, 132, 617-33.
- EGARTER, S., ANDENMATTEN, N., JACKSON, A. J., WHITELAW, J. A., PALL, G., BLACK, J. A., FERGUSON, D. J., TARDIEUX, I., MOGILNER, A. & MEISSNER, M. 2014. The *Toxoplasma* Acto-MyoA motor complex is important but not essential for gliding motility and host cell invasion. *PLoS One*, 9, e91819.
- EL HAJJ, H., LEBRUN, M., FOURMAUX, M. N., VIAL, H. & DUBREMETZ, J. F. 2007. Inverted topology of the *Toxoplasma gondii* ROP5 rhoptry protein provides new

- insights into the association of the ROP2 protein family with the parasitophorous vacuole membrane. *Cellular microbiology*, 9, 54-64.
- FAELBER, K., GAO, S., HELD, M., POSOR, Y., HAUCKE, V., NOE, F. & DAUMKE, O. 2013. Oligomerization of dynamin superfamily proteins in health and disease. *Prog Mol Biol Transl Sci*, 117, 411-43.
- FANG, E. F., SCHEIBYE-KNUDSEN, M., CHUA, K. F., MATTSON, M. P., CROTEAU, D. L. & BOHR, V. A. 2016. Nuclear DNA damage signalling to mitochondria in ageing. *Nature Reviews Molecular Cell Biology*, 17, 308.
- FEAGIN, J. E., GARDNER, M. J., WILLIAMSON, D. H. & WILSON, R. J. 1991. The putative mitochondrial genome of *Plasmodium falciparum*. *J Protozool*, 38, 243-5.
- FENTRESS, S. J., BEHNKE, M. S., DUNAY, I. R., MASHAYEKHI, M., ROMMEREIM, L. M., FOX, B. A., BZIK, D. J., TAYLOR, G. A., TURK, B. E., LICHTI, C. F., TOWNSEND, R. R., QIU, W., HUI, R., BEATTY, W. L. & SIBLEY, L. D. 2010. Phosphorylation of immunity-related GTPases by a *Toxoplasma gondii*-secreted kinase promotes macrophage survival and virulence. *Cell Host Microbe*, 8, 484-95.
- FERGUSON, D., HUTCHISON, W. & SIIM, J. 1975. The ultrastructural development of the macrogamete and formation of the oocyst wall of *Toxoplasma gondii*. *APMIS*, 83, 491-505.
- FICHERA, M. E. & ROOS, D. S. 1997. A plastid organelle as a drug target in apicomplexan parasites. *Nature*, 390, 407.
- FLEGR, J., PRANDOTA, J., SOVIČKOVÁ, M. & ISRAILI, Z. H. 2014. Toxoplasmosis—a global threat. Correlation of latent toxoplasmosis with specific disease burden in a set of 88 countries. *PloS one*, 9, e90203.
- FORD, M. G., JENNI, S. & NUNNARI, J. 2011. The crystal structure of dynamin. *Nature*, 477, 561-6.
- FORTES, P., CUEVAS, Y., GUAN, F., LIU, P., PENTLICKY, S., JUNG, S. P., MARTINEZ-CHANTAR, M. L., PRIETO, J., ROWE, D. & GUNDERSON, S. I. 2003. Inhibiting expression of specific genes in mammalian cells with 5' end-mutated U1 small nuclear RNAs targeted to terminal exons of pre-mRNA. *Proc Natl Acad Sci U S A*, 100, 8264-9.
- FORTSCH, J., HUMMEL, E., KRIST, M. & WESTERMANN, B. 2011. The myosin-related motor protein Myo2 is an essential mediator of bud-directed mitochondrial movement in yeast. *J Cell Biol*, 194, 473-88.
- FOX, B. A., RISTUCCIA, J. G., GIGLEY, J. P. & BZIK, D. J. 2009. Efficient gene replacements in *Toxoplasma gondii* strains deficient for nonhomologous end joining. *Eukaryot Cell*, 8, 520-9.
- FRANCIA, M. E. & STRIEPEN, B. 2014. Cell division in apicomplexan parasites. *Nat Rev Microbiol*, 12, 125-36.
- FRENAL, K., DUBREMETZ, J. F., LEBRUN, M. & SOLDATI-FAVRE, D. 2017. Gliding motility powers invasion and egress in Apicomplexa. *Nat Rev Microbiol*, 15, 645-660.

- FRÉNAL, K., MARQ, J.-B., JACOT, D., POLONAI, V. & SOLDATI-FAVRE, D. 2014. Plasticity between MyoC-and MyoA-glideosomes: an example of functional compensation in *Toxoplasma gondii* invasion. *PLoS pathogens*, 10, e1004504.
- FRÉNAL, K., POLONAI, V., MARQ, J.-B., STRATMANN, R., LIMENITAKIS, J. & SOLDATI-FAVRE, D. 2010. Functional dissection of the apicomplexan glideosome molecular architecture. *Cell host & microbe*, 8, 343-357.
- FRENKEL, J. 1973. *Toxoplasma* in and around us. *Bioscience*, 23, 343-352.
- FRIEDMAN, J. R., LACKNER, L. L., WEST, M., DIBENEDETTO, J. R., NUNNARI, J. & VOELTZ, G. K. 2011. ER tubules mark sites of mitochondrial division. *Science*, 334, 358-62.
- FRIEDMAN, J. R. & NUNNARI, J. 2014. Mitochondrial form and function. *Nature*, 505, 335-43.
- FROHLICH, C., GRABIGER, S., SCHWEFEL, D., FAELBER, K., ROSENBAUM, E., MEARS, J., ROCKS, O. & DAUMKE, O. 2013. Structural insights into oligomerization and mitochondrial remodelling of dynamin 1-like protein. *Embo j*, 32, 1280-92.
- GAJRIA, B., BAHL, A., BRESTELLI, J., DOMMER, J., FISCHER, S., GAO, X., HEIGES, M., IODICE, J., KISSINGER, J. C. & MACKEY, A. J. 2007. ToxoDB: an integrated *Toxoplasma gondii* database resource. *Nucleic acids research*, 36, D553-D556.
- GANDRE-BABBE, S. & VAN DER BLIEK, A. M. 2008. The novel tail-anchored membrane protein Mff controls mitochondrial and peroxisomal fission in mammalian cells. *Mol Biol Cell*, 19, 2402-12.
- GAO, J., WANG, L., LIU, J., XIE, F., SU, B. & WANG, X. 2017. Abnormalities of Mitochondrial Dynamics in Neurodegenerative Diseases. *Antioxidants (Basel)*, 6.
- GAO, S., VON DER MALSBERG, A., PAESCHKE, S., BEHLKE, J., HALLER, O., KOCHS, G. & DAUMKE, O. 2010. Structural basis of oligomerization in the stalk region of dynamin-like MxA. *Nature*, 465, 502-6.
- GARBUZ, T. & ARRIZABALAGA, G. 2017. Lack of mitochondrial MutS homolog 1 in *Toxoplasma gondii* disrupts maintenance and fidelity of mitochondrial DNA and reveals metabolic plasticity. *PLOS ONE*, 12, e0188040.
- GASIUNAS, G., BARRANGOU, R., HORVATH, P. & SIKSNYS, V. 2012. Cas9-crRNA ribonucleoprotein complex mediates specific DNA cleavage for adaptive immunity in bacteria. *Proc Natl Acad Sci U S A*, 109, E2579-86.
- GASKINS, E., GILK, S., DEVORE, N., MANN, T., WARD, G. & BECKERS, C. 2004. Identification of the membrane receptor of a class XIV myosin in *Toxoplasma gondii*. *J Cell Biol*, 165, 383-93.
- GILES, J. R., PETERSON, A. T., BUSCH, J. D., OLAFSON, P. U., SCOLES, G. A., DAVEY, R. B., POUND, J. M., KAMMLAH, D. M., LOHMEYER, K. H. & WAGNER, D. M. 2014. Invasive potential of cattle fever ticks in the southern United States. *Parasites & vectors*, 7, 189.
- GILK, S. D., GASKINS, E., WARD, G. E. & BECKERS, C. J. 2009. GAP45 phosphorylation controls assembly of the *Toxoplasma* myosin XIV complex. *Eukaryot Cell*, 8, 190-6.

- GILL, S. R., SCHROER, T. A., SZILAK, I., STEUER, E. R., SHEETZ, M. P. & CLEVELAND, D. W. 1991. Dynactin, a conserved, ubiquitously expressed component of an activator of vesicle motility mediated by cytoplasmic dynein. *J Cell Biol*, 115, 1639-50.
- GLATER, E. E., MEGEATH, L. J., STOWERS, R. S. & SCHWARZ, T. L. 2006. Axonal transport of mitochondria requires mlt1 to recruit kinesin heavy chain and is light chain independent. *J Cell Biol*, 173, 545-57.
- GOLDMAN, M., CARVER, R. K. & SULZER, A. J. 1958. Reproduction of *Toxoplasma gondii* by internal budding. *J Parasitol*, 44, 161-71.
- GOMES, A. R., BUSHELL, E., SCHWACH, F., GIRLING, G., ANAR, B., QUAIL, M. A., HERD, C., PFANDER, C., MODRZYNSKA, K., RAYNER, J. C. & BILLKER, O. 2015. A genome-scale vector resource enables high-throughput reverse genetic screening in a malaria parasite. *Cell Host Microbe*, 17, 404-413.
- GOMES, L. C., DI BENEDETTO, G. & SCORRANO, L. 2011. During autophagy mitochondria elongate, are spared from degradation and sustain cell viability. *Nat Cell Biol*, 13, 589-98.
- GOMES, L. C. & SCORRANO, L. 2008. High levels of Fis1, a pro-fission mitochondrial protein, trigger autophagy. *Biochimica et Biophysica Acta (BBA) - Bioenergetics*, 1777, 860-866.
- GOODMAN, C. D., BUCHANAN, H. D. & MCFADDEN, G. I. 2017. Is the Mitochondrion a Good Malaria Drug Target? *Trends in parasitology*, 33, 185-193.
- GORDON, J. L. & SIBLEY, L. D. 2005. Comparative genome analysis reveals a conserved family of actin-like proteins in apicomplexan parasites. *BMC Genomics*, 6, 179.
- GORSICH, S. W. & SHAW, J. M. 2004. Importance of mitochondrial dynamics during meiosis and sporulation. *Mol Biol Cell*, 15, 4369-81.
- GOSSEN, M. & BUJARD, H. 1992. Tight control of gene expression in mammalian cells by tetracycline-responsive promoters. *Proceedings of the National Academy of Sciences*, 89, 5547-5551.
- GRIFFIN, E. E., GRAUMANN, J. & CHAN, D. C. 2005. The WD40 protein Caf4p is a component of the mitochondrial fission machinery and recruits Dnm1p to mitochondria. *J Cell Biol*, 170, 237-48.
- GUBBELS, M. J., VAISHNAVA, S., BOOT, N., DUBREMETZ, J. F. & STRIEPEN, B. 2006. A MORN-repeat protein is a dynamic component of the *Toxoplasma gondii* cell division apparatus. *J Cell Sci*, 119, 2236-45.
- GUERIN, A., CORRALES, R. M., PARKER, M. L., LAMARQUE, M. H., JACOT, D., EL HAJJ, H., SOLDATI-FAVRE, D., BOULANGER, M. J. & LEBRUN, M. 2017. Efficient invasion by *Toxoplasma* depends on the subversion of host protein networks. *Nat Microbiol*, 2, 1358-1366.
- GUNDERSON, S. I., POLYCARPOU-SCHWARZ, M. & MATTAJ, I. W. 1998. U1 snRNP inhibits pre-mRNA polyadenylation through a direct interaction between U1 70K and poly(A) polymerase. *Mol Cell*, 1, 255-64.

- HAKANSSON, S., MORISAKI, H., HEUSER, J. & SIBLEY, L. D. 1999. Time-lapse video microscopy of gliding motility in *Toxoplasma gondii* reveals a novel, biphasic mechanism of cell locomotion. *Mol Biol Cell*, 10, 3539-47.
- HARDING, C. R., EGARTER, S., GOW, M., JIMENEZ-RUIZ, E., FERGUSON, D. J. & MEISSNER, M. 2016. Gliding Associated Proteins Play Essential Roles during the Formation of the Inner Membrane Complex of *Toxoplasma gondii*. *PLoS Pathog*, 12, e1005403.
- HARPER, J. M., HUYNH, M. H., COPPENS, I., PARUSSINI, F., MORENO, S. & CARRUTHERS, V. B. 2006. A cleavable propeptide influences *Toxoplasma* infection by facilitating the trafficking and secretion of the TgMIC2-M2AP invasion complex. *Mol Biol Cell*, 17, 4551-63.
- HARTLEY, W. J. & MARSHALL, S. C. 1957. Toxoplasmosis as a cause of ovine perinatal mortality. *New Zealand Veterinary Journal*, 5, 119-124.
- HARTMANN, J., HU, K., HE, C. Y., PELLETIER, L., ROOS, D. S. & WARREN, G. 2006. Golgi and centrosome cycles in *Toxoplasma gondii*. *Mol Biochem Parasitol*, 145, 125-7.
- HEASLIP, A. T., DZIERSZINSKI, F., STEIN, B. & HU, K. 2010. TgMORN1 is a key organizer for the basal complex of *Toxoplasma gondii*. *PLoS Pathog*, 6, e1000754.
- HEASLIP, A. T., NELSON, S. R. & WARSHAW, D. M. 2016. Dense granule trafficking in *Toxoplasma gondii* requires a unique class 27 myosin and actin filaments. *Mol Biol Cell*, 27, 2080-9.
- HELLE, S. C. J., FENG, Q., AEBERSOLD, M. J., HIRT, L., GRÜTER, R. R., VAHID, A., SIRIANNI, A., MOSTOWY, S., SNEDEKER, J. G., ŠARIĆ, A., IDEMA, T., ZAMBELLI, T. & KORNMANN, B. 2017. Mechanical force induces mitochondrial fission. *eLife*, 6, e30292.
- HERM-GOTZ, A., AGOP-NERSESIAN, C., MUNTER, S., GRIMLEY, J. S., WANDLESS, T. J., FRISCHKNECHT, F. & MEISSNER, M. 2007. Rapid control of protein level in the apicomplexan *Toxoplasma gondii*. *Nat Methods*, 4, 1003-5.
- HERM-GOTZ, A., WEISS, S., STRATMANN, R., FUJITA-BECKER, S., RUFF, C., MEYHOFER, E., SOLDATI, T., MANSTEIN, D. J., GEEVES, M. A. & SOLDATI, D. 2002. *Toxoplasma gondii* myosin A and its light chain: a fast, single-headed, plus-end-directed motor. *EMBO J*, 21, 2149-58.
- HERMANN, G. J., THATCHER, J. W., MILLS, J. P., HALES, K. G., FULLER, M. T., NUNNARI, J. & SHAW, J. M. 1998. Mitochondrial fusion in yeast requires the transmembrane GTPase Fzo1p. *J Cell Biol*, 143, 359-73.
- HERSKOVITS, J. S., BURGESS, C. C., OBAR, R. A. & VALLEE, R. B. 1993. Effects of mutant rat dynamin on endocytosis. *J Cell Biol*, 122, 565-78.
- HEYMANN, J. A. & HINSHAW, J. E. 2009. Dynamins at a glance. *J Cell Sci*, 122, 3427-31.
- HIROKAWA, N. 1998. Kinesin and dynein superfamily proteins and the mechanism of organelle transport. *Science*, 279, 519-526.

- HIROKAWA, N., NODA, Y., TANAKA, Y. & NIWA, S. 2009. Kinesin superfamily motor proteins and intracellular transport. *Nature Reviews Molecular Cell Biology*, 10, 682.
- HIROKAWA, N. & TANAKA, Y. 2015. Kinesin superfamily proteins (KIFs): Various functions and their relevance for important phenomena in life and diseases. *Exp Cell Res*, 334, 16-25.
- HLISCS, M., MILLET, C., DIXON, M. W., SIDEN-KIAMOS, I., MCMILLAN, P. & TILLEY, L. 2015. Organization and function of an actin cytoskeleton in *Plasmodium falciparum* gametocytes. *Cellular microbiology*, 17, 207-225.
- HORBAY, R. & BILYY, R. 2016. Mitochondrial dynamics during cell cycling. *Apoptosis*, 21, 1327-1335.
- HOWE, D. K. & SIBLEY, L. D. 1995. *Toxoplasma gondii* comprises three clonal lineages: correlation of parasite genotype with human disease. *Journal of infectious diseases*, 172, 1561-1566.
- HU, K. 2008. Organizational changes of the daughter basal complex during the parasite replication of *Toxoplasma gondii*. *PLoS Pathog*, 4, e10.
- HU, K., JOHNSON, J., FLORENS, L., FRAUNHOLZ, M., SURAVAJJALA, S., DILULLO, C., YATES, J., ROOS, D. S. & MURRAY, J. M. 2006. Cytoskeletal components of an invasion machine—the apical complex of *Toxoplasma gondii*. *PLoS pathogens*, 2, e13.
- HU, K., ROOS, D. S. & MURRAY, J. M. 2002. A novel polymer of tubulin forms the conoid of *Toxoplasma gondii*. *J Cell Biol*, 156, 1039-50.
- HUTCHISON, W. M. 1965. Experimental transmission of *Toxoplasma gondii*. *Nature*, 206, 961-2.
- HUYNH, M.-H. & CARRUTHERS, V. B. 2009a. Tagging of endogenous genes in a *Toxoplasma gondii* strain lacking Ku80. *Eukaryotic cell*, 8, 530-539.
- HUYNH, M. H. & CARRUTHERS, V. B. 2009b. Tagging of endogenous genes in a *Toxoplasma gondii* strain lacking Ku80. *Eukaryot Cell*, 8, 530-9.
- HUYNH, M. H., RABENAU, K. E., HARPER, J. M., BEATTY, W. L., SIBLEY, L. D. & CARRUTHERS, V. B. 2003. Rapid invasion of host cells by *Toxoplasma* requires secretion of the MIC2-M2AP adhesive protein complex. *EMBO J*, 22, 2082-90.
- INGERMAN, E., PERKINS, E. M., MARINO, M., MEARS, J. A., MCCAFFERY, J. M., HINSHAW, J. E. & NUNNARI, J. 2005. Dnm1 forms spirals that are structurally tailored to fit mitochondria. *J Cell Biol*, 170, 1021-7.
- ISHIHARA, N., NOMURA, M., JOFUKU, A., KATO, H., SUZUKI, S. O., MASUDA, K., OTERA, H., NAKANISHI, Y., NONAKA, I., GOTO, Y., TAGUCHI, N., MORINAGA, H., MAEDA, M., TAKAYANAGI, R., YOKOTA, S. & MIHARA, K. 2009. Mitochondrial fission factor Drp1 is essential for embryonic development and synapse formation in mice. *Nat Cell Biol*, 11, 958-66.
- ITO, T., TOH, E. A. & MATSUI, Y. 2004. Mmr1p is a mitochondrial factor for Myo2p-dependent inheritance of mitochondria in the budding yeast. *EMBO J*, 23, 2520-30.

- ITOH, T., WATABE, A., TOH, E. A. & MATSUI, Y. 2002. Complex formation with Ypt11p, a rab-type small GTPase, is essential to facilitate the function of Myo2p, a class V myosin, in mitochondrial distribution in *Saccharomyces cerevisiae*. *Mol Cell Biol*, 22, 7744-57.
- JACOT, D., DAHER, W. & SOLDATI-FAVRE, D. 2013. *Toxoplasma gondii* myosin F, an essential motor for centrosomes positioning and apicoplast inheritance. *Embo j*, 32, 1702-16.
- JACOT, D., TOSETTI, N., PIRES, I., STOCK, J., GRAINDORGE, A., HUNG, Y. F., HAN, H., TEWARI, R., KURSULA, I. & SOLDATI-FAVRE, D. 2016. An Apicomplexan Actin-Binding Protein Serves as a Connector and Lipid Sensor to Coordinate Motility and Invasion. *Cell Host Microbe*, 20, 731-743.
- JACQUOT, G., MAIDOU-PEINDARA, P. & BENICHOUS, S. 2010. Molecular and functional basis for the scaffolding role of the p50/dynamitin subunit of the microtubule-associated dynactin complex. *Journal of Biological Chemistry*, jbc. M110. 100602.
- JIANG, X. & WANG, X. 2004. Cytochrome C-mediated apoptosis. *Annu Rev Biochem*, 73, 87-106.
- JIMENEZ-RUIZ, E., MORLON-GUYOT, J., DAHER, W. & MEISSNER, M. 2016. Vacuolar protein sorting mechanisms in apicomplexan parasites. *Mol Biochem Parasitol*, 209, 18-25.
- JIMENEZ-RUIZ, E., WONG, E. H., PALL, G. S. & MEISSNER, M. 2014. Advantages and disadvantages of conditional systems for characterization of essential genes in *Toxoplasma gondii*. *Parasitology*, 141, 1390-8.
- JINEK, M., CHYLINSKI, K., FONFARA, I., HAUER, M., DOUDNA, J. A. & CHARPENTIER, E. 2012. A programmable dual-RNA-guided DNA endonuclease in adaptive bacterial immunity. *Science*, 337, 816-21.
- JOMAA, H., WIESNER, J., SANDERBRAND, S., ALTINCICEK, B., WEIDEMEYER, C., HINTZ, M., TÜRBACHOVA, I., EBERL, M., ZEIDLER, J. & LICHTENTHALER, H. K. 1999. Inhibitors of the nonmevalonate pathway of isoprenoid biosynthesis as antimalarial drugs. *Science*, 285, 1573-1576.
- JONES, T. C. & HIRSCH, J. G. 1972. The interaction between *Toxoplasma gondii* and mammalian cells. II. The absence of lysosomal fusion with phagocytic vacuoles containing living parasites. *J Exp Med*, 136, 1173-94.
- JULLIEN, N., GODDARD, I., SELMI-RUBY, S., FINA, J. L., CREMER, H. & HERMAN, J. P. 2007. Conditional transgenesis using Dimerizable Cre (DiCre). *PLoS One*, 2, e1355.
- JULLIEN, N., SAMPIERI, F., ENJALBERT, A. & HERMAN, J. P. 2003. Regulation of Cre recombinase by ligand-induced complementation of inactive fragments. *Nucleic Acids Res*, 31, e131.
- KAFSACK, B. F., PENA, J. D., COPPENS, I., RAVINDRAN, S., BOOTHROYD, J. C. & CARRUTHERS, V. B. 2009. Rapid membrane disruption by a perforin-like protein facilitates parasite exit from host cells. *Science*, 323, 530-533.

- KAIDA, D. 2016. The reciprocal regulation between splicing and 3'-end processing. *Wiley Interdiscip Rev RNA*, 7, 499-511.
- KANDIMALLA, R., MANCZAK, M., FRY, D., SUNEETHA, Y., SESAKI, H. & REDDY, P. H. 2016. Reduced dynamin-related protein 1 protects against phosphorylated Tau-induced mitochondrial dysfunction and synaptic damage in Alzheimer's disease. *Hum Mol Genet*, 25, 4881-4897.
- KANFER, G. & KORNMAN, B. 2016. Dynamics of the mitochondrial network during mitosis. *Biochemical Society Transactions*, 44, 510.
- KATRIS, N. J., VAN DOOREN, G. G., MCMILLAN, P. J., HANSSEN, E., TILLEY, L. & WALLER, R. F. 2014. The apical complex provides a regulated gateway for secretion of invasion factors in *Toxoplasma*. *PLoS pathogens*, 10, e1004074.
- KEITHLY, J. S., LANGRETH, S. G., BUTTLE, K. F. & MANNELLA, C. A. 2005. Electron tomographic and ultrastructural analysis of the *Cryptosporidium parvum* relict mitochondrion, its associated membranes, and organelles. *J Eukaryot Microbiol*, 52, 132-40.
- KHAN, A., TAYLOR, S., SU, C., MACKEY, A. J., BOYLE, J., COLE, R., GLOVER, D., TANG, K., PAULSEN, I. T. & BERRIMAN, M. 2005. Composite genome map and recombination parameters derived from three archetypal lineages of *Toxoplasma gondii*. *Nucleic acids research*, 33, 2980-2992.
- KIBBE, W. A. 2007. OligoCalc: an online oligonucleotide properties calculator. *Nucleic Acids Res*, 35, W43-6.
- KIM, K., SOLDATI, D. & BOOTHROYD, J. C. 1993. Gene replacement in *Toxoplasma gondii* with chloramphenicol acetyltransferase as selectable marker. *Science*, 262, 911-4.
- KINTAKA, R., MAKANAE, K. & MORIYA, H. 2016. Cellular growth defects triggered by an overload of protein localization processes. *Scientific reports*, 6, 31774.
- KOCH, A., THIEMANN, M., GRABENBAUER, M., YOON, Y., MCNIVEN, M. A. & SCHRADER, M. 2003. Dynamin-like protein 1 is involved in peroxisomal fission. *Journal of Biological Chemistry*, 278, 8597-8605.
- KOIRALA, S., GUO, Q., KALIA, R., BUI, H. T., ECKERT, D. M., FROST, A. & SHAW, J. M. 2013. Interchangeable adaptors regulate mitochondrial dynamin assembly for membrane scission. *Proc Natl Acad Sci U S A*, 110, E1342-51.
- KONRADT, C., UENO, N., CHRISTIAN, D. A., DELONG, J. H., PRITCHARD, G. H., HERZ, J., BZIK, D. J., KOSHY, A. A., MCGAVERN, D. B. & LODOEN, M. B. 2016. Endothelial cells are a replicative niche for entry of *Toxoplasma gondii* to the central nervous system. *Nature microbiology*, 1, 16001.
- KOROBOVA, F., GAUVIN, T. J. & HIGGS, H. N. 2014. A role for myosin II in mammalian mitochondrial fission. *Curr Biol*, 24, 409-14.
- KOROBOVA, F., RAMABHADRAN, V. & HIGGS, H. N. 2013. An actin-dependent step in mitochondrial fission mediated by the ER-associated formin INF2. *Science*, 339, 464-7.

- KOSAKA, T. & IKEDA, K. 1983. Reversible blockage of membrane retrieval and endocytosis in the garland cell of the temperature-sensitive mutant of *Drosophila melanogaster*, shibirets1. *J Cell Biol*, 97, 499-507.
- KOSHIBA, T., DETMER, S. A., KAISER, J. T., CHEN, H., MCCAFFERY, J. M. & CHAN, D. C. 2004. Structural basis of mitochondrial tethering by mitofusin complexes. *Science*, 305, 858-862.
- KOWALD, A. & KIRKWOOD, T. B. 2011. Evolution of the mitochondrial fusion-fission cycle and its role in aging. *Proc Natl Acad Sci U S A*, 108, 10237-42.
- KRAFT, L. M. & LACKNER, L. L. 2017. Mitochondrial anchors: Positioning mitochondria and more. *Biochemical and biophysical research communications*.
- KRAUS, F. & RYAN, M. T. 2017. The constriction and scission machineries involved in mitochondrial fission. *J Cell Sci*, 130, 2953-2960.
- KREIDENWEISS, A., HOPKINS, A. V. & MORDMULLER, B. 2013. 2A and the auxin-based degron system facilitate control of protein levels in *Plasmodium falciparum*. *PLoS One*, 8, e78661.
- KREMER, K., KAMIN, D., RITTWEGER, E., WILKES, J., FLAMMER, H., MAHLER, S., HENG, J., TONKIN, C. J., LANGSLEY, G., HELL, S. W., CARRUTHERS, V. B., FERGUSON, D. J. & MEISSNER, M. 2013. An overexpression screen of *Toxoplasma gondii* Rab-GTPases reveals distinct transport routes to the micronemes. *PLoS Pathog*, 9, e1003213.
- KUDRYASHEV, M., LEPPER, S., STANWAY, R., BOHN, S., BAUMEISTER, W., CYRKLAFF, M. & FRISCHKNECHT, F. 2010. Positioning of large organelles by a membrane-associated cytoskeleton in *Plasmodium* sporozoites. *Cellular microbiology*, 12, 362-371.
- LABBE, K., MURLEY, A. & NUNNARI, J. 2014. Determinants and functions of mitochondrial behavior. *Annu Rev Cell Dev Biol*, 30, 357-91.
- LABROUSSE, A. M., ZAPPATERRA, M. D., RUBE, D. A. & VAN DER BLIEK, A. M. 1999. *C. elegans* dynamin-related protein DRP-1 controls severing of the mitochondrial outer membrane. *Mol Cell*, 4, 815-26.
- LACKNER, L. L. 2014. Shaping the dynamic mitochondrial network. *BMC Biol*, 12, 35.
- LACKNER, L. L., HORNER, J. S. & NUNNARI, J. 2009. Mechanistic analysis of a dynamin effector. *Science*, 325, 874-7.
- LACKNER, L. L., PING, H., GRAEF, M., MURLEY, A. & NUNNARI, J. 2013. Endoplasmic reticulum-associated mitochondria-cortex tether functions in the distribution and inheritance of mitochondria. *Proc Natl Acad Sci U S A*, 110, E458-67.
- LAEMMLI, U. K. 1970. Cleavage of structural proteins during the assembly of the head of bacteriophage T4. *nature*, 227, 680-685.
- LAMARQUE, M., BESTEIRO, S., PAPOIN, J., ROQUES, M., VULLIEZ-LE NORMAND, B., MORLON-GUYOT, J., DUBREMETZ, J. F., FAUQUENOY, S., TOMAVO, S., FABER, B. W., KOCKEN, C. H., THOMAS, A. W., BOULANGER, M. J., BENTLEY, G. A. &

- LEBRUN, M. 2011. The RON2-AMA1 interaction is a critical step in moving junction-dependent invasion by apicomplexan parasites. *PLoS Pathog*, 7, e1001276.
- LAMARQUE, M. H., ROQUES, M., KONG-HAP, M., TONKIN, M. L., RUGARABAMU, G., MARQ, J.-B., PENARETE-VARGAS, D. M., BOULANGER, M. J., SOLDATI-FAVRE, D. & LEBRUN, M. 2014. Plasticity and redundancy among AMA–RON pairs ensure host cell entry of *Toxoplasma* parasites. *Nature Communications*, 5, 4098.
- LAMBERT, H., HITZIGER, N., DELLACASA, I., SVENSSON, M. & BARRAGAN, A. 2006. Induction of dendritic cell migration upon *Toxoplasma gondii* infection potentiates parasite dissemination. *Cell Microbiol*, 8, 1611-23.
- LANDER, E. S. 2016. The Heroes of CRISPR. *Cell*, 164, 18-28.
- LAU, Y.-L., LEE, W.-C., GUDIMELLA, R., ZHANG, G., CHING, X.-T., RAZALI, R., AZIZ, F., ANWAR, A. & FONG, M.-Y. 2016. Deciphering the draft genome of *Toxoplasma gondii* RH strain. *PloS one*, 11, e0157901.
- LAVY, M. & ESTELLE, M. 2016. Mechanisms of auxin signaling. *Development*, 143, 3226-9.
- LEBRUN, M., MICHELIN, A., EL HAJJ, H., PONCET, J., BRADLEY, P. J., VIAL, H. & DUBREMETZ, J. F. 2005. The rhoptry neck protein RON4 relocates at the moving junction during *Toxoplasma gondii* invasion. *Cellular microbiology*, 7, 1823-1833.
- LEE, H. & YOON, Y. 2016. Mitochondrial fission and fusion. *Biochem Soc Trans*, 44, 1725-1735.
- LEE, J. E., WESTRATE, L. M., WU, H., PAGE, C. & VOELTZ, G. K. 2016. Multiple dynamin family members collaborate to drive mitochondrial division. *Nature*, 540, 139-143.
- LEE, P. Y., COSTUMBRADO, J., HSU, C.-Y. & KIM, Y. H. 2012. Agarose gel electrophoresis for the separation of DNA fragments. *Journal of visualized experiments: JoVE*.
- LEUNG, J. M., HE, Y., ZHANG, F., HWANG, Y. C., NAGAYASU, E., LIU, J., MURRAY, J. M. & HU, K. 2017. Stability and function of a putative microtubule-organizing center in the human parasite *Toxoplasma gondii*. *Mol Biol Cell*, 28, 1361-1378.
- LEUNG, J. M., ROULD, M. A., KONRADT, C., HUNTER, C. A. & WARD, G. E. 2014. Disruption of TgPHIL1 alters specific parameters of *Toxoplasma gondii* motility measured in a quantitative, three-dimensional live motility assay. *PLoS One*, 9, e85763.
- LEVINE, N. D., CORLISS, J. O., COX, F. E., DEROUX, G., GRAIN, J., HONIGBERG, B. M., LEEDALE, G. F., LOEBLICH, A. R., 3RD, LOM, J., LYNN, D., MERINFELD, E. G., PAGE, F. C., POLJANSKY, G., SPRAGUE, V., VAVRA, J. & WALLACE, F. G. 1980. A newly revised classification of the protozoa. *J Protozool*, 27, 37-58.
- LEWIS, S. C., UCHIYAMA, L. F. & NUNNARI, J. 2016. ER-mitochondria contacts couple mtDNA synthesis with mitochondrial division in human cells. *Science*, 353, aaf5549.
- LI, M., WANG, H., LIU, J., HAO, P., MA, L. & LIU, Q. 2015. The Apoptotic Role of Metacaspase in *Toxoplasma gondii*. *Frontiers in Microbiology*, 6, 1560.

- LI, X. & GOULD, S. J. 2003. The dynamin-like GTPase DLP1 is essential for peroxisome division and is recruited to peroxisomes in part by PEX11. *Journal of Biological Chemistry*, 278, 17012-17020.
- LIU, J., HE, Y., BENMERZOUGA, I., SULLIVAN, W. J., JR., MORRISSETTE, N. S., MURRAY, J. M. & HU, K. 2016. An ensemble of specifically targeted proteins stabilizes cortical microtubules in the human parasite *Toxoplasma gondii*. *Mol Biol Cell*, 27, 549-71.
- LIU, J., WETZEL, L., ZHANG, Y., NAGAYASU, E., EMS-MCCLUNG, S., FLORENS, L. & HU, K. 2013. Novel thioredoxin-like proteins are components of a protein complex coating the cortical microtubules of *Toxoplasma gondii*. *Eukaryot Cell*, 12, 1588-99.
- LIU, R. & CHAN, D. C. 2015. The mitochondrial fission receptor Mff selectively recruits oligomerized Drp1. *Molecular Biology of the Cell*, 26, 4466-4477.
- LOPEZ-DOMENECH, G., COVILL-COOKE, C., IVANKOVIC, D., HALFF, E. F., SHEEHAN, D. F., NORKETT, R., BIRSA, N. & KITTLER, J. T. 2018. Miro proteins coordinate microtubule- and actin-dependent mitochondrial transport and distribution. *EMBO J*, 37, 321-336.
- LORESTANI, A., SHEINER, L., YANG, K., ROBERTSON, S. D., SAHOO, N., BROOKS, C. F., FERGUSON, D. J., STRIEPEN, B. & GUBBELS, M. J. 2010. A *Toxoplasma* MORN1 null mutant undergoes repeated divisions but is defective in basal assembly, apicoplast division and cytokinesis. *PLoS One*, 5, e12302.
- LOSON, O. C., SONG, Z., CHEN, H. & CHAN, D. C. 2013. Fis1, Mff, MiD49, and MiD51 mediate Drp1 recruitment in mitochondrial fission. *Mol Biol Cell*, 24, 659-67.
- LOURIDO, S., TANG, K. & SIBLEY, L. D. 2012. Distinct signalling pathways control *Toxoplasma* egress and host-cell invasion. *EMBO J*, 31, 4524-34.
- LUFT, B. J. & REMINGTON, J. S. 1992. Toxoplasmic encephalitis in AIDS. *Clinical Infectious Diseases*, 15, 211-222.
- MACRAE, J. I., SHEINER, L., NAHID, A., TONKIN, C., STRIEPEN, B. & MCCONVILLE, M. J. 2012. Mitochondrial metabolism of glucose and glutamine is required for intracellular growth of *Toxoplasma gondii*. *Cell Host Microbe*, 12, 682-92.
- MAHARANA, B. R., TEWARI, A. K., SARAVANAN, B. C. & SUDHAKAR, N. R. 2016. Important hemoprotozoan diseases of livestock: Challenges in current diagnostics and therapeutics: An update. *Vet World*, 9, 487-95.
- MALI, P., YANG, L., ESVELT, K. M., AACH, J., GUELL, M., DICARLO, J. E., NORVILLE, J. E. & CHURCH, G. M. 2013. RNA-guided human genome engineering via Cas9. *Science*, 339, 823-826.
- MANGANAS, P., MACPHERSON, L. & TOKATLIDIS, K. 2017. Oxidative protein biogenesis and redox regulation in the mitochondrial intermembrane space. *Cell Tissue Res*, 367, 43-57.

- MANN, T. & BECKERS, C. 2001. Characterization of the subpellicular network, a filamentous membrane skeletal component in the parasite *Toxoplasma gondii*. *Molecular and biochemical parasitology*, 115, 257-268.
- MANNELLA, C. A. 2006. Structure and dynamics of the mitochondrial inner membrane cristae. *Biochim Biophys Acta*, 1763, 542-8.
- MANOR, U., BARTHOLOMEW, S., GOLANI, G., CHRISTENSON, E., KOZLOV, M., HIGGS, H., SPUDICH, J. & LIPPINCOTT-SCHWARTZ, J. 2015. A mitochondria-anchored isoform of the actin-nucleating spire protein regulates mitochondrial division. *Elife*, 4.
- MARKS, B., STOWELL, M. H., VALLIS, Y., MILLS, I. G., GIBSON, A., HOPKINS, C. R. & MCMAHON, H. T. 2001. GTPase activity of dynamin and resulting conformation change are essential for endocytosis. *Nature*, 410, 231-5.
- MATHER, M. W. & VAIDYA, A. B. 2008. Mitochondria in malaria and related parasites: ancient, diverse and streamlined. *J Bioenerg Biomembr*, 40, 425-33.
- MAZUMDAR, J., WILSON, E. H., MASEK, K., HUNTER, C. A. & STRIEPEN, B. 2006. Apicoplast fatty acid synthesis is essential for organelle biogenesis and parasite survival in *Toxoplasma gondii*. *Proceedings of the National Academy of Sciences*, 103, 13192-13197.
- MCCOY, J. M., WHITEHEAD, L., VAN DOOREN, G. G. & TONKIN, C. J. 2012. TgCDPK3 regulates calcium-dependent egress of *Toxoplasma gondii* from host cells. *PLoS Pathog*, 8, e1003066.
- MEARS, J. A., LACKNER, L. L., FANG, S., INGERMAN, E., NUNNARI, J. & HINSHAW, J. E. 2011. Conformational changes in Dnm1 support a contractile mechanism for mitochondrial fission. *Nat Struct Mol Biol*, 18, 20-6.
- MEEUSEN, S., DEVAY, R., BLOCK, J., CASSIDY-STONE, A., WAYSON, S., MCCAFFERY, J. M. & NUNNARI, J. 2006. Mitochondrial inner-membrane fusion and crista maintenance requires the dynamin-related GTPase Mgm1. *Cell*, 127, 383-95.
- MEISSNER, M., SCHLUTER, D. & SOLDATI, D. 2002. Role of *Toxoplasma gondii* myosin A in powering parasite gliding and host cell invasion. *Science*, 298, 837-40.
- MELKONIAN, K. A., MAIER, K. C., GODFREY, J. E., RODGERS, M. & SCHROER, T. A. 2007. Mechanism of dynamitin-mediated disruption of dynactin. *J Biol Chem*, 282, 19355-64.
- MELO, E. J., ATTIAS, M. & DE SOUZA, W. 2000. The single mitochondrion of tachyzoites of *Toxoplasma gondii*. *J Struct Biol*, 130, 27-33.
- MERCIER, C., ADJOGLE, K. D., DAUBENER, W. & DELAUW, M. F. 2005. Dense granules: are they key organelles to help understand the parasitophorous vacuole of all apicomplexa parasites? *Int J Parasitol*, 35, 829-49.
- MERCIER, C., DUBREMETZ, J. F., RAUSCHER, B., LECORDIER, L., SIBLEY, L. D. & CESBRON-DELAUW, M. F. 2002. Biogenesis of nanotubular network in *Toxoplasma* parasitophorous vacuole induced by parasite proteins. *Mol Biol Cell*, 13, 2397-409.

- MISKO, A., JIANG, S., WEGORZEWSKA, I., MILBRANDT, J. & BALOH, R. H. 2010. Mitofusin 2 is necessary for transport of axonal mitochondria and interacts with the Miro/Milton complex. *J Neurosci*, 30, 4232-40.
- MITAL, J., MEISSNER, M., SOLDATI, D. & WARD, G. E. 2005. Conditional expression of *Toxoplasma gondii* apical membrane antigen-1 (TgAMA1) demonstrates that TgAMA1 plays a critical role in host cell invasion. *Molecular biology of the cell*, 16, 4341-4349.
- MOJICA, F. J., GARCÍA-MARTÍNEZ, J. & SORIA, E. 2005. Intervening sequences of regularly spaced prokaryotic repeats derive from foreign genetic elements. *Journal of molecular evolution*, 60, 174-182.
- MONDRAGON, R. & FRIXIONE, E. 1996. Ca(2+)-dependence of conoid extrusion in *Toxoplasma gondii* tachyzoites. *J Eukaryot Microbiol*, 43, 120-7.
- MONTESSUIT, S., SOMASEKHARAN, S. P., TERRONES, O., LUCKEN-ARDJOMANDE, S., HERZIG, S., SCHWARZENBACHER, R., MANSTEIN, D. J., BOSSY-WETZEL, E., BASANEZ, G., MEDA, P. & MARTINOU, J. C. 2010. Membrane remodeling induced by the dynamin-related protein Drp1 stimulates Bax oligomerization. *Cell*, 142, 889-901.
- MOORE, R. B., OBORNÍK, M., JANOUŠKOVEC, J., CHRUDIMSKÝ, T., VANCOVÁ, M., GREEN, D. H., WRIGHT, S. W., DAVIES, N. W., BOLCH, C. J. & HEIMANN, K. 2008. A photosynthetic alveolate closely related to apicomplexan parasites. *Nature*, 451, 959.
- MOREJOHN, L. C., BUREAU, T. E., MOLE-BAJER, J., BAJER, A. S. & FOSKET, D. E. 1987. Oryzalin, a dinitroaniline herbicide, binds to plant tubulin and inhibits microtubule polymerization in vitro. *Planta*, 172, 252-64.
- MORIYA, H. 2015. Quantitative nature of overexpression experiments. *Molecular biology of the cell*, 26, 3932-3939.
- MORLINO, G., BARREIRO, O., BAIXAULI, F., ROBLES-VALERO, J., GONZALEZ-GRANADO, J. M., VILLA-BELLOSTA, R., CUENCA, J., SANCHEZ-SORZANO, C. O., VEIGA, E., MARTIN-COFRECES, N. B. & SANCHEZ-MADRID, F. 2014. Miro-1 links mitochondria and microtubule Dynein motors to control lymphocyte migration and polarity. *Mol Cell Biol*, 34, 1412-26.
- MORLON-GUYOT, J., PASTORE, S., BERRY, L., LEBRUN, M. & DAHER, W. 2015. *Toxoplasma gondii* Vps11, a subunit of HOPS and CORVET tethering complexes, is essential for the biogenesis of secretory organelles. *Cell Microbiol*, 17, 1157-78.
- MORRISSETTE, N. 2015. Targeting *Toxoplasma* tubules: tubulin, microtubules, and associated proteins in a human pathogen. *Eukaryot Cell*, 14, 2-12.
- MORRISSETTE, N. S., MURRAY, J. M. & ROOS, D. S. 1997. Subpellicular microtubules associate with an intramembranous particle lattice in the protozoan parasite *Toxoplasma gondii*. *J Cell Sci*, 110 (Pt 1), 35-42.
- MORRISSETTE, N. S. & SIBLEY, L. D. 2002. Disruption of microtubules uncouples budding and nuclear division in *Toxoplasma gondii*. *J Cell Sci*, 115, 1017-25.

- MOZDY, A. D., MCCAFFERY, J. M. & SHAW, J. M. 2000. Dnm1p GTPase-mediated mitochondrial fission is a multi-step process requiring the novel integral membrane component Fis1p. *J Cell Biol*, 151, 367-80.
- MUELLER, C., KLAGES, N., JACOT, D., SANTOS, J. M., CABRERA, A., GILBERGER, T. W., DUBREMETZ, J. F. & SOLDATI-FAVRE, D. 2013. The Toxoplasma protein ARO mediates the apical positioning of rhostry organelles, a prerequisite for host cell invasion. *Cell Host Microbe*, 13, 289-301.
- MUELLER, C., SAMOO, A., HAMMOUDI, P. M., KLAGES, N., KALLIO, J. P., KURSULA, I. & SOLDATI-FAVRE, D. 2016. Structural and functional dissection of Toxoplasma gondii armadillo repeats only protein. *J Cell Sci*, 129, 1031-45.
- MUÑIZ-HERNÁNDEZ, S., GONZÁLEZ DEL CARMEN, M., MONDRAGÓN, M., MERCIER, C., CESBRON, M., MONDRAGÓN-GONZÁLEZ, S., GONZÁLEZ, S. & MONDRAGÓN, R. 2011. Contribution of the residual body in the spatial organization of Toxoplasma gondii tachyzoites within the parasitophorous vacuole. *BioMed Research International*, 2011.
- NAGEL, S. D. & BOOTHROYD, J. C. 1988. The alpha- and beta-tubulins of Toxoplasma gondii are encoded by single copy genes containing multiple introns. *Mol Biochem Parasitol*, 29, 261-73.
- NAIR, S. C., BROOKS, C. F., GOODMAN, C. D., STURM, A., MCFADDEN, G. I., SUNDRIYAL, S., ANGLIN, J. L., SONG, Y., MORENO, S. N. & STRIEPEN, B. 2011. Apicoplast isoprenoid precursor synthesis and the molecular basis of fosmidomycin resistance in Toxoplasma gondii. *J Exp Med*, 208, 1547-59.
- NAYLOR, K., INGERMAN, E., OKREGLAK, V., MARINO, M., HINSHAW, J. E. & NUNNARI, J. 2006. Mdv1 interacts with assembled dnm1 to promote mitochondrial division. *Journal of Biological Chemistry*, 281, 2177-2183.
- NGO, H. M., YANG, M., PAPROTKA, K., PYPAERT, M., HOPPE, H. & JOINER, K. A. 2003. AP-1 in Toxoplasma gondii mediates biogenesis of the rhostry secretory organelle from a post-Golgi compartment. *J Biol Chem*, 278, 5343-52.
- NI NYOMAN, A. D. & LUDER, C. G. 2013. Apoptosis-like cell death pathways in the unicellular parasite Toxoplasma gondii following treatment with apoptosis inducers and chemotherapeutic agents: a proof-of-concept study. *Apoptosis*, 18, 664-80.
- NICHOLLS, D. & FERGUSON, S. 2013. Bioenergetics. Vol. 4. *Norwell, MA, USA: Academic*.
- NICHOLS, B. A. & CHIAPPINO, M. L. 1987. Cytoskeleton of Toxoplasma gondii. *J Protozool*, 34, 217-26.
- NICOLLE, C. & MANCEAUX, L. 1908. Sur une infection à corps de Leishman (ou organismes voisins) du gondi. *CR Acad Sci*, 147, 736.
- NISHI, M., HU, K., MURRAY, J. M. & ROOS, D. S. 2008. Organellar dynamics during the cell cycle of Toxoplasma gondii. *J Cell Sci*, 121, 1559-68.

- NISHIMURA, K., FUKAGAWA, T., TAKISAWA, H., KAKIMOTO, T. & KANEMAKI, M. 2009. An auxin-based degron system for the rapid depletion of proteins in nonplant cells. *Nat Methods*, 6, 917-22.
- NUNNARI, J. & SUOMALAINEN, A. 2012. Mitochondria: in sickness and in health. *Cell*, 148, 1145-59.
- O'DONNELL, R. A., PREISER, P. R., WILLIAMSON, D. H., MOORE, P. W., COWMAN, A. F. & CRABB, B. S. 2001. An alteration in concatameric structure is associated with efficient segregation of plasmids in transfected *Plasmodium falciparum* parasites. *Nucleic Acids Res*, 29, 716-24.
- OBAR, R. A., COLLINS, C. A., HAMMARBACK, J. A., SHPETNER, H. S. & VALLEE, R. B. 1990. Molecular cloning of the microtubule-associated mechanochemical enzyme dynamin reveals homology with a new family of GTP-binding proteins. *Nature*, 347, 256.
- OKAMOTO, P. M., HERSKOVITS, J. S. & VALLEE, R. B. 1997. Role of the basic, proline-rich region of dynamin in Src homology 3 domain binding and endocytosis. *Journal of Biological Chemistry*, 272, 11629-11635.
- OSELLAME, L. D., SINGH, A. P., STROUD, D. A., PALMER, C. S., STOJANOVSKI, D., RAMACHANDRAN, R. & RYAN, M. T. 2016. Cooperative and independent roles of the Drp1 adaptors Mff, MiD49 and MiD51 in mitochondrial fission. *J Cell Sci*, 129, 2170-2181.
- OSSORIO, P. N., SIBLEY, L. D. & BOOTHROYD, J. C. 1991. Mitochondrial-like DNA sequences flanked by direct and inverted repeats in the nuclear genome of *Toxoplasma gondii*. *Journal of molecular biology*, 222, 525-536.
- OTERA, H., MIYATA, N., KUGE, O. & MIHARA, K. 2016. Drp1-dependent mitochondrial fission via MiD49/51 is essential for apoptotic cristae remodeling. *J Cell Biol*, 212, 531-44.
- OTERA, H., WANG, C., CLELAND, M. M., SETOGUCHI, K., YOKOTA, S., YOULE, R. J. & MIHARA, K. 2010. Mff is an essential factor for mitochondrial recruitment of Drp1 during mitochondrial fission in mammalian cells. *J Cell Biol*, 191, 1141-58.
- OTSUGA, D., KEEGAN, B. R., BRISCH, E., THATCHER, J. W., HERMANN, G. J., BLEAZARD, W. & SHAW, J. M. 1998. The dynamin-related GTPase, Dnm1p, controls mitochondrial morphology in yeast. *J Cell Biol*, 143, 333-49.
- OVCARIKOVA, J., LEMGRUBER, L., STILGER, K. L., SULLIVAN, W. J. & SHEINER, L. 2017. Mitochondrial behaviour throughout the lytic cycle of *Toxoplasma gondii*. *Sci Rep*, 7, 42746.
- PADGETT, L. R., ARRIZABALAGA, G. & SULLIVAN, W. J., JR. 2017. Targeting of tail-anchored membrane proteins to subcellular organelles in *Toxoplasma gondii*. *Traffic*, 18, 149-158.
- PAGLIUSO, A., COSSART, P. & STAVRU, F. 2018. The ever-growing complexity of the mitochondrial fission machinery. *Cell Mol Life Sci*, 75, 355-374.

- PALMER, C. S., OSELLAME, L. D., LAINE, D., KOUTSOPOULOS, O. S., FRAZIER, A. E. & RYAN, M. T. 2011. MiD49 and MiD51, new components of the mitochondrial fission machinery. *EMBO Rep*, 12, 565-73.
- PELLETIER, L., STERN, C. A., PYPAERT, M., SHEFF, D., NGO, H. M., ROPER, N., HE, C. Y., HU, K., TOOMRE, D., COPPENS, I., ROOS, D. S., JOINER, K. A. & WARREN, G. 2002. Golgi biogenesis in *Toxoplasma gondii*. *Nature*, 418, 548-52.
- PERIZ, J., WHITELAW, J., HARDING, C., GRAS, S., DEL ROSARIO MININA, M. I., LATORRE-BARRAGAN, F., LEMGRUBER, L., REIMER, M. A., INSALL, R., HEASLIP, A. & MEISSNER, M. 2017. *Toxoplasma gondii* F-actin forms an extensive filamentous network required for material exchange and parasite maturation. *Elife*, 6.
- PERNAS, L. & SCORRANO, L. 2016. Mito-Morphosis: Mitochondrial Fusion, Fission, and Cristae Remodeling as Key Mediators of Cellular Function. *Annu Rev Physiol*, 78, 505-31.
- PHILIP, N. & WATERS, A. P. 2015. Conditional Degradation of Plasmodium Calcineurin Reveals Functions in Parasite Colonization of both Host and Vector. *Cell Host Microbe*, 18, 122-31.
- PIEPERHOFF, M. S., PALL, G. S., JIMENEZ-RUIZ, E., DAS, S., MELATTI, C., GOW, M., WONG, E. H., HENG, J., MULLER, S., BLACKMAN, M. J. & MEISSNER, M. 2015. Conditional U1 Gene Silencing in *Toxoplasma gondii*. *PLoS One*, 10, e0130356.
- PRAEFCKE, G. J. & MCMAHON, H. T. 2004. The dynamin superfamily: universal membrane tubulation and fission molecules? *Nat Rev Mol Cell Biol*, 5, 133-47.
- PREISER, P. R., WILSON, R. J., MOORE, P. W., MCCREADY, S., HAJIBAGHERI, M. A., BLIGHT, K. J., STRATH, M. & WILLIAMSON, D. H. 1996. Recombination associated with replication of malarial mitochondrial DNA. *EMBO J*, 15, 684-93.
- PURKANTI, R. & THATTAI, M. 2015. Ancient dynamin segments capture early stages of host-mitochondrial integration. *Proc Natl Acad Sci U S A*, 112, 2800-5.
- PUTIGNANI, L., TAIT, A., SMITH, H. V., HORNER, D., TOVAR, J., TETLEY, L. & WASTLING, J. M. 2004. Characterization of a mitochondrion-like organelle in *Cryptosporidium parvum*. *Parasitology*, 129, 1-18.
- QUINTYNE, N. J., GILL, S. R., ECKLEY, D. M., CREGO, C. L., COMPTON, D. A. & SCHROER, T. A. 1999. Dynactin Is Required for Microtubule Anchoring at Centrosomes. *The Journal of Cell Biology*, 147, 321.
- QURESHI, B. M., HOFMANN, N. E., ARROYO-OLARTE, R. D., NICKL, B., HOEHNE, W., JUNGBLUT, P. R., LUCIUS, R., SCHEERER, P. & GUPTA, N. 2013. Dynein light chain 8a of *Toxoplasma gondii*, a unique conoid-localized beta-strand-swapped homodimer, is required for an efficient parasite growth. *FASEB J*, 27, 1034-47.
- RAMACHANDRAN, R. 2017. Mitochondrial dynamics: The dynamin superfamily and execution by collusion. *Semin Cell Dev Biol*.

- RAMBOLD, A. S., KOSTELECKY, B., ELIA, N. & LIPPINCOTT-SCHWARTZ, J. 2011. Tubular network formation protects mitochondria from autophagosomal degradation during nutrient starvation. *Proc Natl Acad Sci U S A*, 108, 10190-5.
- RECK-PETERSON, S. L., REDWINE, W. B., VALE, R. D. & CARTER, A. P. 2018. The cytoplasmic dynein transport machinery and its many cargoes. *Nat Rev Mol Cell Biol*, 19, 382-398.
- REUBOLD, T. F., ESCHENBURG, S., BECKER, A., LEONARD, M., SCHMID, S. L., VALLEE, R. B., KULL, F. J. & MANSTEIN, D. J. 2005. Crystal structure of the GTPase domain of rat dynamin 1. *Proc Natl Acad Sci U S A*, 102, 13093-8.
- RIORDAN, C. E., AULT, J. G., LANGRETH, S. G. & KEITHLY, J. S. 2003. Cryptosporidium parvum Cpn60 targets a relict organelle. *Current genetics*, 44, 138-147.
- ROBERT-GANGNEUX, F. & DARDE, M. L. 2012. Epidemiology of and diagnostic strategies for toxoplasmosis. *Clin Microbiol Rev*, 25, 264-96.
- ROBERTS, A. J., KON, T., KNIGHT, P. J., SUTOH, K. & BURGESS, S. A. 2013. Functions and mechanics of dynein motor proteins. *Nature reviews Molecular cell biology*, 14, 713.
- ROUT, M. P., OBADO, S. O., SCHENKMAN, S. & FIELD, M. C. 2017. Specialising the parasite nucleus: Pores, lamins, chromatin, and diversity. *PLOS Pathogens*, 13, e1006170.
- RUSSELL, D. G. & BURNS, R. G. 1984. The polar ring of coccidian sporozoites: a unique microtubule-organizing centre. *J Cell Sci*, 65, 193-207.
- RUSSO, G. J., LOUIE, K., WELLINGTON, A., MACLEOD, G. T., HU, F., PANCHUMARTHI, S. & ZINSMAIER, K. E. 2009. Drosophila Miro is required for both anterograde and retrograde axonal mitochondrial transport. *J Neurosci*, 29, 5443-55.
- SABIN, A. B. & FELDMAN, H. A. 1948. Dyes as Microchemical Indicators of a New Immunity Phenomenon Affecting a Protozoon Parasite (Toxoplasma). *Science*, 108, 660-3.
- SALAMUN, J., KALLIO, J. P., DAHER, W., SOLDATI-FAVRE, D. & KURSULA, I. 2014. Structure of Toxoplasma gondii coronin, an actin-binding protein that relocalizes to the posterior pole of invasive parasites and contributes to invasion and egress. *Faseb j*, 28, 4729-47.
- SANGARÉ, L. O., ALAYI, T. D., WESTERMANN, B., HOVASSE, A., SINDIKUBWABO, F., CALLEBAUT, I., WERKMEISTER, E., LAFONT, F., SLOMIANNY, C., HAKIMI, M.-A., VAN DORSSELAER, A., SCHAEFFER-REISS, C. & TOMAVO, S. 2016. Unconventional endosome-like compartment and retromer complex in Toxoplasma gondii govern parasite integrity and host infection. *Nature Communications*, 7, 11191.
- SANGARE, L. O., ALAYI, T. D., WESTERMANN, B., HOVASSE, A., SINDIKUBWABO, F., CALLEBAUT, I., WERKMEISTER, E., LAFONT, F., SLOMIANNY, C., HAKIMI, M. A., VAN DORSSELAER, A., SCHAEFFER-REISS, C. & TOMAVO, S. 2016. Unconventional endosome-like compartment and retromer complex in Toxoplasma gondii govern parasite integrity and host infection. *Nat Commun*, 7, 11191.

- SAUER, B. & HENDERSON, N. 1988. Site-specific DNA recombination in mammalian cells by the Cre recombinase of bacteriophage P1. *Proc Natl Acad Sci U S A*, 85, 5166-70.
- SCARPELLI, P., ALMEIDA, G. T., VICOSO, K. L., LIMA, W. R., PEREIRA, L. B., MEISSNER, K. A., WRENGER, C., RAFAELLO, A., RIZZUTO, R., POZZAN, T. & GARCIA, C. R. S. 2018. Melatonin activate FIS1, DYN1 and DYN2 Plasmodium falciparum related-genes for mitochondria fission: mitoemerald-GFP as a tool to visualize mitochondria structure. *J Pineal Res*.
- SCHAUSS, A. C., BEWERSDORF, J. & JAKOBS, S. 2006. Fis1p and Caf4p, but not Mdv1p, determine the polar localization of Dnm1p clusters on the mitochondrial surface. *J Cell Sci*, 119, 3098-106.
- SCHINDELIN, J., ARGANDA-CARRERAS, I., FRISE, E., KAYNIG, V., LONGAIR, M., PIETZSCH, T., PREIBISCH, S., RUEDEN, C., SAALFELD, S. & SCHMID, B. 2012. Fiji: an open-source platform for biological-image analysis. *Nature methods*, 9, 676-682.
- SCHINDELIN, J., RUEDEN, C. T., HINER, M. C. & ELICEIRI, K. W. 2015. The ImageJ ecosystem: An open platform for biomedical image analysis. *Molecular reproduction and development*, 82, 518-529.
- SCHRADER, M., COSTELLO, J. L., GODINHO, L. F., AZADI, A. S. & ISLINGER, M. 2016. Proliferation and fission of peroxisomes - An update. *Biochim Biophys Acta*, 1863, 971-83.
- SCHROER, T. A. 2004. Dynactin. *Annu Rev Cell Dev Biol*, 20, 759-79.
- SCHROER, T. A. & SHEETZ, M. P. 1991. Two activators of microtubule-based vesicle transport. *J Cell Biol*, 115, 1309-18.
- SCHULTZ, A. J. & CARRUTHERS, V. B. 2018. Toxoplasma gondii LCAT Primarily Contributes to Tachyzoite Egress. *mSphere*, 3.
- SCHWARZ, T. L. 2013. Mitochondrial trafficking in neurons. *Cold Spring Harb Perspect Biol*, 5.
- SEEBER, F., LIMENITAKIS, J. & SOLDATI-FAVRE, D. 2008. Apicomplexan mitochondrial metabolism: a story of gains, losses and retentions. *Trends Parasitol*, 24, 468-78.
- SESAKI, H. & JENSEN, R. E. 2004. Ugo1p links the Fzo1p and Mgm1p GTPases for mitochondrial fusion. *Journal of Biological Chemistry*, 279, 28298-28303.
- SHARMAN, P. A., SMITH, N. C., WALLACH, M. G. & KATRIB, M. 2010. Chasing the golden egg: vaccination against poultry coccidiosis. *Parasite Immunol*, 32, 590-8.
- SHAW, J. M. & NUNNARI, J. 2002. Mitochondrial dynamics and division in budding yeast. *Trends Cell Biol*, 12, 178-84.
- SHAW, M. K., COMPTON, H. L., ROOS, D. S. & TILNEY, L. G. 2000. Microtubules, but not actin filaments, drive daughter cell budding and cell division in Toxoplasma gondii. *J Cell Sci*, 113 (Pt 7), 1241-54.
- SHAW, M. K., ROOS, D. S. & TILNEY, L. G. 1998. Acidic compartments and rhoptry formation in Toxoplasma gondii. *Parasitology*, 117 (Pt 5), 435-43.

- SHEFFIELD, H. G. & MELTON, M. L. 1968. The fine structure and reproduction of *Toxoplasma gondii*. *J Parasitol*, 54, 209-26.
- SHEINER, L., DEMERLY, J. L., POULSEN, N., BEATTY, W. L., LUCAS, O., BEHNKE, M. S., WHITE, M. W. & STRIEPEN, B. 2011. A systematic screen to discover and analyze apicoplast proteins identifies a conserved and essential protein import factor. *PLoS Pathog*, 7, e1002392.
- SHEINER, L., VAIDYA, A. B. & MCFADDEN, G. I. 2013. The metabolic roles of the endosymbiotic organelles of *Toxoplasma* and *Plasmodium* spp. *Curr Opin Microbiol*, 16, 452-8.
- SHEN, B., BROWN, K. M., LEE, T. D. & SIBLEY, L. D. 2014a. Efficient gene disruption in diverse strains of *Toxoplasma gondii* using CRISPR/CAS9. *MBio*, 5, e01114-14.
- SHEN, B. & SIBLEY, L. D. 2014. *Toxoplasma* aldolase is required for metabolism but dispensable for host-cell invasion. *Proc Natl Acad Sci U S A*, 111, 3567-72.
- SHEN, Q., YAMANO, K., HEAD, B. P., KAWAJIRI, S., CHEUNG, J. T., WANG, C., CHO, J. H., HATTORI, N., YOULE, R. J. & VAN DER BLIEK, A. M. 2014b. Mutations in Fis1 disrupt orderly disposal of defective mitochondria. *Mol Biol Cell*, 25, 145-59.
- SHIRENDEB, U. P., CALKINS, M. J., MANCZAK, M., ANEKONDA, V., DUFOUR, B., MCBRIDE, J. L., MAO, P. & REDDY, P. H. 2012. Mutant huntingtin's interaction with mitochondrial protein Drp1 impairs mitochondrial biogenesis and causes defective axonal transport and synaptic degeneration in Huntington's disease. *Hum Mol Genet*, 21, 406-20.
- SHPETNER, H. S., HERSKOVITS, J. S. & VALLEE, R. B. 1996. A binding site for SH3 domains targets dynamin to coated pits. *Journal of Biological Chemistry*, 271, 13-16.
- SHPETNER, H. S. & VALLEE, R. B. 1989. Identification of dynamin, a novel mechanochemical enzyme that mediates interactions between microtubules. *Cell*, 59, 421-32.
- SIBLEY, L. & BOOTHROYD, J. C. 1992. Construction of a molecular karyotype for *Toxoplasma gondii*. *Molecular and biochemical parasitology*, 51, 291-300.
- SIBLEY, L. D., NIESMAN, I. R., PARMLEY, S. F. & CESBRON-DELAUW, M.-F. 1995. Regulated secretion of multi-lamellar vesicles leads to formation of a tubulo-vesicular network in host-cell vacuoles occupied by *Toxoplasma gondii*. *Journal of cell science*, 108, 1669-1677.
- SIDIK, S. M., HACKETT, C. G., TRAN, F., WESTWOOD, N. J. & LOURIDO, S. 2014. Efficient genome engineering of *Toxoplasma gondii* using CRISPR/Cas9. *PLoS One*, 9, e100450.
- SIDIK, S. M., HUET, D., GANESAN, S. M., HUYNH, M. H., WANG, T., NASAMU, A. S., THIRU, P., SAEIJ, J. P., CARRUTHERS, V. B., NILES, J. C. & LOURIDO, S. 2016. A Genome-wide CRISPR Screen in *Toxoplasma* Identifies Essential Apicomplexan Genes. *Cell*, 166, 1423-1435.e12.

- SINAI, A. P. & JOINER, K. A. 2001. The *Toxoplasma gondii* protein ROP2 mediates host organelle association with the parasitophorous vacuole membrane. *J Cell Biol*, 154, 95-108.
- SINAI, A. P., WEBSTER, P. & JOINER, K. A. 1997. Association of host cell endoplasmic reticulum and mitochondria with the *Toxoplasma gondii* parasitophorous vacuole membrane: a high affinity interaction. *J Cell Sci*, 110 (Pt 17), 2117-28.
- SLOVES, P. J., DELHAYE, S., MOUVEAUX, T., WERKMEISTER, E., SLOMIANNY, C., HOVASSE, A., DILEZITOKO ALAYI, T., CALLEBAUT, I., GAJI, R. Y., SCHAEFFER-REISS, C., VAN DORSSELEAR, A., CARRUTHERS, V. B. & TOMAVO, S. 2012. *Toxoplasma* sortilin-like receptor regulates protein transport and is essential for apical secretory organelle biogenesis and host infection. *Cell Host Microbe*, 11, 515-27.
- SMIRNOVA, E., GRIPARIC, L., SHURLAND, D. L. & VAN DER BLIEK, A. M. 2001. Dynamin-related protein Drp1 is required for mitochondrial division in mammalian cells. *Mol Biol Cell*, 12, 2245-56.
- SMIRNOVA, E., SHURLAND, D. L., RYAZANTSEV, S. N. & VAN DER BLIEK, A. M. 1998. A human dynamin-related protein controls the distribution of mitochondria. *J Cell Biol*, 143, 351-8.
- SOLDATI, D. & BOOTHROYD, J. C. 1993a. Transient transfection and expression in the obligate intracellular parasite *Toxoplasma gondii*. *Science*, 260, 349-52.
- SOLDATI, D. & BOOTHROYD, J. C. 1993b. Transient transfection and expression in the obligate intracellular parasite *Toxoplasma gondii*. *SCIENCE-NEW YORK THEN WASHINGTON-*, 260, 349-349.
- SOLDATI, D. & BOOTHROYD, J. C. 1995. A selector of transcription initiation in the protozoan parasite *Toxoplasma gondii*. *Mol Cell Biol*, 15, 87-93.
- SOLDATI, D. & MEISSNER, M. 2004. *Toxoplasma* as a novel system for motility. *Curr Opin Cell Biol*, 16, 32-40.
- SONG, Z., GHOSHANI, M., MCCAFFERY, J. M., FREY, T. G. & CHAN, D. C. 2009. Mitofusins and OPA1 mediate sequential steps in mitochondrial membrane fusion. *Molecular biology of the cell*, 20, 3525-3532.
- SPEER, C. & DUBEY, J. 1998. Ultrastructure of early stages of infections in mice fed *Toxoplasma gondii* oocysts. *Parasitology*, 116, 35-42.
- SPEER, C. & DUBEY, J. 2005. Ultrastructural differentiation of *Toxoplasma gondii* schizonts (types B to E) and gamonts in the intestines of cats fed bradyzoites. *International journal for parasitology*, 35, 193-206.
- SRIVASTAVA, I. K., ROTTENBERG, H. & VAIDYA, A. B. 1997. Atovaquone, a broad spectrum antiparasitic drug, collapses mitochondrial membrane potential in a malarial parasite. *J Biol Chem*, 272, 3961-6.
- STEINFELDT, T., KONEN-WAISMAN, S., TONG, L., PAWLOWSKI, N., LAMKEMEYER, T., SIBLEY, L. D., HUNN, J. P. & HOWARD, J. C. 2010. Phosphorylation of mouse

- immunity-related GTPase (IRG) resistance proteins is an evasion strategy for virulent *Toxoplasma gondii*. *PLoS Biol*, 8, e1000576.
- STEPANYANTS, N., MACDONALD, P. J., FRANCY, C. A., MEARS, J. A., QI, X. & RAMACHANDRAN, R. 2015. Cardiolipin's propensity for phase transition and its reorganization by dynamin-related protein 1 form a basis for mitochondrial membrane fission. *Mol Biol Cell*, 26, 3104-16.
- STOKKERMANS, T. J., SCHWARTZMAN, J. D., KEENAN, K., MORRISSETTE, N. S., TILNEY, L. G. & ROOS, D. S. 1996. Inhibition of *Toxoplasma gondii* replication by dinitroaniline herbicides. *Exp Parasitol*, 84, 355-70.
- STRACK, S. & CRIBBS, J. T. 2012. Allosteric modulation of Drp1 mechanoenzyme assembly and mitochondrial fission by the variable domain. *J Biol Chem*, 287, 10990-1001.
- STRACK, S., WILSON, T. J. & CRIBBS, J. T. 2013. Cyclin-dependent kinases regulate splice-specific targeting of dynamin-related protein 1 to microtubules. *J Cell Biol*, 201, 1037-51.
- STRIEPEN, B., CRAWFORD, M. J., SHAW, M. K., TILNEY, L. G., SEEBER, F. & ROOS, D. S. 2000. The plastid of *Toxoplasma gondii* is divided by association with the centrosomes. *J Cell Biol*, 151, 1423-34.
- SU, C., EVANS, D., COLE, R., KISSINGER, J., AJIOKA, J. & SIBLEY, L. 2003. Recent expansion of *Toxoplasma* through enhanced oral transmission. *Science*, 299, 414-416.
- SUAREZ, C., BISHOP, R., ALZAN, H., POOLE, W. & COOKE, B. 2017. Advances in the application of genetic manipulation methods to Apicomplexan parasites. *International journal for parasitology*.
- SUEN, D. F., NORRIS, K. L. & YOULE, R. J. 2008. Mitochondrial dynamics and apoptosis. *Genes Dev*, 22, 1577-90.
- SUSS-TOBY, E., ZIMMERBERG, J. & WARD, G. E. 1996. *Toxoplasma* invasion: the parasitophorous vacuole is formed from host cell plasma membrane and pinches off via a fission pore. *Proc Natl Acad Sci U S A*, 93, 8413-8.
- SUVOROVA, E. S., FRANCIJA, M., STRIEPEN, B. & WHITE, M. W. 2015. A novel bipartite centrosome coordinates the apicomplexan cell cycle. *PLoS Biol*, 13, e1002093.
- SWAYNE, T. C., ZHOU, C., BOLDOGH, I. R., CHARALEL, J. K., MCFALINE-FIGUEROA, J. R., THOMS, S., YANG, C., LEUNG, G., MCINNES, J., ERDMANN, R. & PON, L. A. 2011. Role for cER and Mmr1p in anchorage of mitochondria at sites of polarized surface growth in budding yeast. *Curr Biol*, 21, 1994-9.
- SZABADKAI, G., SIMONI, A. M., CHAMI, M., WIECKOWSKI, M. R., YOULE, R. J. & RIZZUTO, R. 2004. Drp-1-Dependent Division of the Mitochondrial Network Blocks Intraorganellar Ca²⁺ Waves and Protects against Ca²⁺-Mediated Apoptosis. *Molecular Cell*, 16, 59-68.

- TAGUCHI, N., ISHIHARA, N., JOFUKU, A., OKA, T. & MIHARA, K. 2007. Mitotic phosphorylation of dynamin-related GTPase Drp1 participates in mitochondrial fission. *Journal of Biological Chemistry*.
- TANG, B. 2018. Miro—Working beyond Mitochondria and Microtubules. *Cells*, 7, 18.
- TARDIEUX, I. & BAUM, J. 2016. Reassessing the mechanics of parasite motility and host-cell invasion. *J Cell Biol*, 214, 507-15.
- TAYLOR, S., BARRAGAN, A., SU, C., FUX, B., FENTRESS, S. J., TANG, K., BEATTY, W. L., HAJJ, H. E., JEROME, M., BEHNKE, M. S., WHITE, M., WOOTTON, J. C. & SIBLEY, L. D. 2006. A secreted serine-threonine kinase determines virulence in the eukaryotic pathogen *Toxoplasma gondii*. *Science*, 314, 1776-80.
- TEALE, W. D., PAPONOV, I. A. & PALME, K. 2006. Auxin in action: signalling, transport and the control of plant growth and development. *Nat Rev Mol Cell Biol*, 7, 847-59.
- TIEU, Q., OKREGLAK, V., NAYLOR, K. & NUNNARI, J. 2002. The WD repeat protein, Mdv1p, functions as a molecular adaptor by interacting with Dnm1p and Fis1p during mitochondrial fission. *J Cell Biol*, 158, 445-52.
- TORREY, E. F. & YOLKEN, R. H. 2013. *Toxoplasma* oocysts as a public health problem. *Trends Parasitol*, 29, 380-4.
- TRAN, J. Q., LI, C., CHYAN, A., CHUNG, L. & MORRISSETTE, N. S. 2012. SPM1 stabilizes subpellicular microtubules in *Toxoplasma gondii*. *Eukaryot Cell*, 11, 206-16.
- TWIG, G., ELORZA, A., MOLINA, A. J., MOHAMED, H., WIKSTROM, J. D., WALZER, G., STILES, L., HAIGH, S. E., KATZ, S., LAS, G., ALROY, J., WU, M., PY, B. F., YUAN, J., DEENEY, J. T., CORKEY, B. E. & SHIRIHAI, O. S. 2008. Fission and selective fusion govern mitochondrial segregation and elimination by autophagy. *Embo j*, 27, 433-46.
- UGARTE-URIBE, B., MULLER, H. M., OTSUKI, M., NICKEL, W. & GARCIA-SAEZ, A. J. 2014. Dynamin-related protein 1 (Drp1) promotes structural intermediates of membrane division. *J Biol Chem*, 289, 30645-56.
- VAIDYA, A. B., AKELLA, R. & SUPLICK, K. 1989. Sequences similar to genes for two mitochondrial proteins and portions of ribosomal RNA in tandemly arrayed 6-kilobase-pair DNA of a malarial parasite. *Molecular and Biochemical Parasitology*, 35, 97-107.
- VAIDYA, A. B. & MATHER, M. W. 2009. Mitochondrial evolution and functions in malaria parasites. *Annu Rev Microbiol*, 63, 249-67.
- VALE, R. D. 2003. The molecular motor toolbox for intracellular transport. *Cell*, 112, 467-480.
- VALETTI, C., WETZEL, D. M., SCHRADER, M., HASBANI, M. J., GILL, S. R., KREIS, T. E. & SCHROER, T. A. 1999. Role of dynactin in endocytic traffic: effects of dynactin overexpression and colocalization with CLIP-170. *Mol Biol Cell*, 10, 4107-20.
- VAN DER BLIEK, A. M. 1999. Functional diversity in the dynamin family. *Trends Cell Biol*, 9, 96-102.
- VAN DER BLIEK, A. M. & MEYEROWITZ, E. M. 1991. Dynamin-like protein encoded by the *Drosophila* shibire gene associated with vesicular traffic. *Nature*, 351, 411-4.

- VAN DER BLIEK, A. M., REDELMEIER, T. E., DAMKE, H., TISDALE, E. J., MEYEROWITZ, E. M. & SCHMID, S. L. 1993. Mutations in human dynamin block an intermediate stage in coated vesicle formation. *J Cell Biol*, 122, 553-63.
- VAN DER BLIEK, A. M., SHEN, Q. & KAWAJIRI, S. 2013. Mechanisms of mitochondrial fission and fusion. *Cold Spring Harb Perspect Biol*, 5.
- VAN DOOREN, G. G., KENNEDY, A. T. & MCFADDEN, G. I. 2012. The use and abuse of heme in apicomplexan parasites. *Antioxidants & redox signaling*, 17, 634-656.
- VAN DOOREN, G. G., REIFF, S. B., TOMOVA, C., MEISSNER, M., HUMBEL, B. M. & STRIEPEN, B. 2009. A novel dynamin-related protein has been recruited for apicoplast fission in *Toxoplasma gondii*. *Curr Biol*, 19, 267-76.
- VAN DOOREN, G. G. & STRIEPEN, B. 2013. The algal past and parasite present of the apicoplast. *Annual review of microbiology*, 67, 271-289.
- VAN DOOREN, G. G., YEOH, L. M., STRIEPEN, B. & MCFADDEN, G. I. 2016. The Import of Proteins into the Mitochondrion of *Toxoplasma gondii*. *J Biol Chem*.
- VARADI, A., JOHNSON-CADWELL, L. I., CIRULLI, V., YOON, Y., ALLAN, V. J. & RUTTER, G. A. 2004. Cytoplasmic dynein regulates the subcellular distribution of mitochondria by controlling the recruitment of the fission factor dynamin-related protein-1. *J Cell Sci*, 117, 4389-400.
- VERCESI, A. E., RODRIGUES, C. O., UYEMURA, S. A., ZHONG, L. & MORENO, S. N. 1998. Respiration and oxidative phosphorylation in the apicomplexan parasite *Toxoplasma gondii*. *J Biol Chem*, 273, 31040-7.
- VERSTREKEN, P., LY, C. V., VENKEN, K. J., KOH, T. W., ZHOU, Y. & BELLEN, H. J. 2005. Synaptic mitochondria are critical for mobilization of reserve pool vesicles at *Drosophila* neuromuscular junctions. *Neuron*, 47, 365-78.
- WANG, J. L., HUANG, S. Y., BEHNKE, M. S., CHEN, K., SHEN, B. & ZHU, X. Q. 2016. The Past, Present, and Future of Genetic Manipulation in *Toxoplasma gondii*. *Trends Parasitol*, 32, 542-53.
- WANG, Z. & WU, M. 2015. An integrated phylogenomic approach toward pinpointing the origin of mitochondria. *Sci Rep*, 5, 7949.
- WATERHAM, H. R., KOSTER, J., VAN ROERMUND, C. W., MOOYER, P. A., WANDERS, R. J. & LEONARD, J. V. 2007. A lethal defect of mitochondrial and peroxisomal fission. *N Engl J Med*, 356, 1736-41.
- WATTS, E., ZHAO, Y., DHARA, A., ELLER, B., PATWARDHAN, A. & SINAI, A. P. 2015. Novel approaches reveal that *Toxoplasma gondii* bradyzoites within tissue cysts are dynamic and replicating entities in vivo. *MBio*, 6, e01155-15.
- WENGER, J., KLINGLMAYR, E., FROHLICH, C., EIBL, C., GIMENO, A., HESSENBERGER, M., PUEHRINGER, S., DAUMKE, O. & GOETTIG, P. 2013. Functional mapping of human dynamin-1-like GTPase domain based on x-ray structure analyses. *PLoS One*, 8, e71835.

- WETZEL, D. M., HAKANSSON, S., HU, K., ROOS, D. & SIBLEY, L. D. 2003. Actin filament polymerization regulates gliding motility by apicomplexan parasites. *Mol Biol Cell*, 14, 396-406.
- WHITELAW, J. A., LATORRE-BARRAGAN, F., GRAS, S., PALL, G. S., LEUNG, J. M., HEASLIP, A., EGARTER, S., ANDENMATTEN, N., NELSON, S. R., WARSHAW, D. M., WARD, G. E. & MEISSNER, M. 2017. Surface attachment, promoted by the actomyosin system of *Toxoplasma gondii* is important for efficient gliding motility and invasion. *BMC Biol*, 15, 1.
- WOLF, A., COWEN, D. & PAIGE, B. 1939. HUMAN TOXOPLASMOSIS: OCCURRENCE IN INFANTS AS AN ENCEPHALOMYELITIS VERIFICATION BY TRANSMISSION TO ANIMALS. *Science*, 89, 226-7.
- XIAO, H., EL BISSATI, K., VERDIER-PINARD, P., BURD, B., ZHANG, H., KIM, K., FISER, A., ANGELETTI, R. H. & WEISS, L. M. 2010. Post-translational modifications to *Toxoplasma gondii* alpha- and beta-tubulins include novel C-terminal methylation. *J Proteome Res*, 9, 359-72.
- YAMAMOTO, M., MA, J. S., MUELLER, C., KAMIYAMA, N., SAIGA, H., KUBO, E., KIMURA, T., OKAMOTO, T., OKUYAMA, M., KAYAMA, H., NAGAMUNE, K., TAKASHIMA, S., MATSUURA, Y., SOLDATI-FAVRE, D. & TAKEDA, K. 2011. ATF6beta is a host cellular target of the *Toxoplasma gondii* virulence factor ROP18. *J Exp Med*, 208, 1533-46.
- YANG, N., FARRELL, A., NIEDELMAN, W., MELO, M., LU, D., JULIEN, L., MARTH, G. T., GUBBELS, M. J. & SAEIJ, J. P. 2013. Genetic basis for phenotypic differences between different *Toxoplasma gondii* type I strains. *BMC Genomics*, 14, 467.
- YAP, G. S. & SHER, A. 1999. Cell-mediated immunity to *Toxoplasma gondii*: initiation, regulation and effector function. *Immunobiology*, 201, 240-7.
- YEH, E. & DERISI, J. L. 2011. Chemical rescue of malaria parasites lacking an apicoplast defines organelle function in blood-stage *Plasmodium falciparum*. *PLoS Biol*, 9, e1001138.
- ZHANG, M., WANG, C., OTTO, T. D., OBERSTALLER, J., LIAO, X., ADAPA, S. R., UDENZE, K., BRONNER, I. F., CASANDRA, D., MAYHO, M., BROWN, J., LI, S., SWANSON, J., RAYNER, J. C., JIANG, R. H. Y. & ADAMS, J. H. 2018. Uncovering the essential genes of the human malaria parasite *Plasmodium falciparum* by saturation mutagenesis. *Science*, 360.
- ZHANG, P. & HINSHAW, J. E. 2001. Three-dimensional reconstruction of dynamin in the constricted state. *Nature Cell Biology*, 3, 922.
- ZHU, G., MARCHEWKA, M. J. & KEITHLY, J. S. 2000. *Cryptosporidium parvum* appears to lack a plastid genome. *Microbiology*, 146, 315-321.
- ZIKOVA, A., HAMPL, V., PARIS, Z., TYC, J. & LUKES, J. 2016. Aerobic mitochondria of parasitic protists: Diverse genomes and complex functions. *Mol Biochem Parasitol*, 209, 46-57.

